



УДК: 616.617-089+617-7

**Умида АБДУЖАББАРОВА,**

*Ассистент Ташкентской медицинской академии*

**Хусниддин НУРИДДИНОВ,**

*Младший научный сотрудник Республиканского специализированного научно-практического медицинского центра урологии*

**Шухрат ГИЯСОВ,**

*Профессор кафедры Урологии ТМА*

**Di TIE,**

*Continuous Extrusion Engineering Research Center of China Ministry of Education, Dalian Jiaotong University*

*На основе рецензии зав.кафедрой Микробиологии и биотехнологии Биологического факультета Национального университета Узбекистана им. М.Улугбека доцента (PhD) Кадировой З.А.*

### STUDY OF THE PROPERTIES OF MAGNESIUM SAMPLES USED IN THE DEVELOPMENT OF BIODEGRADABLE URETERAL STENTS

Annotation

Magnesium is a valuable material for the development of biodegradable ureteral stents due to its biocompatibility, ability to control degradation, and functional advantages. Biodegradable magnesium (Mg) alloys are attractive to medical researchers due to their mechanical properties, excellent biocompatibility, and low risk of rejection and allergic reactions. This article reviews recent advances in the study of biodegradable magnesium alloys, including the development of high-performance magnesium stents. The results of a study of the crystal structure of pure magnesium alloys and magnesium-zinc alloys using X-ray diffraction and electron microscopy are presented.

**Key words:** biodegradable stents, magnesium alloys, zinc, biocompatibility, crystal lattice, X-ray diffraction.

### BIOPARCHALANUVCHI URETERAL STENTLARNI ISHLAB CHIQRISHDA QO'LLANIDIGAN MAGNIY NAMUNALARINING XOSSALARINI O'RGANISH

Annotatsiya

Magniy biologik muvofiqligi, buzilishni nazorat qilish qobiliyati va funksional afzalliklari tufayli biologik parchalanadigan ureteral stentlarni ishlab chiqish uchun qimmatli materialdir. Biologik parchalanadigan magniy (Mg) qotishmalari mexanik xususiyatlari, mukammal biologik muvofiqligi va rad etish va allergik reaksiyalarning past xavfi tufayli tibbiyot tadqiqotchilari uchun jozibador. Ushbu maqolada biologik parchalanadigan magniy qotishmalarini o'rganish bo'yicha so'nggi yutuqlar, shu jumladan yuqori samarali magniy stentlarini ishlab chiqish usullari ko'rib chiqilgan. Sof magniy qotishmalari va magniy-rux qotishmalarining kristall tuzilishini rentgen nurlari difraksiyasi va elektron mikroskopiya yordamida o'rganish natijalari keltirilgan.

**Kalit so'zlar:** biologik parchalanadigan stentlar, magniy qotishmalari, rux, biologik moslik, kristall panjara, rentgen nurlari difraksiyasi.

### ИССЛЕДОВАНИЕ СВОЙСТВ МАГНИЕВЫХ ОБРАЗЦОВ, ИСПОЛЬЗУЕМЫХ ПРИ РАЗРАБОТКЕ БИОРАЗЛАГАЕМЫХ МОЧЕТОЧНИКОВЫХ СТЕНТОВ

Аннотация

Магний является ценным материалом для разработки биоразлагаемых мочеточниковых стентов благодаря своей биосовместимости, способности контролировать деградацию и функциональным преимуществам. Биоразлагаемые магниевые (Mg) сплавы привлекательны для медицинских исследователей благодаря своим механическим свойствам, превосходной биосовместимости и низкому риску отторжения и аллергических реакций. В статье рассматриваются последние достижения в изучении биоразлагаемых магниевых сплавов, включая разработку высокоэффективных магниевых стентов. Представлены результаты исследования кристаллической структуры чистых магниевых сплавов и сплавов магния с цинком, выполненные с использованием рентгеновской дифрактометрии и электронной микроскопии.

**Ключевые слова:** биодegradуемые стенты, магниевые сплавы, цинк, биосовместимость, кристаллическая решетка, рентгеновская дифракция.

**Введение.** Биодegradуемые стенты в медицине, в частности в урологии являются важным направлением в лечении заболеваний мочевыводящих путей. Они имеют несколько значений и преимуществ:

1. Сокращение осложнений: Традиционные металлические стенты могут вызывать различные осложнения, такие как воспаление, инфекция и образование камней. Биоразлагаемые стенты снижают риск этих осложнений, поскольку они растворяются в организме с течением времени.

2. Минимальная необходимость в повторных процедурах: биодegradуемые стенты обеспечивают временное укрепление или открытие мочевыводящих путей, что может сократить количество повторных вмешательств, связанных с удалением стента.

3. Улучшение качества жизни пациентов: поскольку биоразлагаемые стенты исчезают через определенное время, пациентам не нужно беспокоиться о постоянном присутствии инородного тела в организме.

4. Индивидуальная адаптация: Современные технологии позволяют создавать биодеградируемые стенты с учетом особенностей заболеваний и анатомии пациентов.

5. Снижение риска тромбоза и других реакций: биоразлагаемые материалы могут быть разработаны для минимизации негативных реакций в организме.

Использование магния для создания биоразлагаемых мочеточниковых стентов является актуальным и перспективным направлением в медицинской практике по нескольким причинам: это биоразлагаемость и удобство. Как и коронарные стенты, биоразлагаемые магниевые мочеточниковые стенты могут разлагаться в организме после выполнения своей функции.

**Литературный обзор.** Неразлагаемые металлы (например, титан и его сплавы с нержавеющей сталью) широко используются в качестве имплантатов для ортопедических суставов. В последние годы наблюдается рост интереса к биоразлагаемым металлическим материалам, в том числе к магнию и его сплавам, которые считаются перспективными кандидатами для использования в медицине (Witte F. et al., 2009, Sanz -Herrera JA et al., 2017). Магний имеет ряд преимуществ по сравнению с используемыми в настоящее время материалами для стентов. Он привлекает внимание благодаря своей хорошей биосовместимости и механическим свойствам, аналогичным свойствам нативной кости. Кальций, марганец, цинк и цирконий являются основными кандидатами на легирование, так как они нетоксичны для организма человека и способны замедлять скорость биодеградации. Присутствие этих элементов позволяет существенно улучшить физико-механические свойства магниевых сплавов за счет измельчения их микроструктуры и выделения интерметаллических частиц. Исследования показали, что сплавы Mg- Ca, Mg-Zn и Mg- Mn -Zn обладают хорошей биосовместимостью *in vitro* и *in vivo* и повышенной коррозионной стойкостью, постепенно растворяясь в костной ткани (Гиясов, Ш., 2023; Чжао Д.В. и др., 2016).

Сплавы магния с цинком (Mg-Zn) выигрывают от совместимости цинка с телом человека, образуя стабильные защитные слои, которые повышают коррозионную стойкость. Механические свойства сплавов магния с цинком изучались во многих исследованиях (Vrag et al., 2012).

**Методология исследования.** Объектами нашего исследования стали образцы чистого магния и магния с различным количеством цинка. Для изучения внутренней структуры металлов мы использовали такие методы, как электронная микроскопия и рентгеновская дифракция, поскольку они играют решающую роль в обеспечении детального изучения состава, микроструктуры и кристаллографических свойств материалов.

Рентгеновская дифракция позволяет определять кристаллографические параметры, такие как постоянная решетки и ориентация зерен, что дает ценную информацию о внутренней структуре материалов. Уточнение по Ритвелду, распространенный метод рентгеновского дифракционного анализа, позволяет проводить количественный анализ фазового состава и кристаллической структуры (Mc.Cusker, L., et al., 1999). Совместное использование методов электронной микроскопии и рентгеновской дифракции обеспечивает комплексный подход к изучению структуры материалов.

Нами использовался материал на основе магния, полученный методом реэкструзии. Для определения кристаллической структуры фаз использовался дифрактометр PANalytical Empyrean. Для характеристики морфологии поверхности использовался оптический микроскоп (JEOL JSM-IT200LA). Перед анализом наши образцы были очищены в следующей последовательности: Очистка хромовой кислотой (200 г/л CrO<sub>3</sub> + 10 г/л AgNO<sub>3</sub>) в течение 5 мин. для удаления продуктов коррозии поверхности без удаления металлического Mg. Затем образцы были промыты дистиллированной водой, подвергнуты ультразвуковой обработке в ацетоне и высушены на воздухе.

Рентгеновская дифрактометрия является одним из мощных методов исследования материалов

**Анализ и результаты.** В работе использовали чистые образцы Mg и образцы Mg-1Zn. Рентгеновские дифракционные измерения образцов магния проводили на дифрактометре Empyrean Series3 (PANalytical, Нидерланды) с линейным твердофазным детектором X'Celerator с использованием CuK $\alpha$  - излучения и никелевого фильтра. Результаты регистрировали с учетом длин волн 1,54060 Å и 1,54443 Å при соотношении интенсивностей в дублете 2:1. Напряжение и ток на рентгеновской трубке составляли 45 кВ и 40 мА соответственно. Измерения проводили в геометрии Брэгга-Брентано (на отражение) в угловом диапазоне  $2\theta=25^{\circ}-85^{\circ}$ , тип сканирования – непрерывный, скорость сканирования – 0,36 град /мин с шагом 0,013°. Обработка рентгенодифракционных данных проводилась по методу Ритвелда с использованием программы Fullprof. Для определения дифракционных отражений от образцов магния использовалась база данных ICDD: Международный центр дифракционных данных (база данных PDF2).

Обработка рентгеновской дифракции. Изображение чистого образца Mg, полученное на дифрактометре Empyrean, представлено на рис.1. Анализ рентгенограммы образца проводился через базу данных PDF-2 с использованием программы High Score Plus. Результаты анализа показали, что чистый образец Mg имеет гексагональную структуру (пространственная группа P6<sub>3</sub>/mmc).

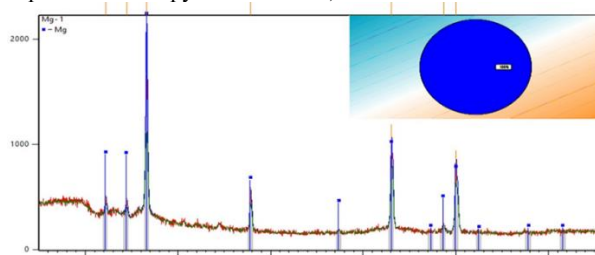


**Рис. 1.** Результат анализа базы данных PDF-2 рентгеновского изображения образца чистого магния.

Обработка данных рентгеновской дифракции проводилась с помощью программы Fullprof методом Ритвелда. Результаты обработки показали (рис. 2), что образцы Mg имеют гексагональную структуру (пространственная группа P6<sub>3</sub>/mmc).

Параметры элементарной ячейки:  $a = 3,2056\text{Å}$ ,  $b = 3,2056\text{Å}$ ,  $c = 5,2053\text{Å}$ ,  $\alpha = 90^{\circ}$ ,  $\beta = 90^{\circ}$  и  $\gamma = 120^{\circ}$ .

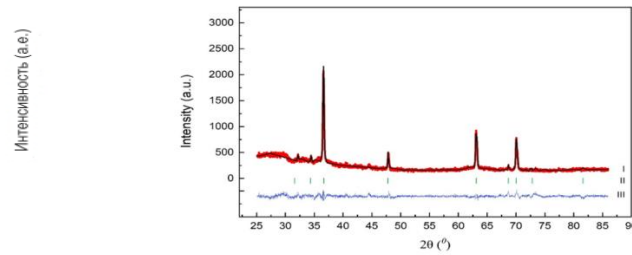


**Рис. 2.** Рентгеновская дифрактограмма Mg с гексагональной фазой (пр. гр.  $P6_3/mmc$ ): I - сравнение наблюдаемого образца с подобранным, II - пики Брэгга, III - разность между наблюдаемым образцом и подобранным.

**Таблица 1.** Координаты атомов образца Mg в гексагональной фазе (пр. гр.  $P6_3/mmc$ )

№	Атомы	Атомные координаты			Термический фактор
		x/a	y/b	z/c	
1	Mg	0.3333	0.6667	0.1300	1.9

(Статистические показатели -  $\chi^2=2,21$ ;  $R_B=2,8$ )

В некоторых образцах часть атомов Mg была заменена атомами Zn. Рентгеноструктурный анализ этих образцов Mg-1Zn, обработанных через базу данных PDF-2, показал, что образец состоит из гексагональной фазы (пространственная группа  $P6_3/mmc$ ). Результаты обработки методом Ритвелда с использованием программы Fullprof показали (рис. 3), что образцы Mg-1Zn имеют гексагональную структуру (пространственная группа  $P6_3/mmc$ ).

Параметры элементарной ячейки образца Mg-1Zn:  $a=3,2094\text{Å}$ ,  $b=3,2079\text{Å}$ ,  $c=5,2126\text{Å}$ ,  $\alpha=90^\circ$ ,  $\beta=90^\circ$  и  $\gamma=120^\circ$ .

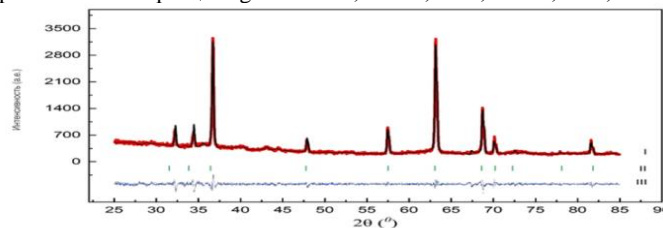


**Рисунок 3.** Рентгеновская дифракционная картина Mg-1Zn с гексагональной фазой (пр. гр.  $P6_3/mmc$ ).

I - сравнение наблюдаемого образца с сопоставленным, II - пики Брэгга, III - разность между наблюдаемым образцом и сопоставленным.

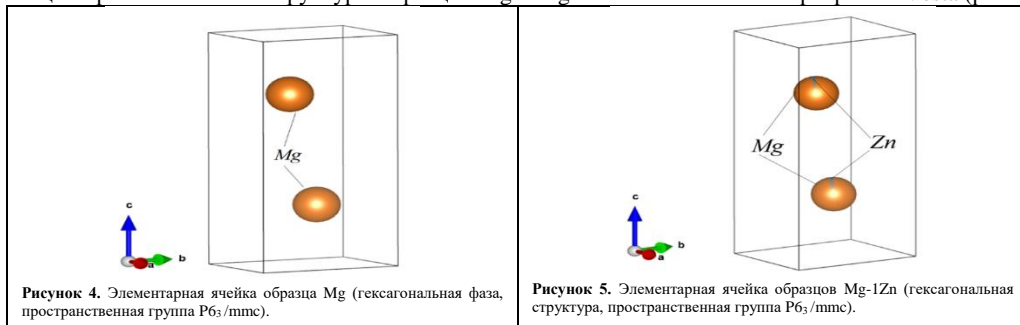
**Таблица 2.** Координаты атомов образца Mg-1Zn в гексагональной фазе (пр. гр.  $P6_3/mmc$ )

№	Атомы	Атомные координаты			Термический фактор
		x/a	y/b	z/c	
1	Mg	0.3333	0.6667	0.2500	1.14
2	Zn	0.3333	0.6667	0.2500	1.14

(Статистический показатель -  $\chi^2=2,2$ ;  $R_B=2,4$ )

Результаты рентгеноструктурного анализа показали, что координаты атомов Mg вдоль оси Z изменились от  $z=0,1300$  до  $z=0,2500$  после замены части атомов Mg на атомы Zn. Это может быть связано с разницей радиуса атомов Mg и радиуса атомов Zn.

Для визуализации кристаллической структуры образцов Mg и Mg-1Zn использовалась программа Vesta (рис. 4 и 5).



Интенсивности дифракционных пиков указывают на то, что эти образцы имеют высокую степень кристаллической регулярности или высокую степень кристаллической ориентации в пространстве. Чем выше значение интенсивности, тем сильнее дифракционные плоскости кристаллической решетки взаимодействуют с рентгеновским излучением при заданном угле дифракции. Значения  $\chi^2$  и  $R_B$  указывают на то, что модель точно представляет экспериментальные данные с небольшими отклонениями. Это указывает на то, что рассчитанная структура, основанная на предоставленных атомных координатах и тепловых факторах, является хорошим представлением фактической структуры изучаемого нами материала.

**Результаты и выводы.** Приведенные атомные координаты и тепловой фактор, а также показатели статистического согласия подтверждают интерпретацию рентгенодифракционных картин. Хорошее соответствие, указанное значениями  $\chi^2$  и  $R_B$ , предполагает, что экспериментальные данные рентгенодифракционного анализа (красная кривая) близко соответствуют расчетным данным, основанным на данной модели кристаллической структуры.

Эти пики соответствуют гексагональной плотноупакованной (ГПУ) структуре магния, что подтверждается стандартными эталонными материалами.

Сплав магния и цинка (Mg-1Zn):

- Эти пики также соответствуют структуре НСР с небольшими сдвигами в положениях пиков из-за присутствия цинка.

Небольшое уменьшение параметров решетки по сравнению с чистым магнием объясняется заменой атомов магния на более мелкие атомы цинка.

Экспериментально определенные параметры решетки близко соответствуют теоретическим значениям для магния и его сплавов, что указывает на высокую точность измерений рентгеновской дифракции. Небольшие отклонения, наблюдаемые в сплаве Mg-1Zn, находятся в пределах ожидаемых значений из-за эффектов легирования. Рентгеновская дифракция подтверждает кристаллическую структуру и параметры решетки чистого магния и сплава Mg-1Zn. Цинк в сплаве приводит к незначительным изменениям параметров решетки, что может повлиять на механические свойства материала и коррозионное поведение. Результаты этого исследования имеют важные последствия для промышленного и медицинского использования магния и его сплавов. Улучшенные свойства сплава Mg-1Zn делают его перспективным кандидатом для биомедицинских устройств, таких как биоразлагаемые мочеточниковые стенты и ортопедические имплантаты.

Таким образом, методы рентгеновской дифракции и электронной микроскопии являются незаменимыми методами исследования внутренней структуры материалов, предлагая дополнительные возможности для детального структурного анализа. Открытие гексагональной структуры в образцах Mg означает, что атомы магния расположены в плотноупакованной гексагональной решетке. Эти результаты способствуют разработке биоразлагаемых материалов на основе магния для биомедицинских и промышленных применений. В заключение следует сказать, что магний и его сплавы являются перспективной альтернативой традиционным неразлагаемым металлическим материалам, поскольку они способны безопасно разлагаться в организме и играть положительную роль в регуляции физиологических процессов в организме в целом.

#### ЛИТЕРАТУРА

1. Agnew, S. R., C. N. Tomé, D. W. Brown, T. M. Holden, and S. C. Vogel. "Study of slip mechanisms in a magnesium alloy by neutron diffraction and modeling." *Scripta materialia* 48, no. 8 (2003): 1003-1008.
2. Botero, M., Yuan, S., Akroyd, J., Martin, J., Dreyer, J., Yang, W., ... & Kraft, M. (2019). Internal structure of soot particles in a diffusion flame. *Carbon*, 141, 635-642. <https://doi.org/10.1016/j.carbon.2018.09.063>
3. Brar, Harpreet S., Joey Wong, and Michele V. Manuel. "Investigation of the mechanical and degradation properties of Mg–Sr and Mg–Zn–Sr alloys for use as potential biodegradable implant materials." *Journal of the mechanical behavior of biomedical materials* 7 (2012): 87-95.
4. Giyasov, Shuxrat. "Innovatsii v meditsinskoy texnologii: perspektivi sozdaniya metallicheskih biorazlagaemih mochetochnikovih stentov." (2023). *Biologiya va tibbiyot muammolari*.
5. Gu, X. N., N. Li, W. R. Zhou, Y. F. Zheng, X. Zhao, Q. Z. Cai, and Liquan Ruan. "Corrosion resistance and surface biocompatibility of a microarc oxidation coating on a Mg–Ca alloy." *Acta Biomaterialia* 7, no. 4 (2011): 1880-1889.
6. Gu, Xuenan N., Nan Li, Yufeng F. Zheng, and Liquan Ruan. "In vitro degradation performance and biological response of a Mg–Zn–Zr alloy." *Materials Science and Engineering: B* 176, no. 20 (2011): 1778-1784.
7. Hedayati R., Ahmadi S.M., Lietaert K., Tümer N., Li Y., Amin Yavari S., Zadpoor A.A. Fatigue and quasi-static mechanical behavior of bio-degradable porous biomaterials based on magnesium alloys. *J Biomed Mater Res A* 2018; 106(7): 1798–1811, <https://doi.org/10.1002/jbm.a.36380>.



UDK: 537.621.5

**Azamatbek ARSLANOV,**

*PhD student Department of Physics, National University of Uzbekistan*

*E-mail: azamat20296@gmail.com*

**Rafael NUSRETOV,**

*Uzbek-Japan Center of Youth, Tashkent State Technical University, Uzbekistan*

**Shavkat YULDASHEV,**

*Center of Nanotechnologies Developments, National University of Uzbekistan*

**Andrey NEBESNIY,**

*Center of Nanotechnologies Developments, National University of Uzbekistan*

*Reviewer: PhD Tursunqulov O.M., Center of advanced technology, Uzbekistan*

### EFFECT OF THE SULFUR DOPING ON STRUCTURAL, MAGNETIC AND OPTICAL PROPERTIES OF ZnMnO THIN FILMS

Annotation

Magnetic semiconductors (MSs) are new functional materials created by doping magnetic ions in non-magnetic semiconductors. The exchange effect between magnetic ions and free charge carriers in semiconductors gives DMSs novel magneto-electric and magneto-optical properties. The widely known ferromagnetic semiconductor GaMnAs is suffered from low Curie temperature, below 200 K. Therefore, the other semiconductor materials are needed in order to get the ferromagnetic semiconductors with the Curie temperature at the room temperature. In this work, structural, optical and magnetic properties of  $Zn_{1-x}Mn_xO_{1-y}S_y$ , additionally doped with nitrogen, thin films grown by ultrasonic spray pyrolysis system are reported. The results of optical transmission measurements demonstrate a successful incorporation of the sulfur ions into ZnMnO crystal lattice. The SQUID measurements demonstrate the ferromagnetism in the sulfur doped ZnMnO thin films with the Curie temperature close to room temperature.

**Key words:** magnetic semiconductors (MS), ZnMnO thin film, Sulfur doping, Curie temperature, magnetic ion, exchange effect

### ЭФФЕКТ ЛЕГИРОВАНИЯ СЕРОЙ НА СТРУКТУРНЫЕ, МАГНИТНЫЕ И ОПТИЧЕСКИЕ СВОЙСТВА ТОНКИХ ПЛЕНОК ZnMnO

Аннотация

Магнитные полупроводники (МП) - это новые функциональные материалы, созданные путем легирования магнитных ионов в немагнитные полупроводники. Эффект обмена между магнитными ионами и свободными носителями заряда в полупроводниках придает МП новые магнитоэлектрические и магнитооптические свойства. Широко известный ферромагнитный полупроводник GaMnAs страдает от низкой температуры Кюри, ниже 200 К. Следовательно, для получения ферромагнитных материалов необходимы другие полупроводниковые материалы. В данной работе описаны структурные, оптические и магнитные свойства  $Zn_{1-x}Mn_xO_{1-y}S_y$ , дополнительно легированного азотом, тонких пленок, выращенных методом ультразвукового распылительного пиролиза. Результаты оптических измерений пропускания демонстрируют успешное включение ионов серы в кристаллическую решетку ZnMnO. Измерения SQUID демонстрируют ферромагнетизм в тонких пленках ZnMnO, легированных серой, при температуре Кюри, близкой к комнатной.

**Ключевые слова:** Магнитные полупроводники (МП), тонких пленках ZnMnO, Легирование серой, температуре Кюри, магнитных ион, эффект обмен.

### OLTINGUGURT BILAN LEGIRLASHNING ZnMnO YUPQA QATLAMLI PLONKALARI STRUKTURAVIY, MAGNIT VA OPTIK XUSUSIYATLARIGA TA'SIRI

Anotatsiya

Magnit yarimo'tkazgichlar (MY) yangi xususiyatlarga ega bo'lgan material bo'lib. Ular yarimo'tkazgichlarni magnit ionlar bilan legirlash orqali hosil qilinadi. Bunday almashtirish erkin zaryad tashuvchilar bilan magnit ionlar o'rtasida ta'siri vujudga keltiradi. Shu sabab yarimo'tkazgichlardagi elektr va optik xususiyatlariga magnit xossasi ham qo'shiladi. Misol uchun GaMnAs magnit yarimo'tkazgich bu sohadagi juda ko'p o'rganilgan material hisoblanadi. Ammo, qilingan ko'p izlanishlarga qaramay uning Kuriy temperaturasi 200 K dan oshmagan. Biz ushbu ishda ultra tovushli spray periolis usuli orqali o'stirilgan azot bilan legirlangan  $Zn_{1-x}Mn_xO_{1-y}S_y$  yupqa qatlamining strukturaviy, magnit va optik xossalarini o'rgandik. Optik o'lchashlar natijalari oltingugurtning ZnMnO ning kristaliga yaxshi o'rmasganini ko'rsatdi. SQUID magnetometrda magnitlanishning temperaturaga bog'lashidan aniqlangan Kuriy temperaturasi xona temperaturasiga yaqinlashgani ko'rsatildi.

**Kalit so'zlar:** magnit yarimo'tkazgichlar (MY), ZnMnO yupqa qatlami, oltingugurt kiritish, Kuriy temperaturasi, magnit ion, o'zaro ta'sir.

**Introduction.** The field of diluted magnetic semiconductors (DMS) holds great promise for various technological applications, particularly in spintronics and magnetic memory devices. However, achieving reliable and reproducible ferromagnetic behavior at or above room temperature remains a significant challenge. Transition metal doping of semiconductor materials, such as zinc oxide (ZnO), is a common approach to create DMS [1]. ZnO-based DMS is particularly attractive due to



its potential for high Curie temperature (TC) exceeding room temperature. However, the reported magnetic properties of ZnO doped with transition metals have been contradictory in various studies [2]. Some research groups have observed high-temperature ferromagnetism in ZnO doped with elements like manganese (Mn) and cobalt (Co), both in bulk and thin film forms [3], while others have reported paramagnetic or spin-glass behaviors [4,5]. Some studies even found the absence of ferromagnetic ordering in single-phase ZnO doped with Mn or Co at low temperatures [6].

**Literature review.** These discrepancies can be attributed to differences in growth methods and conditions for the magnetic semiconductor alloys. The growth process plays a crucial role in determining the structural and magnetic properties of the resulting materials. Variations in doping concentration, growth temperature, and post-growth treatments can significantly influence the observed magnetic behaviors. To address these challenges and enhance the magnetic properties of ZnO-based DMS, researchers have explored various strategies, including bandgap engineering. By doping and alloying ZnO with other materials such as magnesium oxide (MgO) and zinc sulfide (ZnS), it is possible to manipulate the optical, electrical, and magnetic properties of the semiconductor [7]. ZnO-ZnS alloy, for example, exhibits strong valence band (VB) offset bowing as a function of sulfur content, which can be utilized to improve p-type doping and achieve shallower acceptor states [8]. Transition metal doping of ZnO-ZnS alloy, such as with Mn, holds promise for enhancing the ferromagnetic properties and raising the Curie temperature of the resulting DMS.

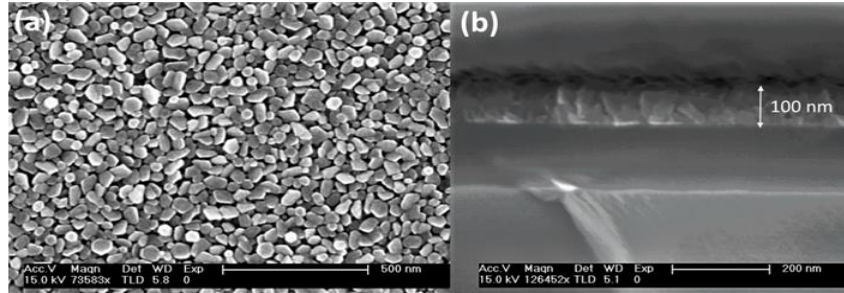
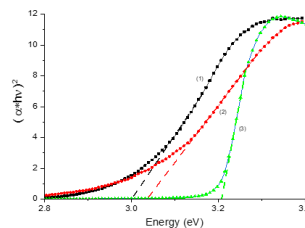


Figure 1 shows the scanning electron microscope (SEM) images of the nitrogen doped  $Zn_{0.95}Mn_{0.05}O_{0.85}S_{0.15}$  thin film grown by ultrasonic spray pyrolysis (USP) method.

Fig.1. SEM images of the nitrogen doped  $Zn_{0.95}Mn_{0.05}O_{0.85}S_{0.15}$  thin film: (a) top view and (b) cross-section view, respectively.

**Research Methodology.**  $Zn_{1-x}Mn_xO_{1-y}S_yN$  thin films were deposited using ultra sonic spray pyrolysis on silicon substrates. The substrates were cleaned for 10 min in hydrofluoric acid, acetone, ethanol for 10 min. each, respectively, and D.I. water to remove impurities and organic solvents. Zinc acetate, ammonium acetate and thiourea were used as the zinc, nitrogen and sulfur sources, respectively. Zinc acetate and ammonium acetate content were added same amount with different sulfur concentration. While aqueous solution of manganese acetate was kept 5% for all samples. After 20 minutes mixing the solutions, we employed an ultrasonic nebulizer with 2.5 MHz frequency for atomization of the solution. Samples were synthesized under atmospheric pressure and substrate temperature was set 4000 C. all samples annealed at 5000 C for 15 minutes in nitrogen ambience. From Fig.1 the thickness of this film was about 100 nm.

**Analysis and results.** Introduced nitrogen into ZnO host gives sufficiently deep acceptor levels [9]. Increasing sulfur content decreases the band gap of ZnO and starts lifting up the valent band edge. The Tauc-Plot results for pure and sulfur doped ZnO was presented at figure 2. Electronegativity of sulfur is sufficiently lower as compared with replaced oxygen. Thus, the energy of valence band edge is increasing, while replacing more oxygen with sulfur. Undoped ZnO shows 3.21 eV band gap energy, but it decreases to almost 200 meV when sulfur content is 15%. The Hall measurements also showed  $5.1 \times 10^{16} \text{ cm}^{-3}$  and



$4.8 \times 10^{17} \text{ cm}^{-3}$  the hole concentrations for  $Zn_{0.95}Mn_{0.05}O_{0.9}S_{0.1}$  and  $Zn_{0.95}Mn_{0.05}O_{0.85}S_{0.15}$ , respectively.

Fig. 2. Tauc plot for undoped and sulfur doped Zinc oxide samples. (1), (2) and (3) are for pure ZnO, 10 % and 15% sulfur added thin films, respectively.

In order to study the magnetic properties of diluted magnetic semiconductors based on  $Zn_{1-x}Mn_xO_{1-y}S_y$  thin films, the magnetization dependencies on the magnetic field and temperature were measured by using a SQUID (superconducting quantum interference device) magnetometer. Fig. 3 shows magnetization dependencies on temperature for 10 % and 15 % sulfur doped thin films. Fig. 3a represents magnetization of  $Zn_{0.95}Mn_{0.05}O_{0.9}S_{0.1}$  going to zero near 250 K, while Fig. 3b shows magnetization of  $Zn_{0.95}Mn_{0.05}O_{0.85}S_{0.15}$  disappears below 300 K.

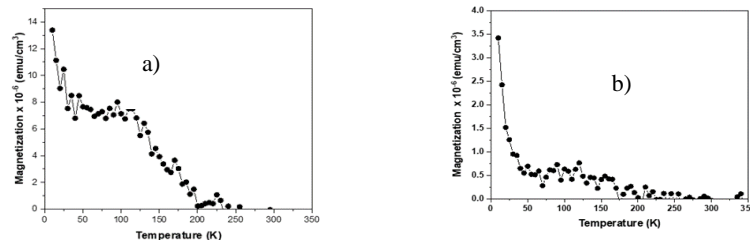


Fig. 3. Dependence of magnetization on temperature for : a)  $Zn_{0.95}Mn_{0.05}O_{0.9}S_{0.1}$ ; b)  $Zn_{0.95}Mn_{0.05}O_{0.85}S_{0.15}$

**Conclusion.** The sulfur doped ZnMnON thin film grown by ultrasonic spray pyrolysis method was studied. Effect of sulfur doping on the band gap of ZnO was measured. And results show that replacing oxygen atoms by sulfur atoms has a significant impact on valence band edge. So, it causes a huge decrease on activation energy of deep acceptor levels. Plus, morphology of the thin films were studied by using scanning electron microscope. Overall, increasing sulfur concentration in the nitrogen doped zinc oxide brings up to increase hole concentration at room temperature. As a result, the Curie temperature of  $Zn_{1-x}Mn_xO_{1-y}S_yN$  thin film could be increased.

#### REFERENCES

1. T. Dietl and H. Ohno, Dilute ferromagnetic semiconductors: Physics and spintronic structures, *Rev. Mod. Phys.* 86 (2014) 187-251.
2. H. T. Lin, T. S. Chin, J. C. Shih, S. H. Lin, T. M. Hong, R. T. Huang, F. R. Chen, and J. J. Enhancement of ferromagnetic properties in  $Zn_{1-x}Co_xO$  by additional Cu doping, *Appl. Phys. Lett.* 85 (2004) 621-623.
3. P. Sharma, A. Gupta, K. V. Rao, F. J. Owens, R. Sharma, R. Ahuja, J. M. Osorio Guillen, B. Johansson, and G. A. Gehring, Ferromagnetism above room temperature in bulk and transparent thin films of Mn-doped ZnO, *Nature Mater.* 2 (2003) 673.
4. T. Fukumura, Z. Jin, M. Kawasaki, T. Shono, T. Hasegawa, S. Koshihara, and H. Koinuma, Magnetic properties of Mn-doped ZnO, *Appl. Phys. Lett.* 78 (2001) 958-960.
5. A. Tiwari, C. Jin, A. Kivt, D. Kumar, J. F. Muth, and J. Narayan, Structural, optical and magnetic properties of diluted magnetic semiconducting  $Zn_{1-x}Mn_xO$  films, *Solid State Commun.* 121 (2002) 371-374.
6. S. Kolesnik, B. Dabrowski and J. Mais, Structural and magnetic properties of transition metal substituted ZnO, *J. Appl. Phys.* 95 (2004) 2582.10
7. H. C. Hsu, C. Y. Wu, H. M. Cheng and W. F. Hsieh, Band gap engineering and stimulated emission of ZnMgO nanowires, *Appl. Phys. Lett.* 89 (2006) 013101.
8. C. Persson, C. Platzer-Björkman, J. Malmström, T. Törndahl, M. Edoff, Strong valenceband offset bowing of  $ZnO_{1-x}S_x$  enhances p-type nitrogen doping of ZnO-like alloys, *Phys. Rev.Lett.* 97 (2006) 146403.
9. M. Joseph, H. Tabata and T. Kawai: *Appl. Phys. Lett.* 74 (1999) 2534.



УДК: 534.2: 58.4: 548.9.

**Фарход АХМЕДЖАНОВ,**

*Институт ионно-плазменных и лазерных технологий, заведующий лабораторией д.ф.-м.н., доцент.*

**Нодир МАХАРОВ,**

*Базовый докторант Институт ионно-плазменных и лазерных технологий*

**Жахонгир КУРБАНОВ,**

*старший научный сотрудник Институт ионно-плазменных и лазерных технологий*

*Рецензент: Институт химии и физики полимеров (PhD) старший научный сотрудник Хакбердиев Э.О.*

### ACOUSTIC PROPERTIES OF KBr, NaBr and RbBr CRYSTALS

Annotation

The anisotropy of the attenuation coefficient of acoustic waves, effective elastic constants and effective anharmonicity constants in KBr, NaBr and RbBr crystals is investigated. It is shown that in these crystals, practically the same dependence of the attenuation coefficient of longitudinal acoustic waves on the direction of propagation in the (110) plane is observed. It is established that in the studied crystals, the effective anharmonicity constants determining the magnitude and anisotropy of attenuation of longitudinal and transverse acoustic waves along the [100] direction change linearly with a change in the radius of the K, Na and Rb cations.

**Key words:** KBr, NaBr and RbBr crystals, velocity and attenuation of acoustic waves, effective elastic constants, effective anharmonicity constants.

### АКУСТИЧЕСКИЕ СВОЙСТВА КРИСТАЛЛОВ KBr, NaBr и RbBr

Аннотация

Исследована анизотропия коэффициента затухания акустических волн, эффективных упругих констант и эффективных констант ангармонизма в кристаллах KBr, NaBr и RbBr. Показано, что в этих кристаллах наблюдается практически одинаковая зависимость коэффициента затухания продольных акустических волн от направления распространения в плоскости (110). Установлено, что в исследованных кристаллах эффективные константы ангармонизма, определяющие величину и анизотропию затухания продольных и поперечных акустических волн вдоль направления [100] изменяются линейно при изменении радиуса катионов K, Na и Rb в этих кристаллах.

**Ключевые слова:** кристаллы KBr, NaBr и RbBr, скорость и затухание акустических волн, эффективные упругие постоянные, эффективные константы ангармонизма.

### KBr, NaBr VA RbBr KRISTALLARINING AKUSTIK XOSSALARI

Annotsiya

KBr, NaBr va RbBr kristallaridagi akustik to'liqlarning so'nish anizotropiyasi, samarali elastik konstantalari va samarali angarnoniklik konstantalari o'rganildi. Ushbu kristallarda bo'ylama akustik to'liqlarning so'nish koeffitsientining (110) tekislikdagi tarqalish yo'nalishiga deyarli bir xil bog'liqligi ko'rsatilgan. O'rganilayotgan kristallarda bo'ylama va ko'ndalang akustik to'liqlarning [100] yo'nalishi bo'yicha so'nishining kattaligi va anizotropiyasini belgilovchi samarali angarnoniklik konstantalari K, Na va Rb ionlari radiusi o'zgarishi bilan chiziqli ravishda o'zgaradi.

**Kalit so'zlar:** KBr, NaBr va RbBr kristallar, akustik to'liqlarning tezligi va so'nishi, effektiv elastik konstantalar, samarali angarnonizm konstantalar.

**Введение.** Щелочно-галогидные кристаллы относятся к кубической точечной группе симметрии  $3m$  и изотропны по многим физическим свойствам. Однако по упругим свойствам эти кристаллы являются анизотропными и их применение в акустических и акустооптических устройствах требует знания ориентационных зависимостей таких важных характеристик как скорость распространения и коэффициент затухания акустических волн [1-3]. В качестве рабочей среды в этих устройствах часто применяются такие щелочно-галогидные кристаллы, как бромиды калия, натрия и рубидия (KBr, NaBr и RbBr), обладающие высокими значениями упругих, а также фотоупругих констант, как в видимой, так и в инфракрасной области электромагнитных волн [1, 4].

Скорость распространения и коэффициент затухания в них, достаточно подробно исследованы в диапазоне низких ультразвуковых частот, в котором затухание зависит от частоты по квадратичному закону, согласно механизму Ахиезера [5-7]. В то же время на высоких частотах такие исследования практически отсутствуют так как основным фактором, ограничивающим их применение, является большая величина коэффициента затухания. В связи с этим в настоящей работе ультразвуковыми методами исследовано скорость распространения, эффективные упругие константы и коэффициент затухания продольных и поперечных акустических волн в гомологическом ряду щелочно-галогидных кристаллов.

#### II. Образцы и экспериментальные методы

Исследованные образцы KBr, NaBr и RbBr представляли собой параллелепипеды, длинная сторона которых была ориентирована с точностью до 1 градуса вдоль главных кубических направлений [100] и [110] и [111]. Ориентация образцов осуществлялась с помощью плоскостей спайности и последующей шлифовки и полировки кристаллических



образцов, с использованием стандартных ориентирующих призм. Исследования проводились при комнатной температуре в диапазоне частот 30 – 400 МГц. Продольные и поперечные акустические волны в образцах возбуждались пьезоэлектрическими преобразователями из кварца, соответственно, X или Y-срезы, толщиной 40-100 микрон.

Измерения скорости и коэффициента затухания акустических волн на относительно низких частотах проводились модифицированным методом «импульсной интерференции» Вильямса–Лэмба [1, 8], в котором сравниваются фазы акустических волн, прошедших различный путь в исследуемом образце. Одним из основных модулей низкочастотной установки является амплитудный селектор, который открывается в определенный промежуток времени, являющийся окном пропускания.

Длительностью такого окна пропускания можно управлять за счет длительности синхроимпульса, открывающего этот селектор. Такая селекция определенного импульса в серии эхо импульсов позволяет измерять его амплитуду с помощью импульсного вольтметра. По измеренным значениям амплитуд соседних импульсов  $A_1$  и  $A_2$  определялся коэффициент затухания акустических волн  $\alpha$  [3, 8]:

$$\alpha = \frac{20 \lg\left(\frac{A_1}{A_2}\right)}{2L} \quad (1)$$

где  $L$  – длина образца. Точность определения коэффициента затухания составляла ~5%, за счет многократного измерения амплитуд импульсов и последующего усреднения.

Наблюдаемые при изменении частоты генератора непрерывных колебаний, интерференционные нули или максимумы амплитуды импульсов, позволяют определить значение скорости акустической волны в образце  $V$  из соотношения [3, 8]:

$$V=2L \cdot \Delta\nu, \quad (2)$$

где  $\Delta\nu$  – разность двух соседних частот высокочастотного генератора, соответствующих противофазной интерференции. Указанные частоты измерялись с помощью цифрового частотомера, обеспечивающего высокую точность определения разности частот (до  $\pm 10$  Гц). При этом точность определения скорости акустической волны ограничивалась точностью измерения длины образца и составляла ~0,01%.

### III. Результаты эксперимента и их обсуждение

Результаты определения коэффициента затухания продольных и поперечных акустических волн вдоль кристаллографических направлений [100] и [110] и рассчитанные значения эффективных действительных и мнимых упругих констант для изученных кристаллов приведены в таблице 1. Значения скорости акустических волн хорошо совпадали с литературными данными и потому не приведены в таблице 1.

**Таблица 1.** Коэффициент затухания акустических волн ( $\nu=1$  ГГц), и эффективные действительные и мнимые упругие константы в кристаллах KBr, NaBr и RbBr

$\varphi$	$\eta$	$c'_{\text{эф}}$ , $10^{10}$ N·m $^{-2}$			$\alpha$ , dB·μs $^{-1}$			$c''_{\text{эф}}$ , $10^7$ N·m $^{-2}$		
		KBr	NaBr	RbBr	KBr	NaBr	RbBr	KBr	NaBr	RbBr
[100]	[100]	3.52	3.96	3.15	38	25	58	4.82	3.7	6.70
	[001]	0.51	0.99	0.38	6.0	3.1	10	0.11	0.11	0.14
[110]	[110]	2.55	3.49	0.48	28	17	41	2.81	2.01	3.29
	[110]	1.48	1.47	2.19	40	34	72	2.12	1.79	3.55
	[001]	0.51	0.99	1.34	6.0	3.1	10	0.11	0.11	0.14
[111]	[111]	2.22	3.33	0.38	26.4	11.9	31	2.14	1.45	2.15
	[110]	1.15	1.31	1.88	34.8	25.6	64.4	1.45	1.23	2.41

Три независимые компоненты действительной и мнимой части тензора упругости для всех исследованных кристаллов определялись из значений скорости и коэффициента затухания продольных и поперечных волн вдоль направлений [100] и [110]. Полученные значения действительных и мнимых компонент тензора упругости:  $c'_{11}$ ,  $c'_{12}$ ,  $c'_{44}$ ,  $c''_{11}$ ,  $c''_{12}$  и  $c''_{44}$  позволяют рассчитать затухание акустических волн по механизму Ахизера вдоль любого направления распространения акустических волн в кристаллах, если выполняется условие  $\omega\tau \ll 1$  ( $\omega$  – круговая частота акустических волн,  $\tau$  – время релаксации тепловых фононов), с помощью выражения [7, 9]:

$$\alpha = \frac{1}{2} \omega \frac{c''_{\text{эф}\varphi\varphi}}{c'_{\text{эф}\varphi\varphi}}. \quad (3)$$

Здесь действительные и мнимые эффективные упругие константы определяются, соответственно, через действительные  $c'_{ijkl}$  и мнимые  $c''_{ijkl}$  компоненты комплексного тензора упругости:

$$c'_{\text{эф}\varphi\varphi} = c'_{ijkl} \kappa_j \kappa_l \eta_i \eta_k, \quad (4)$$

$$c''_{\text{эф}\varphi\varphi} = c''_{ijkl} \kappa_j \kappa_l \eta_i \eta_k, \quad (5)$$

где  $\kappa_j$  и  $\eta_i$  – компоненты единичной волновой нормали  $\mathbf{\kappa}$  и вектора поляризации  $\boldsymbol{\eta}$ . В общем случае, направления векторов  $\mathbf{\kappa}$  и  $\boldsymbol{\eta}$  не совпадают.

В частности, для квазипродольных волн в плоскости (110) при изменении направления волнового вектора относительно оси [110] на некоторый угол ( $\varphi$ ), уравнения Грина–Кристоффеля позволяют определить угол отклонения вектора поляризации ( $\psi$ ) от этой же оси [3]:

$$\psi = \arctg \frac{\sqrt{2}}{2} \cdot \left( \frac{\Gamma'_{12} \Gamma'_{13} - \Gamma'_{23} (\Gamma'_{11} - \rho V^2)}{\Gamma'_{23} \Gamma'_{13} - \Gamma'_{12} (\Gamma'_{33} - \rho V^2)} \right) \quad (6)$$

Здесь  $\Gamma'_{ik}$  – действительные компоненты тензора Грина-Кристоффеля [1, 2]:

$$\Gamma'_{ik} = c'_{ijkl} \mathbf{K}_j \mathbf{K}_l, \quad (7)$$

Результаты расчета показали, что в данной плоскости максимальное отклонение вектора поляризации от волнового вектора в исследованных кристаллах составляет не более 10 угловых градусов. Измерения показали также, что в исследованном диапазоне частот коэффициент затухания как продольных, так и поперечных акустических волн зависит от частоты по квадратичному закону. Это указывает на то, что основным механизмом затухания акустических волн в кристаллах является фоновый механизм, впервые рассмотренный Ахиезером [5], согласно которому выражение для затухания записывается в следующем виде [6]:

$$\alpha = \gamma^2 \frac{\beta \cdot 8.68 \cdot \lambda T \omega^2}{2 \rho V^2 V_D^2} \quad (8)$$

где  $\beta$  – численный множитель,  $T$  – температура,  $\lambda$  – коэффициент теплопроводности,  $\gamma$  – эффективная константа Грюнайзена, зависящая от направления волнового вектора и типа акустической волны [10],  $V_D$  – средняя Дебаевская скорость, которая определяется через скорости продольных и поперечных волн вдоль выбранного направления [1, 2]:

$$V_D = \left[ \frac{1}{3} \left( \frac{2}{V_S^3} + \frac{1}{V_L^3} \right) \right]^{-1/3} \quad (9)$$

Результаты расчета зависимости коэффициента затухания продольных акустических волн с частотой 1 ГГц, от направления волнового вектора в плоскости (110) в кристаллах KBr, NaBr и RbBr с помощью выражений (3), (4) и (5) приведены на рисунке 1.

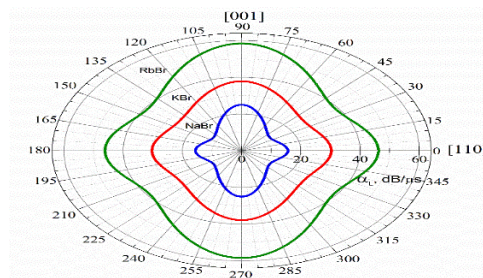


Рис. 1. Анизотропия коэффициента затухания продольных акустических волн с частотой 1 ГГц, распространяющихся в плоскости (110) в кристаллах KBr, NaBr и RbBr

Из рисунка видно, что в исследованных кристаллах анизотропия затухания продольных волн качественно совпадает, но наблюдается количественное расхождение, которое, согласно выражению (8), может быть обусловлено разницей в значениях эффективной константы Грюнайзена и ее зависимостью от направления распространения акустической волны. Используя выражения (3) и (8), можно выразить эффективную константу Грюнайзена через соотношение:

$$\gamma_{эфф} = \left( \frac{c''_{эфф} \cdot V_D^2}{2 \cdot \lambda \cdot T \cdot \omega} \right)^{1/2} \quad (10)$$

Соотношение (10) позволяет определить эффективные константы Грюнайзена для продольных и поперечных акустических волн.

Результаты расчета зависимости коэффициента затухания продольных акустических волн, распространяющихся вдоль направления [100], и эффективной константы Грюнайзена от величины радиуса катионов K, Na и Rb представлены на рисунке 2.

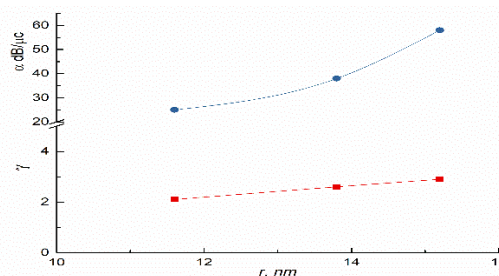


Рис. 2. Зависимость коэффициента затухания  $\alpha$  и константы ангармонизма  $\gamma$  от радиуса положительных ионов в кристаллах KBr, NaBr и RbBr

Из рисунка 2 видно, что в кристаллах KBr, NaBr и RbBr наблюдается практически одинаковая зависимость коэффициента затухания и эффективной константы Грюнайзена от радиуса катионов K, Na и Rb в случае продольных акустических волн, распространяющихся вдоль направления [100]. Таким образом ангармонизм межionных сил взаимодействия, зависящий от расстояния между ионами в кристаллах с ионным типом связи, вносит основной вклад в анизотропию затухания акустических волн.

**Заключение.** Результаты исследования показали, что в кристаллах KBr, NaBr и RbBr эффективные константы ангармонизма, определяющие величину анизотропию затухания продольных и поперечных волн вдоль направления [100] изменяются линейно при изменении радиуса катионов K, Na и Rb в этих кристаллах.

В то же время затухание акустических волн при изменении ионного радиуса изменяется нелинейно с наличием минимума в зависимости коэффициента затухания акустических волн. Такое поведение можно объяснить влиянием времени релаксации тепловых фононов на величину коэффициента затухания в диэлектрических кристаллах [6, 7].

#### ЛИТЕРАТУРА

1. D. Royer, E. Dieulesaint. Elastic Waves in Solids II /Generation/Acousto-optic Interaction/Applications. (Verlag Berlin Heidelberg, Springer, 2000), p. 474.
2. R.E. Newnham. Properties of Materials /Anisotropy/Symmetry/Structure. (New York, Oxford University Press, 2005), p. 378.
3. Ф.Р. Ахмеджанов, Ж.О. Курбанов, Н.М. Махаров. Затухание акустических волн в кубических кристаллах фторида лития. Доклады АН РУз. Вып. 5. 2021, С. 11-15.
4. Акустические кристаллы. Справочник /Под ред. М. П. Шаскольской. – М. Наука, 1982, 632 с.
5. Akhiezer A. About Sound Absorption in Solids, J. of Experimental and Theoretical Physics (SU). - Moscow, 1938. - No 8, - P. 1318-1329.
6. R. Nava, M. P. Vecchi, J. Romero and B. Fernandez. Akhiezer damping and the thermal conductivity of pure and impure dielectrics. Phys. Rev. B. Vol. 14, No 2. 1975, P. 800-807.
7. Логачев Ю. А., Мойжес Б. Я. К теории поглощения звука по Ахиезеру. – ФТТ. - Санкт-Петербург, 1974, - Т. 16. - № 8, - С. 2219-2223.
8. F.R. Akhmedzhanov, J.O. Kurbanov, A.F. Boltabaev, Attenuation of acoustic waves in single-domain and polydomain LiTaO<sub>3</sub> crystals, Sensors & Transducers 246, No.7, 2020. P. 43-47.
9. Ахмеджанов Ф.Р, Леманов В.В, Насыров А.Н. Поверхности акустического затухания в кристаллах. Письма в ЖТФ, 1980. Т. 6, Вып. 10, С. 589-592.
10. Key Samuel. Gruneisen Tensor for Anisotropic Materials. Journal of Applied Physics, 1967. Vol. 38, No 7, P. 2923-2928.



UDK: 544.526.5

**Sherzod BEGIMQULOV,**

*O‘z RFA U.Arifov nomidagi Ion-plazma va lazer texnologiyalari instituti kichik ilmiy xodimi*

*E-mail: sherzodbegimkulov93@gmail.com*

**Anvarjon SHERNIYOZOV,**

*O‘z RFA U.Arifov nomidagi Ion-plazma va lazer texnologiyalari instituti katta ilmiy xodimi, PhD*

**Shermakhmat PAYZIYEV,**

*O‘z RFA U.Arifov nomidagi Ion-plazma va lazer texnologiyalari instituti professori, f.-m.f.d*

*F.-m.f.d., dotsent, A.Kasimov taqrizi asosida*

### LAZER DIODLARINING UZOQ MAYDONDAGI NURLANISH QONUNIYATLARINI RAQAMLI SIMULYATSIYASI

Аннотация

Ushbu ishda lazer diodlarining uzoq masofada nurlanishini simulyatsiya qilish uchun raqamli yondashuvi o‘rganildi. Yorug‘lik tarqalishini modellashtirish uchun foton yo‘lini kuzatish metodi va dioddan chiqqan fotonlarning burchak taqsimotini ifodalash uchun ikki o‘lchovli normal qo‘shma taqsimotidan foydalanildi. Ushbu usul lazerli diodlarning turli nurlanish xususiyatlarini modellashtirishda moslashuvchanlikni ta‘minlaydi.

**Kalit so‘zlar:** Diod, normal taqsimot, lazerli diod, nurlanish qonuniyati.

### ЧИСЛЕННОЕ МОДЕЛИРОВАНИЕ ИЗЛУЧЕНИЯ ЛАЗЕРНОГО ДИОДА В ДАЛЬНОЙ ЗОНЕ

Аннотация

В данной работе представлен численный подход к моделированию моделей излучения лазерных диодов в дальней зоне. Были использованы трассировка фотонов для моделирования распространения света и двумерное нормальное совместное распределение для представления углового распределения испускаемых фотонов. Этот метод обеспечивает адаптируемость в моделировании различных характеристик излучения лазерных диодов.

**Ключевые слова:** Диод, нормальное распределение, Лазерный диод, Диаграмма излучения.

### NUMERICAL SIMULATION OF LASER DIODE FAR-FIELD EMISSION PATTERNS

Annotation

This work studies a numerical approach for simulating the far-field emission patterns of laser diodes. We employ photon tracing to model the light propagation and utilize a bivariate normal joint distribution to represent the angular distribution of emitted photons from diodes. This method offers flexibility in simulating diverse laser diode emission characteristics.

**Key words:** Diode, normal distribution, Laser diode, Emission pattern.

**Introduction.** Laser diodes have transformed laser technology, replacing traditional lamp-pumped systems with more efficient diode-pumped architectures [1]. This paradigm shift has solidified diode pumping as the predominant method for high-power laser generation, especially in solid-state laser systems. Ongoing research actively explores innovative diode configurations, such as stacking and cascading, to push the boundaries of achievable laser power in both continuous-wave and pulsed regimes [1-2]. Given the absence of apparent fundamental limitations in diode-pumped solid-state lasers, this tendency of exploring different techniques for their development is anticipated to persist. Consequently, precise modeling of diode-pumped laser systems is important for optimizing performance and enabling further advancements. An initial step in this process involves modeling the emission pattern of the diode. In this work, we demonstrate a method for simulating the angular distribution of photons emitted from a laser diode using a bivariate normal joint distribution.

**Laser diode basics.** A laser diode is a modified semiconductor optical amplifier with optical feedback via cleaved facets, exploiting refractive index contrast for reflection. Sufficient gain and feedback lead to oscillation, creating a diode laser [3]. Laser diodes generate a narrow spectral output compared to conventional lamps, facilitating efficient excitation of lasing media's active energy levels. Their high wall-plug efficiency and ease of integration into laser cavities contribute to their widespread adoption. A laser diode with an active region of dimensions  $l$  (length) and  $w$  (width) emits light with far-field angular divergences  $\theta_{\perp} = \lambda_c / l$  (radians) in the plane perpendicular to the p-n junction and  $\theta_{\parallel} = \lambda_c / w$  (radians) in the plane parallel to the junction (Fig. 1). In these approximated expressions,  $\lambda_c$  is a central frequency of a diode spectrum. These divergence angles shape the far-field radiation pattern. Due to the limited size of the active region, laser diodes typically exhibit larger angular divergences compared to other laser types. For instance, a diode with  $l = 2 \mu\text{m}$ ,  $w = 10 \mu\text{m}$ , and  $\lambda_c = 808 \text{nm}$  emit photons with divergence angles of  $\theta_{\perp} \approx 4.63^\circ$  and  $\theta_{\parallel} \approx 23.15^\circ$ . Single-transverse-mode laser diodes, with even smaller widths ( $w$ ), possess even larger angular divergences. The precise spatial distribution of the far-field radiation within the resulting cone depends on the number of excited transverse modes and their corresponding optical powers. In this work, we consider single-transverse mode, however generalizing to higher modes are expected to be straightforward.

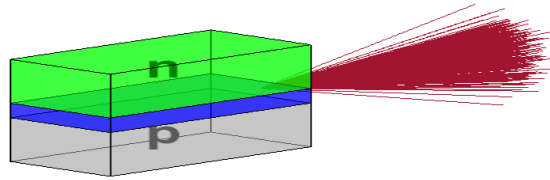


**Figure 1.** Schematic of a typical laser diode structure and its corresponding far-field emission pattern

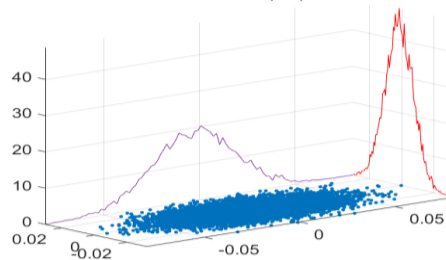
**Simulation of Laser Diode Far-Field Emission Patterns.** The far-field emission pattern of a laser diode exhibits two distinct angular divergences,  $\theta_{\perp}$  (x-axis) and  $\theta_{\parallel}$  (y-axis). To accurately simulate realistic emission characteristics in accumulated simulations, we are considering to employ a bivariate normal distribution for sampling photon directions:

$$f(x, y) = \frac{1}{2\pi\sigma_x\sigma_y\sqrt{1-\rho^2}} \exp\left[-\frac{1}{2(1-\rho^2)}\left[\left(\frac{x-\mu_x}{\sigma_x}\right)^2 - 2\rho\left(\frac{x-\mu_x}{\sigma_x}\right)\left(\frac{y-\mu_y}{\sigma_y}\right) + \left(\frac{y-\mu_y}{\sigma_y}\right)^2\right]\right] \quad (1)$$

where  $\mu_x, \mu_y$  are the means in  $x$  and  $y$  directions,  $\sigma_x, \sigma_y$  are the standard deviations in  $x$  and  $y$  directions, respectively and  $\rho$  is the correlation between  $x$  and  $y$ . In Eq. 1,  $\mu_x$  and  $\mu_y$  represent the center of emitting area of a diode, where  $\sigma_x$  and  $\sigma_y$  are functions of divergence angles determined by the active region dimensions  $l$  (length) and  $w$  (width). We consider the far-field emission pattern at a plane located at distance  $d$  from the laser diode. In this case,  $\sigma_x, \sigma_y$  - the standard deviations can be expressed in following manner

$$\sigma_x \approx d \times \tan\left(\frac{\lambda_c}{w}\right)$$

$$\sigma_y \approx d \times \tan\left(\frac{\lambda_c}{l}\right).$$



These expressions and Eq 1 are used to initialize photon directions emitted from a diode with  $l = 2 \mu m, w = 10 \mu m$ , and  $\lambda_c = 808 nm$  emit photons with divergence angles of  $\theta_{\perp} \approx 4.63^\circ$  and  $\theta_{\parallel} \approx 23.15^\circ$ . We simulated the propagation of 10,000 photons and analyzed their far-field intensity distribution at various distances from the laser diode. Figures 2, 3 and 4 display scattered plots of photons are  $d = 1 mm, d = 1 cm$  and  $d = 1 m$  from the diode.

**Figure 2.** Intensity distribution at  $d=1 mm$ .

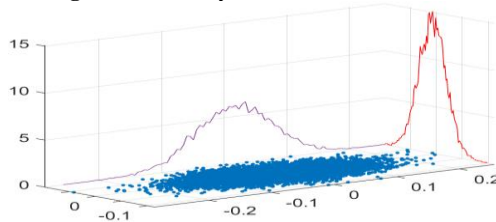


**Figure 3.** Intensity distribution at  $d=1 cm$ .

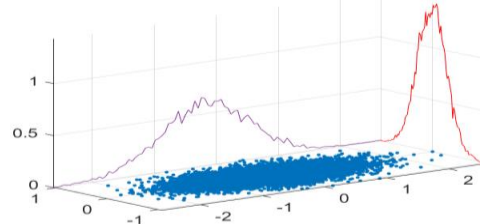
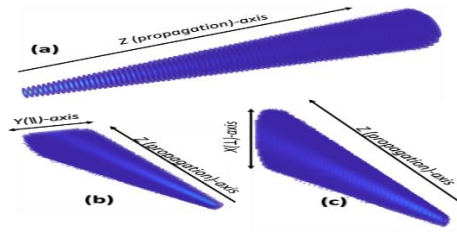


**Figure 4.** Intensity distribution at  $d=1 m$ .

Figures 2-4 illustrate the evolution of the far-field intensity distribution of the simulated photons as they propagate away from the laser diode. The  $x$  and  $y$  axes represent distance in meters, while the  $z$ -axis indicates the photon count, visually depicting the decrease in intensity (attenuation) with increasing distance.





Once the photon directions are established, simulating the laser diode's radiation pattern and its propagation becomes possible. While the emitting area's geometry plays a role in real-world scenarios, it's not crucial for our current simulation. Therefore, we adopted a simplified approach, assuming a small circular emitting area with a radius where photon directions are already sampled/found using the previously described method. With initial photon coordinates and directions determined, we can proceed with simulating their propagation dynamics. We employed methodologies outlined in [4] to achieve this. The results are presented in Figure 5. Figure 5a depicts the propagation of the diode radiation along the z-axis. However, it primarily shows the outer regions, obscuring the core dynamics within the beam. To address this, we virtually sliced the beam. Figure 5b displays the half-beam sliced in the Y-Z plane, while Figure 5c shows the half-beam sliced in the X-Z plane. Both figures illustrate the propagation of the radiation pattern and its evolving size.

**Figure 5.** Propagation of diode radiation from  $0.1\text{ m}$  to  $0.5\text{ m}$ .

In conclusion, this work highlights the importance of modeling laser diode emission patterns for a deeper understanding of experiments utilizing these devices. We presented a method for initializing photon directions using a bivariate normal distribution, capitalizing on the inherent two-dimensional nature of the emitting region in laser diodes. This approach offers a valuable tool for simulating diode photon propagation dynamics

#### REFERENCES

1. Danson, Colin N., Constantin Haefner, Jake Bromage, Thomas Butcher, Jean-Christophe F. Chanteloup, Enam A. Chowdhury, Almantas Galvanauskas et al. "Petawatt and exawatt class lasers worldwide." *High Power Laser Science and Engineering* 7 (2019): e54.
2. Guenter Huber, Christian Kränkel, and Klaus Petermann, "Solid-state lasers: status and future [Invited]," *J. Opt. Soc. Am. B* 27, B93-B105 (2010)
3. Saleh, Bahaa EA, and Malvin Carl Teich. *Fundamentals of photonics*. John Wiley & sons, 2019.
4. Sherniyozov, A. A., & Payziyev, S. D. "Simulating optical processes: Monte Carlo photon tracing method". *Uz. Phy. J*, 24(3), 157-162. (2022). <https://doi.org/10.52304/v24i3.357>



UDK: 538.955; 621.3.082.782

*Saydullo G'AYRATOV,*  
Namangan muhandislik-texnologiya instituti magistranti  
*Ulug'bek ERKABOYEV,*  
Namangan muhandislik-texnologiya instituti professori, f.-m.f.d  
*Jasurbek Mirzayev,*  
Namangan muhandislik-texnologiya instituti, PhD  
*Muzaffar DADAMIRZAYEV,*  
Namangan muhandislik-texnologiya instituti tayanch doktoranti  
*Dilshodbek ERKABOEV,*  
Farg'ona politexnika instituti magistranti  
*Nodirbek NABIJONOV,*  
Namangan davlat universiteti tayanch doktorant  
E-mail: muzaffardadamir81@gmail.com

NamMTI professori, f.-m.f.d. N.Shariboyev taqrizi asosida

### ВЛИЯНИЯ КВАНТУЮЩЕГО МАГНИТНОГО ПОЛЯ И ТЕМПЕРАТУРЫ НА ОСЦИЛЛЯЦИИ ЭНЕРГИИ ФЕРМИ В НАНОРАЗМЕРНЫХ ПОЛУПРОВОДНИКАХ

Аннотация

Получено новое аналитическое выражение, рассчитывающее осцилляции энергии Ферми для закона параболической дисперсии гетероструктурированных полупроводников на основе прямоугольной квантовой ямы под действием квантующего магнитного поля и температуры. Показано, что уровни Ферми наноразмерного полупроводника в квантующем магнитном поле квантована. Предложен метод расчета осцилляции энергии Ферми для двумерного электронного газа при разных магнитных полях и температурах.

**Ключевые слова:** магнитное поле, квантующее магнитное поле, гетероструктура, квантовая яма, плотность состояний, осцилляция, наноразмер, двумерные полупроводники.

### INFLUENCE OF QUANTIZING MAGNETIC FIELD AND TEMPERATURE ON FERMI ENERGY OSCILLATIONS IN NANO-SIZED SEMICONDUCTORS

Annotation

A new analytical expression is obtained for calculating the Fermi energy oscillations for the parabolic dispersion law of heterostructured semiconductors based on a rectangular quantum well under the action of a quantizing magnetic field and temperature. It is shown that the Fermi levels of a nanoscale semiconductor in a quantizing magnetic field are quantized. A method for calculating the Fermi energy oscillations for a two-dimensional electron gas at different magnetic fields and temperatures is proposed.

**Key words:** magnetic field, quantum magnetic field, heterostructure, quantum well, density of states, oscillation, nanosize, two-dimensional semiconductors.

### NANOO'LCHAMLI YARIMO'TKAZGICHLARDA FYERMI ENERGIYASI OSSILLYATSIYALARIGA KVANTLOVCHI MAGNIT MAYDON VA HARORATNING TA'SIRI

Аннотасија

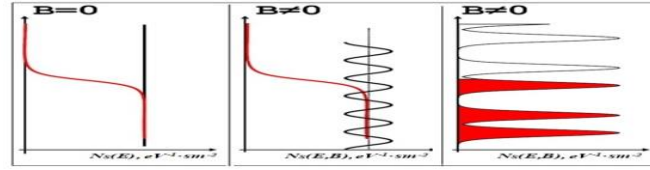
Kvantlovchi magnit maydon va harorat ta'sirida to'g'ri to'rtburchakli kvant o'ra asosidagi geterostrukturali yarimo'tkazgichlarning parabolik dispersiya qonuni uchun Fermi energiyasi ossillyatsiyalarini hisoblaydigan yangi analitik ifoda keltirib chiqarilgan. Kvantlovchi magnit maydon ta'siridagi nanoo'lchamli yarimo'tkazgichlarda Fermi sathi kvantlanishi isbotlangan. Turli harorat va magnit maydonlarda ikki o'lchamli elektron gazlar uchun Fermi energiyasi ossillyatsiyasini hisoblash usuli taklif qilingan.

**Kalit so'zlar:** magnit maydon, kvantlovchi magnit maydon, geterostruktura, kvant o'ra, holatlar zichligi, ossillyatsiya, nanoo'lcham, ikki o'lchamli yarimo'tkazgichlar.

**Kirish.** Elektron va kovaklarning holati  $D_{2f}(E)$  bilan aniqlanadi, bu yerda  $f(E)$  tashuvchining taqsimot funksiyasi. Muvozanat holatidagi zaryad tashuvchilar Fermi – Dirak funksiyasining  $f(E)$  statistikasiga bo'ysinadilar [2]. 1-rasmda  $T=0$ ,  $T>0$  haroratlarda va kvantlovchi magnit maydon ta'siri bo'lmagan ( $B=0$ ) da ikki o'lchamli elektron gazlardagi elektronning muvozanat holati ko'rsatilgan. Ushbu grafiklardan ko'rinib turibdiki, mutlaq nol haroratda elektronlarining joylashishi to'g'ri burchakdir. Bu yerda erkin zaryad tashuvchilarning energiyasi  $E$ , bir tomondan, to'ldirilgan energiya sathining tubi  $E_1$ , boshqa tomondan esa Fermi sathi  $E_F$  bilan cheklangan.  $T>0$  haroratda Fermi sathi  $E_F$  yaqinida yuvilish paydo bo'ladi [3].

Yetarlicha kuchsiz magnit maydonlarda kengaytirilgan Landau sathlari bir-biriga yopishib, energiya bo'shlig'ini yaratmasdan holatlarning zichligini modulyasiya qiladi (1-rasm). Kuchli magnit maydon holatida siklotron energiyasi  $\hbar\omega_c$

Landau sathi kengligidan kattaroq bo'lsa, energiya bo'shlig'i mavjud (hech bo'lmaganda harakatchanlik bo'shlig'i nuqtai nazaridan).



1-rasm. Magnit maydondagi holatlar zichligi (DOS) modulyasiyasi. elektronlarning Fermi taqsimot funksiyasi (qizil) [1].

**Adabiyotlar tahlili.** Hozirgi vaqtda ikki o'lchamli elektron gazlarining xususiyatlarini o'rganishga qiziqish, ularni nanoo'lchamli yarimo'tkazgichlarda qo'llash istiqbollari bilan bog'liq bo'lmoqda. Bunday sistemalarda kvant o'lchamli kattaliklar xarakteristikalarini ossilyatsiyalanuvchi bo'ladi [4, 5]. Ikki o'lchamli materiallarda energetik holatlar zichligi, elektronlarning effektiv massalari, Fermi energiyasi kabi energiyetik xarakteristikalarini kvant o'raning qalininga bog'liq, kichik o'lchamli kristallarda materialning qalinligi  $d$  elektronning de-Broyl to'liq uzunligiga taqriban teng bo'ladi.

Ma'lumki, kvantlovchi magnit maydondagi elektronlarning energetik spektri nanoo'lchamli yarimo'tkazgichlarda Landau sathlariga nisbatan Fermi sathining nisbiy holatiga qarab juda o'zgaruvchan xususiyatlarga ega. Barcha elektron gazlarda Fermi ( $\mu$ ) sathi bor, u mutlaq nol haroratda energiya sohalari elektronlar bilan to'lganlik sathini belgilaydi. Eksperimental va nazariy ma'lumotlardan ma'lum bo'lganidek [7], ikki o'lchamli kristallarda Fermi sirtida mutlaq haroratda Fermi ( $\mu$ ) energiyasini ossilyatsiyalarining yuqori amplitudalari kuzatiladi. Ammo uch o'lchamli elektron gaz uchun, past haroratlarda ham ossilyatsiyalar juda kichik bo'ladi. Uch o'lchamli kristallarda  $\mu$ , klassik magnit maydonlarda bo'lgani kabi faqat chiziqli o'zgaradi.

Ikki o'lchamli elektron sistemalarning elektron va magnit xususiyatlarini o'rganishda Fermi energiyasi muhim ahamiyatga ega, shuning uchun u mikro va nanoo'lchamli materiallarning asosiy parametrlaridan biri hisoblanadi. Bundan kelib chiqqan xolda, ushbu ishning asosiy maqsadi kvant o'ra asosidagi yarimo'tkazgichlarda Fermi sathi ossilyatsiyalariga kuchli magnit maydon va haroratning ta'sirini tahlil qilishdan iborat.

**Tadqiqot metodologiyasi.** Ma'lumki,  $k$ -bo'shliqda  $E(k)=const$  izoenergiya sirtlari yopiq bo'ladi va shar shaklida ifodalanadi. Ruxsat etilgan energiya holatlari doimiy zichlikka ega  $V/8\pi^3$  va  $k$ -bo'shliqda taqsimlanadi. Bu yerda  $V$  - kristalning hajmi. Pa'uli prinsipiga ko'ra: elektronning 2 ta qarama-qarshi spin holati  $k$  ning har bir qiymatini shakllantirishini e'tiborga olsak, barcha to'ldirilgan holatlarning to'liq kattaliklari kristalning  $V$  - birlik hajmida  $k_f$  dan katta bo'lmaydi va  $k_f$  quyidagicha aniqlanadi [8]:

$$\frac{4}{3} \pi k_F^3 \frac{2V}{8\pi^3} = N^{3d} \quad (1)$$

Bundan

$$k_F = \left( \frac{3\pi^2 N^{3d}}{V} \right)^{1/3} \quad (2)$$

Bu yerda,  $N^{3d}$  - uch o'lchamli elektron gaz uchun elektronlar soni.

Erkin elektronlar gazi Fermi-Dirak statistikasiga to'liq bo'ysinadi va asosiy holatdagi energiya mutlaq nol haroratda eng katta bo'ladi:

$$E_F = \frac{\hbar^2 k_F^2}{2m} \quad (3)$$

$E_f$  - uch o'lchamli elektron gaz uchun Fermi energiyasi. Izotopik tarqalish qonuniga asosan Fermi sirti radiusi  $k_f$  bo'lgan sferik shaklga ega bo'ladi. Yuqoridagi faktlar faqat uch o'lchamli materiallar uchun ko'rib chiqilgan bo'lib, ularda kvantlovchi magnit maydondagi ikki o'lchamli elektron gazlarining Fermi energiyasi ossilyatsiyalarini o'zgarishlari batafsil o'rganilmagan.

Endi, Fermi energiyasini ikki o'lchamli elektron gazlarida kvantlovchi magnit maydonga bog'liqligini ko'rib chiqamiz. Ikki o'lchamli elektron gazlarda magnit maydon bo'lmaganda ham, elektron energiyasi  $Z$  o'qi bo'ylab kvantlangan bo'ladi va elektron faqat  $XY$  tekisligida erkin harakat qiladi. Ushbu kvantlanish o'lchamli kvantlanish deyiladi. Agar  $B$  magnit maydon induksiyasi  $XY$  tekisligiga perpendikulyar yo'naltirilgan bo'lsa, u holda erkin elektronning energiyasi  $XY$  tekisligi bo'ylab kvantlanadi.

Yuqorida qayd qilingan ilmiy mulohazalarda bir qator savollar ochiq qoldirilmogda, jumladan kvantlovchi magnit maydon ta'siridagi ikki o'lchamli elektron gazlarida erkin elektronlarning Fermi energiyasi haroratga qanday bog'liq bo'ladi? Yuqori haroratlarda nanoo'lchamli materiallarning zaryad tashuvchilari qanday taqsimlanadi?

Ikki o'lchamli elektron gaz uchun ruxsat etilgan energiya holatlari doimiy sirtiy zichlikka ega deb tasavvur qilib olamiz  $S/4\pi^2$  va  $XY$  tekislikda taqsimlanadi. Bu yerda  $S$  - bu kristalning sirt maydoni. Bundan (1) va (2) formulalar yordamida ikki o'lchamli elektron gaz uchun elektronlar konsentratsiyasini aniqlash mumkin:

$$N^{2d} = 4\pi k_F^2 \frac{2L^2}{4\pi^2} \quad (4)$$

Bundan:

$$k_F^{2d} = \frac{1}{L} \left( \frac{\pi N^{2d}}{2} \right)^{1/2} \quad (5)$$

(5) ni (6) ga almashtirib, magnit maydon bo'lmagan hol uchun ikki o'lchamli elektron gazlaridagi Fermi energiyasini aniqlash mumkin:

$$\mu^{2d} = \frac{p_\mu^2}{2m} = \frac{\pi \hbar^2 N^{2d}}{4mL^2} \quad (6)$$

Bu yerda,  $N^{2d}$  - ikki o'lchamli elektron gaz uchun elektronlar konsentratsiyasi,  $L^2$  - harakat tekisligining yuzasi,  $p_\mu$  - Fermi impulsi.

Magnit maydonga perpendikulyar bo'lgan tekislik harakatida elektronlarning klassik trayektoriyalari davriy aylanalardir. Kvant fizikasida elektronlarning bunday trayektoriyalari (elektronning davriy aylanishi) bir xil masofali diskret Landau sathlaridan tashkil topadi:

$$E_n = \hbar \omega_c \left( n_L + \frac{1}{2} \right) \quad (7)$$

Bu yerda,  $n_L$  - Landau sathlarining soni.  $\omega_c = \frac{eH}{mc}$  - siklotron chastotasi.

Ma'lumki, uch o'lchamli kristallarda (7) formulagacha energiya spektriga uzluksiz kvadratik energiya spektri  $\frac{p_z^2}{2m}$  qo'shiladi. Biroq, ikki o'lchamli materiallarda bu uzluksiz spektr diskret energetik spektrlarga aylanadi. Darhaqiqat,  $d$  kvant o'raning qalinligi o'lchamli kvantlovchi sharti bilan qoplanadi, boshqacha qilib aytganda, qalinlik o'lchami kristaldagi elektronning de-Broyl to'lqin uzunligiga nisbatan yaqin. Elektronning  $Z$  o'qi bo'ylab harakatlanishi  $V_z$  potensialidan hisoblanadi:

$$V(z) = \begin{cases} 0, & 0 < z < d, \\ \infty, & z \leq 0, z \geq d \end{cases} \quad (8)$$

Ikki o'lchamli elektron gazlarda magnit maydon bo'lmaganda, elektronlarning normallashtirilgan to'lqin funksiyalari quyidagi shaklga ega [6]:

$$\psi_{k_{fx}, k_{fy}, n_{fz}}(x, y, z) = \frac{1}{\sqrt{L_{f1}}} \exp(ik_{fx} x) \frac{1}{\sqrt{L_{f2}}} \exp(ik_{fy} y) \varphi_{n_z}(z) \quad (9)$$

Bu yerda,  $k_{fx}$ ,  $k_{fy}$  - elektronlarning Fermi energiyasining to'lqin sonlari,  $n_{fz}$  -  $Z$  o'qi bo'ylab o'lchamli kvantlar soni. (9) formulada (8) ga muvofiq normallashtirilgan  $\varphi_{n_z}(z)$  funksiyalar quyidagi shaklda yozilgan:

$$\varphi_{n_z}(z) = \sqrt{\frac{2}{d}} \sin \frac{\pi n_z z}{d}, \quad n = 1, 2, 3, \dots \quad (10)$$

(9) holatlarga mos keladigan elektronlarning Fermi energiyalari:

$$E(k_{fx}, k_{fy}, n_{fz}) = \frac{\hbar^2}{2m} (k_{fx}^2 + k_{fy}^2) + \frac{\pi^2 \hbar^2 n_{fz}^2}{2md^2} \quad (11)$$

bo'ladi

**U xolda (7), (11) ifodalarni (6) ga almashtirib, magnit maydon ishtirokida quyidagi formulani olamiz:**

$$\mu_F(H) = \frac{\pi \hbar^2 N^{2d}(H)}{4mL^2} + \frac{\pi^2 \hbar^2 n_{fz}^2}{2md^2} \quad (12)$$

Bir birlik ( $L_x L_y = 1$ ) maydon uchun (12) formulalar quyidagicha hisoblanadi:

$$\begin{aligned} \mu_F(H) &= \frac{\pi \hbar^2 N^{2d}(H)}{4m} + \frac{\pi^2 \hbar^2 n_{fz}^2}{2md^2} = \\ &= \frac{1}{8} \frac{\hbar eH}{mc} \cdot \frac{2\pi \hbar N^{2d}(H)c}{eH} + \frac{\pi^2 \hbar^2 n_{fz}^2}{2md^2} = \frac{1}{8} \hbar \omega_c \nu + \frac{\pi^2 \hbar^2 n_{fz}^2}{2md^2} \end{aligned} \quad (13)$$

**Bu yerda,**  $\nu = \frac{2\pi \hbar c N^{2d}(H)}{eH}$  - to'ldirish koeffitsiyenti [9]. Bu Landau sathlarining soni, ular spinini bo'linishini

hisobga olgan holda, kvantlovchi magnit maydonda, mutlaq nol haroratda, elektronlar bilan to'la bo'ladi. Ushbu o'lchovsiz parametr 2D elektron gazlaridagi kvant ossilyatsiya ta'sirlarni muhokama qilishda qulaylik uchun ishlatiladi. (13) formuladan ko'rinib turibdiki, agar to'ldirish koeffitsiyenti butun son bo'lsa, unda Fermi energiyalari kvantlanadi, u holda  $\frac{1}{8} \hbar \omega_c$ , minimal

energiya kvanti bo'ladi, ya'ni (13) formulada birinchi sathdagi energiya uchun aniq qiymat  $\nu = 1$  berilgan

$$\mu_1(H) = \frac{1}{8} \hbar \omega_c + \frac{\pi^2 \hbar^2 n_{fz}^2}{2md^2} \quad (14)$$

Boshqa barcha sathlar uchun nazariya o'z ifodasini beradi

$$\mu(H) = \hbar \omega_c \left( \nu + \frac{1}{8} \right) + \frac{\pi^2 \hbar^2 n_{fz}^2}{2md^2} \quad (15)$$

Bu yerda to'ldirish koeffitsiyenti butun son,  $\nu = 0, 1, 2, 3, \dots$

Bundan tashqari, ikki o'ldamli materiallarda kvantlovchi magnit maydon ta'sir etganda erkin elektronlarning energiya spektri diskret bo'ladi. Fermi energiyasi to'liq diskret energiya spektrida odatda kvant nuqta bo'lib xarakterlanadi. Bunda magnit induksiya vektori  $Z$  o'qi bo'ylab va ikki o'ldamli qatlam tekisligiga perpendikulyar ravishda yo'naltiriladi. Ko'ndalang kvantlovchi magnit maydonida kvant o'ralari kvant nuqtaga o'xshash bo'ladi, bu vaziyatda uchta harakat yo'nalishi ham cheklanadi.

**Xulosa.** Kuchli magnit maydonidagi kvant o'rali yarimo'tkazgichlarning Fermi sathlari kvantlanganligi ko'rsatilgan. Ikki o'ldamli elektron gaz uchun Fermi sathi ossilyatsiyalarini turli magnit maydonlarda va haroratda hisoblash usuli taklif qilingan. Yuqori harorat va kuchsiz magnit maydonlarda Fermi-Dirak taqsimot funksiyasini hisoblash uchun analitik ifoda olingan.

#### ADABIYOTLAR

1. Marcin Z Drozdowa Byszewski. Optical properties of a two-dimensional electron gas in magnetic fields. University Joseph Fourier. 2005. (In English). Ed. "Science technology santé". Part I. pp. 141. <https://tel.archives-ouvertes.fr/tel-00010691>.
2. Леонтович М.А. Введение в термодинамику. Статистическая физика. 1983 г. М. «Наука». 416 С.
3. Григорьев П.Д. Особенности магнитосопротивления в слоистых квазидвумерных проводниках. Дисс. на соиск. уч. степени д.-ф.н. 2015. Черноголовка. 289 С.
4. Коротун А.В. Размерные осцилляции работы выхода металлической пленки на диэлектрической подложке // Физика твердого тела. 2015. Т.57, вып.2, С.371-374.
5. Курбацкий В.П., Погосов В.В. Аналитическая модель размерных осцилляций энергетических и силовых характеристик субатомных металлических пластинок // Физика твердого тела. 2004. Т.46, вып.3, С.526-533.
6. Дымников В.Д. Энергия Ферми электронов в тонкой металлической пластине // Физика твердого тела. 2015. Т.57, вып.5, С.847-852.
7. Кузьмин М.В., Логинов М.В., Митцев М.А. Немонотонные размерные зависимости работы выхода нанопленок иттербия, осаждаемых на поверхность Si(111)7X7 при комнатной температуре // Физика твердого тела. 2008. Т.50, вып.2, С.355-359.
8. Цидильковский И.М. Электроны и дырки в полупроводниках. М. Наука, 1972. С. 620.
9. Шик А.Я., Бакуева Л.Г., Мусихин С.Ф., Рыков С.А., Физика низкоразмерных систем. Санк-Петербург Наука, 2001. С.104-105





UDK 621.315.592

**Shukur G'OFUROV,**

*O'zbekiston-Yaponiya yoshlar innovatsiya markazi kichik ilmiy xodimi*

*Email: schuckur@gmail.com,*

**Dilbar BOZOROVA,**

*Ion-plazma va lazer texnologiyalari instituti tayanch doktoranti*

**Mavonbek ZIYAYEV,**

*Namangan davlat universiteti katta o'qituvchisi, PhD*

**Oksana ISMAILOVA,**

*O'zbekiston-Yaponiya yoshlar innovatsiya markazi, "Energetika" laboratoriyasi mudiri, f.-m.f.n*

**Zuxra KADIROVA,**

*O'zbekiston-Yaponiya Yoshlar innovatsiya markazi, ilmiy ishlar bo'yicha direktor o'rinbosari, k.f.d*

*O'zMU huzuridagi Yarimo'tkazgichlar fizikasi va mikroelektronika ilmiy-tadqiqot instituti laboratoriya mudiri, f.-m.f.n  
A.Mavlyanov taqrizi asosida*

## SOLVATERMAL VA GIDROTERMAL USULDA SINTEZ QILINGAN BISMUT VANADATINING MORFOLOGIK TAHLILI

Annotatsiya

Bismut vanadati fotokatalizatori bir bosqichli solvatermal va ikki bosqichli gidrotermal usullarda sintez qilindi. Sintez qilingan namunalarda SEM-EDS metodi bilan tadqiq qilindi. Namunalarning elemental nisbatlari hamda ularning morfologik tahlillari keltirildi. Xar ikki namunalarda Bi, V hamda O lar yuz bo'ylab bir tekis taqsimlangani kuzatildi. Solvotermal usulda olingan namuna mayda, dag'al va g'ovaksimon strukturalar to'plamidan iboratligi ko'rsatildi. Gidrotermal usulda olingan namunalarda esa 2-3  $\mu\text{m}$  dan 20  $\mu\text{m}$  gacha bo'lgan katta va kichik sferik shakllarga egaligi ko'rsatildi. Ushbu morfologik tahlillar orqali namunalarning sirt yuzasi ularning fotokatalitik faolligiga ta'siri haqida ilmiy tahlillar keltirib o'tildi.

**Kalit so'zlar:** bismut vanadat, vanadat, fotokatalizator, fotodegradatsiya, vodorod energiyasi.

## MORPHOLOGICAL ANALYSIS OF BISMUTH VANADATE SYNTHESIZED BY SOLVOTHERMAL AND HYDROTHERMAL METHODS

Annotation

Bismuth vanadate photocatalyst was synthesized by one-step solvothermal and two-step hydrothermal methods. The synthesized samples were studied by SEM-EDS method. The elemental proportions of the samples and their morphological analysis were presented. Bi, V and O were evenly distributed over the surface in both samples. It was shown that the sample obtained by solvothermal method consists of a set of small, rough and porous structures. It was shown that the samples obtained by the hydrothermal method have large and small spherical shapes from 2-3  $\mu\text{m}$  to 20  $\mu\text{m}$ . Through these morphological analyses, scientific analyzes were made about the effect of the surface of the samples on their photocatalytic activity.

**Key words:** bismuth vanadate, photocatalyst, photodegradation, hydrogen energy.

## МОРФОЛОГИЧЕСКИЙ АНАЛИЗ ВАНДАТ ВИСМУТА, СИНТЕЗИРОВАННЫЙ СОЛЬВОТЕРМАЛЬНЫМИ И ГИДРОТЕРМАЛЬНЫМИ МЕТОДАМИ

Аннотация

Фотокатализатор ванадат висмута синтезирован одностадийным сольватермальным и двухстадийным гидротермальным методами. Синтезированные образцы были исследованы методом SEM-EDS. Представлены элементные соотношения образцов и их морфологический анализ. Bi, V и O были равномерно распределены по поверхности в обоих образцах. Показано, что образец, полученный сольвотермическим методом, состоит из набора мелких, шероховатых и пористых структур. Показано, что образцы, полученные гидротермальным методом, имеют крупную и мелкую сферическую форму от 2-3 мкм до 20 мкм. Посредством этих морфологических анализов был проведен научный анализ влияния поверхности образцов на их фотокалитическую активность.

**Ключевые слова:** ванадат висмута, фотокатализатор, фотодеградация, водородная энергетика.

**Kirish.** Bismut vanadat turli sohalarida, ayniqsa fotokataliz va fotoelektrokimyoviy suvni parchalashda istiqbolli material sifatida qo'llaniladi, bu uning qulay joylashgan hamda nisbatan torroq (2.4 eV) ta'qiqlangan sohaga ega ekanligi, korroziyaga bardoshlilik, narxini nisbatan arzonligi, zararsizligi va yuqori barqarorligi bilan bog'liqdir [1-2]. Uning quyosh energiyasini konvertatsiya qilish samaradorligini oshirish imkoniyati so'nggi yillarda katta e'tibor qozongan. Bismut vanadatning noyob xususiyatlari uni fotoelektrokimyoviy sxema va fotokatalitik tizimlarning samaradorligini oshirish uchun ajoyib nomzodga aylantiradi [3]. Uning samaradorligini optimallashtirishda sintez usullari va hosil bo'lgan material xususiyatlari katta rol o'ynaydi. Shu sababli, bismut vanadat sintezini tushunish va optimallashtirish uning qayta tiklanuvchi energiya texnologiyalaridagi amaliy qo'llanmalari uchun juda muhimdir. Bismut vanadatni turli usullar yordamida sintez qilish mumkin, jumladan qattiq holat reaksiyalari, sol-gel jarayonlari va cho'kma usullari [4]. Ulardan solvotermal va gidrotermal usullar yuqori tozalikdagi va yaxshi kristallangan materiallar ishlab chiqarishda ayniqsa samaralidir [5-6]. Bu usullar erituvchilardan

foydalanib, nazorat qilinadigan harorat va bosim sharoitlarida kerakli kristall strukturalar hosil qilishga olib keladi. Solvotermal sintez odatda organik erituvchilardan foydalanadi, gidrotermal sintez esa suvni erituvchi sifatida qo'llaydi [7-8]. Ikkala usul ham sintez qilingan bismut vanadat xususiyatlarini moslashtirish uchun juda muhim bo'lgan reaksiya muhiti ustidan aniq nazorat qilish imkonini beradi. Ushbu tadqiqot ishida solvotermal va gidrotermal usullar yordamida sintez qilingan bismut vanadat elemental hamda morfologik jihatdan tahlili keltirilgan.

**Tadqiqot metodi.** *Materiallar.* Sigma-Aldrichdan bismut (III) nitrat pentagidrat ( $\text{Bi}(\text{NO}_3)_3 \cdot 5\text{H}_2\text{O}$ ), Vanadil asetilasetonat ( $\text{C}_{10}\text{H}_{14}\text{VO}_5$ ), sirka kislotasi sotib olindi. Ushbu ishda foydalanilgan barcha reagentlar analitik darajada bo'lgan va ular boshqa hech qanday tozalashsiz ishlatilgan. Sintezlangan bismut vanadatni yuvish (tozalash) uchun toza etanol va distillangan suv ishlatilgan.

#### Solvotermal sintez

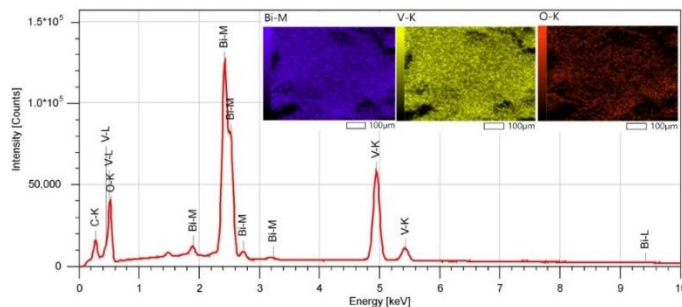
0,01 mol  $\text{Bi}(\text{NO}_3)_3 \cdot 5\text{H}_2\text{O}$  ni 40 ml sirka kislotada eritib, A eritmasi tayyorlandi, 2 soat davomida to'liq eriguncha aralashtirildi. Xuddi shunday, 0,005 mol  $\text{C}_{10}\text{H}_{14}\text{VO}_5$  ni 30 ml sirka kislotada eritib, B eritmasi tayyorlandi, to'liq eriguncha 2 soat davomida aralashtirildi. Doimiy ravishda 500 rpm aylanish tezligida aralashtirib, tomchilab quyish texnikasidan foydalangan holda A eritmasiga asta-sekin B eritmasi qo'shildi va sarg'ish eritma hosil bo'lguncha aralashtirildi. Keyin, biz bu eritmani xona haroratida qorong'i joyda 24 soat ushlab turdik. Cho'kmani 10 daqiqa davomida 2500 rpm tezlikda santrifuga qilish orqali to'plab olindi, so'ngra ortiqcha aralashmalarni olib tashlash uchun etanol va distillangan suv bilan bir necha marta yuvildi. Nihoyat, ajratib olingan modda  $60^\circ\text{C}$  da 12 soat davomida quritildi.

#### Gidrotermik sintez

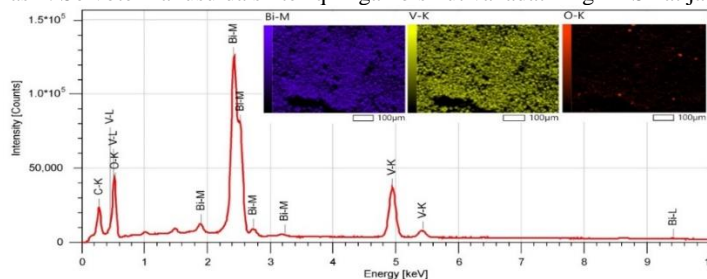
Gidrotermal sintezda solvotermal sintez qilingan aralshmadan foydalanildi. Sarg'ish eritmani olgandan so'ng, uni teflon bilan qoplangan avtoklavga o'tkazildi, uni to'liq yopib, 12 soat davomida  $160^\circ\text{C}$  li pechda qizdirildi. Reaksiyadan so'ng avtoklavni tabiiy ravishda xona haroratiga sovitildi. Aralshma xuddi solvotermal sintezdagi kabi moddaning yig'ib olish va yuvish orqali ajratib olindi.

Solvotermal va gidrotermal yo'llar bilan sintez qilingan namunalar bismut vanadat kristalliligini yaxshilash uchun mufel pechida 1 soat davomida  $500^\circ\text{C}$  da qizdirildi.

**Natijalar va ularning muhokamasi.** 1-rasmda solvotermal usul orqali sintez qilingan bismut vanadat uchun energiya dispersiv spektroskopiyasi (EDS) natijalari keltirilgan. EDS spektri bismut (Bi), vanadiy (V) va kislorod (O) uchun intensive piklarni ko'rsatadi, bu ushbu elementlarning o'rganilayotgan yuza qismida haqiqatdan mavjudligini tasdiqlaydi. Elementar xaritalash tasvirlari Bi, V va O elementlari soha bo'ylab bir xil taqsimlanganini ko'rsatadi. EDS natijalaridagi Bi-M, V-K va O-K kabi spektr chiziqlarining aniq qayd etilishi, bu elementlarning bismut vanadat strukturasi tegishli ekanligini taxmin qilishga asos bo'ladi.



1-rasm. Solvotermal usulda sintez qilingan bismut vanadatining EDS natijalari.



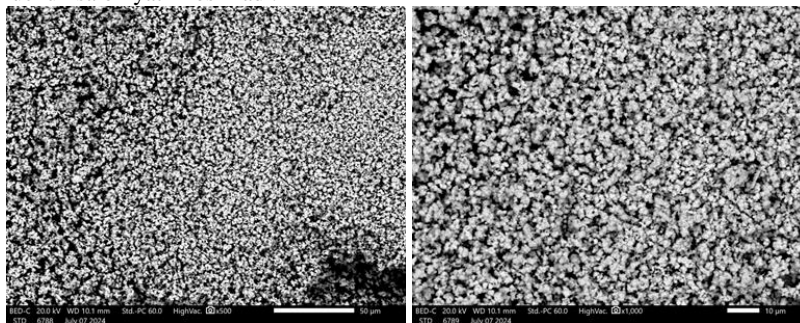
2-rasm. Gidrotermal usulda sintez qilingan bismut vanadatining EDS natijalari.

2-rasm gidrotermal usul yordamida sintez qilingan bismut vanadat uchun EDS natijalarini taqdim etadi. EDS spektri, xuddi solvotermal metod natijalaridagidek Bi, V va O larga tegishli piklarni ko'rsatadi, bu struktura o'xshash ekanligini bildiradi. Elementar xaritalash tasvirlari Bi, V va O ning bir xil taqsimlanishini ko'rsatadi.

Solvotermal usullar bilan sintez qilingan bismut vanadat namunasi Bi, V va O atom foizlari mos ravishda 19.21, 23.97 va 56.83 ni tashkil etdi, gidrotermal usulda sintez qilingan namuna esa 19.36, 15.36 va 65.28 ni ko'rsatdi. Ikkala namunada Bi deyarli bir xil miqdorni ko'rsatdi. Ammo V birinchi namunada ko'proq, ikkinchi namunada esa kamro ekanligini ko'rsatdi. O ham o'z navbatida o'zgargan. Bu esa strukturada extimoliy o'zgarishlar bo'lishi mumkinligini bildiradi. Buning uchun strukturaviy tahlillar kerak bo'ladi. Bu natijalarni kelgusi ishlarda taqdim etish ko'zda tutilgan.

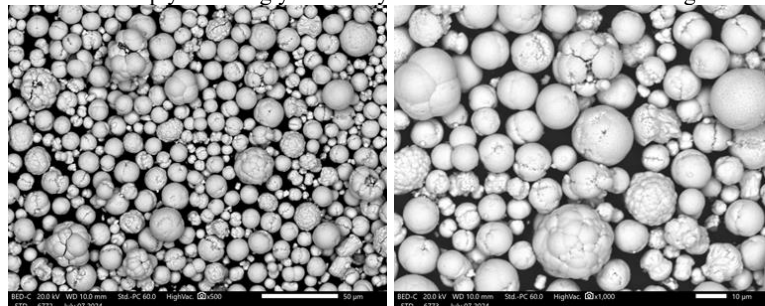
Quyida solvotermal usul yordamida sintez qilingan bismut vanadati namunalarining SEM mikroskopik tasvirlari (3-rasm) x500 va x1000 marta kattalashtirishgan xolati keltirilgan. Zarrachalar zich o'ralgan, donador tuzilishga ega bo'lib, o'lchamlari asosan sub-mikrometr diapazonida ekanligini ko'rish mumkin. Dag'al, teksturali yuzalar va yuqori poroslik ko'proq sirt maydonini ko'rsatadi, bu fotokatalitik ilovalar uchun foydalidir. Kichik kristallitlar va bir-biriga bog'langan zarrachalar bilan

ajralib turadigan bu nozik, bir xil morfologiya bismut vanadatining quyosh energiyasini samarali konvertatsiya qilish va fotokatalitik jarayonlar uchun salohiyatini oshiradi.



3-rasm. Solvotermal usulda sintez qilingan bismut vanadatining x500 va x1000 marta katalashtirilgan SEM mikroskopik tasvirlari.

Keyingi rasm gidrotermal usulda sintez qilingan bismut vanadati namunalarining SEM mikroskopik tasvirlari (4-rasm) x500 va x1000 marta kattalashtirishgan xolatini ifodalagan. Zarrachalar bir necha  $\mu\text{m}$  dan o'nlab  $\mu\text{m}$  gacha bo'lgan keng o'lchamli sferik va yarim sharsimon morfologiyani namoyish etadi. Sirtlar dag'al va g'ovakli bo'lib, agregatsiya va sinterlanishni ko'rsatadi, bu esa faolroq joylarni ta'minlash orqali fotokatalitik faollikni oshirishi mumkin. Yuqori kattalashtirish tasviri (1000x) biriktirilgan sferalar, yoriqlar va kichikroq sun'iy yo'ldosh zarralari kabi batafsil sirt xususiyatlarini ochib beradi, bu sirt maydonini ko'payishiga olib keladi va quyosh energiyasidan foydalanishda ishlash samaradorligini oshiradi.



4-rasm. Gidrotermal usulda sintez qilingan bismut vanadatining x500 va x1000 marta katalashtirilgan SEM mikroskopik tasvirlari.

Shunday qilib, gidrotermik usulda olingan namuna, keng o'lchamli (bir necha mikrometrdan o'nlab mikrometrgacha) sferik va yarim sharsimon zarrachalarni ishlab chiqaradi. Zarrachalar daga'l, g'ovakli yuzalarga ega bo'lib, fotokatalitik reaksiyalar uchun ko'plab faol joylarni ta'minlaydi. Bu usul yorug'likni yutish va zaryadni ajratishni kuchaytiradigan kattaroq, ierarxik tuzilmalarni beradi. Solvotermik usulda olingan namuna, asosan mikrometrdan kichik o'lchamdagi zarrachalar bilan zich o'ralgan, donador tuzilishga ega bo'ladi. Zarrachalar yuqori teksturali va dag'al bo'lib, yuqori sirt maydonini yaratadi. Bu bir xil, nozik morfologiya faol joylarni oshiradi, yorug'lik va reaktivlar bilan yaxshiroq dispersiya va o'zaro ta'sirni taklif qiladi.

Ikkala usul ham foydali fotokatalitik xususiyatlarga ega bismut vanadatini hosil qiladi. Shu bilan birga, solvotermik usul nozikroq, bir xil zarrachalar va yuqori sirt maydoni tufayli yanada qulayroq bo'lib, quyosh energiyasini yanada samarali konvertatsiya qilish va fotokatalitik faollik uchun yorug'lik yutilishi va reaksiya kinetikasini kuchaytiradi.

**Xulosa.** Olib borilgan ushbu tadqiqot ishida biz bismut vanadatini ikki xil usulda sintez qildik. Solvotermal usulda olingan namunalar mayda shakllarga ega va yuqori sirt maydonini ko'rsatmoqda. Gidrotermal usulda olingan namunalar esa, aniq va turli sferik shaklga ega donalarni ifoda etmoqda. Solvotermal usuli, albatta bir qadam kamroq sintez usuli bilan biroz ustunlikka ega bo'lishi mumkin. Lekin, ushbu namunalarning qaysi biri samaraliroq ekanligini kelgusi ishlarimizda rejalashtirilayotgan fotokatalitik faolligini aniqlash testi orqali aniqlab, yakuniy xulosa chiqarishimiz mumkin bo'ladi.

**Tashakkurnoma.** Ushbu tadqiqot ishi O'zbekiston Respublikasi Oliy ta'lim, fan va innovatsiyalar vazirligi huzuridagi Innovatsion rivojlanish agentligi tomonidan moliyalashtirilgan FZ-20200929314 loyihasi tomonidan qo'llab-quvvatlandi.

#### ADABIYOTLAR

1. H. S. Han, S. Shin, D. H. Kim, I. J. Park, J. S. Kim, P.-S. Huang, J.-K. Lee, I. S. Cho, X. Zheng, Energy Environ. Sci., 11, 1299 (2018).
2. J. H. Kim, J.-W. Jang, Y. H. Jo, F. F. Abdi, Y. H. Lee, R. van de Krol, J. S. Lee, Nat. Commun., 7, 13380 (2016).
3. A. Kudo, K. Ueda, H. Kato, I. Mikami, Catal. Lett., 53, 229 (1998).
4. Song, J.; Cha, J.; Lee, M. G.; Jeong, H. W.; Seo, S.; Yoo, J. A.; Kim, T. L.; Lee, J.; No, H.; Kim, D. H.; et al. J. Mater. Chem. A 2017, 5, 18831–18838.
5. Rettie, A. J. E.; Lee, H. C.; Marshall, L. G.; Lin, J. F.; Capan, C.; Lindemuth, J.; McCloy, J. S.; Zhou, J.; Bard, A. J.; Mullins, C. B. J. Am. Chem. Soc. 2013, 135, 11389–11396.
6. Abdi, F. F.; Savenije, T. J.; May, M. M.; Dam, B.; van De Krol, R. J. Phys. Chem. Lett. 2013, 4, 2752–2757.
7. Jiang, Z.; Liu, Y.; Jing, T.; Huang, B.; Zhang, X.; Qin, X.; Dai, Y.; Whangbo, M. H. J. Phys. Chem. C 2016, 120, 2058–2063.
8. Nikam, S.; Joshi, S. RSC Adv. 2016, 6, 107463–107474.



UDK: 577.35

*Shuxrat GULAMOV,*  
Andijon davlat tibbiyot instituti dotsenti, fiz-mat.f.n  
E-mail: shaqfiz@mail.ru,  
*Otabek TASHPULATOV,*  
Andijon davlat tibbiyot instituti o'qituvchisi

AndMI professri, f-m.f.d B.Asqarov taqrizi asosida

### AUTOMATION OF LABORATORY WORK IN BIOPHYSICS (I.BASED ON THE EXAMPLE OF STOKES METHOD)

Annotation

This article contains research on the automation of laboratory work in the subject of Biophysics (using the example of the Stokes method). The traditional method for determining the viscosity of a liquid was analyzed, a block diagram of the automated method was developed, and a laboratory installation was created on its basis. The possibility of using the created laboratory installation in the educational process, as well as in research work, is shown.

**Key words:** laboratory, automation, fluid, viscosity, equipment, temperature, optoelectronic, program, glass tube, heater, thermocouple, program, graphic.

### АВТОМАТИЗАЦИЯ ЛАБОРАТОРНОЙ РАБОТЫ В БИОФИЗИКЕ (I.НА ПРИМЕРЕ МЕТОДА СТОКСА)

Аннотация

В данной статье проведены исследования по автоматизации лабораторной работы по предмету Биофизика (на примере метода Стокса). Проанализирован традиционный метод определения вязкости жидкости, разработана структурная схема автоматизированного метода и создано на его основе лабораторная установка. Показана возможность использования созданной лабораторной установки в учебном процессе, а также в научно-исследовательских работах.

**Ключевые слова:** лаборатория, автоматизация, жидкость, вязкость, оборудование, температура, оптоэлектроника, программа, стеклянная трубка, нагреватель, термомпара, программа, график.

### BIOFIZIKA FANIDAN LABORATORIYA ISHINI AVTOMATLASHTIRISH (I. STOKS USULI MISOLIDA)

Annotatsiya

Uchbu maqolada Biofizika fanidan laboratoriya ishini avtomatlashtirish (Stoks usuli misolida) bo'yicha tadqiqot ishlari olib borilgan. Suyuqliklar qovushoqligini aniqlashning an'anaviy usuli taxlil qilinib, avtomatlashtirilgan usulni blok sxemasi ishlab chiqilgan va u asosida laboratoriya uskunasini yaratilgan. Yaratilgan laboratoriya uskunasini o'quv jarayonida hamda ilmiy tadqiqot ishlarida qo'llash mumkinligi ko'rsatilgan.

**Kalit so'zlar:** laboratoriya, avtomatlashtirish, suyuqlik, qovushoqlik, uskuna, temperature, optoelektron, dastur, shisha nay, qizdirgich, termojuft, dastur, grafik.

**Kirish.** Ta'lim texnologiyalarida va har qanday fizikadan olib boriladigan tajribada, mikroelektronika qurilmalari va kompyuterlar axborotni qabul qilish, saqlash, qayta ishlash va uzatish uchun kuchli vositalar sifatida yetakchi o'rinlardan birini egallaydi [1]. Eksperimental qurilmalarning turli jarayonlarini boshqarish, hozirgi vaqtda fizik tajribani avtomatlashtirishni, mikroelektronika qurilmalari hamda kompyuter texnologiyalarisiz tasavvur qilib bo'lmaydi. Mazkur holat, tibbiyot institutlarida o'qitiladigan Biofizika fanining laboratoriya ishlarida ham katta ahamiyatga ega. Shuning bilan birga, bugungi kunda axborotni tez tarqalishi, uzatilishi va yangi zamonaviy texnologiyalar kirib kelayotgan davrda an'anaviy laboratoriya ishlarini o'rniga avtomatlashtirilgan tizimlarni yaratish va o'quv jarayoniga qo'llash dolzarb masala hisoblanadi.

**Adabiyotlar tahlili va metodologiya.** Ushbu maqolada biofizika fanidan, an'anaviy usulda o'tkiziladigan laboratoriya ishini avtomatlashtirish (Stoks usuli misolida) metodologiyasi yoritilgan. Bu jarayonni amalga oshirishda bir qator adabiyotlarda foydalanilgan. Jumladan, Минеев Л.И., Хромова Л.А. Автоматизация физического эксперимента в лабораторном практикуме. Альманах современной науки и образования. №6 (25), 2009, с. 121 – 123. Ilmiy maqolada laboratoriya ishlarini avtomatlashtirish ushuncha axborot texnologiyalaridan foydalanish lozimligi qayd etilgan. A.N.Remizov. Tibbiy va biologik fizika. T.2006. darsligidan suyuqliklar qovushoqligini fizik ma'nosini va ishchi formulani keltirib chiqarish uchun foydalanilgan. Sh.A.Gulamov, D.T.Komilova. Biofizika fanidan praktikum. O'quv qo'llanma. Andijon. 2021. Ushbu o'quv qo'llanmada qovushoqlikni aniqlashning an'anaviy usuli keltirilgan.

#### Tadqiqot metodologiyasi.

1. Suyuqliklarning qovushoqligini Stoks usulida aniqlash" laboratoriya ishini avtomatlashtirishga oid loyiha-blok sxemalarini ishlab chiqish.

2. Talabalarda, suyuqlardan – glitsirin, paxta va transformator moylari qovushoqliklarini, avtomatlashtirilgan tizimda aniqlash ko'nikmasini hosil qilish bo'yicha tavsiyalar ishlab chiqish u orqali, tirik organizmdagi qon, siydik, o't suyuqligi va suvlarni qovushoqligini aniqlashni o'rganishni osonlashtirishni ta'minlash.

Tajriba usuli va kerakli jixozlar. Avtomatlashtirilgan laboratoriya tizimi "Suyuqliklarni qovushoqligini Stoks usulida aniqlash" laboratoriya ishi asosida yaratildi.



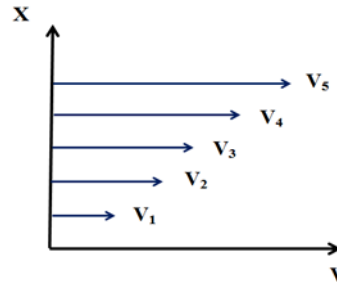
Laboratoriya uskunasi yaratishda quyidagi jixozlardan foydalanildi:

- Uzunligi 0,5 m va diametridi 0,05 m bo'lgan uchta silindrik simon shisha naylar.
- Po'lat sharchalar.
- Shisha silindr idishlarga quyilgan turli qovushoqlikka ega bo'lgan suyuqliklar (paxta moyi, glitsirin, transformator moyi).
- Dasturiy ta'minotga ega bo'lgan kompyuter jamlamasi.

- Optoelektron datchiklar.
- Mikroprotsessorli qurilma (Interfeys blogi).

Nazariy qism: Mazkur maqolada laboratoriya ishini avtomatlashtirish usulini yaratish maqsad qilib qo'yilganligi munosabati bilan bu ishni dasturiy ta'minotini ta'minlash maqsadida suyuqliklar qovushoqligini fizik ma'nolarini eslab o'tish muhim masala hisoblanadi.

Ma'lumki, suyuqliklar ikki turda oqish xususiyatiga ega: birinchisi- laminar oqim, ikkinchisi - turbulent oqim [2]. Nyuton modeliga binoan, suyuqliklar chegarlangan muhitda (masalan-silindr simon naylardan trubalardan, tomirlardan) nisbatan kichikroq tezlikda oqayotgan paytida, laminar oqimni hosil qilishi mumkin, ya'ni oqim qatlam-qatlam bo'lib oqish xususiyatiga egadir (Rasm-1).



Rasm-1

1-rasmdan ko'rinib turibdiki qatlamlarni tezliklari ichki sirtga nisbatan o'zgarib bormoqda, ya'ni  $(dv/dx)$  tezlik gradiyenti xosil bo'lmoqda. Bunday gradiyentni xosil bo'lishi aynan S yuzali qatlamlarni o'zaro ishqalanishga bog'liqdir.

Mazkur ishqalanish - suyuqliklarni qovushoqligini belgilaydi va ishqalanish kuchi quidagi Nyuton tenglamasi bilan aniqlanadi [2]:

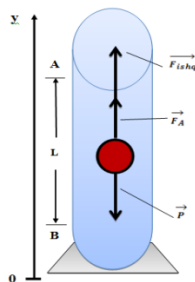
$$F_{ishq} = h (dv/dx) * S \quad (1)$$

bu erda, **h** - qovushoqlik koeffitsienti (ichki ishqalanish) koeffitsienti deyiladi.

Suyuqliklarni qovushoqlik koeffitsienti turli tashqi faktorlarga bog'liqdir. Ayniqsa, organizmdagi biologik suyuqliklarni qovushoqligi haroratga, bosimga suvni miqdoriga va boshqalarga bog'liqdir.

Suyuqliklarni qovushoqligini Sroks usulida aniqlash formulasini ko'rib chiqamiz. Ma'lumki, bu usulda qovushoqlik aniqlanishi lozim bo'lgan suyuqlik silindr-simon shaffof L - uzunlikdagi shisha idishga quyiladi va metall sharchani harakati o'rganiladi (rasm-2).

Suyuqlik ichidagi sharchaga uchta kuch: **P**- og'irlik kuchi, **F<sub>A</sub>** – Arximed kuchi va **F<sub>ishq</sub>** - kuchlari ta'sir qiladi. Statik holat uchun mazkur kuchlarni vector yig'indisini xosil qilib no'lga tenglaymiz (2). Kuchlarni Y-o'qiga nisbatan proyeksiyasini olib (2) formulani skalyar ko'rinishiga olib kelib va uni **h** - qovushoqlik koeffitsientiga nisbatan ychib chiqsak, (3) formulani hosil qilamiz.



Rasm - 1

$$\vec{P} + \vec{F}_A + \vec{F}_{ishq} = 0 \quad (2)$$

$$-\frac{3}{4} \pi r^3 \rho_{sh} g + \frac{3}{4} \pi r^3 \rho_s g + 6\pi r v \eta = 0 \quad (3)$$

$$\eta = \frac{2}{9} \cdot \frac{(\rho_{sh} - \rho_s) r^2 g}{L} \cdot t \quad (4)$$

(3) formulada  $\rho_{sh}$  – metall sharchani zichligi, **r** – sharchani radiusi, **g**- erkin tushish tezlanishi, **L** – metall sharchani shisha nay ichiga quyilgan suyuqlikdagi tekkis harakat masofasi va **t** -metall sharchani, shisha naydagi ikki - **A** va **B** belgilar orasidagi o'tish vaqti. (3) formulani **h** - qovushoqlik koeffitsientiga yechsak, (4) formula hosil bo'ladi.

(4) formuladan ko'rinib turibdiki, tekshirilayotgan suyuqlikning qovushoqligi metall sharchani, shisha naydagi ikki - **A** va **B** belgilar orasidagi o'tish vaqtiga bog'liq bo'lmoqda. Shu munosabat bilan quyidagi belgilashni kiritamiz:

$$\frac{2}{9} \cdot \frac{(\rho_{sh} - \rho_s)}{L} = K$$

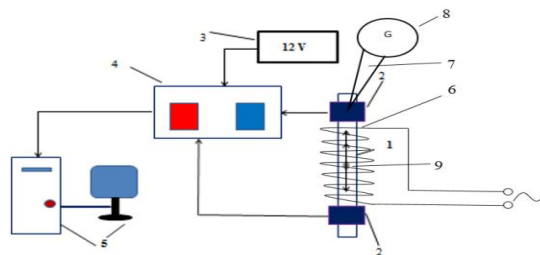
U holda, (4) formulani soddaroq ko'rinishga olib kelamiz:

$$\eta = K(t) \quad (4)$$

Qovushoqlik koeffitsientini topishning (3) formulasini (4) aylantirish orqali, avtomatlashtirilgan laboratoriya ishini dasturiy ta'minotini hosil qilishda qulay imkoniyatlar yaratamiz.

**Tahlil va natijalar.** "Suyuqliklarning qovushoqligini Stoks usulida aniqlash" laboratoriya ishini avtomatlashtirish uskunasi yaratish maqsadida mazkur uskunaning blok sxemasi ishlab chiqildi. (Rasm-3):





Rasm-3

Blok sxema quidagi elementlarda iborat:

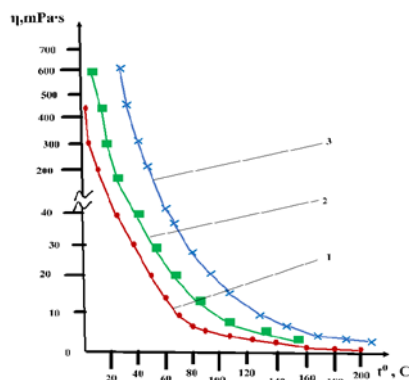
1. Uzunligi 0,5 m va diametrida 0,05 m bo'lgan silindr simon shisha nay.
2. Optoelektron qaytqilgichlar.
3. Tok manbayi (HX-P8045).
4. Interfeys blogi.
5. Pentium-4 rusumli kompyuter jamlamasi.
6. Spiralli qizdirgich.
7. Termojuft.
8. Galvonometr.
9. Metall (po'lat) sharcha.

Ishlab chiqilgan va 3-rasmda tasvirlangan blok sxema yordamida laboratoriya qurilmasi yig'ildi va ishga tushirildi. (4) formulada qayd etilgan qovushoqlik koeffitsienti metall sharchani suyuqlikdagi harakatlanish vaqtiga bogliq ekanligi ko'rsatilgan. An'anaviy usulda [3] mazkur vaqtni aniqlashda o'lchash xatoliklarni ko'lami ancha sezilarli edi. Shuning uchun tadqiqot qilinyotgan bu ishda, aynan yarim o'tkazgichli optoelektron qaytqilgichlar (3-rasmdagi 2-ko'rinish) qo'llanilgan. Qaytqilgichlardan olingan signal 4-interfeys qurilmasiga o'tkaziladi. Interfeys qurilmasidan ma'lumot kompyuter jamlamasining (3-rasmdagi 5-ko'rinish). Shunday qilib, po'lat sharchaning, qovushoqligi aniqlanayotgan suyuqlikdagi harakatlanish vaqtini qiymati kompyuter monitorida aks etadi.

Yuqorida qayd etilgan suyuqliklarning qovushoqligi tashqi faktorlarga bogliqdir. Ayniqsa, bunday omillardan, haroratni oladigan bo'lsak, bu yonalishda tadqiqotlar olib borish va tibbiyot institutlaridagi talabalar uchun ilmiy izlanishlar olib borish dolzarb masala hisoblanadi.

Bunday izlanishlarni olib borish uchun "Suyuqliklarning qovushoqligini Stoks usulida aniqlash" laboratoriya ishini avtomatlashtirish uskunasi shisha nayni spiralli qizdirgichga joylashtirildi (3-rasmdagi 6-ko'rinish). Haroratni o'zgarishi, darajalangan termojuft (3-rasmdagi 7-ko'rinish) yordamida nazorat qilib borildi.

Qovushoqlikni haroratga bog'liqlik tajriba-o'lchash ishlari: paxta moyi (1-ko'rinish), glitsirin (2-ko'rinish) va transformator moyida (3-ko'rinish) olib borildi va quyidagi natijalar olindi (rasm-3):



Rasm-3

Yaratilgan avtomatlashtirilgan laboratoriya uskunasi olib borilgan tadqiqot ishlari natijasida, uchala suyuqliklar uchun ham, qovushoqlikni temperaturaga bog'lanish grafigi  $\eta = f(1/t^0 C)$  qonuniyatni, ya'ni temperatura ortishi bilan o'rganilayotgan suyuqliklarni qovushoqligi kamayib borishini ko'rsatdi. Mazkur holat avtomatlashtirilgan laboratoriya uskunasi o'quv jarayonida va talabalarni ilmiy ishlarida qo'llanilishi mumkinligini isbotlaydi.

Har qanday shaxsiy kompyuterni samarali o'lchash tizimiga aylantirish mumkin. Shundan kelib chiqib, mazkur laboratoriya ishida fizik tajribalarni o'tkazish uchun o'quv jarayonida kompyuterdan o'lchov tizimi sifatida foydalanish hamda mazkur laboratoriya ishini avtomatlashtirish maqsadida Delfi dasturiy ta'minotidan foydalanildi. Dasturiy ishlatish va uskunadagi mikroelektron qurilmalarni ishga tushirish natijasida kompyuter monitorida metall sharchani, shisha naydagi ikki - A va B belgilar orsidagi o'tish t-vaqtni, va talabalarning ro'yxatini aks ettirish imkoniyati yuzaga keldi.

**Xulosa va takliflar.** Suyuqliklarning qovushoqligini Stoks usulida aniqlash" laboratoriya ishini avtomatlashtirishga oid loyiha-blok sxemasi ishlab shiqildi. Suyuqliklarning qovushoqligini Stoks usulida aniqlash" laboratoriya ishini loyiha-blok sxemasi asosida tajriba qurilmasi yaratildi. Yaratilgan avtomatlashtirilgan laboratoriya uskunasi paxta moyi, glitsirin va transformator moylari uchun tadqiqot ishlari olib borildi va qovushoqlikni temperaturaga bog'lanish  $\eta = f(1/t^0 C)$  qonuniyati o'z isbotini topganligi ko'rsatildi. Laboratoriya ishini avtomatlashtirish maqsadida Delfi dasturiy ta'minotidan foydalanildi va bu t-

vaqtini va talabalarning ro'yxatini aks ettirish imkoni yaratdi. Yaratilgan avtomatlashtirilgan laboratoriya uskunasi, tibbiyot institutlaridagi talabalar, biofizika yonalishda, ilmiy izlanishlar olib borishlari taklif etamiz.

#### ADABIYOTLAR

1. Минеев Л.И., Хромова Л.А. Автоматизация физического эксперимента в лабораторном практикуме. Альманах современной науки и образования. №6 (25), 2009, с. 121 – 123.
2. A.N.Remizov. Tibbiy va biologik fizika. T.2006.
3. Sh.A.Gulamov, D.T.Komilova. Biofizika fanidan praktikum. O'quv qo'llanma. Andijon. 2021.
4. Давлетшин Н.Н., Втюрин А.Н., Ципотан А.С., Шамшуринов А.В. Автоматизация физического эксперимента. Лабораторные работы : учебно-методическое пособие. Сиб. федер. ун-т, (СФУ), 2022 (2022-06-16). - 87 с.
5. Хитун В.А., Скляревич Б.Ф., Гофман И.А., Юрьев М.А. Практикум по физике для медицинских вузов., Учебное пособие. М.1972, с.360.
6. Агапов Б.Т., Максютин Г.В., П.И.Островский. Лабораторный практикум по физике., Учебное пособие. М.1982, с.335.
7. Н.А.Ремизов. Практикум по физике., Учебное пособие. М.1958, с.184.
8. J.Nurmatov., M.I.Isroilov., M.Nishonova., A.Avliqulov. Fizika. Laboratoriya ishlari. O'quv qo'llanma. T.2003. b. 286.
9. Sh.A.Gulamov, M.E.Xomidov, G.M.Muminova. Biofizika fanidan laboratoriya ishlari. O'quv qo'llanma. Andijon.2020. b. 119.
10. Gulamov Sh.A. Laboratory work in biophysics. Study Manual. Andijan.2023. p.130.
11. Улуғмуродов Н.Х., Садикова Н.Б., Турсунова З.Б., «Физика», Т., 2019.
12. Улуғмуродов Н.Х. (2-нашр). «Физикадан практикум», М., - Фан, 2014.



UDK: 538.955; 621.3.082.782

**Gafur GULYAMOV**,  
Namangan muhandislik-qurilish instituti professori, f.-m.f.d  
**Ulug‘bek NEGMATOV**,  
Namangan muhandislik-texnologiya instituti tayanch doktoranti  
**Ulug‘bek ERKABOEV**,  
Namangan muhandislik-qurilish instituti professori, f.-m.f.d  
**Nozimjon SAYIDOV**,  
Namangan muhandislik-texnologiya instituti katta o‘qituvchisi  
**Nodirbek NABIJONOV**,  
Namangan davlat universiteti tayanch doktoranti  
E-mail: sayidovnozimjon@gmail.com

NamMQI professori, f.-m.f.d M.Dadamirzayev taqrizi asosida

## NANOSTRUKTURALI YARIMO‘TKAZGICHLARDA OPTIK YUTILISH KOEFFITSIENTINI IKKI O‘LCHAMLI KOMBINIRLANGAN HOLATLAR ZICHLIGIGA BOG‘LIQLIGI

Annotsatsiya

Ushbu ishda, to‘g‘ri zonali nanostrukturali yarimo‘tkazgichlarda magnitooptik yutilish ko‘effitsientlarini haroratga bog‘liqligi tadbiq etilgan. Magnitooptik yutilish ko‘effitsienti ossilyatsiyalarini haroratga bog‘liqligini hisoblashda ikki o‘lchamli kombinirlangan holatlar zichligi  $\alpha_B^{2d}(N_S^{2d}(B), T)$  ossilyatsiyalaridan foydalanilgan. Kvant o‘lchamli to‘g‘ri zonali yarimo‘tkazgichli materiallar uchun  $\alpha_B^{2d}(N_S^{2d}(B), T)$ ni aniqlashning matematik modeli ishlab chiqilgan.

**Kalit so‘zlar:** geterostruktura, nanoo‘lcham, kvant o‘ra, holatlar zichligi, holatlar zichligi, ossilyatsiya, nanoo‘lcham, magnit maydon, ikki o‘lchamli, yarimo‘tkazgichlar.

## DEPENDENCE OF THE OPTICAL ABSORPTION COEFFICIENT IN NANOSTRUCTURED SEMICONDUCTORS ON TWO-DIMENSIONAL COMBINED DENSITY OF STATES

Annotation

In this work, temperature dependence of magneto-optical absorption coefficients in straight-band nanostructured semiconductors was applied. Two-dimensional combined density of states  $\alpha_B^{2d}(N_S^{2d}(B), T)$  oscillations were used to calculate the temperature dependence of magneto-optical absorption coefficient oscillations. A mathematical model for determining  $\alpha_B^{2d}(N_S^{2d}(B), T)$  has been developed for quantum-sized straight-bandgap semiconductor materials.

**Key words:** heterostructure, nanoscale, quantum coil, density of states, density of states, oscillation, nanoscale, magnetic field, two-dimensional, semiconductors.

## ЗАВИСИМОСТЬ КОЭФФИЦИЕНТА ОПТИЧЕСКОГО ПОГЛОЩЕНИЯ В НАНОСТРУКТУРНЫХ ПОЛУПРОВОДНИКАХ ОТ ДВУМЕРНЫХ КОМБИНИРОВАННЫХ ПЛОТНОСТЕЙ СОСТОЯНИЙ

Аннотация

В данной работе применена температурная зависимость коэффициентов магнитооптического поглощения в прямозонных наноструктурных полупроводниках. Двумерная комбинированная плотность состояний  $\alpha_B^{2d}(N_S^{2d}(B), T)$  колебаний была использована для расчета температурной зависимости колебаний коэффициента магнитооптического поглощения. Разработана математическая модель определения  $\alpha_B^{2d}(N_S^{2d}(B), T)$  для квантоворазмерных прямозонных полупроводниковых материалов.

**Ключевые слова:** гетероструктура, наноразмер, квантовая катушка, плотность состояний, плотность состояний, колебание, наноразмер, магнитное поле, двумерность, полупроводники.

**Kirish.** Yorug‘lik nurlarini boshqarish uchun samarali magnitooptik sistemalarni olish va ular asosidagi qurilmalarni yaratish – fotonika, plazmonika, sensorika, spintronika hamda mikro, nano va opto elektronikaning muhim muammolaridan biri hisoblanadi. Nanostrukturali yarimo‘tkazgichlarni zonalar tuzilishini o‘rganish va uni tajribalarda mukammal tekshira olish metodlaridan eng samaralisi magnitooptik effektlar hisoblanadi. Jumladan, har bir materialning ta‘qiqlangan zona kengligini aniqlashning eng ishonchli usuli optik taxlillar yordamida aniqlashdir. Magnitooptik yutilishlardan biri bu zonalararo yutilish mexanizmidir. Zonalararo yutilish qonuniyatini magnitooptik yutilish ko‘effitsienti orqali o‘rganiladi.

**Adabiyotlar tahlili.** Kichik o‘lchamli yarimo‘tkazgichlar va ular asosidagi geterostrukturalarning optik xossalari va xususiyatlarini ifodalaydigan, yorug‘lik chastotasiga bog‘liq bo‘lgan asosiy fizik parametrlari – bu kompleks sindirish ko‘rsatkichi va yorug‘likning yutilish ko‘effitsientlari hisoblanadi [1-2]. Agar yorug‘likning tarqalishi izotrop holatda OX o‘qi bo‘ylab yo‘nalgan bo‘lsa, u holda dispersiya qonuni uchun kompleks sindirish ko‘rsatkichini yorug‘lik vektoriga bog‘liqligi quyidagi ifoda orqali aniqlanadi [3]:

$$F(x, t) = F_0 \exp \left[ i\omega \left( \frac{N(\omega)x}{c} - t \right) \right] \quad (1)$$

Bu yerda,  $F$  – yorug'lik vektori (yorug'likning elektr maydon kuchlanganligi bo'yicha vektori);  $N(\omega) = n(\omega) + iK(\omega)$  – kompleks sindirish ko'rsatkich;  $n(\omega)$  – moddaning sindirish ko'rsatkichi;  $k(\omega)$  – yorug'likning yutilish ko'rsatkichi.

Kombinirlangan holatlar zichligi - bu funksiyaning  $\hbar\omega$  dan  $\hbar\omega + \Delta\hbar\omega$  gacha energiyaga ega bo'lgan fotonlarning yutilishi tufayli energiya va impulsning saqlanish qonunlariga ko'ra valent zona shipi va o'tkazuvchanlik zonasi tub i orasidagi zaryadli zarralarning optik o'tishlari soniga teng. Nanostrukturali yarimo'tkazgichlar uchun kombinirlangan holatlar zichligi yorug'lik chastotasiga bog'liq bo'lgan delta-funksiyalarni qatorga yoyish orqali aniqlanadi [4-5]:

$$\rho_{civj}(\omega) = \sum_k \delta E_{ci}(k) - E_{ci}(k) - \hbar\omega \quad (2)$$

$$\rho_{civj}(\omega) = \frac{d}{d\hbar\omega} \sum_k \theta(\hbar\omega - E_{ci}(k) + E_{vj}(k)) \quad (3)$$

Yuqoridagi ifodalardan ko'rinib turibdiki, hajmiy yoki kichik o'lchamli yarimo'tkazgichlarda yorug'likning yutilish koeffitsientini aniqlashda kombinirlangan holatlar zichligi muxim rol o'ynaydi. Bu keltirilgan ifodalar asosan magnit maydon va harorat ta'siri mavjud bo'lmagan holat uchun o'rinni.

**Tadqiqot metodologiyasi.** Kuchli magnit maydon ta'siridagi kvant o'rali yarimo'tkazgichlarda to'g'ri zonalararo yutilish koeffitsientini haroratga bog'liqligini ko'rib chiqaylik. Bunda, masalani soddaroq yechish uchun, magnit maydon va harorat ta'sirini faqatgina ikki o'lchamli kombinirlangan holatlar zichligi orqali aniqlash maqsadga muvofiq bo'ladi. Yarimo'tkazgichlarning zonalar nazariyasiga ko'ra, magnit maydon ta'siridagi erkin elektronlarning energetik spektri va to'lqin funksiyalarini Shredinger tenglamasini effektiv massa yaqinlashuvida yechimi orqali topiladi, ya'ni:

$$\left\{ -\frac{\hbar^2}{2m^*} \nabla^2 + V(r) \right\} \Psi(r) = E\Psi(r) \quad (4)$$

Bu yerda  $V(r)$  – kuchli magnit maydon ta'siridagi erkin elektron energiyasi.  $Z$  o'qi bo'yicha joylashgan qatlamlarga perpendikulyar bo'lgan kvant o'rali geterostrukturalar uchun (4) tenglama quyidagi ko'rinishga keladi:

$$\left\{ -\frac{\hbar^2}{2m^*} \nabla^2 + V(z) \right\} \Psi(r) = E\Psi(r) \quad (5)$$

(5) tenglamani yechish uchun to'lqin funksiya bilan o'zgaruvchilarni ajratish usulidan foydalaniladi. U holda, (5) tenglamaning yechimi quyidagi ko'rinishga keladi:

$$\Psi_{\mathbf{k}_\perp m}(\mathbf{r}) = \frac{1}{\sqrt{S}} \exp(i\mathbf{k}_\perp \mathbf{r}_\perp) \varphi_m(z) \quad (6)$$

Bu yerda,  $S$  – kvant o'raning  $Z$  o'qiga tik bo'lgan ko'ndalang kesim yuzasi,  $k_\perp = k_{xi} + k_{yj}$  – kvant o'ra tekisligi bo'ylab erkin harakatlanishni ifodalaydigan, ikki o'lchamli to'lqin vektori.

Yuqorida keltirilgan erkin zaryad tashuvchilarning to'lqin funksiyalaridan hamda formulalardan foydalangan holda, kvantlovchi magnit maydon ta'siridagi kvant o'raning valent zonasi shipi va o'tkazuvchanlik zonasi tubidan boshlab hisoblanadigan energiya qiymatlari quyidagicha topiladi:

$$E_c^{2d}(B, d, n_{cz}) = E_c + E_{ci} + \left( N_L^c + \frac{1}{2} \right) \hbar\omega_c^c + \frac{\hbar^2 \pi^2}{2m_c d^2} n_{cz}^2 \quad (7)$$

$$E_v^{2d}(B, d, n_{vz}) = E_v - E_{vi} - \left( N_L^v + \frac{1}{2} \right) \hbar\omega_c^v - \frac{\hbar^2 \pi^2}{2m_v d^2} n_{vz}^2$$

Bu yerda,  $N_L^c, N_L^v$  – kvant o'raning ruxsat etilgan zonasidagi zaryad tashuvchilarning Landau satxlari soni;  $\omega_c^c, \omega_c^v$  – kvant o'raning o'tkazuvchan va valent zonalarida magnit maydonning siklotron chastotasi;  $d$  – kvant o'ra qalinligi;  $n_{cz}^2, n_{vz}^2$  – kvant o'raning o'tkazuvchan va valent zonalarida o'lchamli kvantlash qism-zonasining tartib raqami;  $n_{cz}, n_{vz}$  – mos ravishda  $Z$  o'qi bo'yicha elektronlar va teshiklarning kvantlash satxlari tartib raqamlari; elektron va valent zonalar simmetrik deb faraz qilamiz, u holda,  $n_{cz} = n_{vz} = n_z$  shart bajariladi;  $B$  – magnit maydoni induksiyasi.

Yuqoridagi ifodalarni hisobga olgan holda, to'g'ri zonali kvant o'lchamli yarimo'tkazgichlarning magnitoptik yutilish koeffitsientini harorat va kuchli magnit maydonga bog'liqligini belgilovchi yangi analitik formulani keltirib chiqarish mumkin:

$$\alpha_B^{2d}(\hbar\nu, B, T, d) = \frac{2\pi e^2 |P_{cv}|^2}{nc\epsilon_0 m_0^2 2\pi\nu V} \sum_{ij} |S_{civj}|^2 N_{jds}^{2d}(\hbar\nu, E_{cv}^{2d}(B, T, d, N_L^{cv}, n_z)) \quad (8)$$

yoki

$$\alpha_B^{2d}(\hbar\nu, B, T, d) = \frac{2\pi e^2 |P_{cv}|^2}{nc\epsilon_0 m_0^2 2\pi\nu V} \cdot \frac{eB}{\pi\hbar} \cdot \frac{1}{kT} \cdot \frac{m_{op} S}{2\pi\hbar^2} \times \sum_{ij} |S_{civj}|^2 \sum_{N_L^c, N_L^v, n_z} \exp \left[ -\frac{\left( \hbar\nu - \left( E_g^{2d}(0) + \left( N_L^c + \frac{1}{2} \right) \hbar\omega_c^c + \left( N_L^v + \frac{1}{2} \right) \hbar\omega_c^v + \frac{\hbar^2 \pi^2}{2m_{cv}^* d^2} n_z^2 \right) \right)^2}{(kT)^2} \right] \quad (9)$$

bu yerda,  $m_{op}$  – zaryadli zarralarning optik effektiv massasi, ya'ni:

$$\frac{1}{m_{op}} = \frac{1}{m_n} + \frac{1}{m_p}$$

Agar,  $S/V = a^{-1}$  va  $A_{cv}^{2d} \approx \frac{m_{op} e^2 |P_{cv}|^2}{nc\epsilon_0 m_0^2 \hbar a}$  kabi o'zgarmas kattaliklar kiritib olinsa, (9) ifoda qo'yidagi ko'rinishga keladi:

$$\alpha_B^{2d}(\hbar\nu, B, T, d) = A_{cv}^{2d} \cdot \frac{\omega_s}{\omega_{op}} \cdot \frac{1}{kT} \times \sum_{ij} |S_{civj}|^2 \sum_{N_L^c, N_L^v, n_z} \exp \left[ -\frac{\left( \hbar\nu - \left( E_g^{2d}(0) + \left( N_L^c + \frac{1}{2} \right) \hbar\omega_c^c + \left( N_L^v + \frac{1}{2} \right) \hbar\omega_c^v + \frac{\hbar^2 \pi^2}{2m_{cv}^* d^2} n_z^2 \right) \right)^2}{(kT)^2} \right] \quad (10)$$

Magnit maydon induksiyasi nolga yaqinlashib borsa, (10) formula, magnit maydon ta'siri mavjud bo'lmagandagi kvant o'ralar uchun optik yutilish koeffitsienti ifodasiga qaytadi va u qo'yidagi ko'rinishga keladi:

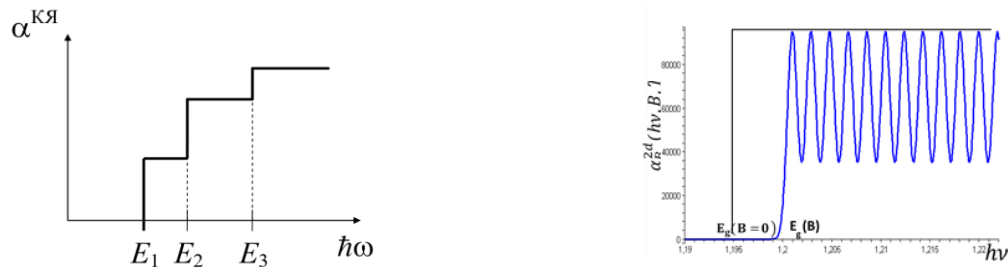
$$\alpha_{cv}^{KYa}(\omega) = A_{cv}^{KYa} \cdot \sum_{\beta} |S_{cv\beta}^{KYa}|^2 \theta(\hbar\omega - E_{cv\beta}) \quad (11)$$

Bu yerda,  $S_{cv}^{ko}$  - bir o'lchovli kvant o'rasi zona ostilari orasidagi zonalararo optik o'tish ehtimoli uchun qo'shimcha tanlab olish qoidalarini belgilaydigan og'ish funksiyalarining bir-birini qoplash integrali. Magnit maydon ta'sirida, ushbu kattalikni o'zgarmas deb olinadi, sababi bu kattalik ossilyatsiya jarayonlarida deyarli o'zini namoyon etmaydi.

**Tahlil va natijalar.** (11) formulaga ko'ra, magnit maydon ta'sir etmagandagi to'g'ri zonali kvant o'rali yarimo'tkazgichlarda zonalararo optik yutilish koeffitsientini yutilayotgan fotonning energiyasiga bog'liqligi "zinasimon" shaklda bo'ladi (1 - rasm).

1 (a)-rasm, magnit maydon ta'siri mavjud bo'lmaganda, kvant o'rali yarimo'tkazgichning yutilish koeffitsientini yutilayotgan foton energiyasiga bog'liqligi namoyon etilgan. Endi, ushbu fizik jarayonlarga kvantlovchi magnit maydonning ta'sirini ko'rib chiqaylik. Bunda, biz albatta, taklif qilayotgan (10) formuladan foydalanamiz. To'g'ri zonali kvant o'rali yarimo'tkazgichli materialni tanlab olaylik. [3] ishda, *InGaAs* kvant o'rali fotoelementning (*InGaAs/GaAs*) fotoelektrik xossalari samaradorligini SimWindows dasturi yordamida modeli ishlab chiqilgan. Bunda, *InGaAs* kvant o'rali qalinligi 9 nm va ta'qiqlangan zona kengligi 1.2 eV ga ( $d=9$  nm bo'lganda) tengligi keltirilgan. Lekin, bu ishda ushbu materialga magnit maydonning ta'siri o'rganilmagan. Agar, magnit maydonni qiymatini 9 Tl, haroratni 8 K deb olsak ( $\hbar\omega_c \gg kT$ ), u holda yuqorida keltirilgan faktlarga asoslanib, (10) formula yordamida 1 (b)-rasm, dagi grafikni quramiz.

1 (b)-rasm, Landau sathlari soni 12 ga teng bo'lib, uni 1(a)-rasm, dan farqi, 9 Tl magnit maydon induksiyasi ta'sirida *InGaAs* kvant o'rali yutilish koeffitsientini ossilyatsiyalanish jarayonlari yaqqol kuzatilmoqda. Ossilyatsiya jarayonlari 1(a)-rasm, da keltirilgan  $E_1$  energiyadan keyingi Landau sathlari hisoblanadi. Ya'ni, 1(a)-rasm, dagi birinchi va ikkinchi "zinasimon" energetik spektrlar orasidagi diskret Landau sathlari soni 1 (b)-rasm, da keltirilgan. Sababi, (10) formula  $n_z=1$  (o'lchamli kvant soni) deb hisoblangan. Bizni matematik modelni asoslash uchun birinchi o'lchamli kvantlar sonidan keyingi Landau sathlarini olish yetarli hisoblanadi.



1 – rasm. a) Magnit maydon mavjud bo'lmagan va b) Magnit maydon mavjud bo'lgan kvant o'rali yarimo'tkazgichlarda optik yutilish koeffitsientini yutilayotgan fotonning energiyasiga bog'liqligi. Bunda,  $T=8$  K,  $B=9$  Tl,  $d=9$  nm,  $E_g(d=9 \text{ nm})=1.2$  eV.

Bundan tashqari, 1 (b)-rasm, dan ko'rinish turibdiki, kvantlovchi magnit maydon ta'siridagi kvant o'rali yutilish koeffitsientini foton energiyasi  $h\nu=1.209$  eV ga teng bo'lganda (qizil chegara), ossilyatsiyalanish jarayoni boshlanmoqda. Bundan xulosa qilish mumkinki, (11) da keltirilgan  $E_1$  energiya 0.09 eV ga siljimoqda.

**Xulosalar.** To'g'ri zonali kvant o'ra asosidagi yarimo'tkazgichli materiallarning optik yutilish koeffitsientiga harorat va magnit maydonning ta'siri tadqiq etildi. Kombinirlangan holatlar zichligi ossilyatsiyalari qonuniyatidan magnitoptik yutilish mexanizmini aniqlashning yangi metodi taklif etildi. Kvant o'rali to'g'ri zonali yarimo'tkazgichli strukturalarning magnitoptik yutilish koeffitsientining harorat, magnit maydon va kvant o'rali qalinligiga bog'liqligini hisoblovchi yangi matematik model ishlab chiqildi. Taklif etilayotgan model asosida, o'zgarish past haroratlardagi magnitoptik yutilish koeffitsientini yuqori haroratlarda oralig'ida ossilyatsiyalarning o'zgarish dinamikasi mukammal tushuntirildi.

#### ADABIYOTLAR

1. Л.С. Бовкун, К.В. Маремьянин, А.В. Иконников, К.Е. Спириин, В.Я. Алешкин, М. Potemski, В. Piot, М. Orlita, Н.Н. Михайлов, С.А. Дворецкий, В.И. Гавриленко. Магнитооптика квантовых ям на основе HgTe/CdTe с гигантским расщеплением Рашби в магнитных полях до 34 Тл // Физика и техника полупроводников, 2018, том.52, вып.11, стр. 1274-1279.
2. С.В. Томилин, В.Н. Бержанский, А.Н. Шапошников, А.Р. Прокопов, А.В. Каравайников, Е.Т. Милукова, Т.В. Михайлова, О.А. Томилина. Вертикальное смещение магнитооптической петли гистерезиса в магнитоплазмонном нанокompозите // Физика твердого тела, 2020, том 62, вып. 1. Стр. 101-109.
3. Л.Е. Воробьев, Е.Л. Ивченко, Д.А. Фирсов, В.А. Шальгин. Оптические свойства наноструктур: Учеб. Пособие // Под ред. Е.Л. Ивченко и Л.Е. Воробьева. СПб.: Наук, 2001.–188 с.
4. G. Gulyamov, U.I. Erkaboev, P.J. Baymatov, A.G. Gulyamov. The effect of pressure on the magneto-absorption in narrow-gap semiconductors. International scientific journal for alternative energy and ecology. 2017. № 07-09. pp. 112-120. <http://dx.doi.org/10.15518/isjaee.2017.07-09.112-120>
5. G. Gulyamov, U.I. Erkaboev, P.J. Baymatov. Simulation of energy dependence of the photon absorption on the magnetic field in semiconductors. International scientific journal for alternative energy and ecology. 2016. № 19-20. pp. 130-138. <http://dx.doi.org/10.15518/isjaee.2016.19-20.130-138>





UDK: 538.955; 621.3.082.782

**Muzaffar DADAMIRZAYEV,**  
Namangan muhandislik- texnologiya instituti tayanch doktoranti  
**Ulug‘bek ERKABOYEV,**  
Namangan muhandislik-texnologiya instituti professori, f.-m.f.d  
Namangan muhandislik-qurilish instituti  
E-mail: muzaffardadamir81@gmail.com

NamMTI professori, f.-m.f.d R.Ikramov taqrizi asosida

### ВЫЧИСЛЕНИЕ ТЕМПЕРАТУРНАЯ ЗАВИСИМОСТЬ ЭНЕРГЕТИЧЕСКИЙ СПЕКТР НОСИТЕЛЕЙ ЗАРЯДОВ В ПОЛУПРОВОДНИКАХ ПРИ ВОЗДЕЙСТВИИ СИЛЬНОГО МАГНИТНОГО ПОЛЯ

Аннотация

Для не квадратичный закон дисперсии вычислена энергетический спектр свободных дырок в сильном магнит поле. Исследовано температурная зависимость уширения уровней Ландау дырок кристаллов с Кейновским законом дисперсии. Предложена новая метод расчета дискретный энергетический спектр в квантующем магнитном поле.

**Ключевые слова:** магнитное поле, свободных дырок, циклотронная частота, модель Кейна, эффективная масса, плотность состояний.

### CALCULATION THE TEMPERATURE DEPENDENCE THE ENERGY SPECTRUM OF CHARGE CARRIERS IN SEMICONDUCTORS EXPOSED TO A STRONG MAGNETIC FIELD

Annotation

The energy spectrum of free holes in a strong magnetic field is calculated for a non-quadratic dispersion law. The temperature dependence of the broadening of the Landau levels of holes in crystals with the Kane dispersion law has been studied. A new method for calculating the discrete energy spectrum in a quantizing magnetic field is proposed.

**Keywords:** Magnetic field, free holes, cyclotron frequency, Kane model, effective mass, density of states.

### KUCHLI MAGNIT MAYDON TA‘SIRDA YARIMO‘TKAZGICHLARDAGI ZARYDA TASHUVCHILARNING ENERGETIK SPEKTRIGA XARORATNI BOG‘LIQLIGINI HISOBLASH

Аннотасија

Kvadrat bo‘lmagan dispersiya qonuni uchun kuchli magnit maydondagi erkin kovaklarning energetik spektri hisoblanadi. Keyn dispersiya qonuni bilan kristallardagi teshiklarning Landau sathlarini kengayishi haroratga bog‘liqligi o‘rganildi. Kvantlovchi magnit maydonda diskret energetik spektrni hisoblashning yangi usuli taklif qilingan.

**Kalit so‘zlar.** Kvantlovchi magnit maydon, erkin kovak, siklatron chastotasi, Keyn modeli, effektiv massa, holatlar zichligi.

**Kirish.** [1, 2] da kvantlovchi magnit maydonlarda holatlar zichligining haroratga bog‘liqligi Landau sathining issiqlik kengayishi natijasida ko‘rib chiqildi. Ushbu ishda suyuq azot haroratida past haroratlarda o‘lchanadigan holatlar zichligining uzluksiz spektri Landau diskret sathlariga aylanishini ko‘rilgan. Holatlar zichligining uzluksiz spektrining eksperimental qiymatlaridan foydalangan holda jarayonlarni matematik modellashtirish Landau diskret sathlarini hisoblash imkonini beradi.

[3] ishda suyuq azot haroratida kuchli magnit maydondagi energetik holatlar zichligi aniqlangan. Ushbu ishlarda tajriba (eksperiment) natijalari tor zonali yarimo‘tkazgichlarda Keyn modeli bilan taqqoslangan. Bu ishlarda kvantlovchi magnit maydonida energetik holatlar zichligiga haroratning ta‘siri ko‘rilmagan.

Ushbu ishning maqsadi kuchli magnit maydon ta‘sirida yarim o‘tkazgichlarda zaryad tashuvchilarning energiya spektrining haroratga bog‘liqligini hisoblashdir.

**Metodlar.** Magnit maydon ta‘sirida parabolik dispersiya qonuniga asosan spinsiz erkin elektronning kvant holatini birinchi marta Landau [4] tomonidan o‘rganilib, metall diamagnetizm nazariyasini ishlab chiqdi. Magnit maydon va osillator tipidagi qo‘shimcha potentsial ta‘sirida elektronning energiya spektri Fock [5] va Darvin [6] tomonidan o‘rganilgan.

Spin-orbital bog‘lanishni hisobga olgan holda spinli elektroni Landau kvantlashni birinchi marta Rashba tomonidan yarimo‘tkazgichlarda o‘tkazuvchanlik elektronlarining ikki diapazonli modeliga asoslangan holda amalga oshirildi [7].

Gamiltonianning diagonal elementlari  $\hbar^2 k^2/2m$  parabolik dispersiya qonuni bilan ifodalangan, diagonal bo‘lmagan elementlar esa birinchi tartibli nosimmetrik shartlari  $k_{\pm} = k_x \pm i k_y$  ga proporsional edi, bu erda  $\vec{k}$ - 3D kristalidagi elektronning to‘lqin vektori. [7] dagi Spin-orbital bog‘lanish va nosimmetrik shartlari z o‘qi bo‘ylab yo‘naltirilgan magnit maydonga parallel bo‘lgan tashqi elektr maydoni  $E_z$  tomonidan generatsiyalanadi. Elektronning to‘lqin funktsiyasi z o‘qi bo‘ylab ikkita yo‘nalishga mos keladigan ikkita komponent bilan spinor shaklida yozilgan. Landau kvantlash energiya sathlari turli spin proyeksiyalariga mos keladigan ikkita n va n' kvant sonlari bilan tavsiflanadi va energetik hosilaning birinchi tartibida 1 ga farqlanadi [7]. Bu [8] da isbotlangan va quyida ko‘rsatib o‘tiladi, umumiy qoida n va n' qiymatlari o‘rtasidagi farqlar energetik sathlar tartiblariga teng: ular uchinchi tartibli energetik sathlar uchun 3 ga va ikkinchi tartibli energetik sathlar uchun 2 ga teng. Rashba tomonidan taklif qilingan usul, [8] da 2D og‘ir kovaklarining Landau kvantlanishini uchinchi tartibli energetik hosilasi nuqta nazaridan tavsiflash uchun qo‘llanilgan va quyida psevdospin komponentlari va ikkinchi tartibli energetik hosilasi bo‘lgan 2D elektroni ko‘chirilgan va ko‘chirilmagan ikki qatlamli grafen namunalariida ko‘rib chiqishda qo‘llaniladi [9].

**Nazariya.** Magnit maydonda Keyn dispersiya qonuni bilan energetik holatlar zichligini aniqlash. Energetik sathlarning spin bo'linishini hisobga olgan holda magnit maydonda kvadratik dispersiya qonuniga ega bo'lgan erkin kovaklarning energiyasi quyidagi ko'rinishda ifodalanadi [10]:

$$E_n^v = \hbar\omega_c^v \left( n_c + \frac{1}{2} \right) + s\mu_B B + \frac{\hbar^2 k_z^2}{2m_e} \quad (1)$$

Bu yerda,  $\omega_c^v$  - kovaklarning siklotron chastotasi,  $\mu_B$  Bor magnetoni, B - magnit maydon induksiyasi.

Magnit maydonda parabolik zona uchun holatlar zichligi quyidagi ifoda bilan ifodalanadi

$$N_H(E, H) = \frac{1}{4\pi^2} \left( \frac{2m^*}{\hbar^2} \right)^{3/2} \hbar\omega_H \sum_n \left( E - \left( n + \frac{1}{2} \right) \hbar\omega_H \right)^{-1/2} \quad (2)$$

Agar energiyaning to'liqin vektoriga bog'liqligi kvadratik funksiya bilan tasvirlanmagan bo'lsa, masalan, InSb dagi elektronlar uchun magnit maydondagi zaryad tashuvchilarning energiya sathlari teng masofada emas, chunki siklotron massasi quyidagi ifoda bilan aniqlanadi.

$$m_c = \frac{\hbar}{2\pi} \frac{\partial S}{\partial E} \quad (3)$$

shuning uchun siklotron chastotasi E va  $k_z$  ga bog'liq.

III-V va II-VI birikmalardagi o'tkazuvchanlik zonasining parabolik bo'lmagan tabiati o'tkazuvchanlik zonasi va uchta valentlik zonalari o'rtasidagi o'zaro ta'sir natijasida yuzaga keladi. Magnit maydonda uchta energetik zona uchun energetik sathlar (ular bilan o'zaro ta'sir qilmaydigan og'ir kovak zonasi bundan mustasno) kubik tenglama bilan berilgan [11]:

$$E_{N\pm} (E_{N\pm} + E_g) (E_{N\pm} + E_g + \Delta) - P^2 \left( k_z^2 + (2N+1) \frac{1}{L^2} \right) * \left( E_{N\pm} + E_g + \frac{2}{3} \Delta \right) \pm \frac{P^2 \Delta}{3L^2} = 0 \quad (4)$$

Bu yerda,  $E_{N\pm}$  -kvantlovchi magnit maydondagi spinni hisobga olgan holda elektronlarning o'tkazuvchanlik zonalaridagi energiyasi;  $E_g$  -taqiqlangan zona kengligi,  $\Delta$ -Spin-orbitaning bo'linish qiymati, P - matritsa elementi.

Bizning ishimizda tor tirqichli yarimo'tkazgichlar ko'rib chiqiladi va elektronlar quyidagi shartlarda Keyn dispersiya qonuniga ega bo'ladi [12]:

$$\left\{ \begin{array}{l} E(p) - E_c \ll E_g + \frac{2}{3} \Delta \\ \frac{2}{3} \Delta \gg E_g \end{array} \right\}$$

Ushbu shartdan kubik tenglama (4) kvadratik tenglamaga keltiriladi, uning yechimi o'tkazuvchanlik zonasining elektronlari uchun quyidagi ifoda orqali ifodalanadi

$$E_N^c = -\frac{E_g}{2} + \frac{1}{2} \sqrt{E_g^2 + 4E_g \left[ \left( N + \frac{1}{2} \right) \hbar\omega_c^c + \frac{\hbar^2 k_z^2}{2m_n^*} \pm \frac{g_0 \mu_B H}{2} \right]} \quad (5)$$

Xuddi shu tarzda, valent zonadagi yengil kovaklar uchun quyidagi ifoda olingan:

$$E_g = E_N^c - E_N^v; E_N^v = E_N^c - E_g$$

$$E_N^v = -\frac{3E_g}{2} + \frac{1}{2} \sqrt{E_g^2 + 4E_g \left[ \left( N + \frac{1}{2} \right) \hbar\omega_c^v + \frac{\hbar^2 k_z^2}{2m_p^*} \right]}$$

(6)

(6) ifoda faqat tor zonali yarimo'tkazgichlar uchun amal qiladi.

Endi ikkita Landau satxlar orasidagi energiyaga ega bo'lgan holatlar sonini topamiz.

Energiyalari farq qiladigan ikkita izoenergetik sirtning bo'lirlari orasidagi farqni aniqlaymiz  $\Delta E = \hbar\omega_c^v$ :

Energiyalari farq qiladigan ikkita izoenergetik sirtning bo'lirlari orasidagi farqni aniqlaymiz

$$\Delta S = \frac{2\pi m_p}{\hbar^2} \Delta E = \frac{2\pi m_p}{\hbar^2} \hbar\omega_c^v$$

Sikl shartlariga ko'ra kvantlash uchun,  $k_x k_y$  tekisligida maydon birligiga to'g'ri keladigan holatlar soni  $\frac{L_x L_y}{(2\pi)^2}$  ga

teng. Ikki kvant orbita orasidagi holatlar soni

$$\frac{L_x L_y}{(2\pi)^2} \Delta S = \frac{m\omega_c^v}{2\pi\hbar} L_x L_y$$

(6) tenglamadan biz spinni hisobga olmasdan  $k_z$  ni aniqlaymiz:

$$\left(E_N^v + \frac{3E_g}{2}\right)^2 = \frac{1}{4} \left[ E_g^2 + 4E_g \left( \left(N + \frac{1}{2}\right) \hbar\omega_c^v + \frac{\hbar^2 k_z^2}{2m_p^*} \right) \right]$$

$$k_z = \frac{(2m_p^*)^{1/2}}{\hbar} \left( \frac{(E_N^v + 2E_g)(E_N^v + E_g)}{E_g} - \left(N + \frac{1}{2}\right) \hbar\omega_c^v \right)^{1/2} \quad (7)$$

Endi magnit maydon ta'sirida parabolik bo'lmagan dispersiya qonuniga ega bo'lgan holatlar zichligini hisoblaylik. Elektronning harakati z o'qi bo'ylab erkin va  $k_z$  bo'ylab kvantlanmaydi. Ya'ni:

$$k_z = \frac{2\pi}{L_z} n_z \quad (8)$$

(7) va (8) ifodalarga ko'ra,  $\left(N + \frac{1}{2}\right) \hbar\omega_c^v$  E energiya oralig'idagi holatlar soni:

$$n_z = \frac{L_z k_z}{2\pi}$$

$$n_z = \frac{L_z \sqrt{2m_p^*}}{2\pi\hbar} \left( \frac{(E_N^v + 2E_g)(E_N^v + E_g)}{E_g} - \left(N + \frac{1}{2}\right) \hbar\omega_c^v \right)^{1/2}$$

$$n_z = \frac{L_z \sqrt{2m_p^*}}{2\pi\hbar} \left( \frac{(E_N^v)^2 + 3E_N^v E_g + 2E_g^2}{E_g} - \left(N + \frac{1}{2}\right) \hbar\omega_c^v \right)^{1/2}$$

$$n_z = \frac{L_z \sqrt{2m_p^*}}{2\pi\hbar} \left( \frac{(E_N^v)^2}{E_g} + 3E_N^v + 2E_g - \left(N + \frac{1}{2}\right) \hbar\omega_c^v \right)^{1/2} \quad (9)$$

Energiyalari E dan kichik bo'lgan hajmiy kvant holatlarining umumiy soni:

$$N^v(E_N^v) = \frac{L_x L_y L_z 2^{1/2} m_p^{*3/2}}{4\pi^2 \hbar^3} \hbar\omega_c^v \sum_{N=0}^{N_{max}} \left( \frac{(E_N^v)^2}{E_g} + 3E_N^v + 2E_g - \left(N + \frac{1}{2}\right) \hbar\omega_c^v \right)^{1/2}$$

(10)

Natijada, magnit maydonda Keyn dispersiya qonuni bilan spinni hisobga olmagan holda, hajm birligidagi energetik holatlar zichligini aniqlaymiz:

$$N_S^v(E_N^v, H) = \frac{dN^v(E)}{dE_N^v}$$

Hajm birligida  $L_x L_y L_z = 1$

$$N_S^v(E_N^v, H) = \frac{2^{1/2} m_p^{*3/2}}{4\pi^2 \hbar^3} \frac{\hbar\omega_c^v}{2} \sum_{N=0}^{N_{max}} \frac{\frac{2E_N^v}{E_g} + 3}{\left( \frac{(E_N^v)^2}{E_g} + 3E_N^v + 2E_g - \left(N + \frac{1}{2}\right) \hbar\omega_c^v \right)^{1/2}}$$

$$N_S^v(E_N^v, H) = \frac{3}{2} \frac{2^{1/2} m_p^{*3/2}}{4\pi^2 \hbar^3} \hbar\omega_c^v \sum_{N=0}^{N_{max}} \frac{\frac{2E_N^v}{3E_g} + 1}{\left( \frac{(E_N^v)^2}{E_g} + 3E_N^v + 2E_g - \left(N + \frac{1}{2}\right) \hbar\omega_c^v \right)^{1/2}}$$

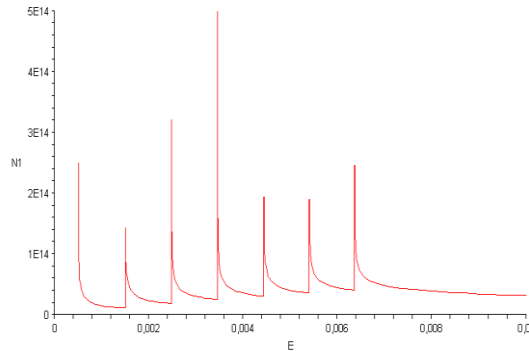
(11)

$$E_N^v = E_N^c - E_g$$

$$N_S^v(E_N^v, H) = \frac{3}{2} \frac{2^{1/2} m_p^{*3/2}}{4\pi^2 \hbar^3} \hbar \omega_c^v \sum_{N=0}^{N_{max}} \frac{\frac{2(E_N^c - E_g)}{3E_g} + 1}{\left( \frac{(E_N^c - E_g)^2}{E_g} + 3(E_N^c - E_g) + 2E_g - \left(N + \frac{1}{2}\right) \hbar \omega_c^v \right)^{1/2}} \quad (12)$$

Bu yerda,  $N_S^v(E_N^v, H)$  - kvant magnet maydonda Keyn dispersiya qonuni bo'yicha energetik holatlar zichligi.

$E_g \rightarrow \infty$  da (11) ifoda parabolik dispersiya qonuni (2) ga aylanadi. Bu ifoda energetik sathlarning harorat kengayishini hisobga olmaydi.



1-Rasm. Kvant magnet maydonda Keyn dispersiya qonuni bo'yicha valent zonadagi kovaklarni energetik holatlar zichligi

**Xulosa.** Kuchli magnet maydon ta'sirida yarimo'tkazgichlarda zaryad tashuvchilarning energiya spektrining haroratga bog'liqligini hisoblash uchun formula olingan. Kvadrat bo'lmagan dispersiya qonuni uchun kuchli magnet maydondagi erkin kovaklarning energiya spektri hisoblanadi. Keyn dispersiya qonuni bilan kristallardagi kovaklarning Landau sathlarining kengayishining haroratga bog'liqligi o'rganildi. Kvantlovchi magnet maydonda diskret energiya spektrini hisoblashning yangi usuli taklif qilingan.

#### ADABIYOTLAR

1. G. Gulyamov, U.I.Erkaboev, N.Yu.Sharibaev. Effect of temperature on the thermodynamic density of states in a quantizing magnetic field. *Semiconductor (springer)*, (2014) 48 (10), pp.1323-1328
2. G. Gulyamov, U.I.Erkaboev, N.Yu.Sharibaev. Simulation of the temperature dependence of the density of states in a strong magnetic field. *Journal of Modern Physics*. (2014) 5(8), pp.680-685. <http://dx.doi.org/10.4236/jmp.2014.58079>
3. Yu.I. Ravich, V. A. Efimova, I.A. Smirnov. *Investigation methods of semiconductors in application to plumbum halcogenids PbTe, PbSe and PbS* (Nauka, Moscow, 1968) ch.5, p.229 [in Russian].
4. L.D. Landau, *Z. Phys.* 64 (1930) 629; L.D. Landau, *Collection of Papers*, vol. 1, Nauka, Moscow, 1969 p. 47 (in Russian).
5. V. Fock, *Z. Phys.* 47 (1928) 446.
6. C.G. Darwin, *Math. Proc. Cambridge Philos. Soc.* 27 (1931) 86.
7. E.I. Rashba, *Fiz. Tverd. Tela (Leningrad)* 2 (1960) 1224 [Sov. Phys. Solid State 2 (1960) 1109].
8. T. Hakioglu, M.A. Liberman, S.A. Moskalenko, I.V. Podlesny, *J. Phys.: Condens. Matter*. 23 (2011) 345405.
9. Eduardo V. Castro, K.S. Novoselov, S.V. Morozov, N.M.R. Peres, J.M.B. Lopes dos Santos, Johan Nilsson, F. Guinea, A.K. Geim, A.H. Castro Neto, *J. Phys.: Condens. Matter* 22 (2010) 175503.
10. N.B. Brandt, V.A. Kulbachinsky. *Quasiparticles in condensed matter physics*. (Fizmatlit, Moscow, 2007) ch.6, p.283 [in Russian].
11. I.M. Tsidilkovsky. *Electrons and holes in semiconductors*. (Nauka, Moscow, 1972) ch.5, p.457 [in Russian].
12. I.S. Dubitskiy, A.M. Yafyasov. On the field effect in thin films of semiconductors with Kane's charge-carrier dispersion relation. *Semiconductor (springer)*, (2014) 48 (3), pp.312-319.



UDK: 538.945.9

**Davron DJURAYEV**,  
Professor of Bukhara State University, d.ph-m.s  
**Akmal TURAYEV**,  
Associate Professor of Bukhara State University, PhD  
**Ozodjon TURAYEV**,  
Doctoral student of Bukhara State University  
E-mail: [ozodjonturayev@gmail.com](mailto:ozodjonturayev@gmail.com)

Based on the review of L.N. Niyazov, associate professor of the Bukhara State Medical Institute, PhD

## INVESTIGATION OF THE STRUCTURE, SURFACE STATE AND ELECTROPHYSICAL PARAMETERS OF BSCCO CUPRATE

Annotation

In this article, the available technologies for the production of bismuth-based cuprates belonging to the BSCCO (Bismuth Strontium Calcium Copper Oxide) family are studied. As a result of scientific research, the production technology of cuprate based on the formula  $\text{Bi}_2\text{Sr}_2\text{CaCu}_2\text{O}_x$  and its physical characteristics were studied. In this case, the composition of the Bi-(2212) sample was checked by the Raman spectroscopy method, a chemical imaging analysis of its structure was obtained, and the dependence of electrical resistance on temperature was studied.

**Key words:** Bismuth-based cuprate, Bi-(2212), Raman spectroscopy, solid-state reaction, electrical probe, chemical imaging.

## BSCCO KUPRATINING TUZILISHI, SIRT HOLATI VA ELEKTROFIZIK PARAMETRLARINI O‘RGANISH

Annotatsiya

Ushbu maqolada BSCCO (vismut stronsiy kalsiy mis oksidi) oilasiga tegishli vismut asosidagi supratlarni ishlab chiqarishning mavjud texnologiyalari o‘rganiladi. Ilmiy-tadqiqotlar natijasida  $\text{Bi}_2\text{Sr}_2\text{CaCu}_2\text{O}_x$  formulasi asosida kupratlar tayyorlash texnologiyasi va uning fizik xarakteristikalarini o‘rganildi. Bunda Bi-(2212) namunasining tarkibi Raman spektroskopiyasi usuli yordamida aniqlandi, uning sirt holati kimyoviy tasvirlash tahlili bilan tekshirildi va elektr qarshiligining haroratga bog‘liqligi o‘rganildi.

**Kalit so‘zlar:** vismut asosli kuprat, Bi-(2212), Raman spektroskopiyasi, qattiq holat reaksiyasi, elektr zond, kimyoviy tasvir.

## ИССЛЕДОВАНИЕ СТРУКТУРЫ, СОСТОЯНИЯ ПОВЕРХНОСТИ И ЭЛЕКТРОФИЗИЧЕСКИХ ПАРАМЕТРОВ КУПРАТА BSCCO

Аннотация

В данной статье изучены доступные технологии производства купратов на основе висмута, принадлежащих к семейству BSCCO (Bismuth Strontium Calcium Copper Oxide). В результате научных исследований изучена технология производства купрата на основе формулы  $\text{Bi}_2\text{Sr}_2\text{CaCu}_2\text{O}_x$  и его физические характеристики. При этом был проверен состав образца Bi-(2212) методом рамановской спектроскопии, получен химико-визуальный анализ его структуры и изучена зависимость электрического сопротивления от температуры.

**Ключевые слова:** купрат висмута, Bi-(2212), рамановская спектроскопия, твердотельная реакция, электрический зонд, химическая визуализация.

**Introduction.** Bi-based superconductor (BSCCO) was discovered around 1988 [1], and those materials have been investigated extensively in recent years. One of the most important areas of application of bulk HTS is represented by the electric power, in particular current leads for LTS devices to reduce refrigeration loads and fault-current limiters as superconducting screens. Bi-(2212) is an elective material for those applications due to its resistance to environmental degradation and its relatively easy workability. Nevertheless the preparation of high purity Bi-(2212) powders is still a limiting factor in the production and industrialization of this material, in addition powder's characteristics strongly affect the process parameters and the designed final properties [5]. The Bi-(2212) superconductor family contains three phases having the generalized chemical formula  $\text{Bi}_2\text{Sr}_2\text{Ca}_{n-1}\text{Cu}_n\text{O}_{2n+4+x}$  where  $n = 1, 2$  and  $3$  (where  $n$  is referring to the number of  $\text{CuO}_2$  layers in the crystal structure) [2–3]. Bi-(2212) was the first high-temperature superconductor containing various oxides. Superconductivity in such cuprates is due to the copper atoms in the nodes of the crystal lattice and the cavities formed from them. It has general formula  $\text{Bi}_2\text{Sr}_2\text{Ca}_{n-1}\text{Cu}_n\text{O}_{2n+4+x}$  with specific transition temperature ranging from  $T_c=20$  K ( $n=1$ , 2201 phase), 85 K ( $n=2$ , 2212 phase), 110 K ( $n=3$ , 2223 phase) and 104 K ( $n=4$ , 2234 phase) [4].

**Experimental methods.** We analyzed several methods of the world's researchers for the synthesis of samples and its research, and used the most current methods for synthesis and study of samples.

**Synthesis method.** BSSSO composition can be prepared using several different methods. Examples include solid state, sol-gel, wet chemical, and melt quenching. We used a solid-state reaction method to obtain a sample of Bi-(2212). The solid-state reaction method is one of the most widely used methods for the preparation of high-temperature and crystalline solids. At room temperature, solids do not naturally react with each other, and in order to do so, they must be heated to a much higher temperature. [6] In the process of synthesis, oxide substances are first taken as a basis. The required amount of chemical products is measured with high precision and ground into a fine powder using an agate mortar. The reaction starts spontaneously during



mixing, as the temperature rises, the reaction accelerates, the crystal lattice begins to form, and the excess carbon and oxygen contained in the oxides are released into the air in the form of carbon dioxide. Mixing the powder is repeated several times. Prolonged mixing of the components is a very important factor for the correct formation of the crystal lattice [9].

**Methods of sample research.** Raman spectroscopy probes molecular and crystal lattice vibrations and is therefore very sensitive to molecular structures, chemical environment, bonding, and crystal morphology. Changes in the parameters of Raman modes: wave numbers, polarization, width, band shape and their intensity can reveal any structural changes. Raman intensity measurements are mainly used to identify different phases in the material, to quantitatively assess the degree of crystallization [10]. We used laser Raman spectroscopy to study the Bi-(2212) sample. In this case, the laser light interacts with molecular vibrations and other excitations in the system, as a result of which the energy of the laser photons is shifted up or down. Energy transfer provides information about vibrational modes in the system.

The four point electrical probe method. A four-point electrical probe is a very versatile device widely used in physics to investigate electrical phenomena. With the help of a four-point probe, it is possible to observe that the constant resistance tends to zero. The scheme of the four-point probe is shown in Figure 1 below. In this graph, four wires (or probes) are attached to the test specimen. A constant electric current is generated from the sample through the probes marked 1 and 4 in the figure. This can be done using a power source as shown. Most power supplies have a built-in current output indicator. An ammeter in series with this current source can be used to determine the value of this current. A 5 W power supply producing up to 0.5 Amps is required for the experiments described for our semiconductor devices.

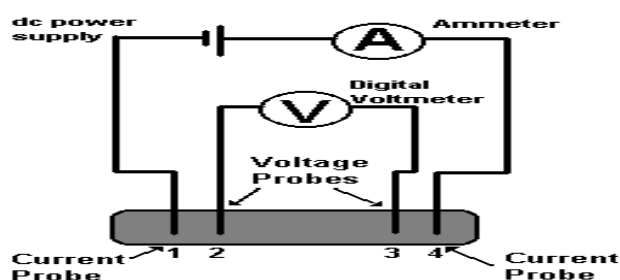


Fig. 1 .Schematic of Four-Point Probe

If electricity is passed through the sample, the potential (or voltage) between probes 2 and 3 drops as the temperature drops, and the voltage drop can be measured with a digital voltmeter. The resistance of the sample between probes 2 and 3 is the ratio of the voltage recorded on the digital voltmeter to the value of the output current of the power source. The high impedance of a digital voltmeter reduces the current flow through the circuit that contains the voltmeter [11].

**Results and Discussion.** According to the methods mentioned above, the sample was synthesized and then its parameters were measured.

**Synthesis of Bi-(2212).** As mentioned above, the solid state reaction method was used to obtain the samples. The constituent elements of the selected composite material were selected according to the Bi(Pb)-Sr-Ca-Cu-O system. For this purpose, powders of high purity  $\text{Bi}_2\text{O}_3$  (99.9%),  $\text{SrCO}_3$  (99.9%),  $\text{CaO}$  (99.9%) and  $\text{CuO}$  (99.9%) were taken in appropriate proportions. The mass fractions of elements in 10 g of the mixture based on the formula  $\text{Bi}_2\text{Sr}_2\text{CaCu}_2\text{O}_y$  are given in Table 1 below [6].

Table 1. The mass fraction of the elements in the mixture.

№	Element n=3	Mass fraction (gr)
1	$\text{Bi}_2\text{O}_3$	5,761177
2	$\text{SrCO}_3$	2,908644
3	$\text{CaO}$	0,346672
4	$\text{CuO}$	0,983507

The sample is prepared by solid state synthesis.  $\text{Bi}_2\text{O}_3$ ,  $\text{SrCO}_3$ ,  $\text{CaO}$  and  $\text{CuO}$  powders were obtained in the ratio of Bi:Sr:Sa:Su in the ratio 2:2:1:2 and were ground and mixed in an agate mortar for a period of time. The powder is then placed in a muffle furnace at 705° C for 12 hours and allowed to cool naturally for 12 hours. Then it is removed from the oven and crushed for another 1 hour and placed in an oven at 780° C for 12 hours. After that, the same grinding process is repeated. Finally, the sample is pressed into a pellet of 10 mm diameter and 5 mm thickness by dry pressing method and sintered at 880°C for 12 hours. The process of cooling the sample took 15 hours in a natural state. The samples, cooled to room temperature, were sent to the laboratory to study their physical parameters.

**Results of Raman spectroscopy.** After sintering the sample, the elements contained in it were confirmed by Raman spectroscopy. The substance sample composition was studied depending on the wave number of the peaks in the spectrogram.

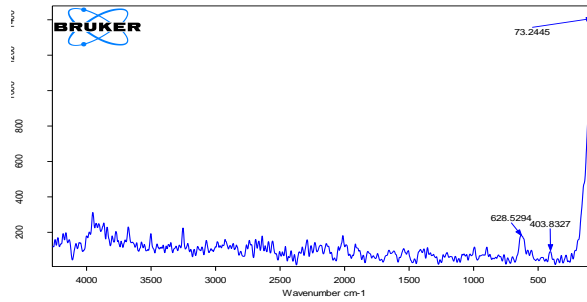


Fig. 2. Compressed Raman spectrum of Bi-(2212).

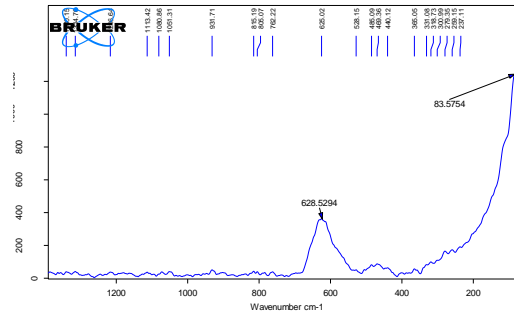


Fig. 3. Extended Raman spectrum of Bi-(2212).

The peak observed at  $552.46 \text{ cm}^{-1}$  corresponds to the stretching vibrations of the Bi-O bond, indicating bismuth-oxygen bonding. The peak at  $628.52 \text{ cm}^{-1}$  represents the stretching vibrations of the Cu-O bond, indicating the copper-oxygen bond. The peak at  $403.83 \text{ cm}^{-1}$  corresponds to Ca-O bond vibrations, reflecting the calcium-oxygen bond.

**Resistance measurement.** The scheme of The four point electrical probe method presented above was created. The sample was placed and cooled to the boiling temperature  $T=77\text{K}$  of dilute nitrogen. A constant current of  $5\text{mA}$  was allowed to pass through the sample. The dependence of the temperature on the resistance was measured by means of a potential difference with Rigol DM3068 and Rigol DM3058E devices.

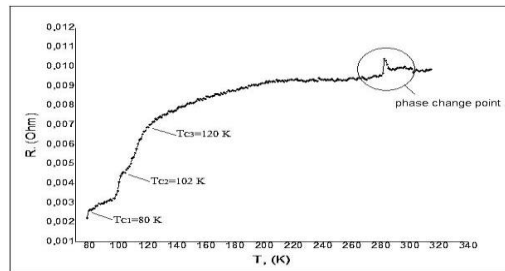


Fig. 6. Temperature dependence of Bi-(2212) sample resistance

The temperature change was recorded by a thermocouple. As can be seen in the graph, different jumps were observed in the resistance change as the temperature increased. Each jump points were marked with  $T_c$  and they were  $T_{C1}=80\text{K}$ :  $T_{C2}=102\text{K}$ :  $T_{C3}=120\text{K}$  respectively. At approximately  $T=284 \text{ K}$ , a peak appeared in the graph line, indicating that a phase change was observed in the sample.

**Conclusion.** From the analysis of many literatures and the results of our scientific research, it became clear that the technology of obtaining bismuth cuprates is a complex process, and it is very important to choose the right temperature during the calcination and sintering process. To obtain a single-phase superconductor from Bi-based cuprates, it is necessary to sinter the sample at a temperature very close to its melting temperature. When the surface of the Bi - (2212) sample was examined by the Chemical Imaging method, a number of irregularities were seen, and measures will be taken to reduce them as much as possible in the next samples.

Since we tested the samples at the boiling temperature of Nitrogen, no resistance was observed. Because the critical temperature of such samples in  $R=0$  state is  $T_C \leq 75\text{K}$ , it was determined by the analysis of scientific research. In our sample, we observed jumps in the subsequent increase in resistance. At the same time, a phase change was noted in the sample at a temperature close to room temperature  $T = 284$ .

**Acknowledgements.** We would like to thank all the laboratory staff headed by Professor D.D. Gulamova of the Institute of Materials Science of the Republic of Uzbekistan who helped us to obtain the above results.

At the same time, we are grateful to the staff of the scientific laboratory of the National University of Uzbekistan for providing Raman spectra and chemical imaging results.

## REFERENCES

1. H. Maeda, Y. Tanaka, M. Fukutumi, and T. Asano, Jpn. J. Appl. Phys. 27 (2) (1988).
2. Yildirim, G., Varilci, A., Terzioglu, C.: Anisotropic nature and scaling of thermally activated dissipation mechanism in Bi-2223 superconducting thin film. J.Alloy.Comp. 554, 327–334 (2013).

3. Dogruer, M., Yildirim, G., Varilci, A., Terzioglu, C.: MgB<sub>2</sub> inclusions in Bi-2223 matrix: the evaluation of microstructural, mechanical and superconducting properties of new system, Bi-2223+MgB<sub>2</sub>. *J. Alloys Compd.* 556, 143–152 (2013).
4. Shreelekha Mishra Synthesis and characterization of superconductor composite Bi<sub>2</sub>Sr<sub>2</sub>Ca<sub>1</sub>Cu<sub>2</sub>O<sub>8</sub>/La<sub>0.85</sub>Sr<sub>0.15</sub>MnO<sub>3</sub>, National Institute of Technology, Rourkela Rourkela-769008, Orissa, India May-2012
5. A. Tampieri, G. Calestani, G. Celotti, R. Masini, S. Lesca Multi-step process to prepare bulk BSCCO 2223 superconductor *Ž / with improved transport properties* A. Tampieri et al. *Physica C* 306 1998 21–33.
6. A. Coşkun, G. Akça, E. Taşarkuyu, Ö. Battal, A. Ekicibil, Structural, Magnetic, and Electrical Properties of Bi<sub>1.6</sub>Pb<sub>0.4</sub>Sr<sub>2</sub>Ca<sub>2</sub>Cu<sub>3</sub>O<sub>10+x</sub> Superconductor Prepared by Different Techniques, <https://doi.org/10.1007/s10948-020-05618-8> *Journal of Superconductivity and Novel Magnetism* (2020) 33:3377–3393.
7. A.R. West, *Solid State Chemistry and Its Applications*, Wiley and Sons, 2005.
8. Vinod Kumara, S.P. Tiwarib, O.M. Ntwaeaborwa, Hendrik C. Swart, Luminescence properties of rare-earth doped oxide materials, *Spectroscopy of Lanthanide-Doped Oxide Materials*. <https://doi.org/10.1016/B978-0-08-102935-0.00010-1>, © 2020 Elsevier Ltd. All rights reserved.
9. Navas D.; Fuentes, S.; Castro-Alvarez, A.; Chavez-Angel, E. Review on Sol-Gel Synthesis of Perovskite and Oxide Nanomaterials. *Gels* 2021, 7, 275. <https://doi.org/10.3390/gels7040275>.
10. Philippe Colomban, Aneta Slodczyk, Raman intensity: An important tool to study the structure and phase transitions of amorphous/crystalline materials, *Optical Materials* 31 (2009) 1759–1763, <https://doi.org/10.1016/j.optmat.2008.12.030>.
11. Images Scientific Instruments / 2007-2024 Images SI, Inc. All rights reserved.
12. [http://www.malvern.com/LabEng/products/sdi/bibliography/sdi\\_bibliography.htm](http://www.malvern.com/LabEng/products/sdi/bibliography/sdi_bibliography.htm) E. N. Lewis, E. Lee and L. H. Kidder, Combining Imaging and Spectroscopy: Solving Problems with Near-Infrared Chemical Imaging. *Microscopy Today*, Volume 12, No. 6, 11/2004.
13. Hagen, Nathan; Kudenov, Michael W. (2013). “[Review of snapshot spectral imaging technologies](#)”. *Optical Engineering*.52 9): 090901. [Bibcode: 2013OptEn..52i0901H](#). [doi:10.1117/1.OE.52.9.090901](#). [S2CID 215807781](#). Archived from the original on 20 September 2015. Retrieved 2 February 2017.
14. Gulamova, D. D., and D. E. Uskenbaev. “Effect of substrate composition and crystal structure on the BSCCO texture with the 2223 composition obtained under the action of solar radiation.” *Applied Solar Energy* 42.4 (2006): 40-42.



UDC: 539.12.01

**Bakhadir IRGAZIEV,**  
*O'zbekiston Milliy universiteti professori, fiz.-mat.f.d*  
*E-mail:irgaziev@yahoo.com*  
**Javlonbek XASANOV,**  
*O'zbekiston Milliy universiteti stajyor-tadqiqotchisi*

*O'zRFA Yadro instituti laboratoriya mudiri, fiz.-mat.f.d prof. E.Tursunov taqrizi asosida*

### BIR TESHIKLI YADROLAR $\beta$ – PARCHALANISHINING YARIM YEMIRILISH DAVRI

Аннотация

Biz  $^{15}_8\text{O}$  va  $^{11}_6\text{C}$  bir teshikli yadrolarining yarim yemirilish davrini hisobladik. Bu hisoblashlarda biz [1], [2] adabiyotlarda keltirilgan yangi kinematik doimiylar va koeffitsiyentlardan foydalandik. Shu bilan birga, biz fazaviy fazoni hisoblashda avvalgi [3] ishdan farqli o'laroq uni yaqinlashuv holatini emas balki sonli hisoblashlardan olingan natijalarni ishlatdik. Olingan natijalar tajribada olingan natijalar bilan taqqoslandi.

**Kalit so'zlar:** kuchsiz ta'sir, yarim yemirilish davri, bir teshikli yadro.

### ПОЛУПЕРИОД $\beta$ – РАСПАДА ОДНО ДЫРОЧНЫХ ЯДЕР

Аннотация

Мы рассчитали полупериод одно дырочных ядер для  $^{15}_8\text{O}$  и  $^{11}_6\text{C}$ . Мы рассчитали полупериоды этих элементов, используя новые кинематические константы и коэффициенты, которые описаны в [1], [2]. При этом фазовое пространство не рассматривается как приближенное состояние, в отличие от предыдущей работы [3]. Полученные результаты сравнивались с экспериментальными данными.

**Ключевые слова:** слабое взаимодействие, полупериод, функция фазовое пространство, одно дырочное ядро.

### $\beta$ – DECAY HALF-LIFE OF ONE-HOLE NUCLEI

Annotation

We have calculated of the half-life of the one-hole nuclei for  $^{15}_8\text{O}$  and  $^{11}_6\text{C}$ . We calculated half-lives of these elements using new kinematic constants and coefficients, which are covered in [1], [2]. At the same time, the phase space has not treated as approximate state, unlike in previous work [3]. The results have obtained by numerical calculation method. The findings were compared to the experimental data.

**Key words:** weak decay, half-life, phase-space function; one-hole nuclei.

**Introduction.** Nuclear  $\beta$ -decay is a type of radioactive decay that can occur in many nuclei. It involves weak, strong, and Coulomb interactions. The decay energy and wave functions of the parent and daughter nuclei determine the nuclear  $\beta$ -decay half-life. Research on  $\beta$ -decay helps to give us a better understanding of the nuclear structure and the fundamental interactions between nucleons.

Study  $\beta$  – decay gives us much information about the structure of nuclei. Nuclear  $\beta$ -decay has three types, namely  $\beta^-$ -decay,  $\beta^+$ -decay, and electron capture. The atomic number  $Z$  only changes by one unit in all three types of  $\beta$ -decay processes, but the mass number  $A$  of the parent and daughter nuclei remains constant. All transitions from the ground state of the parent nucleus to ground and excited states of the daughter nucleus that fall within the energy window provided by the  $Q$ -value have allowed by the  $\beta$ -decay selection rules. In this work, we study allowed beta decay (Fermi transition and Gamow-Teller transition), and we calculate the half-life of the one-hole nuclei for transitions between ground energy states. Then we compare our results with experimental data.

The nucleus is composed of protons and neutrons. According to the nuclear-shell model, protons and neutrons fill the shells according to the Pauli principle. In this work, we have one hole for this neutron shell to be filled, and it is filled by the conversion of a proton to a neutron, and at the same time, one hole is created in the protons. In this work, we have selected oxygen and carbonates. Previously, these substances were studied in works [3] and [4]. Unlike them, we used numerical integrations instead of approximations to calculate the phase space factor and used new values of the kinematic constants.

**Selection rule of  $Q$  – value.** The  $Q$ -value of a reaction is defined as the difference in the total kinetic energies of the system before and after a reaction [5]. “The following useful relations (1), (2), (3) connect the  $Q$  value to the energy difference the nuclear energy initial and final states” (equal to electron and neutrino energy) [3]. For a nuclear  $\beta$ -decay, the parent nucleus may be assumed to be at rest in the laboratory, the initial kinetic energy in the system is zero [6], and  $m_\nu c^2$  is neglected. So, the  $Q$  value of nuclear beta decay is the total kinetic energy of the final-state leptons. In our case,  $W_0$  is the difference in energy final and initial nuclear states. [3]

$$\begin{aligned}Q_{\beta^-} &= T_{e^-} + T_{\bar{\nu}} = E_{e^-} + E_{\bar{\nu}} - m_e c^2 = W_0 m_e c^2 - m_e c^2 \\Q_{\beta^+} &= T_{e^+} + T_{\nu} = E_{e^+} + E_{\nu} - m_e c^2 = W_0 m_e c^2 - m_e c^2 \\Q_{EC} &= T_{\nu} - T_{e^-} = W_0 m_e c^2 + m_e c^2\end{aligned}$$

$$W_0 = \frac{Q_{\beta^-} + m_e c^2}{m_e c^2} \quad (1)$$

$$W_0 = \frac{Q_{\beta^+} + m_e c^2}{m_e c^2} = \frac{Q_{EC} - m_e c^2}{m_e c^2} \quad (2)$$

$$W_0 = \frac{Q_{EC} - m_e c^2}{m_e c^2} \quad (3)$$

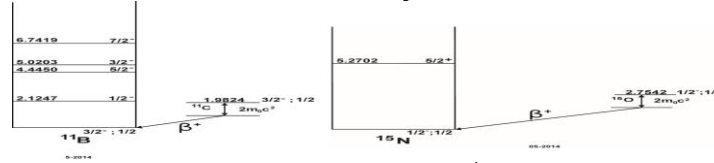


Figure 1: this pictures show us  $\beta^+$  decay. [8]

The  $Q$  values  $Q_{\beta^-}$  and  $Q_{EC}$  are the ones tabulated in the Table of Isotopes [7] and elsewhere. Therefore the  $\beta^+$  endpoint energy is here expressed also in terms of  $Q_{EC} = Q_{\beta^+} + 2m_e c^2$ .

Figure 1 shows the  $Q_{EC}$  results used in subsequent calculations. Here it can be seen that  $Q_{EC} = 1.9824 \text{ MeV}$  for  $^{11}\text{C} \rightarrow ^{11}\text{B}$  transition and  $Q_{EC} = 2.7542 \text{ MeV}$  for  $^{15}\text{O} \rightarrow ^{15}\text{N}$  transition.

**The half-life of  $\beta$  decay.** The beta decay half-life is determined by the equation:

$$t_{1/2} = \frac{\ln 2}{T_{fi}} \quad (4)$$

where  $T_{fi}$  is transition probability,  $t_{1/2}$  is the nuclear  $\beta$ -decay half-life. It is known that (see ref. [6]) Fermi's "Golden rule" for calculating the nuclear  $\beta$ -decay probability is as follows:

$$T_{fi} = \frac{2\pi}{\hbar} |\langle \phi_k(r) | H' | \phi_0(r) \rangle|^2 \rho(E_f) \quad (5)$$

where  $\rho(E_f)$  is density of final states. The initial states is simple, involving only the parent nucleus,

$$|\phi_0(r)\rangle = |J_i M_i \xi_i\rangle |\varphi_i\rangle. \quad (6)$$

The final state consists of three particles: a neutral lepton, a charged lepton, and the daughter nucleus. For simplicity, we shall begin by ignoring any Coulomb effect between the charged lepton and the daughter nucleus. In this limit, both leptons are free particles and are described by plane waves traveling with wave numbers  $\mathbf{k}_e$  and  $\mathbf{k}_\nu$ , respectively. The final state wave function is then a product of three parts:

$$|\phi_k(r)\rangle = \frac{1}{\sqrt{V}} e^{i\mathbf{k}_e \cdot \mathbf{r}} \frac{1}{\sqrt{V}} e^{i\mathbf{k}_\nu \cdot \mathbf{r}} |J_f M_f \xi_f\rangle |\varphi_f\rangle. \quad (7)$$

In this paper we study allowed  $\beta$ -decay. So  $kr \ll 1$  and this matrix element don't depend on  $r$ .

**The Nuclear transition matrix element.** Nuclear matrix element formula is given by [6].

$$\begin{aligned} \sum_{\mu M_f} \langle J_f M_f \xi_f | O_{\lambda\mu} | J_i M_i \xi_i \rangle &= G_V \sum_{\mu M_f} \langle J_f M_f \xi_f | \sum_{j=1}^A \tau_{\mp} | J_i M_i \xi_i \rangle + \\ &+ G_A \sum_{\mu M_f} \langle J_f M_f \xi_f | \sum_{j=1}^A \sigma(j) \tau_{\mp}(j) | J_i M_i \xi_i \rangle \end{aligned} \quad (8)$$

The nuclear matrix element for single particle nucleon can be written as:

$$\begin{aligned} \sum_{\mu M_f} |\langle J_f M_f \xi_f | O_{\lambda\mu} | J_i M_i \xi_i \rangle|^2 &= \\ &= G_V^2 \left( \sum_{\mu M_f} \langle J_f M_f \xi_f | \mathbf{1} | J_i M_i \xi_i \rangle + g_A \sum_{\mu M_f} \langle J_f M_f \xi_f | \boldsymbol{\sigma} | J_i M_i \xi_i \rangle \right) \\ &= G_V^2 (B_F + B_{GT}) \end{aligned} \quad (9)$$

Here  $G_V = G_F \cos \theta_C$  and  $g_A = \frac{G_A}{G_V}$  axial vector coupling constant.  $B_F$  and  $B_{GT}$  are reduced transition probabilities [3].

Isospin lowering and rising operators are written with operators annihilation and creation and this matrix element is calculated using the Wigner-Eckart theorem.

$$\langle J_f M_f \xi_f | T_{\lambda\mu} | J_i M_i \xi_i \rangle = \sum_{\alpha\beta} \langle \alpha | T_{\lambda\mu} | \beta \rangle \langle J_f M_f \xi_f | c_{\alpha}^{\dagger} c_{\beta} | J_i M_i \xi_i \rangle \quad (10)$$

$$T_{\lambda\mu} = \sum_{\alpha\beta} \langle \alpha | T_{\lambda\mu} | \beta \rangle c_{\alpha}^{\dagger} c_{\beta} = \frac{1}{\sqrt{2\lambda+1}} \sum_{ab} (a || T_{\lambda\mu} || b) [c_{\alpha}^{\dagger} \tilde{c}_b]_{\lambda\mu} \quad (11)$$

(one-body operator) is written with annihilation and creation operators here.

$$\langle J_f M_f \xi_f | T_{\lambda\mu} | J_i M_i \xi_i \rangle = \frac{(J_f M_f \lambda \mu | J_i M_i)}{\sqrt{2J_i+1}} (J_f \xi_f || T_{\lambda} || J_i \xi_i) \quad (12)$$

$$(J_f \xi_f || T_{\lambda} || J_i \xi_i) = \frac{1}{\sqrt{2\lambda+1}} \sum_{a,b} (a || T_{\lambda} || b) (J_f \xi_f || [c_{\alpha}^{\dagger} \tilde{c}_b]_{\lambda} || J_i \xi_i) \quad (13)$$

"The basic property of the allowed beta decay is that final-state leptons are emitted in an  $s$  ( $l=0$ ) state relative to the nucleus. Similarly, in allowed electron capture, the initial electron forms an  $s$  shell and the final neutrino is in an  $s$  state relative to the nucleus. Thus, the orbital angular momentum of the leptons cannot change the nuclear total angular momentum" [3].

The above formulas have written only for single-particle nuclei. We must change creation and annihilation operators and these formulas are suitable for one-hole nuclei.

$$(\Phi_f || [c_{\alpha}^{\dagger} \tilde{c}_b]_{\lambda} || \Phi_i) = \delta_{aj} \delta_{bi} (-1)^{j_i + j_f + \lambda} \sqrt{2\lambda+1} \quad (14)$$



$\lambda = 0$  is the Fermi transition and  $\lambda = 1$  is the Gamow-Teller transition. Orbital momentum doesn't change in our case and this condition corresponds to allowed decay (see Fig. 2). Fermi transitions express antiparallel spins and Gamow-Teller transitions express parallel spins.

$$B_F = \delta_{fi}, \quad B_{GT} = g_A^2 \frac{3}{2j_i + 1} |M_{GT}(fi)|^2 \quad (15)$$

$$M_{GT}(fi) = \frac{1}{\sqrt{3}} (f \| \sigma \| i) = \frac{1}{\sqrt{3}} (n_f l_f j_f \| \sigma \| n_i l_i j_i) = \sqrt{2} \delta_{n_i n_f} \delta_{l_f l_i} \sqrt{(2j_f + 1)(2j_i + 1)(-1)^{l_f + j_f + 3/2}} \begin{pmatrix} 1/2 & 1/2 & 1 \\ j_f & j_i & l_f \end{pmatrix} \quad (16)$$

$^{15}_8O$  ground state spin equal to  $1/2$  and located p shell,  $^{11}_6C$  ground state equal to  $3/2$  and located p shell.

Type of transition	$\Delta J =  J_f - J_i $	$\pi_i \pi_f$
Fermi	0	+1
Gamow-Teller	1 ( $J_i = 0$ or $J_f = 0$ )	+1
Gamow-Teller	0, 1 ( $J_i > 0, J_f > 0$ )	+1

Here  $J_i$  ( $J_f$ ) is the angular momentum of the initial (final) nuclear state and correspondingly for the parity  $\pi$ .

Figure 2: Selection rules for allowed beta decay transitions [3]

“However, in some cases we must assume a predominant value of the orbital angular momentum  $L$  which is hardly consistent with the measured magnetic moment, unless there are large exchange magnetic moments. For example, the comparative lifetime for the  $^{11}_6C \rightarrow ^{11}_5B$  transition seems to imply a predominant  $D$  state ( $L = 2$ ), whereas the magnetic moment of  $^{11}_6C$  is much closer to that of a  $P$  state ( $L = 1$ ).” [9]

**Phase-space factor.** When we calculate the density of final state energy, the Coulomb interaction between beta particles and daughter nuclei affects the result. So, we have to give our consent to this phase-space factor. Without considering screening of the nuclear charge by orbital electrons, the relativistic Coulomb correction factor is given (Fermi 1934) by [10], [11] as

$$f^+(Z, E_0) = \int_0^{p(E_0)} F(Z, E) p_e^2 (E_0 - E)^2 dp_e \quad (18)$$

$$F(Z, p_e) = \frac{2(1+S)}{\Gamma(1+2S)^2} (2p_e \rho)^{2S-2} e^{\pi\eta} |\Gamma(S+i\eta)| \quad (19)$$

$$S = \sqrt{1 - \alpha^2 Z^2}, \eta = \pm \frac{Ze^2 E}{\hbar c p_e}, \rho = \frac{r_N m_e c}{\hbar}, r_N = r_0 A^{1/3}$$

$$p_e = \frac{1}{c} \sqrt{E - m_e c^2}, \quad dp_e = \frac{E}{c \sqrt{E^2 - m_e c^2}} dE$$

$$f^+(Z, E_0) = \frac{1}{m_e^2 c^{10}} \int_{m_e c^2}^{E_0} F(Z, E) \sqrt{E^2 - m_e c^2} (E_0 - E)^2 E dE, \quad (20)$$

where  $E$  is energy of electron.

We know that there are three particles in the final state of beta-decay. In this condition, the kinetic energy of the electron (positron) changes between zero and the  $Q$  value. So, we try to find this phase-space factor with a numerical integral. In this case, we use natural units  $\hbar = c = 1$ ,  $\hbar c \approx 197 \text{ MeV} \cdot \text{fm}$ ,  $e^2 = \alpha$  and  $\alpha \approx 1/137$ ,  $m_e = 0,511 \text{ MeV}$ ,  $W = E/m_e c^2$ ,  $W_0 = Q/m_e c^2$ .

$$f^+(Z, W_0) = \int_0^{W_0} F(Z, W) \sqrt{W^2 - 1} (W_0 - W)^2 dW \quad (21)$$

$$F(Z, W) = \frac{2(1+S)}{\Gamma(1+2S)^2} (2\sqrt{W^2 - 1} \rho)^{2S-2} e^{\pi\eta} |\Gamma(S+i\eta)| \quad (22)$$

$$S = \sqrt{1 - \alpha^2 Z^2}, \eta = \pm \frac{\alpha Z W}{\sqrt{W^2 - 1}}, \rho = \frac{r_0 m_e}{197} A^{1/3}, \quad (23)$$

here  $r_0 = 1,25 \text{ fm}$ .

The phase-space factor of electron capture for the relativistic treatment is

$$f_k = 2\pi (2\rho)^{2S-2} \frac{1+S}{(2S)!} \gamma^{1+2S} (W_0 + s)^2, \quad (24)$$

here  $\gamma = Z\alpha$ ,  $Z$  is nuclear charge of parent nuclei. [9]

**Calculation of half-life time.** Final half-life time formula is given by [1]

$$t_{1/2} = \frac{k}{(f^+(Z, W_0) + f_k) \langle \varphi_f | \varphi_i \rangle^2 (B_F + B_{GT})}, \quad (25)$$

where  $\varphi_i(r)$  and  $\varphi_f(r)$  are the radial wave functions of the initial and final states of the hole-neutron and hole-proton, respectively [1]. The overlap integral  $\langle \varphi_f | \varphi_i \rangle = 0,994$  in the case of  $^{11}C \rightarrow ^{11}B$  and  $^{15}O \rightarrow ^{15}N$  transitions.  $k$  is the universal constant value in accordance with ref. [2] provided as:

$$k = \frac{2\pi^3 \hbar^7 \ln 2}{m_e^5 c^4 (G_F \cos(\theta_C))^2} = 6289 \text{ s}, \quad (26)$$

and  $\theta_C$  stands for the Cabibo angle and  $m_e$  is the electron mass. The term  $G_F$  denotes the Fermi constant, i.e., effective coupling constant. In Eq. (8)  $O_{\lambda\mu}$  means the operator of the  $\beta$ -decay transition and the summation over  $M_f$  takes care of the requirement to include all the possible nuclear final states and averaging over the initial states. The phase-space factor  $f(Z, W_0)$  contains the lepton kinematics,  $J_i$  is the angular momentum of the initial nuclear state,  $J_f$  is the final angular momentum of the final state.

The quantity  $\log[f(Z, W_0)t_{1/2}]$  is called the  $\log ft$  value. “It depends exclusively on nuclear structure, which is contained in the reduced matrix elements. In the literature it has also called the comparative half-life” [9].

We have used  $g_A = g \frac{G_A}{G_V} = -1,27641g$  in our calculation and the results are presented in this Table. We take into account from Ref. [4]  $g = 0.927$ .

**Analysis and results.** The nuclear shell model describes the lower energy levels of the nucleus well. Although, transition probability and half-life calculated using the shell model differ somewhat from the experimental values. The results we have obtained are closer to the experiment compared to the previous work. Even so, our results are slightly different from the experimental data.

We can see from table 1 above that the relative errors compared to the results of the experiment are 11.33% for  $^{11}\text{C} \rightarrow ^{11}\text{B}$  and 0.2% for  $^{15}\text{O} \rightarrow ^{15}\text{N}$ . On the other hand, this condition is one of the defects of the nuclear shell model. In addition, it is clear that EC happens at the same time. We may predict probability  $\beta^+$  and EC.  $^{11}\text{C} \rightarrow ^{11}\text{B}$ ,  $\beta^+$  - 99,75 % and EC - 0,25 %. In case  $^{15}\text{O} \rightarrow ^{15}\text{N}$ ,  $\beta^+$  - 99,9 % and EC - 0,1 %.

Table-1

Transition	Our results		Experiment	
	$t_{1/2}$	$\log ft$	$t_{1/2}$ [8], [12]	$\log ft$ [8], [12]
$^{11}\text{C} \rightarrow ^{11}\text{B}$	18.0565 min	3.53789	$20.364 \pm 0.014$ min	$3.5921 \pm 0.0019$
$^{15}\text{O} \rightarrow ^{15}\text{N}$	122.49 sec	3.63702	$122.24 \pm 0.16$ sec	$3.637 \pm 0.001$

**Conclusion.** The provided document is a study on nuclear beta decay, a type of radioactive decay involving weak, strong, and Coulomb interactions. The research focuses on understanding nuclear structure and fundamental interactions between nucleons through beta decay, specifically allowed beta decay (Fermi and Gamow-Teller transitions).

The study calculates the half-life of one-hole nuclei in transitions between ground energy states, comparing results with experimental data. Beta decay types discussed include  $\beta^-$ ,  $\beta^+$ , and electron capture, where the atomic number changes by one unit but the mass number remains constant.

Key aspects include the use of numerical integration for the phase-space factor, the impact of Coulomb interactions, and the calculation of the beta decay half-life using Fermi's "Golden rule." The results demonstrate a close match between theoretical calculations and experimental data for transitions in carbon and oxygen isotopes.

#### REFERENCES

1. B. F. Irgaziev and Jameel-Un Nabi and Abdul Kabir, "Analysis of  $\beta^+$  decay of  $^{13}\text{N}$  nucleus using a modified one-particle approach," Canadian Journal of Physics, vol. 99, pp. 176-184, 2021.
2. Particle Data Group and C. Patrignani and K. Agashe and G. Aielli and C. Amsler and M. Antonelli and Asner, D. M. and H. Baer and Sw Banerjee and Barnett, R. M. and T. Basaglia and Bauer, C. W. and Beatty, J. J. and Belousov, V. I. and J. Beri, "Review of particle physics," Chinese Physics C, 2016.
3. J. Suhonen, From Nucleons to Nucleus: Concepts of Microscopic Nuclear Theory, Springer Berlin Heidelberg, 2007.
4. D. Wilkinson, "Renormalization of the axial-vector coupling constant in nuclear  $\beta$ -decay (III)," Nuclear Physics A, vol. 225, no. 3, pp. 365-381, 1974.
5. K. S. Krane, Introductory nuclear physics, New York: Wiley, 1988.
6. S. S. Wong, Introductory Nuclear physics, WILEY-VCH, 2004.
7. Firestone, R.B. and Zipkin, J. and Chu, S.Y.F. and Shirley, V.S. and Baglin, C.M., Table of Isotopes, John Wiley & Sons, 1996.
8. T. N. D. E. Group. [Online]. Available: <https://nucldata.tunl.duke.edu/nucldata/>.
9. F., Blatt M. John and Weisskopf Victor, Nuclear reactions; Application of the Theory to Experiments, New York, NY: Springer New York, 1979.
10. G. K. Schenter and P. Vogel, "A Simple Approximation of the Fermi Function in Nuclear Beta Decay," Nuclear Science and Engineering, pp. 393-396, 1983
11. P Venkataramaiah and K Gopala and A Basavaraju and S S Suryanarayana and H Sanjeeviah, "A simple relation for the Fermi function," Journal of Physics G: Nuclear Physics, pp. 359-364, 1985
12. Burdette, D. P. and others, "Precise half-life determination of the mixed-mirror beta-decaying  $\text{O}15$ ," Phys. Rev. C, p. 055504 Burdette, D. P. and others, "Precise half-life determination of the mixed-mirror beta-decaying  $\text{O}15$ ," Phys. Rev. C, p. 055504, 2020



UDK: 538.955; 621.3.082.782

*Jasurbek MIRZAYEV,*  
*Namangan muhandislik-texnologiya instituti, f.-m.f.n.PhD*  
*Ulug'bek ERKABOYEV,*  
*Namangan muhandislik-texnologiya instituti professori, f.-m.f.d*  
*Muzaffar DADAMIRZAYEV,*  
*Namangan muhandislik-texnologiya instituti tayanch doktoranti*  
*E-mail: muzaffardadamir81@gmail.com*

*NamMTI professori f.-m.f.d. N.Shariboyev taqrizi asosida*

### ОСЦИЛЛЯЦИИ ПЛОТНОСТИ ЭНЕРГЕТИЧЕСКИХ СОСТОЯНИЙ В НАНОРАЗМЕРНЫХ ПОЛУПРОВОДНИКАХ ПРИ ПРОДОЛЬНЫХ И ПОПЕРЕЧНЫХ КВАНТУЮЩИХ МАГНИТНЫХ ПОЛЯХ

Аннотация

С учетом гауссовой функции распределения удастся рассчитать влияние квантованного магнитного поля на температурную зависимость колебаний плотности энергии состояний в квантоворазмерных полупроводниках на основе метода растекания дельта-функции. С помощью численных методов расчета разработана новая математическая модель температурной зависимости колебаний плотности энергии состояний разрешенного поля в наноразмерных полупроводниках под действием поперечного квантующего магнитного поля.

**Ключевые слова:** магнитное поле, квантующее магнитное поле, гетероструктура, квантовая яма, плотность состояний, осцилляция, наноразмер, двумерные полупроводники.

### OSCILLATIONS OF THE ENERGY DENSITY OF STATES IN NANO-SIZED SEMICONDUCTORS IN LONGITUDINAL AND TRANSVERSE QUANTIZING MAGNETIC FIELDS

Annotation

Taking into account the Gaussian distribution function, it is possible to calculate the effect of a quantized magnetic field on the temperature dependence of fluctuations in the energy density of states in quantum-sized semiconductors based on the delta-function spreading method. Using numerical calculation methods, a new mathematical model of the temperature dependence of fluctuations in the energy density of states of the allowed field in nanosized semiconductors under the action of a transverse quantizing magnetic field has been developed.

**Key words:** magnetic field, quantum magnetic field, heterostructure, quantum well, density of states, oscillation, nanosize, two-dimensional semiconductors.

### BO'YLAMA VA KO'NDALANG KVANTLOVCHI MAGNIT MAYDONDAGI NANOO'LCHAMLI YARIMO'TKAZGICHLARDA ENERGETIK HOLATLAR ZICHLIGI OSSILLYATSIIYASILARI

Аннотация

Gauss taqsimot funksiyasini hisobga olgan holda kvant o'lchamli yarimo'tkazgichlarda energetik holatlar zichligi ossillyatsiyalarini haroratga bog'liqligiga kvantlovchi magnit maydonning ta'sirini hisoblash mumkinligi delta – funktsiyalarni qatorga yoyish usuli yordamida asoslangan. Sonli hisoblash usullaridan foydalanib, ko'ndalang kvantlovchi magnit maydon ta'siridagi nano o'lchamli yarimo'tkazgichlarda ruhsat etilgan sohasining energetik holatlar zichligi ossillyatsiyalarini haroratga bog'liqligi aniqlangan.

**Kalit so'zlar:** magnit maydon, kvantlovchi magnit maydon, geterostruktura, kvant o'ra, holatlar zichligi, ossillyatsiya, nanoo'lcham, ikki o'lchamli yarimo'tkazgichlar.

**Kirish.** Hozirgi vaqtda yarimo'tkazgichlar fizikasi sohasidagi amaliy va fundamental tadqiqotlarga bo'lgan qiziqish hajmi materiallardan nanoo'lchamli materiallarga o'tdi. Ayniqsa, kvantlovchi magnit maydon ta'sirida bo'lgan nanoo'lchamli yarimo'tkazgichlarda zaryad tashuvchilarning energetik spektrining xususiyatlarini tubdan o'zgarishi, olimlarning spintronika va nanoelektronika sohalari bilan ilmiy tadqiqot ishlarini olib borishga qiziqish uyg'otdi. Natijada kvantlovchi magnit maydonidagi erkin elektronlar va teshiklarning energetik sathlarini kvantlantirish kvant o'rali yarimo'tkazgichlardagi energetik holatlar zichligi ossillyatsiyalarini sezilarli o'zgarishlarga olib kelishi tajribalarda kuzatilmoqda.

**Adabiyotlar tahlili.** Kvant o'rali yarimo'tkazgichlarda energetik holatlar zichligini kvantlovchi magnit maydonning kattaligiga bog'liqligini o'rganish zaryad tashuvchilarning energetik spektrlari to'g'risida muhim ma'lumotlarni olish imkonini beradi. Kinetik, dinamik va termodinamik kattaliklar, jumladan magnit qarshilik, magnit singdiruvchanlik, elektronlarning issiqlik sig'imi, Fermi sathi va boshqa kattaliklarning ossillyatsiya jarayoni asosan energetik holatlar zichligining ossillyatsiyalanishi hisobiga hosil bo'ladi.

Bundan kelib chiqadiki, ko'ndalang va bo'ylama magnit maydon ta'siridagi to'g'ri burchakli kvant o'rali yarimo'tkazgichning o'tkazuvchanlik sohasida energetik holatlar zichligi ossillyatsiyalarini o'rganish zamonaviy qattiq jismlar fizikasining dolzarb muammolaridan biri hisoblanadi.

Jumladan, ushbu ishlarda, [1, 2, 3], bir jinsli perpendikulyar magnit maydonidagi va tasodifiy ixtiyoriy korrelyatsiya maydonidagi ikki o'lchamli elektron gazlarda Landau sathlari holatlar zichligi hisob-kitoblari ko'rib chiqilgan. Keskin

o'zgaraydigan trayektoriya bo'yicha integrallar yarim klassik usuli yaratilgan korrelyasiyaning tasodifiy maydoni uchun yo'lli integrallarning noan'anaviy yondashuvi ishlab chiqilgan va bu Landau sathlari holatlar zichligi uchun analitik yechim beradi. Magnit maydonning zaiflashishi va korrelyasiya uzunligining kamayishi bilan holatlar zichligining og'ishi Gauss shaklidan ortadi [1, 2]

Bu ishlarda erishilgan yutuqlarga qaramay, ularda ba'zi savollar ochiq qolmoqda. Masalan: ko'ndalang va bo'ylama magnit maydondagi kvant o'rali yarimo'tkazgichlarning energetik holatlar zichligini haroratga bog'liqligini termik o'zgarishni hisobga olgan holda qanday aniqlash mumkin? Umuman, uning harorat bo'yicha o'zgarish dinamikasi qanday bo'ladi kabi muammolar hozirgacha ochiq qolmoqda.

**Tadqiqot metodologiyasi.** Keling, ko'ndalang kvantlovchi magnit maydon ta'sirida kichik o'lchamli qattiq jismlardagi holatlar zichligi ossillyatsiyalarining haroratga bog'liqligini ko'rib chiqaylik. Ma'lumki, Landau sathlariga haroratning ta'sirini aniqlashda, energetik holatlar zichligi ossillyatsiyalarini delta o'xshash funksiyalar bo'yicha qatorga yoyish usulidan foydalaniladi [4, 5, 6, 7]. Delta shaklidagi funksiyalarning ketma-ket qatorga yoyish yo'li bilan energetik holatlar zichligi ossillyatsiyalarini o'rganish orqali kvant o'rali yarimo'tkazgichlarda o'tkazuvchanlik sohasini diskret Landau sathining haroratga bog'liqligini tushuntirish mumkin bo'ladi. Kvantlovchi magnit maydonda holatlar zichligi ossillyatsiyalarining haroratga bog'liqligi diskret Landau sathlarining termik kengayishi bilan aniqlanadi. Mutloq nol haroratda Gauss taqsimot funksiyasi delta shaklida bo'lib, quyidagi ifoda bilan hisoblanadi [8]:

$$Gauss(E, T) = \frac{1}{kT} \cdot \exp\left(-\frac{(E - E_i)^2}{(kT)^2}\right) \quad (1)$$

U holda, termik kengayishni Gauss taqsimot funksiyasini haroratga bog'liqligi bilan tavsiflash mumkin. Cheksiz chuqur to'g'ri burchakli kvant o'ra uchun, zaryad tashuvchilarning  $E_i$  chuqur sathidan o'tkazuvchanlik sohasiga va  $E$  energiyali valentlik

sohasiga termik chiqarish vaqti eksponent faktor  $\exp\left(-\frac{(E - E_i)^2}{(kT)^2}\right)$  bilan belgilanadi. Demak, chuqur to'ldirilgan diskret

Landau sathlari eksponent sifatida energetik holatlar zichligi ossillyatsiyalariga va haroratga bog'liq. Energetik holatlarning zichligi ossillyatsiyalarining haroratga bog'liqligini aniqlash uchun  $T = 0$  holatidagi energiya zichligi ma'lum energiya  $E_i$  ( $N_L$ ,  $N_Z$ ) funksiyasiga teng deb faraz qilamiz. Ikki o'lchamli elektron gazlar uchun, ko'ndalang kvantlovchi magnit maydonda, holatlar zichligining ossillyatsiyalari (2) formula bo'yicha hisoblanadi.

$$N_{S,Z}^{2d}(E, B) = \frac{eB}{\pi\hbar} \sum_{N_L, N_Z} \delta(E - E(N_L, N_Z)) \quad (2)$$

Haroratning oshishi bilan har bir holat energiya  $E_i(N_L, N_Z)$  bilan o'zgaradi. Diskret Landau sathlarini  $E_i(N_L, N_Z)$  energiya bilan termik kengayishi Shokli-Rid-Xoll statistikasiga bo'ysinadi [9]. Shunday qilib, o'tkazuvchanlik va valent sohaslarida, barcha holatlarning termik kengayishini hisobga olgan holda, hosil bo'ladigan holatlar zichligi ossillyatsiyalari barcha termik kengayishlarni yig'indisi bilan aniqlanadi. Demak kvant o'rali yarimo'tkazgichlar uchun  $T$  cheklangan haroratda energetik holatlar zichligi ossillyatsiyalari  $N_{S,Z}^{2d}(E, B, T, d)$  Gauss funksiyani qatorga yoyish orqali termik kengayishini (haroratga bog'liqligini) tushuntirishga imkon beradi.

Agar  $N_{S,Z}^{2d}(E, B, T, d)$  ni Gauss funksiyalari bo'yicha qatorga yoyib kengaytirsak, u holda ikki o'lchamli elektron gazlardagi energetik holatlar zichligi ossillyatsiyalarining haroratga bog'liqligini hisoblash mumkin. Bundan, ko'ndalang kvantlovchi magnit maydonidagi energetik holatlar zichligi ossillyatsiyalarining haroratga bog'liqligini olish mumkin.

**Tahlil va natijalar.** Ko'ndalang kvantlovchi magnit maydonda Landau sathining termik kengayishi diskret sathlarning silliqlashiga olib keladi va termik kengayish Gauss funksiyasi yordamida aniqlanadi. Past haroratlarda Gauss taqsimot funksiyalari delta shaklidagi funksiyaga aylanadi:

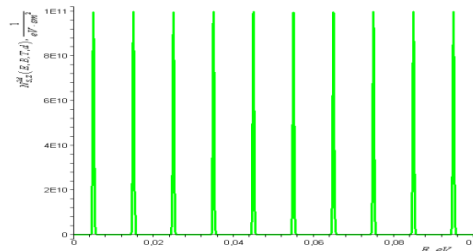
$$Gauss(E, E_i, T) \xrightarrow{T \rightarrow 0} \delta(E - E_i) \quad (3.21)$$

Shunday qilib, to'g'ri burchakli kvant o'ra uchun energetik holatlar zichligi ossillyatsiyalarini quyidagi analitik ifoda orqali olamiz:

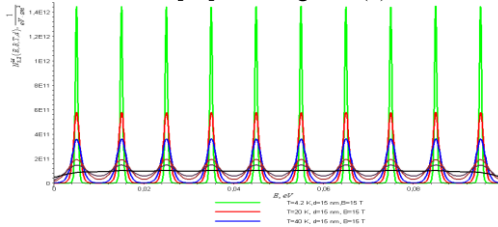
$$N_{S,Z}^{2d}(E, B, T, d) = \sum_{N_L, N_Z} \frac{eB}{\pi\hbar} \cdot \frac{1}{kT} \cdot \exp\left(-\frac{\left(E - \left(\hbar\omega_c \left(N_L + \frac{1}{2}\right) + \frac{\pi^2\hbar^2}{2m^*d^2} N_Z^2\right)\right)^2}{(kT)^2}\right) \quad (3)$$

Bu yerda,  $d$  - kvant o'raning qalinligi;  $N_L$  - to'g'ri burchakli kvant o'ra uchun Landau sathlari soni;  $N_Z$  -  $Z$  o'qi bo'yab o'lchamli kvantlar soni;  $B$  - ko'ndalang kvantlovchi magnit maydonning induksiyasi. Bu formula ko'ndalang kvantlovchi magnit maydon ta'siridagi kvant o'rali yarimo'tkazgichlarda, energetik holatlar zichligi ossillyatsiyasining haroratga bog'liqligini anglatadi. Olingan ifoda turli harorat va ko'ndalang magnit maydonda, ikki o'lchamli elektron gazlarda energetik holatlar zichligi ossillyatsiyalari bo'yicha eksperimental ma'lumotlarni qayta ishlash uchun qulaydir. Shunday qilib, nanoo'lchamli yarimo'tkazgichlardagi energetik holatlar zichligi ossillyatsiyalarining haroratga bog'liqligini ifodalaydigan yangi matematik model ishlab chiqildi. Taklif etilayotgan model yordamida kvantlovchi magnit maydondagi nanoo'lchamli yarimo'tkazgichlarning energetik xolatlar zichligini haroratga bog'liqligini tahlil qilaylik. Ushbu ishda [10], HgCdTe/CdHgTe kvant o'rali assimetrik yarimo'tkazgichlarda klassik va kvantlovchi magnit maydonlar ta'siridagi erkin elektronlarning siklotron rezonans spektrlarining o'zgarishi o'rganilgan. Bu yerda Cd<sub>x</sub>Hg<sub>1-x</sub>Te kvant o'raning qalinligi  $d=15$  nm, magnit maydoni  $B=15$  T va harorati  $T=4,2$  K ni tashkil etadi. Bu ishda materiallar uchun energetik holatlar zichligining haroratga bog'liqligi muhokama qilinmagan. 1-rasmda ko'ndalang kvantlovchi magnit maydon  $B=15$  Tl. va harorat  $4.2$  K bo'lganda kvant o'raning qalinligi  $d=15$

nm uchun  $\text{Cd}_x\text{Hg}_{1-x}\text{Te}$  ni energetik holatlar zichligi ossillyatsiyalari keltirilgan. Rasmda keltirilgan kvant o'raning o'tkazuvchanlik sohasidagi diskret energetik sathlari (3) formula bo'yicha hisoblangan. Bunda diskret energetik sathlari soni 10 ga teng. Har bir diskret energiya cho'qqilari Landau sathlari deyiladi. Grafikda diskret Landau sathlarini kuzatilishiga sabab,  $B=15\text{ Tl}$  da,  $\hbar\omega_c = 0,02\text{ eV}$ ,  $T=4.2\text{ K}$  da  $kT=4.10\text{--}4\text{ eV}$  hamda  $\frac{\hbar\omega_c}{kT} = 50$  yoki  $kT \ll \hbar\omega_c$  sharti bajariladi. Bunday holda Landau sathining termik kengayishi juda kuchsiz va energetik holatlar zichligining ossillyatsiyasi, ideal shakldan chetga chiqishni sezmaydi. Birinchi diskret Landau sathi ( $N_L=0$ ) kvant o'raning o'tkazuvchanlik sohasining pastki qismida paydo bo'ldi. Ikkinchi ( $N_L=1$ ), uchinchi ( $N_L=2$ ) va boshqa diskret Landau sathlari kvant o'raning o'tkazuvchanlik sohasi tubidan yuqorida joylashgan. Shu tarzda, past haroratlarda kvant o'raning valentlik sohasida ham Landau sathining cho'qqilarini hisoblash mumkin. Ushbu hisob-kitoblarga dissertatsiyaning keyingi bobida ko'rib o'tamiz. 2-rasmda energetik xolatlar zichligi  $N_{S,Z}^{2d}(E, B, T, d)$  4.2 K, 20 K, 40 K, 60 K, 80 K va 100 K haroratlar uchun ossillyatsiya keltirilgan. Bu rasmdan ko'rinib turibdiki, harorat ko'tarilishi bilan Landau sathining cho'qqilari keskin silliqlasha boshlaydi va etarlicha yuqori haroratlarda holatlarning diskret energetik holatlar zichligi uzluksiz energetik spektrlariga aylanadi.



1 -rasm.  $\text{HgCdTe}/\text{CdHgTe}$  kvant o'radagi energetik holatlar zichligi ossillyatsiyalari. Kvant o'ra  $\text{Cd}_x\text{Hg}_{1-x}\text{Te}$  ning qalinligi  $d=15\text{ nm}$ ,  $B=15\text{ T}$  va  $T=4.2\text{ K}$ , [10]. Ushbu grafik (3) formula bo'yicha olingan



2-rasm. Ko'ndalang kvantlovchi magnit maydon ( $B=15\text{ Tl}$ ) gacha  $\text{HgCdTe}/\text{CdHgTe}$  kvant o'raning ( $d=15\text{ nm}$ ) o'tkazuvchanlik sohasidagi energetik holatlar zichligi ossillyatsiyalarining haroratga bog'liqligi. Rasmda keltirilgan energetik spektrlar (3) formula bo'yicha hisoblangan

**Xulosa.** Parabolik dispersiya qonuni asosida bo'yilama va ko'ndalang magnit maydon ta'siridagi ikki o'lchamli materiallarning energetik holatlar zichligi ossillyatsiyalarini hisoblash uchun yangi analitik ifodalar olindi. Ko'ndalang kvantlovchi magnit maydon ta'sirida ikki o'lchamli yarimo'tkazgichli materiallarda energetik holatlar zichligi ossillyatsiyalarining haroratga bog'liqligini aniqlash uchun yangi matematik model ishlab chiqildi. Kvant o'rali yarimo'tkazgichlarda harorat ortishi bilan termik kengayish hisobiga diskret Landau sathlari yuvilishi ko'rsatildi va energetik holatlar zichligi ossillyatsiyalari kuzatilmadi.

#### ADABIYOTLAR

1. Дубровский И.М. Новая теория электронного газа в магнитном поле задачи для теории и эксперимента // Успехи физ. мет. 2016. Т.17, С.53–81.
2. Kytin V.G., Bisquert J., Abayev I., Zaban A. Determination of density of electronic states using the potential dependence of electron density measured at nonzero temp // Physical review B. 2004. Vol.70, pp.193304-1- 193304-4.
3. Sablikova V. A., Tkacha Yu.Ya. Singularity of the density of states and transport anisotropy in a two-dimensional electron gas with spin-orbit interaction in an in-plane magnetic field // Semiconductors, 2018. Vol. 52, No.12, pp.1581–1585.
4. Gulyamov G., Erkaboev U.I., Sharibaev N.Yu. Effect of temperature on the thermodynamic density of states in a quantizing magnetic field // Semiconductors. 2014, Vol. 48, No.10, pp. 1323-1328.
5. Gulyamov G., Erkaboev U.I., Sharibaev N.Yu. The de Haas-van Alphen effect at high temperatures and in low magnetic fields in semiconductors // Modern physics letters B. 2016. Vol. 30, No.7. pp.1650077-1-1650077-7.
6. Gulyamov G., Erkaboev U.I., Baymatov P.J. Determination of the density of energy states in a quantizing magnetic field for model Kane // Advances in condensed matter physics. 2016. Vol.2016. pp.5434717-1-5434717-1.
7. Gulyamov G., Erkaboev U.I., Gulyamov A.G. Influence of pressure on the temperature dependence of quantum oscillation phenomena in semiconductors // Advances in condensed matter physics. 2017. Vol.2017. pp.6747853-1-6747853-6.
8. Schoenberg D. Magnetic oscillations in metals. New York, Wiley. 1986. pp.350-400.
9. Стильбанс Л.С. Физика полупроводников. Москва, «Советское радио». 1967. С.416-421.
10. Бовкун Л.С., Маремьянин К.В., Иконников А.В., Спириин К.Е., Алешкин В.Я., Potemski M., Piot B., Orlita M., Михайлов Н.Н., Дворецкий С.А., Гавриленко В.И. Магнитооптика квантовых ям на основе  $\text{HgTe}/\text{CdTe}$  с гигантским расщеплением Рашбы в магнитных полях до 34 Тл // ФТП. 2018. Т.52, вып.11, С.1274-1279.





UDK:52(03) (575.1)

*Durdona NAJMIDDINOVA,*  
*Toshkent davlat pedagogika universiteti o'qituvchisi*  
*E-mail: najmiddinavadurdona@gmail.com*

*O'zMU professori, f.-m.f.d S.Nuritdinov alohitdin taqrizi asosida*

## THE CHALLENGES AND SOLUTIONS OF CREATING AN ASTRONOMY DICTIONARY IN UZBEKISTAN

Annotation

The article underscores the necessity of creating an astronomy dictionary in the Uzbek language, not merely as a list of terms, but as a means of exploring and understanding the mysteries of space and the universe. It sheds light on the linguistic, cultural, and technical challenges involved in this undertaking. The article discusses the concerns raised about the need for various types of dictionaries aimed at astronomers, students, and graduates, as well as the efforts to address their challenges. By highlighting the nuances of astronomical terminology and ensuring accurate translations that resonate with Uzbek-speaking audiences, this noble initiative underscores its significant contributions. Furthermore, it emphasizes the importance of enhancing scientific literacy among Uzbek-speaking audiences and the pivotal role such a dictionary plays in deepening understanding of astronomy within the community.

**Key words:** Terminological dictionary, explanatory dictionary, astronomical dictionaries, astronomical terms.

## ПРОБЛЕМЫ СОЗДАНИЯ АСТРОНОМИЧЕСКОГО СЛОВАРЯ В УЗБЕКИСТАНЕ И ИХ РЕШЕНИЯ

Аннотация

Создание астрономического словаря – это не просто список слов, это путешествие по Вселенной и познание тайн Вселенной. Данная статья проливает свет на лингвистические, культурные и технические проблемы, возникшие при создании астрономического словаря на узбекском языке. Ставятся вопросы о типах словарей, необходимых астрономам, прежде всего студентам и аспирантам, и изучаются их решения. В статье рассматриваются тонкости этого амбициозного предприятия: от изучения тонкостей астрономической терминологии до обеспечения точных переводов, подходящих для носителей узбекского языка. Кроме того, говорится о важности такого словаря в повышении научной грамотности узбекоязычной аудитории и углублении понимания Вселенной.

**Ключевые слова:** Терминологический словарь, толковый словарь, астрономические словари, астрономические термины.

## O‘ZBEKISTONDA ASTRONOMIYADAN LUG‘AT YARATISH MUAMMOLARI VA ULAR YECHIMLARI

Annotatsiya

Astronomiyadan lug‘at yaratish shunchaki so‘zlar ro‘yxatini tuzish emas, balki bu Koinot bo‘ylab sayohat va olam sirlarini o‘rganishdir. Ushbu maqola o‘zbek tilida astronomiya lug‘atini yaratish yo‘lida duch kelgan lingvistik, madaniy va texnik muammolarga oydinlik kiritadi. Unda astronomlar, birinchi navbatda talabalar va magistrantlar uchun zarur lug‘at turlari haqida muammolar ko‘tarilib, ular yechimlari o‘rganiladi. Maqolada astronomik terminologiyaning nozik jihatlari bilan kurashishdan tortib, o‘zbek tilida so‘zlashuvchilarga mos keladigan to‘g‘ri tarjimalarni ta‘minlashgacha bo‘lgan ushbu ulug‘vor tashabbusning nozik tomonlari ko‘rib chiqiladi. Bundan tashqari, unda o‘zbek tilida so‘zlashuvchi auditoriyada ilmiy savodxonlikni oshirish va Koinotni chuqurroq anglashda bunday lug‘atning ahamiyati haqida so‘z boradi.

**Kalit so‘zlar:** Terminologik lug‘at, izohli lug‘at, astronomik lug‘atlar, astronomik atamalar.

**Kirish.** Koinot sirlarini ochuvchi ulug‘vor fan bo‘lmish astronomiya nafaqat hayrat uyg‘otadi, balki insoniyatning Koinotni tushunishga intilishini aks ettiruvchi boy atamalar leksikasini ham taqdim etadi. Yulduzlarga qaraydigan qadimiy sivilizatsiyalardan tortib, Koinotning noyob obyektlarini o‘rganuvchi zamonaviy teleskoplarga boy astronomiya bizga atamashunoslik xazinasini hadya etdi. Ushbu maqolada biz astronomiyadan lug‘atlar yaratish muammolarini o‘rganamiz, koinot haqidagi tushunchamizni boyitadigan samoviy lug‘atni yaratilishi haqida so‘zlashamiz.

Kosmosning ulkan kengligida astronomik atamalar Koinot sirlarini tushunish uchun ko‘prik bo‘lib xizmat qiladi. Eng kichik subatomik zarrachalardan tortib eng uzoq galaktikalargacha, astronomlar o‘z sohalarining murakkabliklarini tushunish va mulqot qilish uchun maxsus leksikaga tayanadilar. Shunga qaramay, ushbu leksikada hatto eng tajribali olimni ham chalkashtirib yuborishi mumkin bo‘lgan juda ko‘p qirrali atamalar, tushunchalar va tarixiy kontekstlar mavjud.

**Mavzuga oid adabiyotlar tahlili.** Ko‘pgina astronomik atamalarining kelib chiqishi qadimiy bo‘lib, ularning ildizlari bobilliklar, yunonlar va misrlilar kabi sivilizatsiyalarga borib taqaladi. Ushbu atamalar ortidagi tarixiy kontekstni tushunish ularning ma‘nosini va qadrini chuqurlashtiradi. Kuzatishlar misli ko‘rilmagan aniqlik bilan olib boriladigan aniq astronomiya davrida standartlashtirilgan terminologiyaga ehtiyoj katta. Astronomik lug‘atlar tadqiqotchilar o‘rtasidagi mulqotda aniqlik va izchillikni ta‘minlash uchun muhim vosita bo‘lib xizmat qiladi. Astronomiya atamalarini turli tillarga tarjima qilish nafaqat xalqaro hamkorlikni osonlashtiradi, balki kosmosning universaligini chuqurroq tushunishga yordam beradi. Astronomik lug‘atlar koinot mo‘jizalariga kirish eshigini ta‘minlab, talabalar va ishqibozlar uchun bebaho manba bo‘lib xizmat qiladi.

Lug‘atlar turli maqsadlarda tuziladi va ularni o‘rganish, o‘z tilining imkoniyatlarini to‘laroq egallashda, savodxonlikni oshirishda, nutq madaniyatini yuksaltirishda hamda bizning so‘z boyligimizni kengaytirishda muhim rol o‘ynaydi.

Bu masala bo'yicha shug'ullanganlardan 1971-yil A.Mel'nikov, A.Nemiro, Z.Kadla va M.Pererveral [1] tomonidan 2000 ta terminni o'z ichiga olgan "Англо-русский словарь" deb nomlangan terminologik lug'atni misol tariqasida keltirishimiz mumkin.

Bundan tashqari 1989- yilda chop yetilgan R. Guseynov, B. Babayev va G. Axmedovlar [2] muallifligidagi lug'atni keltirib o'tishimiz mumkin. Bu lug'at 9000 ta so'zni o'z ichiga olgan bo'lib, ko'p tilli lug'at hisoblanadi. Bu lug'at ozarbayjonlar lug'ati bo'lib, unda terminlarni ruschadan va inglizchadan ozarbayjon tiliga tarjima qilishda foydalaniladi.

R.A.Matzner [3] ham lug'atshunoslik bilan shug'ullangan va uning 2001-yili 4000 ta atamani o'z ichiga olgan "Dictionary of Geophysics, Astrophysics and Astronomy" lug'ati chop etilgan.

Shuningdek, 2010-yil A.K.Murtazov [4] tomonidan "Русско-английский астрономический словарь" deb nomlangan lug'ati yaratilib 10000 ga yaqin so'z va so'z birikmalari tarjima qilingan va kitob holiga keltirilgan.

Bu lug'atlarning kamchiliklari shundaki keltirilgan terminlar son jihatdan kamligi, fanga kirib kelgan yangi so'z (jet, kvazar, kollaps, karlik) va so'z birikmalari (absolyut qora materiya) kiritilmaganligi, lug'atlarning ko'pchiligi ikkita tilda yaratilganligi va bu lug'atlar asosida izohli lug'at yaratilmaganligidir. Bundan tashqari yana bir kamchiligi O'zbekistonda Astronomiya fanidan ko'p sonli terminologik lug'at yo'qligi va izohli lug'at yaratilmaganligini keltirish mumkin

**Tadqiqot metodologiyasi.** Gap shundaki aniq hamda maxsus fanlardagi qator terminlar izohga muhtoj, yangi yoki bizga ko'pincha boshqa tillardan kirib kelgan bu atamalar (masalan, kvazar, blazar, gravitatsion linza, pulsar, qora tuynuk va h.k) alohida lug'atlarda batafsil yoritilishi zarur. Biroq bunday izohli lug'atlarni ishlab chiqishda yetarlicha muammolar mavjud. Shu jumladan, astronomiyadan o'zbek tilida izohli lug'at umuman yo'q, terminologik lug'atdan esa faqat bitta kichik [5] turi mavjud, lekin qator atamalar ma'no jihatidan o'zbek tiliga tarjima qilinmay, chet tilidagi o'qilishi bilan chegaralanib qolingan. Bundan tashqari, ba'zi atamalarga turli izohli lug'atlarda turlicha ta'riflar berilgan bo'ladi. Bu esa foydalanuvchining ilmiy adabiyot bilan ishlashini qiyinlashtiradi. Shu bilan birga, yildan yilga aniq va maxsus fanlar ham rivojlanib boradi, bu esa o'z navbatida yangi atamalarning kelib chiqishiga va yig'ilib borishiga sabab bo'ladi, ya'ni oldin terminologik lug'atni yangilab chiqish zarur. Mavjud yagona terminologik lug'at [5] atiga 3800 atamadan iborat bo'lib, bugungi ilmiy maqolalar va adabiyotlarni to'la o'zlashtirish uchun kamida 10000 dan ortiq atamani bilish zarur.

**Tahlil va natijalar.** Endilikda biz yuqorida ko'rsatilgan muammolarni va ayrim kamchiliklarini bartaraf etish maqsadida astronomiyadan ruscha-o'zbekcha-inglizcha atamalar lug'atini yaratdik. Bu lug'at 10 mingga yaqin atama va so'z birikmalarini o'z ichiga oladi. Lug'atni tuzishda o'zbek tilining boy imkoniyatlaridan foydalanilib, ko'pgina atamalar o'rniga o'zbek so'zlari asosida takomil atamalar yasalgan. Bunda ilmiy-uslubiy, leksikografik, didaktik va psixologik talab va mezonlarga rioya qilindi. Quyida shunday terminlardan namunalar keltiriladi: tizim (система), jarayon (процесс), tahlil (анализ), donador (зернистый), faol (активный), radiofaol (радиоактивный), jadal (интенсив), o'tish (переход) va boshqalar.

Astronomiyaga doir kattagina guruh tushunchalar ilmiy mazmuni jihatidan shunday o'ziga xoslikka egaki, ularga ham tarkibi, ham lug'aviy mazmuni (semantikasi) jihatidan hamohang milliy so'z yoki so'z birikmasini topishning imkoni bo'lmaydi. Bunday hollarda milliy til tarkibiga baynalmilal astronomiya atamasi qabul qilinadi. Masalan, atom, elektron, potensial, energiya, magnit, barion va h.k.

Lug'atda har bir atama alfabit tartibiga ko'ra joylashtirildi. Osmon jismlari va olimlarning ism-sharflari katta harf bilan berilgan, qolgan terminlar esa kichik harflarda yozilgan. Unga asosan umumiy astronomiyada keng foydalaniladigan va fanga yangi kirib kelayotgan atamalar va so'z birikmalari kiritilgan. Lug'atda astronomiya fanining bir qancha yo'nalishlari, ya'ni, umumiy astronomiya, astrofizika, radioastronomiya, osmon mexanikasi, galaktikalar fizikasi, yulduzlar fizikasi, kosmologiya va kosmogoniya bo'yicha atamalar yig'ilib lug'atga kiritilgan. O'zbek tiliga tarjima qilinuvchi astronomik atamalari qo'shma so'z va so'z birikmalari miqdorini ma'lum darajada qamrab olishga harakat qilindi. Bunda astronomiya fanining barcha bo'limlarini qamrab oluvchi astronomik hodisalar, o'lchov birliklari astronomik holatlar xususiyatiga tegishli atamalar va so'z birikmalari tanlab olindi.

Astronomiyadan terminologik lug'at yaratilgandan so'ng O'zbek tilidagi izohli lug'atni tuzishga kirishdik. Lekin nima uchun bizga bunday manba kerak? Astronomiya, har qanday ilmiy fan kabi, aniq til poydevoriga qurilgan. "Qora tuynuk", "kvazar" va "tumanlik" kabi atamalar o'zlari bilan boy tarix, rivojlanayotgan ta'riflar va boshqa samoviy hodisalar bilan murakkab munosabatlarni olib boradi. Izohlar yordamisiz, bu atamalar faqat bir nechta tanlanganlar tomonidan tushuniladigan sirli gliflarga aylanishi mumkin.

Darsliklar, o'quv qo'llanmalarida atama mazmuni bir necha sahifa davomida, hattoki bir necha bo'limlar doirasida ochib beriladi. Bunday holat o'qitish jarayonida ham yuz berib turadi. Bir qator hollarda mualliflar o'quv adabiyotida yangi atamani ishlatganlari holda uning mazmunini ochib berishga uncha e'tibor bermaydilar. Ushbu izohli lug'at o'quv adabiyotlari mualliflariga, o'quvchilarga atama va uning ta'rifiga tayangan holda ilmiy mazmunni aniq va ihsam tarzda bayon qilish imkonini beradi.

Astronomiyaning izohli lug'ati nafaqat ta'riflarni beradi, balki etimologiyasini, tarixiy ahamiyatini, tegishli tushunchalarni va ko'rgazmali qo'llanmalarni ochib beruvchi bebaho izohlarni ham taqdim etadi. Bu yangi ishqibozlar va tajribali mutaxassislarni astronomik terminologiyaning labirint yo'laklarida yo'naltirish uchun puxta ishlab chiqilgan vositadir.

Qolaversa, astronomiyaning fanlararo aloqadorligi tilga yaxlit yondashishni taqozo etadi. Fizika, matematika, kimyo va hatto falsafadagi tushunchalar astronomik tamoyillar bilan o'zaro bog'lanib, sinchkovlik bilan tushuntirishni talab qiladigan bilim ko'nikmalarini yaratadi. Astronomiyaning izohli lug'ati ushbu fanlararo landshaftga kirish eshigi bo'lib xizmat qiladi, u aloqalarni yoritib, chuqurroq tushunishga yordam beradigan o'zaro bog'liq tushunchalarni taklif qiladi.

Astronomiya bo'yicha izohli lug'atni yaratishga kirishish tizimli yondashuvni va tafsilotlarga diqqat bilan qarashni talab qiladi. Har qanday izohli lug'atning asosi uning mazmunida yotadi. Ilmiy jurnallar, darsliklar, onlayn ma'lumotlar bazalari va nufuzli veb-saytlar kabi nufuzli manbalardan olingan astronomiya atamalarining to'liq ro'yxatini tuzishdan boshladik. Har bir atamaning to'g'riligi va dolzarbligini ta'minlash, ilmiy konsensusning kengligini olish uchun bir nechta [6], [7], [8], [9] va boshqa manbalar bo'ylab ta'riflarni tekshirish juda muhimligini inobatga oldik.

Ushbu lug'atdan foydalanuvchilarga qulaylik uchun atamalar alifbo tartibida joylashtirilgan bo'lib, lug'atga hozirgi kunda astronomiyada keng qo'llaniladigan umumastronomiya atamalarini kiritilgan va ularga aniq va qisqa ko'rinishda izohlar berilgan. Masalan, Afeliy - Quyosh atrofida harakatlanuvchi jism orbitasining Quyoshdan eng uzoq nuqtasi. Kosmologik doimiy - gravitatsion maydonga ega bo'lmagan fazoning egriligini o'lchovchi doimiy. Habbl doimiysi - Koinotning kosmologik

kengayishi tufayli galaktikalar uzoqlashishi tezliklari bilan ulargacha bo'lgan masofalar orasidagi bog'lanishning mutanosiblik koeffitsiyenti. Sayyoraning siderik aylanish davri - sayyoraning Quyosh atrofida yulduzlarga nisbatan bir marta to'la aylanib chiqish davri.

Ushbu tadqiqot bosqichida astronomik terminologiyaning nuanslari va murakkabliklariga alohida e'tibor berildi. Ba'zi atamalar vaqt o'tishi bilan rivojlanib, yangi ma'nolarga ega bo'lishi yoki eskirgan ma'nolarni yo'qotishi mumkin. Boshqalar muqobil talqinlar va nuqtai nazarlarni sinchiklab ko'rib chiqishni talab qiladigan ilmiy hamjamiyat ichida davom etayotgan munozaralarga duchor bo'lishi mumkin. Aynan shu muammolarga alohida ahamiyat qaratildi. Izohlar izohli lug'atning markazi bo'lib xizmat qiladi, qo'shimcha kontekst, tarixiy ma'lumotlar, etimologik tushunchalar va tegishli tushunchalarga o'zaro havolalar beradi. Izohlar yaratishda chuqurlik va aniqlikdan voz kechmasdan, murakkab tushunchalarni hazm bo'ladigan bilim zarralariga aylantirib, ravshanlik va qulaylikka intilish talab qilinadi.

**Xulosa va takliflar.** O'zbek tilida astronomik lug'at yaratish birinchi navbatda talabalar va magistrantlar uchun ilmiy ishlarida foydalanish imkoniyatlarini oshirishga qaratilgan salmoqli ishdur. Ushbu loyiha muhim astronomik atamalar va tushunchalarni aniq va tushunarli tilda yig'ish, tarjima qilish va tushuntirishni o'z ichiga oladi. Bu ishda albatta o'zbek tilshunosligi bo'yicha mutaxassislar bilan hamkorlik lug'at mazmunining to'g'ri va dolzarbligini ta'minlaydi, madaniy manbalarni ko'rib chiqish uning madaniy ahamiyatini boyitadi. Lug'at illyustratsiyalar va ko'rgazmali qurollarni birlashtirish orqali murakkab astronomik hodisalarni tushunishni kuchaytiradi. Mutaxassislar va foydalanuvchilarning ko'rib chiqishlari va fikr-mulohazalari lug'atni nashr etish va tarqatishdan oldin takomillashtirishga hissa qo'shadi. Oxir oqibat, astronomik lug'at o'zbek tilida olam mo'jizalarini o'rganish va baholashga xizmat qilib, o'qituvchilar, talabalar va ixlosmandlar uchun qimmatli manba bo'lib xizmat qiladi.

#### ADABIYOTLAR

1. O.A.Melnikov, A.A.Nemiro, Z.I.Kadla, V.M.Pererva., Англо-русский словарь, М., 1971.
2. R. Guseynov, B. Babayev va G. Axmedov., Astronomiya terminlar lyg'ati. 1989
3. R.A.Matzner., Dictionary of Geophysics, Astrophysics and Astronomy. 2001
4. A.K.Murtazov., Русско-английский астрономический словарь, Ryazan., 2010
5. A.Latipov, A.Rahimov, A.Qodirov, H.Ishmuxamedov va A. Ramazonov., Astronomiyadan ruscha-o'zbekcha terminologik lug'at, Fan, T., 1974
6. G.J. Ellard., An Astronomical Glossary. Or Dictionary of Terms Used in Astronomy . 1983
7. P.Habibullayev, E.Nazirov, Sh.Otajonov, D.Nazirov., Fizika izohli lug'ati T., 2002
8. G'. Jalolov., O'zbekcha – ruscha – inglizcha – arabcha astronomik atamalar lug'ati, T., 2000
9. M.G. Saidova., История формирования астрономической терминологии в сопоставляемых языках., Серия наук, 2012
10. www.astronet.ru



*Ulug'bek NEGMATOV,*  
*Namangan muhandislik-texnologiya instituti tayanch doktoranti*  
**Rustamjon RAHIMOV,**  
*Namangan Institute of Engineering and Technology, PhD*  
**Ulugbek ERKABOEV,**  
*Namangan Institute of Engineering and Technology, DSc professor*  
*E-mail: rgrakhimov@gmail.com*  
*Phone: 93) 499 99 29*

*Based on the review of Doctor of Physical and Mathematical Sciences, Professor of NamICI M. G. Dadamirzaev*

**MATHEMATICAL MODELING OF SHUBNIKOV-DE HAAS OSCILLATIONS IN NARROW-GAP SEMICONDUCTORS UNDER THE INFLUENCE OF TEMPERATURE AND ABSORPTION OF MICROWAVE RADIATION**

Annotation

In this article, a mathematical model for Shubnikov-de Haas oscillations in semiconductors upon absorption of microwave radiation is obtained and its temperature dependence is studied. A two-dimensional image of microwave magnetoabsorption oscillations in narrow-gap semiconductors is constructed.

**Key words:** semiconductor, electron gas, oscillation, microwave, Landau levels, mathematical model, Shubnikov-de Haas oscillations.

**МАТЕМАТИЧЕСКОЕ МОДЕЛИРОВАНИЕ ОСЦИЛЛЯЦИЙ ШУБНИКОВА-ДЕ ГАЗА В УЗКОЗОННЫХ ПОЛУПРОВОДНИКАХ ПОД ВОЗДЕЙСТВИЕМ ТЕМПЕРАТУРЫ И ПОГЛОЩЕНИЯ МИКРОВОЛНОВОГО ИЗЛУЧЕНИЯ**

Аннотация

В данной статье получена математическая модель осцилляций Шубникова-де Гааза в полупроводниках при поглощении микроволнового излучения и изучена ее температурная зависимость. Построено двумерное изображение осцилляций магнитопоглощения в узкозонных полупроводниках.

**Ключевые слова:** полупроводник, электронный газ, осцилляция, СВЧ, уровни Ландау, математическая модель, осцилляция Шубникова-де Гааза.

**HARORAT VA MIKROTO'LQINLI NURLANISH TA'SIRIDAGI TOR ZONALI YARIMO'TKAZGICHLARDA SHUBNIKOV-DE GAAZ OSSILLYATSİYALARINI MATEMATİK MODELASH TIRISH**

Annotatsiya

Ushbu maqolada mikroto'lqinli nurlanishni yutishda yarim o'tkazgichlarda Shubnikov-de Gaaz ossillyatsiyalarining matematik modeli olingan va uning haroratga bog'liqligi o'rganilgan. Tor zonali yarimo'tkazgichlarda magnit yutilish ossillyatsiyalarning ikki o'lchovli tasviri hosil qilingan.

**Kalit so'zlari:** yarimo'tkazgich, elektron gaz, ossillyatsiya, mikroto'lqinli pech, Landau sathlari, matematik model, Shubnikov-de Gaaz ossillyatsiyalari.

**Introduction.** In recent years, much attention has been paid to the definition and study of quantum oscillation phenomena under the influence of temperature, a strong electromagnetic field, and deformation in bulk and low-dimensional semiconductors [1-4]. With the help of such phenomena, it is possible to determine some basic physical quantities (the effective masses of charge carriers, magnetoresistance, magnetic susceptibility, etc.) and study the band energy spectra of electrons in new semiconductor materials.

Shubnikov-de Haas, de Haas-van Alphen oscillations and the quantum Hall effect were discovered at ultralow temperatures and superstrong magnetic fields [5]. In this case, oscillation phenomena were observed in bulk semiconductors and metals.

**Model.** As is known, all quantum oscillation phenomena strongly depend on the spectral density of states in semiconductors. In works [6-7], the temperature dependence of the spectral density of states in narrow-gap semiconductors in quantizing magnetic fields was studied. However, these papers did not consider the influence of microwave radiation absorption on quantum oscillation phenomena.

Let us consider the Shubnikov-de Haas oscillations in narrow-gap semiconductors under the action of temperature and a strong electromagnetic field. The power of absorbed microwave radiation per unit volume is determined by the following expression [8]:

$$P = \sigma \cdot E_E^2 \quad (1)$$

Here,  $\sigma$  is the conductivity of the semiconductor,  $E_E$  is the electric field strength of the wave.

In a quantizing magnetic field, the distribution function satisfies the kinetic equation [9]:

$$\frac{\partial f_N}{\partial t} + \frac{eE_z}{\hbar} \frac{\partial f_N}{\partial k_z} = -\frac{f_N - f_{0N}}{\tau_N}. \quad (2)$$

From (15), one can determine the current density of  $\dot{j}_{zN}$  and the longitudinal electrical conductivity of  $\sigma_{zz}$  for each N-th quantum level:

$$j_{zN} = -\frac{e^2 E_z}{\pi m} \int k_z \tau_N \frac{\partial f_{0N}}{\partial k_z} dk_z. \quad (3)$$

$$\sigma_{zz} = -\frac{(2m)^{\frac{1}{2}} e^2}{\pi^2 \hbar^3} \hbar \omega_c \int_{\hbar \omega_c / 2}^{\infty} \sum_N \tau_N(E) N_s(E_N, H) \frac{\partial f_0(E)}{\partial E} dE \quad (4)$$

As seen from (4), in a quantizing magnetic field, the longitudinal conductivity of  $\sigma_{zz}$  strongly depends on the oscillations of the spectral density of states and the  $\tau(E)$  relaxation time.

For a unit volume of a semiconductor, the following condition is satisfied:  $\rho_{zz} \approx R_{zz} = \frac{1}{\sigma_{zz}}$ . Here,  $\rho_{zz}$  is the longitudinal specific magnetoresistance.

In the general case, the relaxation time is determined by the following expression [10]:

$$\tau(E) = \tau_0 E^r \quad (5)$$

where,  $\tau_0$  and  $r$  - have different values for different semiconductors.

Substituting previous expressions, we obtain the following expression:

$$P[Gauss(E, E_i, T), H, E_E] = \sum N^k [Gauss(E, E_i, T), H] \cdot \tau(E) \cdot E_E^2 \quad (6)$$

$$P\left[\frac{\partial f_0(E_i, \mu, T)}{\partial E}, H, E_E\right] = \sum N^k \left[\frac{\partial f_0(E_i, \mu, T)}{\partial E}, H\right] \cdot \tau(E) \cdot E_E^2 \quad (7)$$

$$P[Lorentz(E, E_i, T), H, E_E] = \sum N^k [Lorentz(E, E_i, T), H] \cdot \tau(E) \cdot E_E^2 \quad (8)$$

We differentiate expressions (6), (7) and (8) with respect to H, that is,  $\frac{dP^k(H, T, E, E_E)}{dH}$ .

From here, we obtain the expression for the dependence of the Shubnikov-de Haas oscillations on the absorption of microwave radiation and temperature in narrow-gap semiconductors:

$$\frac{dP[Gauss(E, E_i, T), H, E_E]}{dH} = C \cdot \sum N^k [Gauss(E, E_i, T), H] \cdot \left(1 + \frac{AH(N + \frac{1}{2})}{2\left(\frac{E^2}{E_g} + E - (N + \frac{1}{2})AH\right)}\right) \cdot \tau(E) \cdot E_E^2 \quad (9)$$

$$A = \frac{\hbar e}{mc}; \quad C = \frac{(m)^{\frac{3}{2}}}{(2)^{\frac{1}{2}} \pi^2 \hbar^3}$$

$$\frac{dP\left[\frac{\partial f_0(E_i, \mu, T)}{\partial E}, H, E_E\right]}{dH} = C \cdot \sum N^k \left[\frac{\partial f_0(E_i, \mu, T)}{\partial E}, H\right] \cdot \left(1 + \frac{AH(N + \frac{1}{2})}{2\left(\frac{E^2}{E_g} + E - (N + \frac{1}{2})AH\right)}\right) \cdot \tau(E) \cdot E_E^2 \quad (10)$$

$$\frac{dP[Lorentz(E, E_i, T), H, E_E]}{dH} = C \cdot \sum N^k [Lorentz(E, E_i, T), H] \cdot \left(1 + \frac{AH(N + \frac{1}{2})}{2\left(\frac{E^2}{E_g} + E - (N + \frac{1}{2})AH\right)}\right) \cdot \tau(E) \cdot E_E^2 \quad (11)$$

Here,  $P^k$  is the microwave absorption power for the Kane model.

Using previous expressions one can determine the  $\frac{dP(H, T, E, E_E)}{dH}$  oscillations for wide-gap semiconductors.

The working formula for the Shubnikov-de Haas oscillations in the absorption of microwave radiation and temperature for wide-gap materials is as follows:

$$\frac{dP(H, T, E, E_E)}{dH} = C \sum_{N=0}^{\max} \frac{1}{\sqrt{E - (N + \frac{1}{2})AH}} \cdot \left(1 + \frac{AH(N + \frac{1}{2})}{\left(E - (N + \frac{1}{2})AH\right)}\right) \cdot \sum_{i=1}^{m_k} Gauss(E, E_i, T) \cdot \tau(E) \cdot E_E^2 \quad (12)$$

From here, we have the opportunity, using formulas (9), (10), (11) and (12), to calculate the  $\frac{dP(H, T, E, E_E)}{dH}$  oscillations in narrow-gap and wide-gap semiconductors in a strong electromagnetic field and at various temperatures.

Thus, a new mathematical model has been created to determine the oscillations of the absorption of microwave radiation in narrow-gap semiconductors. On the basis of the proposed model, it is possible to investigate to explain the experimental oscillations at different temperatures.

Let us consider Shubnikov-de Haas oscillations in the presence of absorption of microwave radiation in narrow-gap semiconductors. In particular, we will obtain the  $\frac{dP^k(H, T, E, E_E)}{dH}$  oscillation plot for *InSb* using formula (11).

Figure 1 shows the dependence of  $\frac{dP}{dH}$  on the magnetic field strength *H* in *InSb* ( $E_g(0) = 0.234$ ) at  $T=3$  K and  $E_E = 10^3 \frac{V}{sm}$ . In this case,  $E_E = const$ .

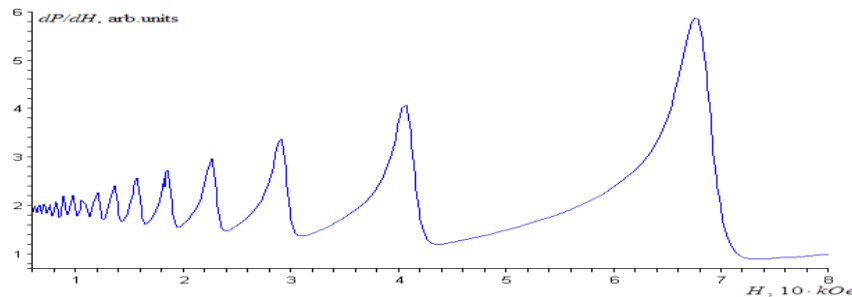


**Fig.1.** Oscillations  $\frac{dP}{dH}$  in *InSb* at temperature  $T=3$  K and electromagnetic wave strength  $E_E = 10^3 \frac{V}{sm}$ , calculated using formula (9).

As the power of the electromagnetic wave increases, the amplitude of the  $\frac{dP}{dH}$  oscillations increases. This can be seen

from Fig.2, which shows the  $\frac{dP}{dH}$  oscillations for two different values of the power of the absorbed electromagnetic wave.

Figure 2 shows oscillations of absorption of microwave radiation at various strengths of the electromagnetic field and constant low temperatures. Where,  $E_{E1} = 10^3 \frac{V}{cm}$ ,  $E_{E2} = \sqrt{2} \cdot 10^3 \frac{V}{cm}$ .

As can be seen from Fig. 2, the amplitude of quantum oscillation phenomena can be controlled using the power of microwave radiation.

Let us now calculate the microwave magnetoabsorption in semiconductors using the above model. In particular, we will obtain the  $\frac{dP^k(H, T, E, E_E)}{dH}$  oscillation plot for *InAs* using formulas (9), (10) and (11).

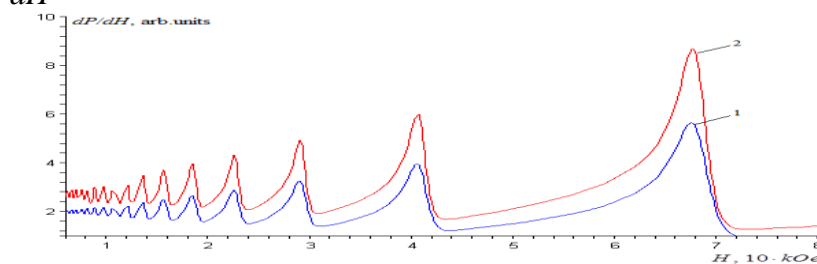


**Fig.2.**  $\frac{dP}{dH}$  oscillations in *InSb* at various electromagnetic wave intensities.

$$1 - E_{E1} = 10^3 \frac{V}{cm}; \quad 2 - E_{E2} = \sqrt{2} \cdot 10^3 \frac{V}{cm}$$

**Conclusion.** Based on the study, the following conclusion can be drawn:

Mathematical modeling of the temperature dependence of the oscillations of microwave magnetoabsorption in semiconductors has been carried out using the Gaussian, Lorentzian functions and the derivative of the Fermi-Dirac function with respect to energy.



Using this model, the dependences of quantum oscillation phenomena on microwave fields and temperature in semiconductors are calculated.

Using the Gaussian function, the oscillation of the absorption of microwave radiation in narrow-gap semiconductors at various temperatures is calculated. The calculation results are compared with experimental data.

#### REFERENCES

1. Alhun Aydin, Altug Sisman. Quantum oscillations in confined and degenerate Fermi gases. I. Half-vicinity model // *Physics letters A*. 2018. Vol.382. pp.1807-1812.
2. Klaus von Klitzing. 25 Years of quantum Hall effect (QHE): A personal view on the discovery, physics and applications of this quantum effect // *Seminaries Poincare*. 2004. Vol.2, pp.1-10.
3. Bagraev N.T., Grigoryev V.Yu., Klyachkin L.E., Malyarenko A.M., Mashkov V.A., Romanov V.V., Rul' N.I. High-temperature quantum kinetic effect in silicon nanosandwiches // *Low temperature physics*, 2017. Vol.43, No.1, pp.132-142.
4. Kazuma Eto, Zhi Ren, Taskin A.A, Kouji Segawa, Yoichi Ando. Angular-dependent oscillations of the magnetoresistance in Bi<sub>2</sub>Se<sub>3</sub> due to the three-dimensional bulk Fermi surface // *Phys.Rev. B*, 2010. Vol.81, Iss.19. pp.5309-5310.
5. Schoenberg D. *Magnetic oscillations in metals*. New York, Wiley. 1986. pp.350-400.
6. U.I. Erkaboev, R.G. Rakhimov, N.A. Sayidov. Mathematical modeling determination coefficient of magneto-optical absorption in semiconductors in presence of external pressure and temperature. *Modern Physics Letters B*. 2021, 2150293 pp, (2021).
7. U.I. Erkaboev., G. Gulyamov, J.I. Mirzaev, R.G. Rakhimov. Modeling on the temperature dependence of the magnetic susceptibility and electrical conductivity oscillations in narrow-gap semiconductors. *International Journal of Modern Physics B*. 34, 7, 2050052 pp, (2020).
8. G. Gulyamov, U.I. Erkaboev, R.G. Rakhimov, J.I. Mirzaev. On temperature dependence of longitudinal electrical conductivity oscillations in narrow-gap electronic semiconductors. *Journal of Nano- and Electronic Physics*. 12, 3, 03012 pp, (2020).
9. G. Gulyamov, U.I. Erkaboev, N.A. Sayidov, R.G. Rakhimov. The influence of temperature on magnetic quantum effects in semiconductor structures. *Journal of Applied Science and Engineering*. 23, 3, 453-460 pp, (2020).
10. Dmitriev I.A., Mirlin A.D., Polyakov D.G. Theory of Fractional Microwave-Induced Resistance Oscillations // *Phys. Rev. Lett*. 2007. Vol.99, pp. 206805-1-206805-7.



*Salakhutdin NURITDINOV,*  
Professor of National university of Uzbekistan  
E-mail: nur200848@mail.ru  
*Sobir TURAEV,*  
PhD student of National university of Uzbekistan

*O'zRFA Astronomiya instituti professori Mirtadjiyeva Karomat taqrizi asosida*

## PROBLEMS OF THE ACCELERATING EXPANSION OF THE UNIVERSE

Annotation

Observational data from the James Webb Telescope pose significant challenges to the  $\Lambda$ CDM model. This could lead to significant changes to the standard model. The accelerated expansion of the Universe is associated with the redshift of distant objects, and standard cosmology assumes that this redshift is caused by cosmological expansion. In this paper, we consider the alternative possibility that the redshift of distant objects may also be due to the phenomenon of redshift of light in the intergalactic and interstellar media.

**Key words:** accelerating expansion, cosmology, intergalactic medium, interstellar medium, modeling, redshift.

## О ПРОБЛЕМЕ УСКОРЯЮЩЕГОСЯ РАСШИРЕНИЯ ВСЕЛЕННОЙ

Аннотация

Данные наблюдений телескопа Джеймса Уэбба представляют собой серьезные проблемы для модели  $\Lambda$ CDM. Это может привести к существенным изменениям в стандартной модели. Ускоренное расширение Вселенной связано с красным смещением далеких объектов, и стандартная космология предполагает, что это красное смещение вызвано космологическим расширением. В этой статье мы рассматриваем альтернативную возможность того, что красное смещение далеких объектов также может быть связано с явлением красного смещения света в межгалактической и межзвездной среде.

**Ключевые слова:** ускоряющееся расширение, космология, межгалактическая среда, межзвездная среда, моделирование, красное смещение.

## KOINOTNING TEZLANISH BILAN KENGAYISHI MUAMMOLARI

Аннотация

Jeyms Webb teleskopidan olingan kuzatuv ma'lumotlari  $\Lambda$ CDM modeli uchun jiddiy qiyinchiliklar tug'diradi. Bu standart modelda sezilarli o'zgarishlarga olib kelishi mumkin. Olamning tezlashtirilgan kengayishi uzoqdagi jismlarning qizilga siljishi bilan bog'liq va standart kosmologiyada bu qizilga siljish kosmologik kengayish tufayli yuzaga keladi deb taxmin qilinadi. Ushbu maqolada biz uzoq obyektning qizilga siljishi ham galaktikalararo va yulduzlararo muhitda yorug'likning qizilga siljishi fenomeni bilan bog'liq bo'lishi mumkin bo'lgan muqobil imkoniyatni ko'rib chiqamiz.

**Kalit so'zlar:** tezlanuvchan kengayish, kosmologiya, galaktikalararo muhit, yulduzlararo muhit, modellashtirish, qizilga siljish.

**Introduction.** Observing very young massive objects with JWSP poses significant challenges for modern cosmology. In this case, it is useful to introduce new alternatives to standard cosmology and increase the demand for existing alternatives. The new model of the Universe proposed by Perlmutter and his co-authors [1,2] is known to be expanding with acceleration, which was established by them on the basis of observations of type Ia supernovae (SNe Ia) in distant galaxies and the discovery of regular deviations of distances to them from Hubble's law towards them increase. However, without disputing in any way the possibility of the existence of dark energy in the Universe, it is useful to look for an alternative to its expansion with acceleration, if only because the processing of observational data and the calculations of the above authors need clarification on a number of factors. Riess et al. considered some factors of affecting the distance modulus, including effect of a Local Void-very small, Weak Gravitational Lensing, Evolution, Extinction and Light Curve Fitting Method [1]. They consider that all these factors cannot explain for the  $0.28^m$  difference in the template-fitting SNe Ia distances and the  $\Omega_\Lambda=0$  prediction. Among them, the procedure for determining the distance to a light source requires special attention, since a natural question arises: is the regular deviation of distances related to the effect of a decrease in the brightness of supernova light as it moves in intergalactic space and inside our Galaxy?

Let us first turn to the results of modern observational data performed on the Hubble Space Telescope and large ground-based telescopes. These results show that the understanding of the physical state, structure and distribution of baryonic and dark matter in intergalactic space today is clearly far from the concept accepted in [1,2], and only now we have deep observations indicating a patchy structure of the distribution of these types of matter in intergalactic space. An example is the work of Whitaker et al. [3], where in the redshift interval  $0.5 < z < 2.5$  young galaxies and systems of globular clusters of stars were found inside dark matter in Coma Berenices [4]. Both articles [3,4] were written based on the results of research in 2017. If several dark dwarf galaxies were previously known, now dark spiral galaxies have been discovered [5]. The work of Farrah et al. [6] even discovered super-luminous infrared galaxies with a redshift of  $1.5 < z < 3$  inside a dark matter halo with a mass of  $6 \times 10^{13} M_\odot$ . These super-luminous infrared galaxies are likely the precursors of galaxy clusters or superclusters. Thus, if stars in the Milky Way are born in dark molecular clouds, then it turns out that protogalaxies and young galaxies should be sought within dark

matter. The complex, patchy structure of intergalactic matter, which may contain protogalaxies and other types of baryonic matter, suggests that neglecting the effect of weakening the brightness of distant supernovae in intergalactic space, and especially in our Galaxy, is generally unacceptable.

### I. Alternatives to the cosmological redshift

Masanori Sato [7] proposed an alternative interpretation of the theory of the accelerating Universe using experimental data on redshift. At small  $z$  ( $<0.1$ ), there is no slowdown in the width of the light curve. At large  $z$  ( $>0.1$ ), a slowing down of the width of the light curve appears. We know Zwicky tired light mechanism based on gravitational redshift is proposed for a diffusion-free and dispersion-independent frequency redshift mechanism.

Although Tired Light Theory is mainly suggested for the static Universe, however, this theory could be attached to the expanding Universe (non-accelerating). Partial correctness of the theory may also damage to the existing standard model. In Tired light theory, redshift is caused not by the cosmological expansion, as in the  $\Lambda$ CDM model, but by the loss of a portion of photon's energy during the intergalactic motion. This loss may be owing to electrons, neutral hydrogen and other substances in the intergalactic medium. Accordance with New Tired Light (NTL) oscillating electrons in the intergalactic environment absorb and reproduce photon, resulting in reduced its energy, wavelengths, and redshift [8]. As photons irradiated by intergalactic electrons are coherent, light cannot dim (interference is not observed). Current intergalactic medium models contend that it's mass density:  $\rho_M \approx 10^{-27}$  kg/m<sup>3</sup>. Using identic electron number density,  $n \approx 0.498$  giving a mean free path of  $7.13 \times 10^{21}$ m. If redshift due to interaction between photon and intergalactic medium matter it can't be used it in calculations. Then this result may be sufficient to damage to the SNe Ia cosmology calculations.

Frank R. Tangherlini developed an alternative theory for the expansion of the Universe with acceleration. This theory doesn't keep out the existence of dark energy, although opposed to acceleration, but assumes that there is no negative compressive force (no acceleration) [9]. At  $z = 1.65 \pm 0.15$ , the Universe expansion coincides with a non-accelerating period [10]. In another paper [11], when  $z \approx 0.5$ , the visibility of SNe Ia fits to the maximum brightness. This theory opposes the accelerating expansion by supporting the expanding Universe.

The Timescape cosmological model [12] was supposed as a potentially vital Smale & Wiltshire alternative to homogeneous and accelerating model with fluid-like dark energy. This model considered that the redshift value could be greater in Voids, and less in intergalactic and interstellar medium. At present, about 40-50% of the universe is in voids of order  $30h^{-1}$  Mpc in diameter. According to observations of voids, the present epoch Universe is inhomogeneous on scales below the BAO (Baryon Acoustic Oscillation) in scale of  $100h^{-1}$  Mpc, while exhibiting the density difference of order 8% in density for sample volumes larger than this scale [13,14]. Timescape cosmology predicted the values that are comparably low at  $61.7 \pm 3.0$  km s<sup>-1</sup> Mpc<sup>-1</sup>, being a non-linear average of  $50.1 \pm 1.7$  km s<sup>-1</sup> Mpc<sup>-1</sup> for walls and an apparent maximum of  $75.2_{-2.6}^{+2.0}$  km s<sup>-1</sup> Mpc<sup>-1</sup> across voids [51].

**Photon transmission in different media.** The effect of partial loss of radiation in intergalactic and interstellar space occurs in completely different ways and is cumulative in nature, as a result of which it is lost through absorption.  $A''(r) > 0$  in units of magnitude  $m$ , which directly enters into the expression for the "absolute magnitude" of the supernova at the moment of its maximum brightness

$$M_{max} = m_{max} - 5lgr - A''(r), \quad (1)$$

Moreover, the value  $M_{max} = -19^{m.07}$  (filter B) was established for many supernovae. Formula (1) makes it possible to determine the distance  $r$  to the supernova (i.e. to the galaxy), if only we know the value of the total absorption  $A''(r)$  in a given direction, which is not a simple task. Note that the authors of [1,2] it is believed that there is a critical value of redshift  $z_{cr} = 0.7$ , and for  $z_{cr} > z$  the light source is in a state where the Universe was expanding at a slower rate and in this case absorption can be neglected. However, in our opinion, the absorption effect must be taken into account regardless of the value of redshift of the supernova. These authors determine the absorption value using an approximate formula known in stellar astronomy, where excess color is involved [3,4]. Numerous calculations of the value known in the literature show that its value depends not only on the type of objects, but also on the direction in our Galaxy. In this regard, below we present another way to calculate the absorption effect.

In (1), the value of the absorption function  $A''(r)$  is determined by the absorption coefficient  $a(r)$ , which in general depends on the distance  $r$  and consists of at least two parts: interstellar  $a_{is}(r)$  and intergalactic  $a_{ig}(r)$  coefficients absorption, i.e.

$$A''(r) = \int_0^r a(r)dr = \int_0^R a_{is}(r)dr + \int_0^r a_{ig}(r)dr = J_S + J_G, \quad (2)$$

where  $R$  is the distance from us to the boundary of the characteristic size of our Galaxy in the observed direction, which is a function of galactic latitude  $b$ .

Analysis of observational data assessing the absorption of light in various directions in the Milky Way shows that the magnitude of absorption is maximum in the equatorial plane of symmetry of our Galaxy and decreases rapidly with increasing galactic latitude  $b$ . The Sun is located just near this plane, along which the gas-dust layer of matter is located, since the Galaxy is a system flattened along the  $z$ -coordinate with a mass concentration towards this plane. The absorption coefficient  $a_{ig}(r)$  is proportional to the distribution density of the gas-dust layer, for which the barometric formula is a fairly good approximation

$$a_{is}(r) = a_0 \exp\left(\frac{-z}{\Delta}\right) = a_0 \exp\left(\frac{-r \sin b}{\Delta}\right), \quad (3)$$

where  $a_0$  is the absorption value in the plane itself,  $a_{is}$  is the characteristic half-thickness of the substance layer. Therefore, in (2)

$$J_S = \frac{a_0 \Delta}{\sin b} \left[ 1 - \exp\left(-\frac{r \sin b}{\Delta}\right) \right] \quad (4)$$

According to observations,  $a_0 = 2.^m23 \pm 0.^m19$ ,  $\sim 100$  pc, and the value of  $R$  depends on  $b$ .

As for determining the value of  $J_S$ , today this task seems quite difficult due to the lack of observational data and requires, first of all, an analysis of the distribution of gas-dust matter in galaxy clusters and superclusters, since it is believed that electromagnetic radiation interacts very weakly with dark matter, in dense areas in which accumulation of ordinary, observable matter occurs

To estimate the average value of  $J_G$  in (2), you can use the normal density distribution

$$a_{ig}(r) = \bar{g}_0 N \sqrt{\frac{a}{\pi}} \exp(-ar^2). \quad (5)$$

here  $\bar{g}_0$  is the average value of the absorption coefficient in a galaxy cluster,  $N$  is the number of clusters in a given direction,  $a$  is the proportionality coefficient. Substituting (5) and (2) and representing the integral from  $R$  to  $r$  as the difference of integrals for the intervals  $[0, R]$  and  $[0, r]$  we find that

$$J_G = \frac{1}{2} \bar{g}_0 N [(\Phi\sqrt{ar}) - (\Phi\sqrt{aR})], \quad (6)$$

where  $\Phi$  is the symbol of the special function "probability integral". A more accurate estimate of the value obviously requires the accumulation of observational data and the implementation of appropriate additional analysis.

**Conclusion.** Redshift is a very important concept in astrophysics. It explains the expansion of the Universe and determines the distances to distant objects. In standard cosmology, the cosmological redshift is assumed to be related to the cosmological expansion. But there are a number of alternatives to the occurrence of redshift. In this work, we propose that light experiences external influences as it passes through different media and that the cosmological redshift arises from the absorption and re-emission of light in the intergalactic and interstellar medium. There are a number of alternatives for the origin of the redshift. We assume that the redshift is caused in part by the absorption and re-emission of photons in the interstellar and intergalactic medium, and modulate the passage of light through various media. We need further research to draw a definitive conclusion on our supporting proposal, and we will develop our results in future work.

#### REFERENCE

1. Adam G. Riess et al., Observational evidence from supernovae for an accelerating Universe and a cosmological constant, *Astrophysical journal*, 116:1009-1038, 1998 September, p.1009,1020, 1028-1034
2. S. Perlmutter et al., measurements of  $\Omega$  and  $\lambda$  from 42 high-redshift supernovae, *The Astrophysical Journal*, 517 : 565-586, 1999 June 1
3. Whitaker, Katherine E et al., Predicting Quiescence: The Dependence of Specific Star Formation Rate on Galaxy Size and Central Density at  $0.5 < z < 2.5$ , *The Astrophysical Journal*, 838:19 (19pp), 2017 March 20
4. Pieter van Dokkum et al., Extensive Globular Cluster Systems Associated with Ultra Diffuse Galaxies in the Coma Cluster, *The Astrophysical Journal Letters*, 844:L11 (7pp), 2017 July 20
5. Pieter van Dokkum et al., A high stellar velocity dispersion and  $\sim 100$  globular clusters for the ultra-diffuse galaxy dragonfly 44, *The Astrophysical Journal Letters*, 828:L6 (6pp), 2016 September 1
6. D. Farrah et al., Ultraluminous Infrared Galaxies at  $1.5 < z < 3$  Occupy Dark Matter Haloes of Mass  $\sim 6 \times 10^{13} M_{\odot}$ , *ASP Conference Series*, Vol. 380, 2007
7. Masanori Sato, Tired Light: An Alternative Interpretation of the Accelerating Universe, 20181225 Revised, 20 Oyamazuka, Oiwa-cho, Toyohashi, Aichi 441-3193, Japan, 2019, p.2
8. Lyndon E Ashmore, Calculating the redshifts of distant galaxies from first principles by the new tired light theory (NTL), *IOP Conf. Series: Journal of Physics: Conf. Series* 1251 (2019) 012007, p.1
9. Frank R. Tangherlini, A Possible Alternative to the Accelerating Universe I, II, III, IV, *Journal of Modern Physics*, 2015, 6, 78-87; 2015, 6, 1360-1370; 2016, 7, 1829-1844; 2017, 8, 622.
10. Riess A. G., et al., The farthest known supernova: support for an accelerating Universe and a glimpse of the epoch of deceleration, *The Astrophysical Journal*, 560, 49-71. 2001, p.49.
11. Tonry J. L., Cosmological results from high- $z$  supernovae, *The Astrophysical Journal*, 594, 1-24, 2003, p.2
12. David L Wiltshire, Cosmic clocks, cosmic variance and cosmic averages, *New Journal of Physics* 9 (2007) 377, p.3
13. David W. Hogg et al. Cosmic homogeneity demonstrated with luminous red galaxies. arXiv:astro-ph/0411197v1 8 Nov 2004, p.1
14. Sylos Labini F. et al. Testing the Copernican and Cosmological Principles in the local Universe with galaxy surveys, arXiv:1006.0801v1 [astro-ph.CO] 4 Jun 2010, p.1



UDK: 534.112

**Abdutilib PARMONOV,**  
*O‘zbekiston Milliy universiteti Jizzax filiali, O‘zbekiston*  
*E-mail:pabdutolib@gmail.com*

*PhD,dotsent R.Abduraxmanov taqrizi asosida*

## DINAMIK SO‘NDIRGICH O‘RNATILGAN BALKA KO‘NDALANG TEBRANISHLARINING USTIVORLIGI

Аннотация

Dinamik so‘ndirgich o‘rnatilgan balka ko‘ndalang tebranishlarining ustivorligi. Balka va unga o‘rnatilgan dinamik so‘ndirgichdan iborat mexanik sistemaning kinematik qo‘zg‘atishlardagi tebranishlari ustivorligi masalasi qaralgan. Sistemaning ustivorlik shartlari topilgan.

**Kalit so‘zlar:** tebranishlardan himoyalalanuvchi sistema, tebranishlar, ustivorlik, tebranishlar dekrementi, elastik dissipativ xarakteristika.

## ПРИОРИТЕТ ПОПЕРЕЧНЫХ КОЛЕБАНИЙ МОЛОТА С ДИНАМИЧЕСКИМ ДЕМПФЕРОМ

Аннотация

Устойчивость балки с динамическим гасителем колебаний. Рассматривается задача устойчивости механической системы, состоящей из балки и динамического гасителя колебаний при кинематических воздействиях. Найдены условия устойчивости системы.

**Ключевые слова:** виброзащитная система, колебания, устойчивость, декремент колебаний, упругодиссипативная характеристика.

## PRIORITY OF TRANSVERSE VIBRATION OF THE BEAM WHEN INSTALLING A DYNAMIC DAMPER

Annotation

Stability of bar with dynamic absorber of oscillations. It was tinned the problem of bar stability with dynamic absorber on kinematic influences. It was found conditions of the system stability.

**Keywords:** vibroprotection system, oscillations, stability, vibration decrement, elastic-dissipate characteristics.

**Kirish.** Strukturaviy muhandislik sohasida, ayniqsa, yuqori aniqlik va chidamlilikni talab qiladigan tizimlarda tebranishlarni nazorat qilish juda muhim masala. Turli tuzilmalarning asosiy komponentlari bo‘lgan nurlar, ularning nozik tabiati va yuk ko‘taruvchi ilovalarda keng qo‘llanilishi tufayli tebranish buzilishlariga ayniqsa sezgir. Nurlar boshdan kechirishi mumkin bo‘lgan turli xil tebranish usullari orasida ko‘ndalang tebranishlar - nur uzunligiga perpendikulyar bo‘lganlar - ayniqsa zararli hisoblanadi. Ushbu tebranishlar stress konsentratsiyasining oshishi, tizimli charchoq va hatto ekstremal holatlarda halokatli nosozlik kabi muhim muammolarga olib kelishi mumkin.

Ushbu muammolarni hal qilish uchun dinamik amortizatorlar odatda kiruvchi tebranishlarni kamaytirishning samarali vositasi sifatida qo‘llaniladi. Ushbu qurilmalar tebranish energiyasini tarqatadigan va shu bilan tebranishlar amplitudasini kamaytiradigan qarshi kuchni kiritish orqali ishlaydi. Biroq, dinamik dampning samaradorligi ko‘p jihatdan uning muayyan tebranish rejimlarini nishonga olish qobiliyatiga bog‘liq. Nurlar bo‘ylama, buralish va ko‘ndalang tebranishlarni boshdan kechirishi mumkin bo‘lsa-da, ko‘pincha ko‘ndalang tebranishlar jiddiy struktura buzilishiga olib kelishi mumkinligi sababli ko‘pincha e‘tiborni talab qiladi.

Ushbu maqola nurlarga dinamik amortizatorlarni o‘rnatishda ko‘ndalang tebranishlarning ustivorligiga qaratilgan. Transvers tebranishlarni boshqarish muhimligini ta‘kidlab, biz asosiy mexanikani har tomonlama tushunishni va turli muhandislik ilovalarida dinamik amortizatorlarning ishlashini optimallashtirish bo‘yicha amaliy ko‘rsatmalarni taklif qilishni maqsad qilganmiz. Nurlarning dinamik xarakteristikalari va damping mexanizmlari o‘rtasidagi o‘zaro ta‘sir o‘rganilib, tebranishlarni samarali boshqarish uchun hisobga olinishi kerak bo‘lgan muhim parametrlarni ta‘kidlaydi. Nazariy tahlil va amaliy tadqiqotlar orqali ushbu maqola nurga asoslangan tizimlarning strukturaviy yaxlitligi va uzoq umrini ta‘minlash uchun ko‘ndalang tebranishlarga ustunlik berish zarurligini ko‘rsatadi.

Ichki nomukammallikka ega taqsimlangan parametrlil mexanik sistemalar dinamikasini tadqiq etish masalasi sistema harakat differensial tenglamalarining murakkab tuzilishga egaligi sababli yechilishi murakkab bo‘lgan masalalardan hisoblanadi. Bu tipdagi masalalarning yechilishi maxsus metodlarni qo‘llashni talab etadi [1]. da gisterezis elastik dissipativlik xususiyatlari e‘tiborga olingan holda dinamik so‘ndirgich o‘rnatilgan balkaning harakat differensial tenglamalari tuzilgan va tebranish tenglamalari uzatish funksiyalari ko‘rinishida olingan. Ushbu ishda bu yechimlarning ustivorligi masalasi qaraladi.

Sistema harakat differensial tenglamalari quyidagicha:

$$EJ[1 + C_0(-\eta_1 + i\eta_2)]\frac{\partial^4 w}{\partial x^4} + \frac{24}{h^3}EJ(-\eta_1 + i\eta_2)\frac{\partial^2}{\partial x^2}\left[\frac{\partial^2 w}{\partial x^2}\int_0^{h/2} f(\xi_{or})z^2 dz\right] + \quad (1)$$

$$+ \rho F \frac{\partial^2 w}{\partial t^2} - c[1 + (-\theta_1 + i\theta_2)(D_0 + f(\zeta_{or}))]\zeta \delta(x - x_0) = -\rho F \frac{\partial^2 w_0}{\partial t^2};$$

$$m \frac{\partial^2 w(x_0)}{\partial t^2} + m \frac{\partial^2 \zeta}{\partial t^2} + c[1 + (-\theta_1 + i\theta_2)(D_0 + f(\zeta_{or}))]\zeta = -m \frac{\partial^2 w_0}{\partial t^2},$$

bunda  $E$ —balka elastiklik moduli;  $J$ —balka kesimining inersiya momenti;  $f(\xi_{or})$  va  $f(\zeta_{or})$  — tebranishlar dekrementi bo'lib,

$\xi_{or}$  va  $\zeta_{or}$  nisbiy deformatsiyalarning funksiyalari:

$$f(\xi_{or}) = C_1 \xi_{or} + C_2 \xi_{or}^2 + \dots + C_{n_1} \xi_{or}^{n_1}; \quad f(\zeta_{or}) = D_1 \zeta_{or} + D_2 \zeta_{or}^2 + \dots + D_{n_2} \zeta_{or}^{n_2}, \quad (2)$$

$\eta_1, \eta_2, \theta_1, \theta_2$  — o'zgarma koeffitsientlar.

Sistema uchun quyidagi uzatish funksiyalari olingan [1]:

$$\Phi(q_{ka}) = |q_{ka}| = \frac{W_0}{|\Delta|} \left\{ [d_k \omega^2 - n^2(1 - \theta_1 Q)(\mu \mu_k u_0 + d_k)]^2 + [\theta_2 Q n^2 (\mu \mu_k u_0 + d_k)]^2 \right\}^{1/2}; \quad (3)$$

$$\Phi(\zeta_a) = |\zeta_a| = \frac{W_0}{|\Delta|} \left\{ [(1 - d_k u_0) \omega^2 - p^2(1 - \eta_1 R)]^2 + [\eta_2 p^2 R]^2 \right\}^{1/2}.$$

bunda

$$\Delta = [\omega^2 - p^2(1 + (-\eta_1 + i\eta_2)R)][\omega^2 - n^2(1 + (-\theta_1 + i\theta_2)Q)] -$$

$$- n^2(1 + (-\theta_1 + i\theta_2)Q)\mu \mu_k u_0^2 \omega^2.$$

bunda  $\mu = \frac{m}{m_C}$ ;  $\mu_k = \frac{\ell}{d_{2k}}$ ;  $m_C$  — balka massasi;  $d_k = \frac{d_{1k}}{d_{2k}}$ ;  $p_k$  — energiya tarqalishi e'tiborga olinmagan

holdagi xususiy chastota;

$$d_{1k} = \int_0^\ell u_k dx; \quad d_{2k} = \int_0^\ell u_k^2 dx; \quad R = C_0 + \frac{3EJ\mu_k}{m_C p_k^2} \sum_{i=1}^{r_2} C_i q_{ka}^i \frac{h^i}{2^i(i+3)} G_{ki};$$

$$Q = D_0 + f(\xi_{or}); \quad G_{ki} = \int_0^\ell u_k \frac{\partial^2}{\partial x^2} \left( \frac{\partial^2 u_k}{\partial x^2} \left| \frac{\partial^2 u_k}{\partial x^2} \right|^i \right) dx.$$

Olingan yechimlarning ustivorligini tekshiramiz. Bunda 2 ta xususiy hollarni qarab o'tamiz: 1) balkaning elastiklik xarakteristikasi chiziqli bo'lgan hol —  $R = const$  va  $\eta_2 = 0$ , 2) dinamik so'ndirgich elastik xarakteristikasi chiziqli bo'lgan hol —  $Q = const$  va  $\theta_2 = 0$ .

(3) tenglamalar bilan aniqlanuvchi egri chiziqlar chiziqlimas mexanik sistemalarning o'ziga xos jihati — tebranishlar amplitudasining chastotaga bog'liqligi sababli ma'lum shartlar bajarilganda argument ( $\omega$ ) bo'yicha bir qiymatli aniqlanmasligi mumkin. Tebranishlar chastotasining bu qiymatlariga mos soha qaralayotgan mexanik sistema (3) yechimi uchun noustivorlik

sohasi bo'ladi. Ushbu sohani topish uchun (3) tenglamalarning har biridan to'liq differensiallarni hisoblab,  $\frac{d\Phi(q_{ka})}{d\omega}$  ni

topamiz. Oshkormas funksiyalarning bir qiymatli bo'lishligining Lagranj teoremasiga asosan, ushbu hosila chekli qiymatlarga ega bo'lishlik shartlarini topamiz.

Hisoblashlarni bajarib, qaralayotgan sistema uchun ustivorlik oraliqlarini aniqlash imkonini beruvchi quyidagi munosabatlarni olamiz:

birinchi hol uchun

$$\omega^4 - \omega^2(n^2(1 + \mu \mu_k u_0^2) + p_k^2(1 - \eta_1 R)) + p_k^2(1 - \eta_1 R)n^2 = \quad (6)$$

$$= \beta_{1,2} [(1 + \mu \mu_k u_0^2)\omega^2 - p_k^2(1 - \eta_1 R)]n^2,$$

bunda

$$\beta_{1,2} = \frac{1}{2} \left[ -\theta_1(2Q + Q'\zeta) \pm \sqrt{\theta_1^2 \zeta^2 Q'^2 - 4Q(Q'\zeta)\theta_2} \right]. \quad (7)$$

ikkinchi hol uchun



$$\left(2A + \left(2R + \frac{\partial R}{\partial q_k} q_k\right) \eta_1 B\right)^2 = B^2 \left[ \left(\eta_1 \frac{\partial R}{\partial q_k} q_k\right)^2 - 4\eta_2^2 R \frac{\partial(Rq_k)}{\partial q_k} \right], \quad (8)$$

bunda

$$A = (\omega^2 - p^2)(\omega^2 - n^2(1 - \theta_1 Q)) - n^2(1 - \theta_1 Q)\mu\mu_k u_0^2 \omega^2;$$

$$B = p^2(\omega^2 - n^2(1 - \theta_1 Q)).$$

Olingan (6) – (8) tengliklar biror haqiqiy  $\omega$  larda bajarilsa, (3) bilan aniqlanuvchi egri chiziq (oshkormas funksiya) argumentning bu qiymatlarida chekli hosilaga ega bo'lmashligini va oshkormas funksiya bir qiymatli bo'lmashligini ifodalaydi. Demak, bu tengliklarni sistema ustivorlik oraliqlarini topish ifodalari hisoblanadi.

(8) tenglikni  $m$ -ga ko'paytirib,  $m$ ning o'rniga nol qo'yisak (dinamik so'ndirgichsiz) balkaning chiziqalmas tebranishlarining ustivorlik shartlarini hosil qilamiz.

$$\begin{aligned} (\omega^2 - p^2 - p^2 \eta_1 R)^2 - q_k \frac{\partial R}{\partial q_k} p^2 \eta_1 (\omega^2 - p^2 - p^2 \eta_1 R) + \\ + p^4 \eta_2^2 \left( R + q_k \frac{\partial R}{\partial q_k} \right) = 0. \end{aligned} \quad (9)$$

Xuddi shunga o'xshash munosabat [2] da olingan natijalarga mos keladi.

**Xulosa.** Nurlardagi ko'ndalang tebranishlarni nazorat qilish turli muhandislik dasturlarida strukturaning yaxlitligi va ishlashini saqlashning muhim jihati hisoblanadi. Ushbu tadqiqot dinamik amortizatorlarni o'rnatishda ko'ndalang tebranishlarga ustunlik berish muhimligini ta'kidladi, chunki bu tebranishlar ko'pincha struktura barqarorligi uchun eng katta xavf tug'diradi. Nazariy tahlil va amaliy misollar orqali tebranishlarni samarali boshqarishga dinamik amortizatorlarni nurning o'ziga xos ko'ndalang rejimlariga ehtiyotkorlik bilan sozlash orqali erishish mumkinligi ko'rsatildi.

Ko'ndalang tebranishlarni muvaffaqiyatli yumshatish nafaqat tuzilmalarning uzoq umrini va xavfsizligini oshiradi, balki stress konsentratsiyasini kamaytirish va yuzaga kelishi mumkin bo'lgan nosozliklarning oldini olish orqali ularning ishlash samaradorligini oshiradi. Muhokama qilingan strategiyalar, jumladan, chastotalarni moslashtirish, amortizatorlarni optimal joylashtirish va damping koeffitsientlarini to'g'ri tanlash, dinamik amortizatorlarning samaradorligini maksimal darajada oshirish uchun muhimdir.

Ushbu sohadagi kelajakdagi yutuqlar o'zgaruvchan tebranish sharoitlarini real vaqt rejimida sozlash, nurlarda tebranishlarni boshqarishning aniqligi va samaradorligini yanada oshirishga qodir bo'lgan adaptiv damping tizimlarini ishlab chiqishni o'z ichiga olishi mumkin. Oxir oqibat, ko'ndalang tebranishlarni boshqarishga ustunlik berish orqali muhandislar tuzilmalarning ishlash muddati davomida mustahkam, ishonchli va xavfsiz bo'lishini ta'minlashi mumkin.

#### ADABIYOTLAR

1. Дусматов О.М. Исследование поперечных колебаний стержня с динамическим гасителем/ Киев. – 1987.-11с.-Рус.-Деп. в УкрНИИИТИ. 11.05.87, №1431-Ук87.
2. Рыжков Л.М. О стационарных поперечных колебаниях стержня с гистерезисным рассеянием энергии.// Пробл. прочности. №4. 1987. – с. 102-105.
3. Писаренко Г.С. Обобщенная нелинейная модел учета рассеяния энергии при колебаниях. – Киев: Науково думка, 1985. – 240 с.
4. Буранов Х., Рахмонов А. Поперечные колебания упругого стержня с динамическим гасителем колебаний//Современные проблемы механики грунтов ва сложных реологических систем. Материалы межд. научно-технической конфренсии. Самарканд-2013. 123-125 с.



UDK: 621.315.592

**Rustamjon RAHIMOV**,  
Namangan Institute of Engineering and Technology, PhD  
**Ulugbek ERKABOEV**,  
Namangan Institute of Engineering and Technology, DSc professor  
**Dilshodbek ERKABOEV**,  
Fergana Polytechnic Institute, master  
E-mail: rgrakhimov@gmail.com

Based on the review of Doctor of Physical and Mathematical Sciences, Professor of NamICI M. G. Dadamirzaev

### CALCULATION OF OSCILLATIONS OF THE DENSITY OF ENERGY STATES IN TWO-DIMENSIONAL MATERIALS IN THE PRESENCE OF A LONGITUDINAL AND TRANSVERSE STRONG MAGNETIC FIELD

Annotation

In this article, we investigated the effect of temperature and a quantizing magnetic field on oscillations of the density of energy states in the conduction band of nanoscale semiconductor structures. A new mathematical model has been developed for calculating the temperature dependence of the oscillations of the density of states in a rectangular quantum well under the influence of a transverse quantizing magnetic field.

**Key words:** semiconductor, nanoscale semiconductor structures, quantizing magnetic field, quantum well, oscillation, density of energy states.

### РАСЧЕТ ОСЦИЛЛЯЦИЙ ПЛОТНОСТИ ЭНЕРГЕТИЧЕСКИХ СОСТОЯНИЙ В ДВУМЕРНЫХ МАТЕРИАЛАХ ПРИ НАЛИЧИИ ПРОДОЛЬНОГО И ПОПЕРЕЧНОГО СИЛЬНОГО МАГНИТНОГО ПОЛЯ

Аннотация

В этой статье мы исследовали влияние температуры и квантующего магнитного поля на колебания плотности энергетических состояний в зоне проводимости наноразмерных полупроводниковых структур. Разработана новая математическая модель для расчета температурной зависимости колебаний плотности состояний в прямоугольной квантовой яме под воздействием поперечного квантующего магнитного поля.

**Ключевые слова:** полупроводник, наноразмерные полупроводниковые структуры, квантующее магнитное поле, квантовая яма, осцилляция, плотность энергетических состояний.

### BO‘YLAMA VA KO‘NDALANG KUCHLI MAGNIT MAYDON TA‘SIRIDAGI IKKI O‘LCHOVLI MATERIALLARDA ENERGETIK HOLATLARI ZICHLIGI OSSILLYATSIYALARINI HISOBLASH

Annotatsiya

Ushbu maqolada kichik o‘lchovli yarimo‘tkazgichli tuzilmalarning o‘tkazuvchanlik zonasidagi energiya holatlari zichligi ossillyatsiyalariga harorat va kvantlovchi magnit maydonning ta‘sirini o‘rganilgan. Ko‘ndalang kvantlovchi magnit maydon ta‘sirida to‘g‘ri burchakli kvant o‘rasidagi holatlar zichligi ossillyatsiyalarining haroratga bog‘liqligini hisoblash uchun yangi matematik model ishlab chiqilgan.

**Kalit so‘zlar:** yarimo‘tkazgich, kichik o‘lchovli yarimo‘tkazgichli tuzilmalar, kvantlovchi magnit maydon, kvant o‘ra, ossillyatsiya, energetik holatlar zichligi.

**Introduction.** Currently, the interest in applied and fundamental research in the field of condensed matter physics has shifted from bulk materials to nanoscale semiconductor structures. Of particular interest are the properties of the energy spectrum of charge carriers in low-dimensional semiconductor structures exposed to a quantizing magnetic field. Quantization of the energy levels of free electrons and holes in a quantizing magnetic field leads to a significant change in the form of oscillations of the density of energy states in two-dimensional semiconductor structures.

In particular, in works [1-3], calculations of the density of states of Landau levels in two-dimensional electron gases, with a uniform perpendicular magnetic field and with a random field of arbitrary correlation are considered. A semiclassical nonperturbative approach of path integrals is developed for a random field of arbitrary correlation, and this provides an analytical solution for the density of states of Landau levels. The deviation of the density of states from the Gaussian form increases with decreasing correlation length and weakening the magnetic field [1-3.]

Model. According to the band theory of a solid, the wave function of a free electron, in the presence of an external field, is a solution of the stationary Schrödinger equation with a parabolic dispersion law [4-9]:

$$\left\{ -\frac{\hbar^2}{2m^*} \nabla^2 + V(r) \right\} \psi(r) = E\psi(r) \quad (1)$$

Here,  $V(r)$  is the energy of free electrons in the presence of an external field,  $E$  is the energy of charge carriers in the absence of an external field,  $\psi(r)$  is the wave function. The dependence of the quantizing magnetic field on the wave function

of electrons and the energy spectra of charge carriers in two-dimensional electron gases is determined using equation (1), in which the momentum operator should be replaced by the generalized momentum operator in a quantizing magnetic field:

$$\left\{ \frac{1}{2m^*} (-i\hbar\nabla - eA)^2 + V(z) \right\} \psi(r) = E\psi(r) \quad (2)$$

Here,  $A$  is the vector potential of the induction of a strong magnetic field,  $[B = rot(A)]$ . To solve equation (2), the direction of the vector  $B$  is chosen in two different ways. In the first case, this vector will be directed along the plane of the two-dimensional layer (along the X-axis) and perpendicular to the Z-axis. For a longitudinal quantizing magnetic field, vector potential  $A$  can be chosen in the form of  $A = (0, -Bz, 0)$ .  $\psi_{k_{\perp m}}$  from the Schrödinger equation (2), for a deep rectangular quantum well, takes the following form:

$$\psi_{k_{\perp m}}(r) = \frac{1}{\sqrt{S}} \exp(ik_{\perp} r_{\perp}) \varphi_n(z - z_0) \quad (3)$$

Then it can be solved by the method of separation of variables, using the function from work [4]. This function describes localized motion in the YZ plane and the state of motion of a free electron along the X axis. In equation (3), the  $\varphi_n(z - z_0)$  function is responsible for localized motion. Then the solution to equation (3) will be as follows:

$$\left\{ -\frac{\hbar^2}{2m^*} \frac{d^2}{dz^2} + V(z) + \frac{1}{2} m^* \omega_c^2 (z - z_0)^2 \right\} \varphi_n(z - z_0) = E_n \varphi_n(z - z_0) \quad (4)$$

Here,  $z_0 = -\frac{\hbar k_y}{eB}$ ,  $\omega_c = \frac{eB}{m^*}$ . Equation (4) is called the equation of a quantum harmonic oscillator, the motion of which is additionally limited by a quantum well, and  $E_n$  is a discrete level.

In a quantizing magnetic field, if the width of the quantum well increases, the energy spectrum of free electrons will increase. That is,  $a \gg \lambda = \sqrt{\frac{\hbar}{eB}}$ . Here,  $a$  is the width of the quantum well,  $\lambda$  is the magnetic length, which is equal in magnitude to the radius of the characteristic orbit of an electron in a quantizing magnetic field. Hence, the discrete energy levels  $E_n$  will be equal to the energies of the harmonic quantum oscillator:

$$E_N = \hbar\omega_c \left( N + \frac{1}{2} \right), \quad N = 0, 1, 2, 3, \dots \quad (5)$$

According to equation (2), the velocity and momentum of charge carriers in the direction of the quantizing magnetic field can take any values. In other words, the motion of free electrons and holes in the direction of the XY plane (i.e., along the X axis) is not quantized. Hence, the total energy of free electrons in two-dimensional electron gases in the presence of a magnetic field directed along the X axis is determined by the following expression:

$$E_N = \hbar\omega_c \left( N + \frac{1}{2} \right) + \frac{\hbar^2 k_x^2}{2m} \quad (6)$$

Where,  $\hbar\omega_c \left( N + \frac{1}{2} \right)$  is the energy of motion of a free electron in the YZ plane, these energies are called discrete Landau levels.  $\frac{\hbar^2 k_x^2}{2m}$  is the energy of continuous motion along the X axis. Thus, in the presence of a longitudinal magnetic field, due to the quantization of the orbital motion of charge carriers in the YZ plane, the allowed energy zone is split into one-dimensional magnetic subbands, that is, into discrete Landau levels.

In three-dimensional and two-dimensional electron gases, a change in the energy spectrum of charge carriers leads to a change in the oscillations of the density of states in a quantizing magnetic field. In works [10-11], an analytical expression is derived for the oscillations of the density of states in three-dimensional electron gases in the presence of a quantizing magnetic field with a non-parabolic dispersion law. There, the temperature dependence of the oscillations of the density of energy states with a transverse strong magnetic field was discussed.

Now, let us first calculate the oscillations of the density of energy states in two-dimensional electron gases in the presence of a longitudinal strong magnetic field. When the width of the quantum well becomes comparable to the de Broglie wavelength, in two-dimensional semiconductor materials, then quantization occurs. That is,  $L_z \approx \lambda_D$  and  $L_y \gg L_z$ . Hence, in the YZ plane, the cyclotron mass is calculated by the expression:

$$m_c = \frac{\hbar}{2\pi} \frac{\partial L_y}{\partial E} \quad (7)$$

For a parabolic dispersion law, the effective cyclotron mass will be constant. The energy in the interval between the two Landau levels is  $\Delta E = \hbar\omega_c$ . Hence, for a two-dimensional semiconductor material, we find the difference in the section length of two isoenergy surfaces:

$$\Delta L_Y = \frac{2\pi m_c \hbar \omega_c}{\hbar} \tag{8}$$

The number of states for quantization, in the presence of a longitudinal quantizing magnetic field, in the YZ plane, due to the cyclic conditions, is equal to  $\frac{L_Y}{2\pi}$ . In expression (8), the number of states between two quantum orbits is:

$$\frac{L_Y}{2\pi} \Delta L_Y = \frac{2\pi m_c}{\hbar} \hbar \omega_c \frac{L_Y}{2\pi} = m \omega_c L_Y \tag{9}$$

From formula (6) we find  $k_x$

$$k_x = \frac{(2m)^{1/2}}{\hbar} \left( E_N - \hbar \omega_c \left( N + \frac{1}{2} \right) \right)^{1/2} \tag{10}$$

In the presence of a longitudinal strong magnetic field, the movement of charge carriers along the X axis is not quantized in  $k_x$  and takes the following form:

$$k_x = \frac{2\pi}{L_x} n_x \tag{11}$$

With the help formulas (10) and (11), in the energy range from  $\hbar \omega_c \left( N + \frac{1}{2} \right)$  to E, it is possible to determine the number of states along the X axis:

$$n_x = \frac{L_x (2m)^{1/2}}{2\pi \hbar} \left( E_N - \hbar \omega_c \left( N + \frac{1}{2} \right) \right)^{1/2} \tag{12}$$

Using formulas (9) and (12), in the presence of a longitudinal magnetic field and for a rectangular quantum well, we obtain the total number of quantum states by the following expression:

$$N_X^{2d}(E, H) = \frac{L_x L_y (m)^{3/2}}{2^{1/2} \pi \hbar^2} \hbar \omega_c \sum_{N=0}^{N_{\max}} \left( E_N - \hbar \omega_c \left( N + \frac{1}{2} \right) \right)^{1/2} \tag{13}$$

Differentiate expression (13) with respect to energy E per unit area ( $L_x L_y = 1$ ) and define  $N_{SX}^{2d}(E, H)$ :

$$N_{SX}^{2d}(E, H) = \frac{(m)^{3/2}}{2^{1/2} \pi \hbar^2} \hbar \omega_c \sum_{N=0}^{N_{\max}} \frac{1}{\left( E_N - \hbar \omega_c \left( N + \frac{1}{2} \right) \right)^{1/2}} \tag{14}$$

This formula is called the density of energy states, in two-dimensional electron gases (that is, in a rectangular quantum well), in the presence of a longitudinal quantizing magnetic field. This formula is analogous to the quantum thread equation (Fig.1). Obviously, with a longitudinal quantizing magnetic field, in a two-dimensional electron gas, the energies of free electrons in the YZ plane can take only some fixed values, but the electron energy along the X axis remains free (not quantized). Formula (14), at  $H \rightarrow 0$ , turns into work [19]:

$$N_S^{2d}(E) = \frac{m}{\pi \hbar^2} \tag{15}$$

This formula describes the density of energy states in two-dimensional electron gases in the absence of a magnetic field (Fig.1). In conclusion, we note that the main feature of the oscillation of the density of energy states for a two-dimensional electron gas, in the presence of a longitudinal strong magnetic field, is that it does not depend on the width of the quantum well or the size of the size quantization and is determined only by the magnitude of the magnetic field induction and energy. And also the densities of states oscillate only in accordance with changes in the longitudinal

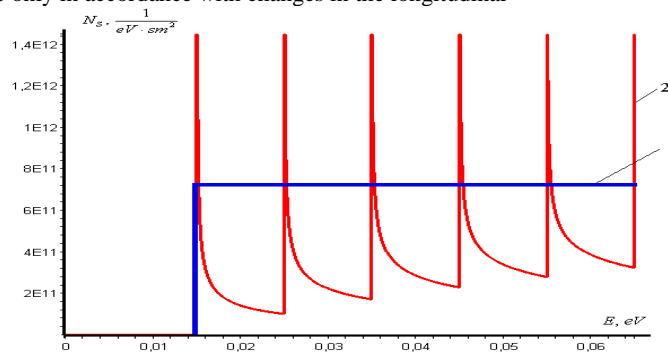


**Fig. 1.** Dependence of the density of energy states on the energy of charge carriers in two-dimensional electron gases in the presence and in the absence of a longitudinal quantizing magnetic field.  
1. B = 0, calculated by the formula (15) [9];

2.  $B = 10$  T, calculated by the formula (14)

**Conclusion.** Based on the study, the following conclusions can be drawn: Analytical expressions for the oscillations of the density of states in two-dimensional electron gases in the presence of longitudinal and transverse quantizing magnetic fields with a parabolic dispersion law are derived. A new mathematical model has been developed to determine the temperature dependence of the oscillations of the density of energy states in two-dimensional semiconductor materials when exposed to a transverse quantizing magnetic field. It is shown that with increasing temperature, discrete Landau levels are smoothed out due to thermal smearing and no oscillations of the energy density of states are observed in two-dimensional electron gases. Using the proposed model, graphs of the effect of the thickness of the quantum well on the oscillations of the density of states in the presence of a quantizing magnetic field were created.

#### REFERENCES

1. Glutsch S *et al.* (2003). "Density of states of a two-dimensional electron gas in a perpendicular magnetic field and a random field of arbitrary correlation". *Journal of physics: condensed matter*. Vol.15, pp.1305 – 1323.
2. Dubrovsky I.M. (2016). "A new theory of an electron gas in a magnetic field and problems for theory and experiment". *Uspekhi fiz. met.* Vol. 17, pp. 53–81.
3. Kytin V.G. *et al.* (2004). "Determination of density of electronic states using the potential dependence of electron density measured at nonzero temp". *Physical review B*. Vol.70, pp.193304-1- 193304-4.
4. Dragunov V.P. *et al.* (2019). *Nanoelectronics*. Part 1. Moscow, "Yurayt". 2019. p.248-257. (in Russian)
5. Devyatov E.V. (2014). "Fundamentals of physics of low-dimensional systems and the regime of the quantum Hall effect". *Chernogolovka, Editorial and Publishing Department of the IPCP RAS*. pp.20-25.(in Russian)
6. Burmistrov I.S.(2015). "An introduction to the theory of the integer quantum Hall effect.". *Moscow, Editorial and Publishing Department of IPCP RAS*. p.23-30.
7. Glazkov V.N. (2016). "Two-dimensional electronic systems in a magnetic field. Quantum Hall effect". *Moscow, MIPT*. pp.15-27.
8. Borisenko S.I. (2010). "Physics of semiconductor nanostructures". *Tomsk, ed. "Tomsk Polytechnic University"*. pp.33-43.
9. Neverov V.N. and Titov A.N. (2008). "Physics of low-dimensional systems". *Yekaterinburg, ed. "IONTS nanotechnology and advanced materials"*. pp.71-80.
10. Erkaboev U.I. (2017). "Influence of temperature and pressure on oscillatory phenomena in semiconductors in a quantizing magnetic field". *Thesis. Doctor of Philosophy (PhD) in Physics and Mathematics Tashkent. ANRUz FTI*. pp.27-43.
11. Erkaboev U.I. (2019). "Quantum oscillatory phenomena in semiconductor structures under the influence of external fields". *Thesis. Doctor of Physical and Mathematical Sciences (DSc). Tashkent. Tashkent State Technical University*. pp. 68-85.



УДК: 537.311.1

**Достон САИТКУЛОВ,**  
Докторант НУУз  
E-mail: [dostonsaidkulov@gmail.com](mailto:dostonsaidkulov@gmail.com)  
**Мунира КАРАБАЕВА,**  
Доцент НУУз, к.ф.-м.н  
**Яйра РАХИМОВА,**  
Старший преподаватель НУУз, PhD  
**Шерзод КАМИЛОВ,**  
Доцент НУУз, к.ф.-м.н  
E-mail: [sherkamilov19@gmail.com](mailto:sherkamilov19@gmail.com)  
**Умарбек АБДУРАХМАНОВ,**  
Профессор НУУз, д.ф.-м.н

Под редакцией профессора ТГТУ, д.ф.-м.н. Зикриллаева Н.

## TRANSFER OF CHARGE CARRIERS IN HETEROGENEOUS MATERIALS CONTAINING ELECTRICALLY CONDUCTING NANOPARTICLES

Annotation

Based on a comparison and analysis of the conductivity of pyropolymers, as well as ceramics and polymers containing nickel nanoparticles, it is concluded that the formation of such heterogeneous materials, to a first approximation, can be represented as a process of filling a dielectric with nanodispersed “metallic” particles - similar to doped compensated semiconductors. The results obtained were explained based on the concepts of the spatial-structural hierarchical model proposed by Balberg et al. for heterogeneous materials.

**Key words:** pyropolymer, polyacrylonitrile,  $\pi$ -electrons, percolation threshold, semiconductor.

## ПЕРЕНОС НОСИТЕЛЕЙ ЗАРЯДА В ГЕТЕРОГЕННЫХ МАТЕРИАЛАХ СОДЕРЖАЩИХ ЭЛЕКТРОПРОВОДЯЩИЕ НАНОЧАСТИЦЫ

Аннотация

На основе сравнения и анализа проводимости пирополимеров, а также керамики и полимеров содержащих наночастицы никеля, заключено, что формирование таких гетерогенных материалов в первом приближении можно представить в виде процесса наполнения диэлектрика нанодисперсными «металлическими» частицами – подобно легированному компенсированному полупроводникам. Полученные результаты были объяснены на основе понятий пространственно-структурной иерархической модели предложенной Balberg и др. для гетерогенных материалов.

**Ключевые слова:** пирополимер, полиакрилонитрил,  $\pi$ -электроны, порог перколяции, полупроводник.

## ELEKTR O‘TKAZUVCHAN NANOZARRALARI BO‘LGAN GETEROGEN MATERIALLARDA ZARYAD TASHUVCHILARNING KO‘CHISHI

Annotatsiya

Piropolimerlar, shuningdek, nikel nanozarrachalari bo‘lgan keramika va polimerlarning o‘tkazuvchanligini taqqoslash va tahlil qilish asosida bunday geterogen materiallarning hosil bo‘lishini birinchi yaqinlashuvda dielektrikni nanodispers bilan to‘ldirilgan "Metall" zarralar - qo‘shilgan kompensatsiyalangan yarimo‘tkazgichlarga o‘xshash degan xulosaga kelindi. Olingan natijalar geterogen materiallar uchun Balberg va boshqalar tomonidan taklif qilingan fazoviy-strukturali ierarxik model tushunchalari asosida tushuntirildi.

**Kalit so‘zlar:** piropolimer, poliakrilonitrit,  $\pi$  - elektronlar, perkolyatsiya chegarasi, yarimo‘tkazgich.

**Введение.** Гетерогенные материалы, содержащие наночастицы, с проводящими свойствами имеют большой прикладной потенциал, что стимулирует изучение переноса носителей заряда в таких системах.

Целью данной работы является сравнение и анализ полученных результатов по исследованию электропроводности гетерогенных материалов на основе органических проводящих пирополимеров, а также керамики и полимеров содержащих наночастицы металлов, для выяснения механизма переноса носителей заряда в них.

**Литературный обзор.** В работе [1.2] показано, что пирополимеры-типичным представителем которых является термообработанные продукты полиакрилонитрила (ПАН), при низких температурах термообработки ( $T_t \leq 200^\circ\text{C}$ ) является диэлектриком, а при  $T_t \geq 200^\circ\text{C}$  приобретает полупроводниковые свойства. Ответственными за электрические свойства полупроводникового ПАН являются области полисопряжения, появляющиеся при  $T_t \geq 200^\circ\text{C}$ . Они представляют собой более плотные по сравнению с исходным полимером хорошо проводящие образования линейным размером  $\sim 5 - 10 \text{ nm}$ , в которых носителями заряда являются  $\pi$  - электроны двойных связей, подобно как в органических проводящих полимерах, к примеру полианилине или полипирроле. Менее плотные и потому более широкозонные промежутки между областями сопряжения представляют собой потенциальные барьеры для электронов. Формирование пирополимеров можно представить в виде процесса наполнения диэлектрика нанодисперсными «металлическими» частицами – областями полисопряжения.



**Методология исследования.** Термообработанный продукт ПАН, при  $200^{\circ} \leq T_t \leq 600^{\circ} C$ , когда объем областей полисопряжения увеличивается (рис.1) за счет увеличения их количества, полупроводниковый ПАН представляет собой электронно-неоднородную систему. При  $T_t \geq 600^{\circ} C$  происходит рост и объединение областей сопряжения, в результате чего пирополимер представляет собой уже однофазную систему, образованную бесконечным кластером из областей полисопряжения.

Нами, методом термического разложения формиата металлов, были получены гетерогенные материалы, представляющие собой металлосодержащие наночастицы, стабилизированные в объеме матриц из керамик (рис.2) и полимеров (рис.3), исследованы зависимости их электропроводности ( $\sigma$ ) от объемного содержания наночастиц металлов ( $V_1$ ) [3-6].

**Анализ и результаты.** Согласно перколяционной теории проводимость  $s$  систем, содержащих металлические частицы, распределенных случайным образом в диэлектрической матрице, используя граничные условия ( $V_1 = 0$  и  $V_1 = 1$ ), описывается следующими формулами:

$$\sigma(V_1) = \sigma_2 \left( \frac{V_1 - V_c}{V_c} \right)^{-q} \text{ при } V_1 < V_c \quad (2)$$

$$\sigma(V_1) = \sigma_1 (V_1 - V_c) / (1 - V_c)^t \text{ при } V_1 > V_c \quad (3)$$

здесь  $\sigma_1$  - проводимость металлических частиц;  $\sigma_2$  - проводимость диэлектрической матрицы;  $V_c$  - критическая концентрация (порог протекания), при которой впервые образуется бесконечный кластер (БК) из частиц наполнителя;  $t$  и  $q$  - параметры, называемые критическими индексами.

Для изучаемых пирополимеров  $V_c$  была определена при помощи дифференцирования  $\lg \sigma$  по  $V_1$ . Критический индекс  $t$  были получены из экспериментальных данных, представляя их как график в координатах  $\lg \sigma - \lg \left[ \frac{V_1 - V_c}{1 - V_c} \right]$ , угол наклона графика, есть  $t$ . Величина  $\sigma_1$  была получена экстраполяцией этого графика к  $V_1 = 1$ . Найдено, что  $V_c = 0,50$  ( $T_t = 600^{\circ}C$ ) и  $t = 2,20$

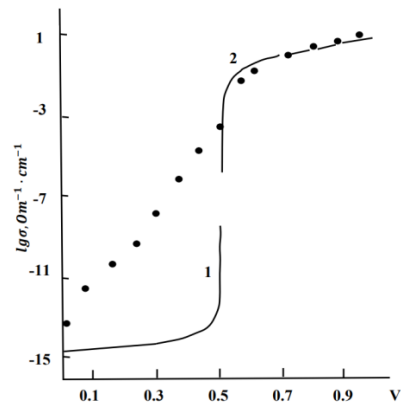


**Рис. 1.** Сравнение экспериментальных (точки) и расчетных (сплошные кривые) величин проводимости как функции объемного содержания нанодисперсными «металлическими» частицами – областями полисопряжения ( $V_1$ ). 1 –  $\sigma_{\text{рас}}$  по (1), 2 –  $\sigma_{\text{рас}}$  по (2).

Как видно из рис. 1 для изучаемых пирополимеров соответствие между расчетными и экспериментальными данными наблюдается при  $V_1 > V_c$ . Следовательно для полученных пирополимеров значение  $V_c$  намного больше, чем теоритического значение порога протекания = 0,15.

Установлено, что перколяционно-подобное поведение  $\sigma$  в гетерогенных материалах, представляющие собой металлосодержащие наночастицы, стабилизированные в объеме матриц из керамик (рис.2) и полимеров (рис.3), которое наблюдается, когда частицы металлов имеют размер  $1 - 3 \mu m$  (высокодисперсные частицы), сменяется другим поведением, характеризуемым дополнительным вкладом в  $\sigma$  ниже перколяционного порога, когда частицы никеля имеют размер  $\sim 10 nm$  (наночастицы)

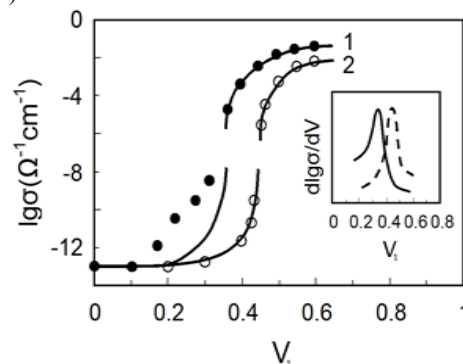


**Рис. 2.** Сравнение экспериментальных (точки) и расчетных (сплошные кривые) величин проводимости как функции объемного содержания ( $V_1$ ) никелевых частиц для керамических материалов, содержащих наночастицы (заполненные точки, кривая 1) и микродисперсные частиц (пустые точки, кривая 2). На вставке показана кривая зависимости  $d \lg \sigma / dV_1$  от  $V_1$  (сплошная линия для материалов, содержащих наночастицы, штриховая линия для материалов, содержащих микродисперсные частицы)

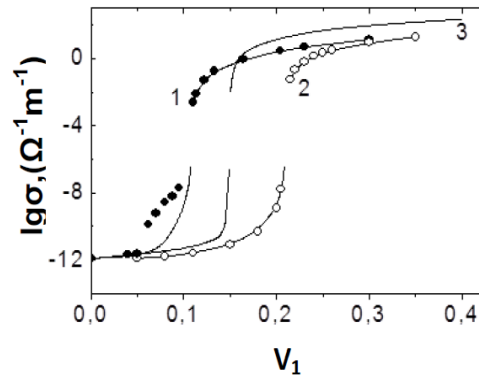


**Рис. 3.** Сравнение экспериментальных (точки) и теоретических (сплошные кривые) величин проводимости как функций объемного доля ( $V_1$ ) никелевых частиц для полимерных материалов, содержащих наночастицы (заполненные точки, кривая 1) и микродисперсные частицы (пустые точки, кривая 2). Кривая 3 вычислена с помощью формул (1) и (2) при значениях  $V_c = 0,15$ ;  $t = 1,6$ ;  $q = 1$ ;  $\sigma_2 = 1,2 \cdot 10^{-12} \text{ Ом}^{-1} \text{ м}^{-1}$ ; и  $\sigma_1 = 1,6 \cdot 10^3 \text{ Ом}^{-1} \text{ м}^{-1}$

Найдено, что  $V_c = 0,355$ ;  $t = 2,21$  для керамического материала с наноразмерными частицами никеля и  $V_c = 0,443$ ;  $t = 1,81$ ;  $q = 1,02$  для керамического материала с микродисперсными частицами никеля, а также  $V_c = 0,105$ ;  $t = 2,2$  для композита на основе фенилона с наноразмерными частицами никеля и  $V_c = 0,210$ ;  $t = 1,78$ ;  $q = 1,02$  для композита с микродисперсными частицами никеля.

Существование порога при большой концентрации, чем предсказываемой теорией протекания в керамических и полимерных композитах, говорит, как показано и в [7], о высокой степени асимметрии между характерными формами проводящих и непроводящих областей.

Отклонение экспериментальной зависимости электропроводности пирополимеров, а также в керамических и полимерных композитах при  $V_1 < V_c$  могут быть объяснены на основе предложенной Бальбергом модели электрической проводимости в композитах [8]. Согласно этой модели, все металлические частицы в композитах, в которых металлические частицы случайным образом распределены в диэлектрической матрице, являются электрически связанными, и проводимость этих композитов определяется как туннелированием носителей заряда между соседними частицами, так и туннелированием между частицами, находящимися на удалении. Перколяционное поведение наблюдается, когда вклад туннелирования между частицами, удаленными друг от друга в макроскопическую проводимость, является пренебрежимо малым. Это имеет место, когда радиус частиц ( $b$ ) значительно превосходит параметр области туннелирования (или параметр распада туннелирования) ( $d$ ). В том случае, когда  $b \sim d$ , туннелирование носителей заряда между не соседними частицами вносит вклад в макроскопическую проводимость наряду с туннелированием между соседними частицами и зависимость макроскопической проводимости от концентрации металлсодержащих частиц отличается от той, которая диктуется классической перколяционной теорией.

В керамических и полимерных композитах, в которых наблюдается вклад в электропроводности дают туннелирование носителей заряда между ближайше-соседними так и не ближайше-соседними частицами, существуют два перколяционных порога. Один из них наблюдается при высоких значениях  $V$ , он и есть перколяционный порог  $V_c$ . Другой порог (дополнительный перколяционный  $V_{cd}$ ) наблюдается при низких значениях  $V$ , он и есть критический долевой объем металлических частиц, который инициирует первый бесконечный кластер из туннельно-связанных проводников. Для изучаемых композитов, содержащих никелевые наночастицы, перколяционно-туннельный процесс является причиной "низкого" перколяционного порога  $V_{cd}$ , что и определяет поведение электропроводности в области ниже классического перколяционного порога. Было установлено, что  $V_{cd} = 0,145$  и  $t = 3,2$  для керамических композитов и  $V_{cd} = 0,05$  и  $t = 3,0$  для полимерного композита

**Заключение.** На основе сравнения и анализа проводимости пирополимеров, а также керамики и полимеров содержащих наночастицы никеля, заключено, что формирование таких гетерогенных материалов в первом приближении можно представить в виде процесса наполнения диэлектрика нанодисперсными «металлическими» частицами – подобно легированным компенсированным полупроводникам.

В отличие от композиций с нанодисперсными металлическими частицами, в пирополимерах хорошо электропроводящие области возникают под действием физических факторов в результате сложных химических превращений и находятся в химически связанном состоянии с непроводящими участками. Поэтому существование порога при большой концентрации, чем предсказываемой теорией протекания в пирополимерах, требует дополнительные исследования.

Практическая значимость полученных нами результатов исследований определяется возможностью использования разработанных гетерогенных материалов содержащих наночастицы в качестве элементов с относительно высоким и регулируемым значением диэлектрической проницаемости, необходимой для электротехники и в качестве преобразователей тепловой энергии в электрическую.

#### ЛИТЕРАТУРА

1. Магруппов М.А. Успехи химии, 1981, т.50, №11, с.2106-2131
2. М.А.Магруппов, У.Абдурахманов. Высокомолек. соед., 22А, 10 2279 (1980)
3. U. Abdurakhmanov, Sh. Sharipov, Y. Rakhimova, M. Karabaeva, M. Baydjanov. Conductivity and Permittivity of Nickel-Nanoparticle-Containing Ceramic Materials in the Vicinity of Percolation Threshold.// J. Am. Ceram.Soc.2006.V.89.№ 9. pp. 2946–2948.

4. Abdurahmanov U., Rakhimova Y, Mukhamedov G., Balberg I. Temperature Dependence of the Conductivity in Ceramic Materials Containing Nickel Nanoparticles // J. Am. Ceram. Soc. 2009, Vol. 92, No. 3, pp. 661-664.
5. U. Abdurakhmanov, F. T. Boitmuratov, G. I. Mukhamedov, A. S. Fionov, and G. Yu. Yurkov. Electric Conductivity of Composite Materials Based on Phenylon Matrices and Nickel Particles.// Journal of Communications Technology and Electronics, 2010, Vol. 55, No. 2, pp.
6. Abduraxmanov Umarbek, Abdusalom Vaxitovich, Yayra Raximova, Munira Karabayeva, Doston Saidkulov, Bekzod Matyakubov. An Investigation Of The Electrophysical Properties Of Composite Ceramic Materials Containing Nickel Nanoparticles // Phys. Chem. Res., 2023, Vol. 11, No. 2, pp. 231-239, 221–224.
7. С. Киркпатрик. В. Сб. «Теория и свойства неупорядоченных материалов», под ред. В.Л. Бонч-Бруевича, «Мир» 1977г.
8. Balberg I, Azulay D, Toker D, and Millo O “Percolation and Tunneling in Composite materials”, 2004 Int. J.Mod. Phys. B 18 2091-2121



UDK: 538.955; 621.3.082.782

**Ulug‘bek ERKABOEV,**  
*Namangan muhandislik-texnologiya instituti professori, f.-m.f.d*  
**Nozimjon SAYIDOV,**  
*Namangan muhandislik-texnologiya instituti katta o‘qituvchisi*  
**Ulug‘bek NEGMATOV,**  
*Namangan muhandislik-texnologiya instituti tayanch doktoranti*  
*E-mail: sayidovnozimjon@gmail.com*

*NamMQI professori, f.-m.f.d. M.Dadamirzayev taqrizi asosida*

**KVANT O‘RALI GETEROSTRUKTURALI YARIMO‘TKAZGICHLARNING ELEKTR O‘TKAZUVCHANLIGI  
OSSILYATSIYALARINI KUCHLI ELEKTROMAGNIT MAYDON VA HARORATGA BOG‘LIQLIGINI  
MODELLASHTIRISH**

Annotatsiya

Ushbu ishda kvant o‘rali yarimo‘tkazgichli strukturalarni o‘rganishga qiziqish uni kichik o‘lchamli diapazonda ishlaydigan nanotexnologik asboblarning sifatida, shuningdek, turli xil spintronik qurilmalarda qo‘llash imkoniyati bilan belgilanmoqda. Olimlar tomonidan ushbu kvant o‘lchamli strukturalarning katta e‘tibor bilan o‘rganishiga asosiy sabab, bunday materiallarning fizik xususiyatlari bir qator qiziqarli ilmiy jarayonlarga ega bo‘lib, bu jarayonlarning turli xil tashqi omillar ta‘sirida tubdan o‘zgarishlarini to‘liqroq tushunishga imkon beradi.

**Kalit so‘zlar:** Geterostruktura, nanoo‘lcham, kvant o‘ra, holatlar zichligi, holatlar zichligi, ossilyatsiya, nanoo‘lcham, magnit maydon, ikki o‘lchamli, yarimo‘tkazgichlar.

**MODELING OF THE DEPENDENCE OF OSCILLATIONS OF ELECTRICAL CONDUCTIVITY OF  
HETEROSTRUCTURAL SEMICONDUCTORS WITH QUANTUM WELLS ON A STRONG ELECTROMAGNETIC  
FIELD AND TEMPERATURE**

Annotation

In this work, the interest in the study of quantum-wound semiconductor structures is determined by the possibility of its application as nanotechnological devices operating in the small size range, as well as in various spintronic devices. The main reason why these quantum-scale structures are studied with great attention by scientists is that the physical properties of such materials have a number of interesting scientific processes, which lead to a more complete understanding of the fundamental changes of these processes under the influence of various external factors. allows.

**Key words:** Heterostructure, nanoscale, quantum coil, density of states, density of states, oscillation, nanoscale, magnetic field, two-dimensional, semiconductors.

**МОДЕЛИРОВАНИЕ ЗАВИСИМОСТИ ОСЦИЛЛЯЦИЙ ЭЛЕКТРОПРОВОДНОСТИ ГЕТЕРОСТРУКТУРНЫХ  
ПОЛУПРОВОДНИКОВ С КВАНТОВЫМИ ЯМАМИ ОТ СИЛЬНОГО ЭЛЕКТРОМАГНИТНОГО ПОЛЯ И  
ТЕМПЕРАТУРЫ**

Аннотация

В данной работе интерес к исследованию полупроводниковых структур с квантовой ямой определяется возможностью их применения в качестве нанотехнологических устройств, работающих в малоразмерном диапазоне, а также в различных устройствах спинтроники. Основная причина, по которой эти квантовые структуры изучаются учеными с большим вниманием, заключается в том, что в физических свойствах таких материалов происходит ряд интересных научных процессов, которые приводят к более полному пониманию фундаментальных изменений этих процессов под влиянием позволяют различные внешние факторы.

**Ключевые слова:** Гетероструктура, наноразмер, квантовая катушка, плотность состояний, плотность состояний, колебание, наноразмер, магнитное поле, двумерность, полупроводники.

**Kirish.** So‘nggi yillarda, kvant o‘rali yarimo‘tkazgichli strukturalarni o‘rganishga qiziqish uni kichik o‘lchamli diapazonda ishlaydigan nanotexnologik asboblarning sifatida, shuningdek, turli xil spintronik qurilmalarda qo‘llash imkoniyati bilan belgilanmoqda. Olimlar tomonidan ushbu kvant o‘lchamli strukturalarning katta e‘tibor bilan o‘rganishiga asosiy sabab, bunday materiallarning fizik xususiyatlari bir qator qiziqarli ilmiy jarayonlarga ega bo‘lib, bu jarayonlarning turli xil tashqi omillar ta‘sirida tubdan o‘zgarishlarini to‘liqroq tushunishga imkon beradi. Jumladan, bunday tashqi omillardan biri kvantlovchi magnit maydon va kuchli elektromagnit to‘lqin bo‘lib, u hajmiy yoki kichik o‘lchamli materiallarning kristall panjarasi bo‘ylab erkin harakatlanayotgan zaryadli zarralarning traektoriyalarini o‘zgartirib yuboradi. Bu esa, kvant Xoll effekti, Shubnikov – de Gaaz va de Gaaz – van Alfen effektlari kabi kvant – fizik hodisalarning paydo bo‘lishiga olib keladi.

**Adabiyotlar tahlili.** [1] Ishlarda tajriba tadqiqotlari, ya‘ni kvant o‘lchamli materiallarning elektr o‘tkazuvchanlik ossilyatsiyalarini kuchli elektromagnit maydon ta‘sirini aniqlashda elektroparamagnit rezonans (EPR) o‘rnatish bo‘yicha o‘tkazilgan. Sababi, EPR usuli kvant o‘rali geterostrukturali materiallarning magneto qarshilik yoki elektr o‘tkazuvchanlik ossilyatsiyalarini tashqi maydonlarga bog‘liqligini aniqlash imkonini beradi. Bunda, kuchli elektromagnit maydon quvvatining

maksimal kamayishi ( $dP$ ) EPR ta'sirini to'g'ridan-to'g'ri o'lchashda elektromagnit to'lqinining energiyasi tufayli energetik sathlar o'rtasida (bir sathdan ikkinchi sathga) o'tishlar hisobiga sodir bo'ladi. Ya'ni,  $dP$  ning yo'qolishlari elektromagnit to'lqinining energiyasi kvanlovchi magnit maydondagi ( $H$ ) erkin zaryad tashuvchilarini tezlashtirishlariga xizmat qiladi. Bu energetik sathlar Landau sathlari bo'lib, ushbu sathlar soni magnit maydon kuchlanganligi ( $dH$ ) ga bog'liq. Bundan kelib chiqadiki, kvant o'raning o'tkazuvchanlik zonasidagi elektr o'tkazuvchanlik ossilyatsiyalarida ko'proq mikroto'lqinli maydon yutulishini kuzatish uchun o'ta yuqori chastotali elektromagnit maydon quvvatini oshirib borish darkor. Aniqroq qilib aytadigan bo'lsak,  $dH$  qanchalik ortsa Landau sathlari soni ortib boradi.

**Tadqiqot metodologiyasi.** Har bir Landau diskret sathlarida EPR hodisasini kuzatish uchun  $dP$  ni orttirib borish kerak.

Umuman olganda  $\frac{dP^{2d}(H,T,d,E_E,N_L,n_z)}{dH}$  nisbat kvant o'lchovli yarimo'tkazgichlarda EPR tajribalarini o'tkazishida muhim ahamiyatga ega. Bu tajribalar nazariyasini, uning yangi modulini ishlab chiqishda formuladan foydalanish mumkin.

Kvant o'rali geterostrukturalarda o'ta yuqori chastotali elektromagnit maydonning elektr o'tkazuvchanlik ossilyatsiyalari sezgirligini kuzatish maqsadida formuladan magnit maydon kuchlanganligi bo'yicha birinchi tartibli hosila olinadi [3]. Natijada quyidagi formula:

$$\frac{dP^{2d}(H,T,d,E_E,N_L,n_z)}{dH} = \frac{d \left[ \frac{e^3 B}{2\pi m^* c} \sqrt{\frac{21}{\pi G}} \int_0^\infty \sum_{n_L} \exp \left[ -2 \left( \frac{E - \left[ \hbar \frac{eH}{m^* c} (n_L + \frac{1}{2}) + \frac{\pi^2 \hbar^2}{2m^* d^2 n_z^2} \right]^2 \right) \right] \gamma_1(k_0 T)^\beta E^{\alpha + \frac{3}{2}} \left( \frac{\partial f_0(E,T)}{\partial E} \right) dE \right]}{dH} \cdot E_E^2 \quad (1)$$

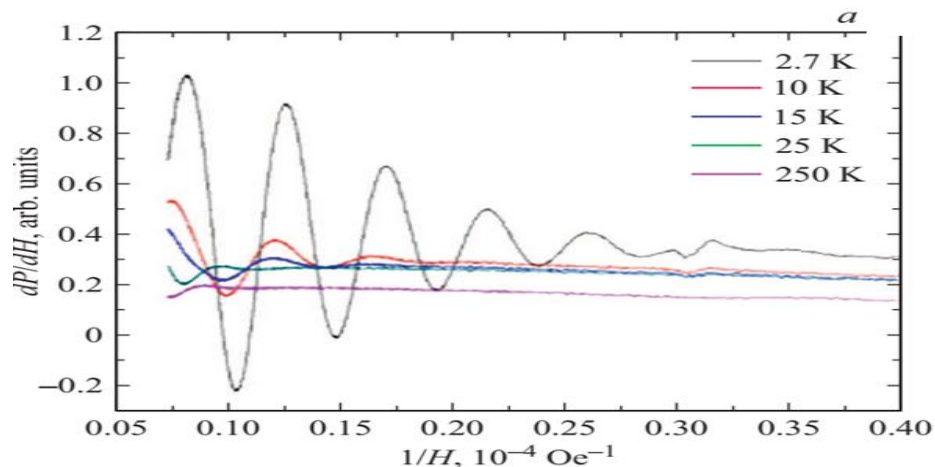
Ushbu (1) formula yordamida o'ta yuqori chastotali maydondagi kvant o'rali geterostrukturalarning elektr o'tkazuvchanlik ossilyatsiyalarini hisoblash mumkin.

Agar, yanada kvant o'raning har bir diskret Landau sathlaridagi mikroto'lqinli maydon yutulishini yuqoriroq aniqlikda kuzatishga sabab tug'lsa, (1) dan magnit maydon kuchlanganligi bo'yicha hosila olinadi [4-6]. Ya'ni:

$$\frac{d^2 P^{2d}(H,T,d,E_E,N_L,n_z)}{dH^2} = \frac{d^2 \left[ \frac{e^3 B}{2\pi m^* c} \sqrt{\frac{21}{\pi G}} \int_0^\infty \sum_{n_L} \exp \left[ -2 \left( \frac{E - \left[ \hbar \frac{eH}{m^* c} (n_L + \frac{1}{2}) + \frac{\pi^2 \hbar^2}{2m^* d^2 n_z^2} \right]^2 \right) \right] \gamma_1(k_0 T)^\beta E^{\alpha + \frac{3}{2}} \left( \frac{\partial f_0(E,T)}{\partial E} \right) dE \right]}{dH^2} \cdot E_E^2 \quad (2)$$

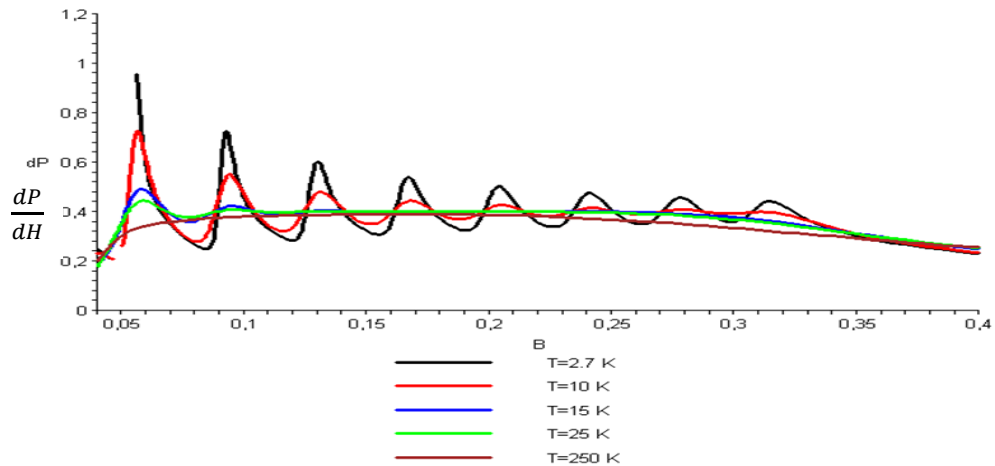
(1) va (2) formulalar asosida yangi matematik model ishlab chiqildi. Bu yangi matematik model, albatta bir qator tajriba natijalarini tushuntirishga xizmat qiladi.

**Tahlil va natijalar.** Jumladan, 1-rasmda kvant o'ra qalinligi  $d=8\text{nm}$  ( $GaSb$  uchun) kuchli magnit maydondagi mikroto'lqinli yutulish koeffitsientini ( $\frac{dP}{dH}$ )ni haroratga bog'liqligi ossilyatsiyalari keltirilgan. Bu ushbu tajriba natijalari EPR ustanovkasida harorat  $T=2.7\text{K} - 250\text{K}$  intervalida olingan. Magnit maydon kuchlanganligi vektori  $Z$  o'qi bo'ylab ( $H/Z$ ) yo'nalgan, bu yerda  $Z$  – kvant o'ra qalinligi yo'nalishiga to'g'ri keladi. Tajribada, kuchli mikroto'lqinli elektr maydon kattaliklari quyidagicha olingan: mikroto'lqin chastotasi  $\nu = 9.35\text{ GGrtz}$ , kvant energiyasi  $E = \hbar\omega = \hbar 2\pi\nu = 0.04\text{ meV}$ , elektromagnit maydon quvvati  $P=1\text{mVt}$  [1]. Ushbu kattaliklar yordamida elektromagnit maydonning elektr maydon kuchlanganligini hisoblash mumkin:



1-rasm.  $InAs/GaSb$  kvant o'rali yarimo'tkazgichlar uchun  $\frac{dP}{dH}$  ni haroratga bog'liqligi [1]

Ushbu tajribada keltirilgan fizik kattaliklardan foydalanib, nazariy tahlilni boshlaymiz. Taklif etilayotgan model yordamida ((1) formula asosida)  $dP/dH$  ni  $1/H$  ga bog'liqligini aniqlash mumkin. Lekin, (1) formuladan ko'rinib turibdiki, ushbu tenglama transtendent bo'lib, nazariy yo'l bilan yechimini topib bo'lmaydi. Buni, kompyuter dasturlari yordamida (Maple, Matchad, Matlab, Matematika) va grafik usulida kerakli natijalarga erishiladi [7]. Matematik modelni dasturiy taminotini (Maple) yaratishda protsedura funksiyalardan foydalaniladi.



2-rasm. *InAs/GaSb* kvant o'rali yarimo'tkazgichlar uchun  $\frac{dP}{dH}$  ni haroratga bog'liqligi. Ushbu grafiklar taklif etilayotgan model (1) bo'yicha olingan [7]

Chunonchi, (1) formuladan ko'rinib turibdiki, kvant ossilyatsiya jarayonlarini tubdan o'zgartiruvchi kattaliklar  $H$ ,  $T$ ,  $d$ ,  $E_E$ ,  $N_L$ ,  $n_z$  bo'lgani uchun dasturda  $\text{proc}(H, T, d, E_E, N_L, n_z)$  buyruqdan foydalaniladi [8].

Xulosa qilib shuni aytish mumkinki, biz taklif qilayotgan model ( $\frac{dP}{dH}(H, T)$  funksiya) nafaqat 2D materiallarda, balki uni hajmiy yarimo'tkazgichlarga ham tadbiq etishga imkon bermoqda.

**Xulosalar.** Kvant o'lchamli yarimo'tkazgichlar uchun elektr o'tkazuvchanlik ossilyatsiyalari kuchli elektromagnit maydonga bog'liqligi tadbiq etiladi. Kvant o'rali geterostrukturali yarimo'tkazgichlarda mikroto'lqinli maydon quvvatidan ( $dP$ ) magnit maydon kuchlanganligi ( $dH$ ) bo'yicha olingan birinchi va ikkinchi tartibli differensial ifodalarni ( $\frac{dP}{dH}, \frac{d^2P}{dH^2}$ ) analitik ko'rinishi keltirib chiqarildi. Hajmiy va kichik o'lchamli yarimo'tkazgichli materiallar uchun kvant ossilyatsiya effektlarini mikro to'lqinli maydon quvvati, kvantlovchi magnit maydon kuchlanganligi va haroratlargabog'liqligini aniqlovchi matematik model ishlab chiqildi. Kvant o'lchamli va hajmiy yarimo'tkazgichli strukturalarda olingan eksperiment natijalarini taklif qilinayotgan model asosida yuqori haroratlar dinamikasi uchun tushuntirishga imkon topildi.

#### ADABIYOTLAR

1. Кочман И.В., Михайлова М.П., Вейнгер А.И., Парфеньев Р.В. Магнитофонные осцилляции магнитосопротивления в квантовой яме *InAs/GaSb* с инвертированным зонным спектром // Физика и техника полупроводников, 2021, том 55, вып. 4, стр.313-318. <http://dx.doi.org/10.21883/FTP.2021.04.50731.9569>
2. А.И. Вейнгер, И.В. Кочман, Д.А. Фролов, В.И. Окулов, Т.Е. Говоркова, Л.Д. Паранчич. Микроволновое магнитопоглощение в *HgSe* с примесью *Co* и *Ni* // Физика и техника полупроводников, 2019, том 53, вып. 10. Стр.1413-1418. <http://dx.doi.org/10.21883/FTP.2019.10.48299.9149>
3. Erkaboev U.I., Rakhimov R.G., Sayidov N.A. Mathematical modeling determination coefficient of magneto-optical absorption in semiconductors in presence of external pressure and temperature // *Modern Physics Letters B*. 2021. Vol.35, Iss.17, pp. 2150293-1-2150293-10. (№3, Scopus. IF: 1.9, Q3; <https://www.scopus.com/sourceid/29055>).
4. Erkaboev U.I., Negmatov U.M., Rakhimov R.G., Mirzaev J.I., Sayidov N.A. Influence of a quantizing magnetic field on the Fermi energy oscillations in two-dimensional semiconductors // *International Journal of Applied Science and Engineering*. 2022. Vol.19, Iss.2, pp. 2021123-1-2021123-8. (№3, Scopus. IF: 1.4, Q3; <https://www.scopus.com/sourceid/21100822732>).
5. Erkaboev U.I., Rakhimov R.G., Negmatov U.M., Sayidov N.A., Mirzaev J.I. Influence of a strong magnetic field on the temperature dependence of the two-dimensional combined density of states in *InGaN/GaN* quantum well heterostructures // *Romanian Journal of Physics*. 2023. Vol.68, Iss.5-6, pp.614-1-614-14. (№3, Scopus. IF: 1.5, Q2; <https://www.scopus.com/sourceid/11500153309>).
6. Erkaboev U.I., Rakhimov R.G., Mirzaev J.I., Negmatov U.M., Sayidov N.A. Influence of a magnetic field and temperature on the oscillations of the combined density of states in two-dimensional semiconductor materials // *Indian Journal of Physics*. 2024. Vol.98, pp.189-197. (№3, Scopus. IF: 2.0, Q3; <https://www.scopus.com/sourceid/145208>).
7. Gulyamov G., Erkaboev U.I., Rakhimov R.G., Mirzaev J.I., Sayidov N.A. Determination of the dependence of the two-dimensional combined density of states on external factors in quantum-dimensional heterostructures // *Modern Physics Letters B*. 2023. Vol.37, No.10, pp.2350015-1-2350015-14. (№3, Scopus. IF: 1.9, Q3; <https://www.scopus.com/sourceid/29055>).
8. Erkaboev U.I., Rakhimov R.G., Mirzaev J.I., Sayidov N.A., Negmatov U.M., Mashrapov A. Determination of the band gap of heterostructural materials with quantum wells at strong magnetic field and high temperature // *AIP Conference Proceedings*. 2023. Vol.2789, Iss.1, pp.040056-1-040056-7. (№3, Scopus. IF: 0.5, Q4; <https://www.scopus.com/sourceid/26917>).





UDK: 534.2: 58.4: 548.9.

**Ibrat TOSHPULATOV,**  
*Institute of Ion-Plasma and Laser Technologies, PhD*  
**Jakhongir KURBANOV,**  
*Institute of Ion-Plasma and Laser Technologies, senior researcher*  
**Vladimir AVDIYEVICH,**  
*Institute of Ion-Plasma and Laser Technologies, senior researcher*  
E-mail: [ibrat.toshpolatov96@gmail.com](mailto:ibrat.toshpolatov96@gmail.com)  
Tel: +998912189238

*Reviewer: National University of Uzbekistan named after Mirzo Ulugbek Professor of the Department of Semiconductor Physics, doctor of physics and mathematics Sh.U Yuldoshev*

### ACOUSTIC CHARACTERISTICS OF GaAs CRYSTAL

#### Annotation

In this article we present a detailed investigation of the acoustic properties of Gallium Arsenide (GaAs) crystal. Utilizing advanced experimental techniques, we have measured the acoustic wave velocities, elastic coefficients, and acoustic attenuation in Gallium Arsenide (GaAs) crystal on the direction of propagation in the (001) and (110) plane is observed at room temperature. The data obtained reveal significant anisotropy in the acoustic behavior of these materials. These findings provide crucial insights for the design and optimization of optoelectronic and semiconductor devices that incorporate GaAs. Our study offers a valuable reference for future research and practical applications in the fields of engineering.

**Key words:** GaAs crystal, speed, attenuation, acoustic waves, effective elastic constants, elastic constants.

### АКУСТИЧЕСКИЕ СВОЙСТВА КРИСТАЛЛА GaAs АННОТАЦИЯ

#### Аннотация

В этой статье мы представляем подробное исследование акустических свойств кристалла арсенида галлия (GaAs). Используя передовые экспериментальные методы, мы измерили скорости акустических волн, упругие коэффициенты и акустическое затухание в кристалле арсенида галлия (GaAs) в направлении распространения в плоскости (001) и (110), наблюдаемом при комнатной температуре. Полученные данные показывают значительную анизотропию в акустическом поведении этих материалов. Эти результаты дают важную информацию для проектирования и оптимизации оптоэлектронных и полупроводниковых приборов, включающих GaAs. Наше исследование дает ценную ссылку для будущих исследований и практических приложений в областях машиностроения.

**Ключевые слова:** Кристалл GaAs, скорость, затухание, акустические волны, эффективные упругие константы, упругие константы.

### GaAs KRISTALLINING AKUSTIK XOSSALARI

#### Annatsiya

Ushbu maqolada biz Galiy Arsenid (GaAs) kristallining akustik xususiyatlarini batafsil o'rgandik. Ilg'or eksperimental usullardan foydalangan holda, biz xona haroratida kuzatilgan (001) va (110) tekislikdagi tarqalish yo'nalishi bo'yicha Galiy Arsenid kristallidagi akustik to'lqin tezligini, elastik koeffitsientlarini va akustik so'nish koeffitsientlarini o'lchadik. Olingan keng qamrovli ma'lumotlar ushbu materiallarning akustik harakatidagi anizotropiyasini aniqlashga yordam beradi. Ushbu olingan natijalar GaAsni o'z ichiga olgan optoelektronik va yarimo'tkazgichli qurilmalarni loyihalash va optimallashtirish uchun muhim ma'lumotlarni beradi. Bizning tadqiqotimiz muhandislik sohaslarida kelajakdagi tadqiqotlar va amaliy qo'llanmalar uchun muhimdir.

**Kalit so'zlar:** GaAs kristalli, tezlik, so'nish, akustik to'lqinlar, samarali elastik konstantalar, elastik konstantalar.

**Introduction.** The primary thermal mechanisms responsible for acoustic wave attenuation in solids at room temperature are the phonon-viscosity mechanism and the thermoelastic phenomenon. The phonon-viscosity mechanism involves energy conversion at various temperatures due to the thermal conduction of phonons. In contrast, the thermoelastic phenomenon results from thermal conduction between the compressed and rarefied regions of the propagating wave [1]. The predominant factor contributing to attenuation in these crystals is the interaction between thermal phonons and ultrasonic waves. To evaluate the attenuation experienced by compressional and shear acoustic waves in GaAs, propagating along the (100) and (110) directions, and shear waves polarized along the (100) and (001) directions, second- and third-order elastic moduli were utilized, considering phonon viscosity and thermoelastic phenomena at 293 K.

**Samples and experimental methods.** The studied sample of GaAs was cubic crystal, the long side of which was oriented with an accuracy of 5 degree along the main cubic directions [100] and [110] and [111]. The orientation of the samples was achieved using cleavage planes and subsequent grinding and polishing of the crystalline sample, using standard orienting prisms. The studies were carried out at room temperature in the frequency range of 30 – 400 MHz. Longitudinal and transverse acoustic waves in the samples were excited by piezoelectric transducers made of quartz, respectively, of X or Y-cut, with a thickness of 40-100 microns. The measurements of the velocity and attenuation coefficient of acoustic waves at relatively low

frequencies were carried out using a modified Williams-Lamb "pulse interference" method [1, 10], which compares the phases of acoustic waves that have passed different paths in the studied sample. One of the main modules of the low-frequency installation is the amplitude selector, which opens at a certain time interval, which is the transmission window.

The duration of such a transmission window can be controlled by the duration of the synchronization pulse that opens this selector. Such selection of a specific pulse in a series of echo pulses allows its amplitude to be measured using a pulse voltmeter. The attenuation coefficient of acoustic waves  $\alpha$  was determined from the measured values of the amplitudes of adjacent pulses  $A_1$  and  $A_2$  [4, 10].

$$\alpha = \frac{20 \lg\left(\frac{A_1}{A_2}\right)}{2L} \quad (1)$$

where  $L$  is the length of the sample. The accuracy of the attenuation coefficient was  $\sim 5\%$ , due to the multiple increase in the pulse amplitude and subsequent averaging. The interference zero or maximum pulse amplitudes observed during the formation of the continuous oscillation generator frequency allow us to determine the value of the acoustic wave velocity in the sample  $V$  from the relationship [4]:

$$V = 2L \cdot \Delta\nu \quad (2)$$

Where  $\Delta\nu$  is the difference between two adjacent frequencies of the high-frequency generator, corresponding to antiphase interference. The specified measurements were carried out using a frequency converter, ensuring the accuracy of determining the frequency difference (up to  $\pm 10$  Hz). In this case the determination of the accuracy of the acoustic wave velocity was limited by the limits of measuring the sample length and the value of  $\sim 0.01\%$  [2].

**Experimental results and discussion of the attenuation coefficient.** The results of longitudinal and transverse acoustic waves along the crystallographic directions [100] and [110], and the calculated values of the effective constants and minimum elastic constants for the studied crystals are given in Table 1.

The effective elastic constants are found from this equation.

$$c'_{eff} = c'_{eff} + ic''_{eff} = c'_{ijkl} \kappa_j \kappa_l \eta_i \eta_k + ic''_{ijkl} \kappa_j \kappa_l \eta_i \eta_k \quad (3)$$

where  $\kappa_j$  and  $\eta_i$  are the traveling cosines of the wave vector and displacement vectors [4, 11]. Effective elastic constants  $c'_{ijkl}$  are located at source  $V$  of acoustic waves.

$$c'_{eff} = \rho V^2 \quad (4)$$

Three independent components of the real and imaginary parts of the elasticity tensor for all the crystals studied were determined from the values of the velocity and attenuation coefficient of longitudinal and transverse waves along the directions [100] and [110].

**Table 1.** Velocity of acoustic waves in GaAs crystals ( $\nu=1$  GHz), acoustic attenuation, effective real and imaginary elastic constants at room temperature.

q	$\eta$	$c_{eff}$	$V$ , $10^3$ m·s <sup>-1</sup>	$c'_{eff}$ , $10^{10}$ N·m <sup>-2</sup>	$\alpha$ , dB· $\mu$ s <sup>-1</sup>	$c''_{eff}$ , $10^7$ N·m <sup>-2</sup>
[100]	[100]	$c_{11}$	4.73	11.88	3.43	2.24
	[001]	$c_{44}$	3.35	5.96	1.21	3.96
[110]	[110]	$(c_{11}+c_{12}+2c_{44})/2$	5.24	14.6	2.88	23.09
	[110]	$(c_{11}-c_{12})/2$	2.48	3.27	2.08	3.73
	[001]	$c_{11}$	3.35	5.96	1.21	3.96
[111]	[111]	$(c_{11}+2c_{12}+4c_{44})/3$	5.40	15.5	2.76	23.49
	[110]	$(c_{11}-c_{12}+c_{44})/3$	2.79	4.15	1.21	2.76

Three independent components of the real and imaginary parts of the elasticity tensor for all the crystals studied were determined from the values of the velocity and attenuation coefficient of longitudinal and transverse waves along the directions [100] and [110]. The obtained values of the real and imaginary components of the elasticity tensor:  $c'_{11}$ ,  $c'_{12}$ ,  $c'_{44}$ ,  $c''_{11}$ ,  $c''_{12}$  and  $c''_{44}$  allow us to calculate the attenuation of acoustic waves by the Akhiezer mechanism along any direction of propagation of acoustic waves in crystals, if the condition  $\omega\tau \ll 1$  is met ( $\omega$  is the circular frequency of acoustic waves,  $\tau$  is the relaxation time of thermal phonons), using the expression [8, 11].

$$\alpha = \frac{1}{2} \omega \frac{c''_{eff}}{c'_{eff}} \quad (5)$$

Here the real and imaginary effective elastic constants are defined respectively, through the real  $c'_{ijkl}$  and imaginary  $c''_{ijkl}$  components of the complex elasticity tensor:

$$c'_{eff} = c'_{ijkl} \kappa_j \kappa_l \eta_i \eta_k \quad (6)$$

$$c''_{eff} = c''_{ijkl} \kappa_j \kappa_l \eta_i \eta_k \quad (7)$$

where  $\kappa_j$  and  $\eta_i$  are the components of the unit wave normal  $\kappa$  and the polarization vector  $\eta$  [4,11]. In the general case, the directions of the vectors  $\kappa$  and  $\eta$  do not coincide.

In particular, for quasi-longitudinal waves in the (110) plane, when the direction of the wave vector changes relative to the [110] axis by a certain angle ( $\varphi$ ), the Green-Christoffel equations allow us to determine the angle of deviation of the polarization vector ( $\psi$ ) from the same axis [4]:

$$\psi = \arctg \frac{\sqrt{2}}{2} \cdot \left( \frac{\Gamma'_{12} \Gamma'_{13} - \Gamma'_{23} (\Gamma'_{11} - \rho V^2)}{\Gamma'_{23} \Gamma'_{13} - \Gamma'_{12} (\Gamma'_{33} - \rho V^2)} \right) \quad (8)$$

Here  $\Gamma'_{ik}$  are the real components of the Green-Christoffel tensor [1, 2].

$$\left| \Gamma'_{il} - \rho v^2 \delta_{il} \right| = 0 \quad (9)$$

By virtue of the symmetry properties of the stiffness tensor,  $\Gamma'_{ij}$  is symmetric [5].

$$\Gamma'_{ik} = c'_{ijkl} K_j K_l, \quad (10)$$

The calculation results show that in this plane the maximum deviation of the polarization vector from the wave vector in the studied crystals is no more than 5 angular degrees. The measurements also show that in the experimental direction the attenuation frequency coefficient of both longitudinal and transverse acoustic waves depends on the frequency according to a quadratic law. This indicates that the main mechanism of attenuation of acoustic waves in crystals is the phonon-phonon mechanism, first considered by Akhiezer [6], according to the indication of the expression for attenuation for recording in the following view [7]:

The results of calculating the attenuation coefficient of short acoustic waves with a band of 1 GHz from the direction of the wave vector in the plane (110) in GaAs crystals using expressions (5) are shown in Figure 1.

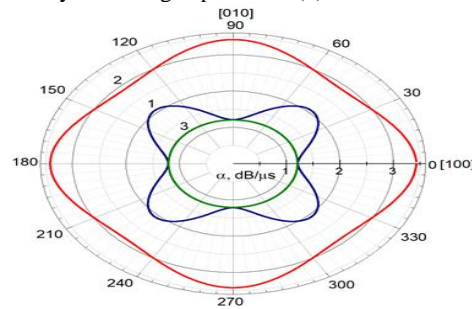


**Fig. 1.** Quasi-longitudinal (1), quasi-transverse (2) and purely transverse (3) attenuation surfaces of acoustic waves in the (001) plane of a GaAs crystal.

The image is a polar plot illustrating the attenuation surfaces of three types of acoustic waves in the (001) plane of a Gallium Arsenide (GaAs) crystal. The plot provides a visual representation of how the attenuation of each type of wave varies with direction within the crystal plane. Quasi-longitudinal waves are primarily longitudinal with a small transverse component. The least attenuation is observed for purely transverse waves, as indicated by the green curve being closest to the center. Quasi-transverse waves have a motion that is mainly perpendicular to the direction of propagation but with a small longitudinal component. The attenuation is higher than that of purely transverse waves but less than quasi-longitudinal waves, as shown by the blue curve. Purely transverse waves have a motion completely perpendicular to the direction of wave propagation. The highest attenuation is observed for quasi-longitudinal waves, as represented by the red curve being farthest from the center. The shape of each curve shows the anisotropic nature of the crystal, indicating how the attenuation of acoustic waves varies with direction. The distinct shapes for each type of wave highlight the directional dependence of attenuation in the GaAs crystal. The variation in curve shape and distance from the center indicates that the GaAs crystal exhibits different attenuation properties depending on the direction of wave propagation within the (001) plane.

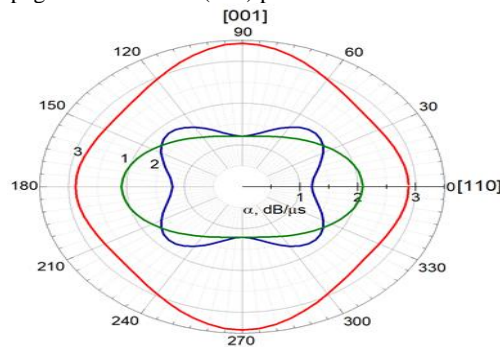


**Fig. 2.** Quasi-longitudinal (1), quasi-transverse (2) and purely transverse (3) attenuation surfaces of acoustic waves in the (110) plane of a GaAs crystal.

**Conclusion.** The attenuation surfaces for quasi-transverse waves reflect the crystal's response to waves that are not purely transverse. This can give insights into how attenuation is distributed between longitudinal and transverse modes, especially under high-frequency conditions. Purely transverse waves will have attenuation characteristics that are directly influenced by the material's transverse acoustic properties. In GaAs, these waves are sensitive to the crystal structure and imperfections, and their attenuation surfaces will reveal information about how well the crystal supports purely transverse wave propagation at 1 GHz.

**Quasi-transverse waves** will reflect a mix of attenuation factors and how the crystal transitions between longitudinal and transverse behaviors. **Purely transverse waves** will highlight the crystal's ability to support transverse wave propagation and how scattering or other interactions affect them. This information can be critical for applications like ultrasonic testing, material characterization, and the design of acoustic devices using GaAs. As seen in the provided polar plots, the attenuation surfaces in the (001) plane have more regular and symmetric patterns, while those in the (110) plane are more elliptical and anisotropic.

#### REFERENCES

1. Kor, U.S. Tandon, and G. Rai, Phys. Rev. B5, 4143 (1972)

2. R.E. Newnham. Properties of Materials /Anisotropy/Symmetry/Structure. (New York, Oxford University Press, 2005), p. 378.
3. Yu.I. Sirotin and M.P. Shaskolskaya, "Fundamentals of crystal physics," 2d ed. (Mir Publishers, Moscow, 1982), Chap. 6.
4. Ф.Р. Ахмеджанов, Ж.О. Курбанов, Н.М. Махаров. Затухание акустических волн в кубических кристаллах фторида лития. Доклады АН РУз. Вып. 5. 2021, С. 11-15.
5. F.R. Akhmedzhanov M.M., F.R. Akhmedzhanova. A guide to calculating the characteristics of elastic waves in crystals when performing coursework and dissertations., 1982. Ch. I.
6. Akhiezer A. About Sound Absorption in Solids, J. of Experimental and Theoretical Physics (SU). - Moscow, 1938. - No 8, - P. 1318-1329.
7. R. Nava, M. P. Vecchi, J. Romero and B. Fernandez. Akhiezer damping and the thermal conductivity of pure and impure dielectrics. Phys. Rev. B. Vol. 14, No 2. 1975, P. 800-807.
8. Логачев Ю. А., Мойжес Б. Я. К теории поглощения звука по Ахиезеру. – ФТТ. - Санкт-Петербург, 1974, - Т. 16. - № 8, - С. 2219-2223.
9. F.I. Fedorov, Theory of elastic waves in crystals, Plenum Press: New York (1968)
10. F.R. Akhmedzhanov, J.O. Kurbanov, A.F. Boltabaev, Attenuation of acoustic waves in single-domain and polydomain LiTaO<sub>3</sub> crystals, Sensors & Transducers 246, No.7, 2020. P. 43-47.
11. Ахмеджанов Ф.Р., Леманов В.В., Насыров А.Н. Поверхности акустического затухания в кристаллах. Письма в ЖТФ, 1980. Т. 6, Вып. 10, С. 589-592.
12. Key Samuel. Gruneisen Tensor for Anisotropic Materials. Journal of Applied Physics, 1967. Vol. 38, No 7, P. 2923-2928.
13. Kor, U.S. Tandon, andG. Rai, Phys. Rev. B5, 4143 (1972)



UDK: 524

*Sobir TURAEV,*  
PhD student of National university of Uzbekistan  
E-mail: [sobr8488@mail.ru](mailto:sobr8488@mail.ru)

*O'zRFA Astronomiya instituti professori K. Mirtadjiyeva taqrizi asosida*

### PROBLEMS OF DISTANCE MEASUREMENT TO DISTANT SUPERNOVAE

Annotation

This article analyzes the procedure for measuring distances to distant objects in cosmology and possible systematic and statistical errors, uncertainties in distance measurement. In particular, the errors that occur due to absorptions in the intergalactic medium, extragalactic and host galaxies, possible errors in determining the absolute magnitude: nuisance coefficients, color parameter, light curve shape parameter in finding the distance modulus are analyzed. It is also taken into account possible errors in measuring the distance via redshift. As a result, the necessity for dark energy in cosmology is estimated due to these uncertainties.

**Key words:** absorption, color parameter, cosmology, dark energy, distance measuring, error, nuisance coefficients

### ПРОБЛЕМЫ ИЗМЕРЕНИЯ РАССТОЯНИЙ ДО ДАЛЕКИХ СВЕРХНОВЫХ

Аннотация

В статье анализируется процедура измерения расстояний до далеких объектов в космологии и возможные системные и статистические ошибки, погрешности измерения расстояний. В частности, анализируются ошибки, возникающие из-за поглощения в межгалактической среде, внегалактических и родительских галактиках, возможные ошибки в определении абсолютной звездной величины: коэффициенты помех, параметр цвета, параметр формы кривой блеска при нахождении модуля расстояния. Также учитываются возможные ошибки измерения расстояния через красное смещение. В результате из-за этих неопределенностей оценивается необходимость темной энергии в космологии.

**Ключевые слова:** поглощение, цветовой параметр, космология, темная энергия, измерение расстояния, погрешность, мешающие коэффициенты.

### UZOQ O'TA YANGI YULDUZLARGACHA BO'LGAN MASOFALARNI O'LCHASH MUAMMOLARI

Annotatsiya

Ushbu maqolada kosmologiyada uzoq ob'ektlarga masofani o'lchash tartibi va yuzaga kelishi mumkin bo'lgan sistematik va statistik xatolar, masofani o'lchashdagi noaniqliklar tahlil qilingan. Xususan, galaktikalararo muhitda, galaktikalararo va mezbon galaktikalardagi yutilishlar tufayli yuzaga keladigan xatoliklar, o'ta yangi yulduzlarning absolyut yulduz kattaligini aniqlashdagi mumkin bo'lgan xatoliklar; jumladan, noqulaylik koeffitsientlari, rang parametri, yorug'lik egri shakli parametri kabilarning masofa modulini topishda yuzaga keltirishi mumkin bo'lgan xatoliklari tahlil qilinadi. Shuningdek, masofani qizil siljish orqali o'lchashda yuzaga kelishi mumkin bo'lgan xatolar ham hisobga olinadi. Natijada, ushbu noaniqliklar tufayli kosmologiyada qoramtir energiyaga bo'lgan ehtiyoj tahlil qilinadi.

**Kalit so'zlar:** yutilishsh, rang parametri, kosmologiya, qorong'u energiya, masofani o'lchash, xatoliklar, noqulaylik koeffitsientlari.

**Introduction.** The accelerated expansion of the Universe was discovered during 1998, by two independent projects, the Supernova Cosmology Project and the High-Z Supernova Search Team, which both used distant supernovae Ia (SNe Ia) to measure the acceleration. The idea was that as SNe Ia have almost the same intrinsic brightness (a standard candle), and since objects that are further away appear dimmer, it is used the observed brightness of these supernovae to measure the distance to them. The observational fact is that the SNe Ia at  $z \approx 0.5$  are  $\sim 0.28^m$  dimmer ( $\sim 14\%$  farther) than expected [1]. The unexpected result was that objects in the Universe are moving away from one another at an accelerating rate. Cosmologists at the time expected that recession velocity would always be decelerating, due to the gravitational attraction of the matter. To explain the acceleration they introduced into science a new term "Dark Energy". It is said that this energy, which causes the accelerating expansion Universe, covers about 70% of the Universe [2].

In cosmology, distance is calculated in two main ways, through the distance modulus and the cosmological redshift. The calculation of distance using the distance module is mainly based on observational data, which takes into account the absolute and apparent magnitudes of objects, absorption coefficients, color parameter, light curve shape parameter, nuisance coefficients, etc. The calculation of distance by redshift is based mainly on theoretical data, with only the cosmological redshift based on the measurement results.

First method is considered to have a high degree of reliability because it relies mainly on observational data, but is more likely to have systematic and statistical errors. Second method is based on theoretical data and is less likely to contain errors and inaccuracies in calculations, but has a much lower level of reliability. Therefore, Reiss, Perlmutter, and Schmidt, in their study, proposed a modification to the second method to correct the difference in distances found in these two methods, and introduced a new term into cosmology called "Dark Energy" [2]. But could this difference be due to the errors and inaccuracies of the first



method, or due to the inaccuracies in the measurement of the redshift? In their view, these errors are insufficient to close the difference between two distance measuring methods.

**Distance measurement in intergalactic medium.** Before the effects of light absorption were discovered, various photometric methods were quite successfully used in astronomy to determine the distances to stars and other space objects. Based on various astrophysical or statistical assumptions, the absolute magnitude  $M$  of the studied objects was determined. Then, comparing it with the apparent magnitude  $m$ , we calculated the distance  $r'$  to the object by the formula:

$$lgr' = 0.2(m - M) + 1 \quad (1)$$

Since the discovery of the fact of the existence of interstellar matter, formula (1) has ceased to be correct and has been replaced by another:

$$lgr = 0.2(m - M) + 1 - 0.2A \quad (2)$$

or:

$$M = m + 5 - 5lgr - A, \quad (3)$$

where  $A$  denotes the loss of light in magnitude as a result of its passage through the interstellar medium. The distances  $r$  previously determined were magnified, because if we compare formulas (1) and (2), we have:

$$r' = r \cdot 10^{0.2A}, \quad A \geq 0 \quad (4)$$

From this equation we can see that apparent distance is always greater than real distance ( $r' > r$ ). In addition, the discovery of dark matter also entailed a decrease in almost all previously measured distances. For example, the size of our Galaxy decreased by about half [3].

This formula is mainly used for objects in our Galaxy. However, we can realise from this formula that as the distance increases, the distance-measure errors increase significantly under the affect of the interstellar matter. For example, when the extinction  $A = 2.5$  at a distance of 1000 pc, the error is  $\sim 3$ , which means that the object appears to be about 3 times farther away from the real distance. Especially calculating the distance to the distant SNe, taking into account the Galaxy extinction, extragalactic and SNe host galaxy extinctions, the distance measurement becomes more sophisticated and the uncertainties increase even more. Measuring distance is hard there is no easily-determined standard of length for calibration. This has always been a central problem in astronomy. The distance to a light cannot be estimated from its apparent brightness. There are too many factors which can change the perceived intensity [4].

**Distance measurement based on SNe Ia data.** Six of the principal galaxy distance indicators are discussed: Cepheid variables, the Tully-Fisher relation, the  $D_n$ - $\sigma$  relation, Surface Brightness Fluctuations, Brightest Cluster Galaxies, and SNe Ia [5]. Below we take a closer look at the last method.

Finding the distance to distant supernovae, the distance modulus is calculated by the following formula:

$$\mu = m_B^* - M_B + \alpha x_1 - \beta c \quad (5)$$

where:  $m_B^*$ , the apparent magnitude at maximum,  $M_B$  is the absolute magnitude of SNe (in the rest frame B-band).  $\alpha$  and  $\beta$  are nuisance coefficients and their value can be constrained in several methods (Table 1).  $x_1$ -light curve shape parameter,  $c$ -color parameter, these parameters have a particular value for each SNe. Based on the observed values of SNe stretch and color distributions, the limits are  $-4.5 < x_1 < 2$  and  $-0.3 < c < 0.6$ . These limits were identified based on the results of 234 SNe Ia [6].

Table 1. Best fit  $\Lambda$ CDM parameters for SNe Ia

	$\Omega_M$	$\alpha$	$\beta$	$M_B$
JLA (stat+sys)	$0.295 \pm 0.034$	$0.141 \pm 0.006$	$3.101 \pm 0.075$	$-19.05 \pm 0.02$
JLA (stat)	$0.289 \pm 0.018$	$0.140 \pm 0.006$	$3.139 \pm 0.072$	$-19.04 \pm 0.01$
SDSS+SNLS (stat+sys)	$0.311 \pm 0.042$	$0.140 \pm 0.007$	$3.140 \pm 0.082$	$-19.04 \pm 0.03$
SDSS+SNLS (stat)	$0.305 \pm 0.022$	$0.139 \pm 0.007$	$3.178 \pm 0.079$	$-19.03 \pm 0.01$
lowz+SDSS (stat+sys)	$0.337 \pm 0.072$	$0.145 \pm 0.007$	$3.059 \pm 0.093$	$-19.02 \pm 0.03$
lowz+SDSS (stat)	$0.298 \pm 0.052$	$0.144 \pm 0.007$	$3.096 \pm 0.090$	$-19.04 \pm 0.02$
lowz+SNLS (stat+sys)	$0.281 \pm 0.043$	$0.138 \pm 0.009$	$3.024 \pm 0.107$	$-19.08 \pm 0.03$
lowz+SNLS (stat)	$0.282 \pm 0.023$	$0.139 \pm 0.009$	$3.074 \pm 0.104$	$-19.05 \pm 0.02$

In this table It is given nuisance coefficients average values  $\alpha \approx 0.14$  and  $\beta \approx 3.1$ , absolute magnitude  $M_B \approx -19.05$  [7]. However, these values are differed from other papers, for example:

- SALT Light-Curve Fit Parameters  $\rightarrow M_B = -19.46$ ,  $\alpha = 1.34 \pm 0.08$  and  $\beta = 2.59 \pm 0.12$ ,
- SALT2 Light-Curve Fit Parameters  $\rightarrow M_B = -19.44$ ,  $\alpha = 0.104 \pm 0.018$ , and  $\beta = 2.48 \pm 0.10$  [6],
- The best-fit Light-Curve parameters in YONSEI SNe catalog for SALT2 are  $\alpha = 0.15$ ,  $\beta = 3.69$ , and  $M_B = -19.06$  [1515].

Two different light curve fitting methods, MLCS (multicolor light curve shape) and a template-fitting approach, were employed to determine the distances to the nearby and high-redshift samples. Both methods use relations between light curve shape and luminosity as defined from SNe Ia in the nearby Hubble flow [12]. Both methods employ extinction correction from the measured color excess using relations between intrinsic color and light curve shape, then the Galaxy and SNe host galaxy extinctions are corrected by using following formula:

$$R_V = A_V / E_{B-V} \quad (6)$$

This ratio normally has an average value of 3.1 for interstellar dust in the

Galaxy, although it can vary between 2.1 and 5.8 [8]. The same value ( $R_V = 3.1$ ) was also detected by other researchers [9,10]. However, A. G. Riess et al. defined this ratio:  $R_V = 1.7-2.2$  [12].

Based on a new approach for determining the absorption-to-reddening ratio  $R_V$  for host galaxies using color excess probability functions, it was found for a sample of 34 SNe Ia observed in Sbc-Scp galaxies, and 21 SNe Ia observed in Sab-Sbp galaxies,  $R_V = 2.71 \pm 1.58$  and  $R_V = 1.70 \pm 0.38$  respectively [9]. SNe Ia in passive hosts favour a dust law of  $R_V = 1.0 \pm 0.2$ , while SNe Ia in star-forming hosts require  $R_V = 1.8 \pm 0.2$  [6]. On average, the distance modulus increase by  $0.019^m$ , with an average increase for the fixed  $R_V$  subsample of  $0.014^m$ . It is supposed that these results agree with  $\sim 1\%$  increase in distance [13].



All these constraints and values are defined with a certain confidence level, which means that these limits and values are not appropriate for all SNe Ia. In addition, each method has some uncertainties. For example, Hicken M. et al. combine the CfA3 SNe Ia sample with samples from SALT, SALT2, MLCS17, MLCS31 to calculate improved constraints and found uncertainties MLCS17 has  $0.02^m$ , MLCS31 and SALT have  $0.03^m$ , and SALT2 has  $0.06^m$ . In addition, some factors (not all) affecting the distance modulus have been considered by Riess et al., Including Effect of a Local Void-very small, Weak Gravitational Lensing  $0.02^m$ , Evolution  $0.05^m$  Extinction  $0.05^m$ , (according to the latest researches  $\sim 0.10^m$ - $0.25^m$ ), Light Curve Fitting Method  $0.03^m$  [14]. And they consider that all these factors cannot explain for the  $0.28^m$  difference in the template-fitting SNe Ia distances and the  $\Omega_\Lambda=0$  prediction. But if it is collected that all the factors and uncertainties that affect the modulus of distance, perhaps the observational data of SNe Ia can be explained without dark energy.

**Distance measurement via redshift.** The distance to the long supernovae can also be measured by redshift:

$$\mu \equiv 25 + 5 \log_{10}(d_L/Mpc), \quad (7)$$

$$d_L = (1+z) \frac{d_H}{\sqrt{\Omega_k}} \sinh\left(\sqrt{\Omega_k} \int_0^z \frac{H_0 dz'}{H(z')}\right), \quad d_H = \frac{c}{H_0}, \quad (8)$$

$$H_0 \equiv 100h \text{ km s}^{-1} \text{ Mpc}^{-1},$$

$$H = H_0 \sqrt{\Omega_M(1+z)^3 + \Omega_k(1+z)^2 + \Omega_\Lambda} \quad (9)$$

This way is more theoretical, so it is considered that there are no any uncertainties as statistical and systematic errors. But while measuring spectroscopic redshift there could be some uncertainties. Srivatsan Sridhar and Yong-Seon Song claimed that there are significantly contaminated by the uncertainty on redshift measurements obtained through multiband photometry, which makes it difficult to get cosmic distance information measured from baryon acoustic oscillations, or growth functions probed by redshift distortions [16]. They test their method using simulated galaxy maps with photometric uncertainties of  $\sigma_0 = (0.01, 0.02, \text{ and } 0.03)$ .

**Conclusion.** In cosmology, calculating distance is a very complex process. Calculations become more complicated, especially when calculating the distance to a long supernova. In this study, the factors that cause uncertainties and errors in distance calculation were discussed in detail. From this it can be concluded that the difference in the calculation of the distance to the long supernovae in the two methods ((7) and (8) equations) may be due to the above possible errors and uncertainties. As a result, cosmology may not need "Dark Energy" .

#### REFERENCES

1. Weidong Li and Filippenko A. V. Observations of Type Ia Supernovae, and Challenges for Cosmology, arXiv:astro-ph/0310529v1 19 Oct 2003, p.2
2. Adam G. Riess et al., Observational evidence from supernovae for an accelerating Universe and a cosmological constant, *Astrophysical journal*, 116:1009-1038, 1998 September, p.1009,1020, 1028-1034
3. Кутузов С. А., Марданова М. А., Осипков Л. П., *Математические методы моделирования галактик, Санкт-Петербург*, 2012, ISBN 978-5-98340-266-9, p.51
4. Type Ia supernovae as distance indicators, Article in *Astrophysics and Space Science* · July 1989, p.5,7
5. Jeffrey A. WILLICK, Measurement of Galaxy Distances, arXiv:astro-ph/9610200, 1996, p.1
6. Lampeit H. et al. The effect of host galaxies on type Ia supernovae in the SDSS-II supernova survey, the *astrophysical journal*, 722:566–576, 2010 October 10, p.568
7. Betoule M. et al. Improved cosmological constraints from a joint analysis of the SDSS-II and SNLS supernova samples, arXiv:1401.4064v2 [astro-ph.CO] 4 Jun 2014, p.16
8. Hicken M. et al. Improved dark energy constraints from  $\sim 100$  new CfA supernova type Ia light curves, *The Astrophysical Journal*, 700:1097–1140, 2009 August 1, p.1107-1113
9. Mandel K. S. et al. The type Ia supernova color–magnitude relation and host galaxy dust: a simple hierarchical Bayesian model, *The Astrophysical Journal*, 842:93 (26pp), 2017 June 20, p.2
10. Linlin Li. Et al. The galactic extinction and reddening from the south galactic cap u-band sky survey: u band galaxy number counts and u – r color distribution, *The Astronomical Journal*, 153:88 (9pp), 2017 February, p.1
11. Cikota A. et al. Determining type Ia supernova host galaxy extinction probabilities and a statistical approach to estimating the absorption-to-reddening ratio  $R_V$ , *The Astronomical Journal*, 819:152 (13pp), 2016 March 10, p.1
12. A. G. Riess et al. Is the dust obscuring supernovae in distant galaxies the same as dust in the Milky Way? *The Astrophysical Journal*, 473:588-594, 1996 December 20, p.593
13. Jha S. et al. Improved distances to type Ia supernovae with multicolor light-curve shapes: MLCS2K2, *The Astrophysical Journal*, 659:122Y148, 2007 April 10, p.144
14. Adam G. Riess et al. Observational evidence from supernovae for an accelerating Universe and a cosmological constant, *Astrophysical journal*, 116:1009-1038, 1998 September, p.1009,1020, 1028-1034
15. Young-Lo Kim et al. Environmental dependence of type Ia supernova luminosities from the YONSEI supernova catalog, *Journal of the Korean Astronomical Society* - Vol. 53 , No. 3, p.199
16. Srivatsan Sridhar and Yong-Seon Song. Cosmic distance determination from photometric redshift samples using BAO peaks only, arXiv:1903.09651v2 [astro-ph.CO] 12 Jul 2019, p.1



UDK: 538.955; 621.3.082.782

*Azambek TURAKULOV,*  
*Namangan muhandislik-texnologiya instituti dotsenti, f.-m.f.n*

*NamMTI professori f.-m.f.d. R.Ikramov taqrizi asosida*

## ВОЗМОЖНОСТИ ИСПОЛЬЗОВАНИЯ ПОЛУПРОВОДНИКОВЫХ СЕНСОРОВ В МОНИТОРИНГЕ ЗДОРОВЬЯ ЧЕЛОВЕКА

Аннотация

В статье рассмотрены возможности и результаты применения современных датчиков, являющихся результатом достижений в области физики полупроводников, в устройствах, предназначенных для непрерывного мониторинга здоровья человека. Также были предложены некоторые методы устранения трудностей, возможные в этом процессе.

**Ключевые слова:** полупроводник, датчик, полупроводниковый датчик, p-n переход, магнитное поле, терморезистор, магнитный датчик.

## POSSIBILITIES OF USING SEMICONDUCTOR SENSORS IN HUMAN HEALTH MONITORING

Annotation

The article discusses the possibilities and results of using modern sensors, which are the product of advances in semiconductor physics, in devices designed for continuous monitoring of human health. Some troubleshooting methods available in this area have also been suggested.

**Key words:** semiconductor, sensor, semiconductor sensor, p-n junction, magnetic field, thermistor, magnetic sensor.

## YARIMO‘TKAZGICHLI SENSORLARDAN INSON SALOMATLIGINI MONITORING QILISHDA FOYDALANISH IMKONIYATLARI

Annotatsiya

Maqolada yarimo‘tkazgichlar fizikasi sohasining yutuqlari mahsuli bo‘lgan zamonaviy sensorlardan inson salomatligini doimiy monitoring qilib borishga mo‘ljallangan qurilmalarda qo‘llash imkoniyatlari va natijalari muhokama qilingan. Shuningdek, ushbu sohada mavjud ba‘zi muammolarni bartaraf qilish usullari taklif qilingan.

**Kalit so‘zlar:** yarimo‘tkazgich, sensor, yarimo‘tkazgichli sensor, p-n o‘tish, magnit maydon, termorezistor, magnit sensor.

**Kirish.** Jamiyatimiz misli ko‘rilmagan darajada jadal suratlar bilan rivojlanib bormoqda. Insoniyat tarixida birinchi hisoblash asbobi – “Abak sanog‘i” (Eramizdan avvalgi 3000 yillar) kashf qilingandan to birinchi elektron hisoblash mashinasi ishlab chiqilgunga qadar (1942 yil, ENIAK) qariyb 5000 yil vaqt o‘tgan bolsa, undan birinchi inson koinotga chiqqunga qadar (1961 yil Yuriy Gagarin) atigi 19 yil vaqt o‘tdi.

Bugungi kunda hayotimizni qo‘l telefonlari, hisoblash tizimlari, axborot almashish tizimlari, avtomatlashtirilgan boshqaruv tizimlari, elektron maishiy texnikalar, bort kompyuterli avtomashinalar kabi qulaylikarsiz tasavvur ham qila olmaymiz.

Informatsiya almashish tezligining o‘ta yuqoriligi odatiy holga aylanib bormoqda. Yaqin o‘tmishda bir habarni boshqa qit‘aga yetkazish va javobini olish uchun oylab vaqt sarflangan. Bugungi kunda ushbu habar bir necha soniya ichida manzilga yetib borayotgan bo‘lsada, uni yuklab olish tezligiga (u, xattoki, Gbit/sek bo‘lganda ham) e‘tiroz bildiramiz.

Agar televizorning boshqaruv pulti orqali bir kanaldan boshqasiga o‘tkazish tugmasini bosganingizda uni bajarish atigi bir necha soniyaga kechiksa, uning nozozligi bo‘yicha mutaxassisga murojaat qilamiz.

Yuqorida keltirilgan taraqqiyotga erishshda zamonaviy elektron tizimlarning asosini tashkil qiluvchi “Yarimo‘tkazgichlar fizikasi” ilmiy tadqiqotlari natijalarining o‘rni beqiyosdir.

Ushbu maqolada zamonaviy avtomatlashtirilgan boshqaruv tizimlarining eng zarur ajralmas qismi hisoblangan yarimo‘tkazgichli sensorlardan inson salomatligini saqlash maqsadlarida foydalanish imkoniyatlari muhokama qilingan.

**Adabiyotlar tahlili.** Ma‘lumki, inson tanasi o‘zida ro‘y berayotgan fizik, kimyoviy va biologik jarayon yordamida o‘zining haroratini optimall (o‘rtacha 36,6 °C) holatda ushlab turadi. Ushbu haroratdan atiga 1°C ga chetlanish ham inson tanasida qandaydir kasallik borligidan dalolat beradi. Shu ma‘noda inson tanasi haroratini uning salomatlik ko‘zgusi deb hisoblash mumkin.

Odatda inson tanasi harorati shifoxonalarda muntazam ravishda grafik bo‘yicha, yoki uy hamda safar sharoitlarida kasallik alomati sezilganda, turli termometrlar yordamida tananing ma‘lum bir joyida o‘lchanadi. Bu esa turli kasalliklardi dastlabki boshlanish davrida sezib qolish ehtimolini kamaytiradi. Buning ustiga biz tana haroratini faqat bir joyda (odatda peshona yoki qo‘ltiqda) o‘lchashga odatlanganmiz. Bir vaqtning o‘zida tananing turli joylaridagi haroratni uzluksiz o‘lchash va natijalarni qiyosiy qayta ishlab xulosa chiqarish amaliyoti yetarli darajada ommalashmagan.

Asrlar osha chaqaloqlar va bolalar tanasi haroratini o‘lchash uchun kasallikning qandaydir tashqi belgilari, katta yoshdagi insonlar uchun ularning shikoyatlari turtki bo‘lib kelgan. Masalan bolaning ishtaxasi bo‘lmasa yoki kamharakat bo‘lib qolsa birinchi galda uning peshonasi ushlab ko‘riladi. Agar harorat keragidan yuqori ekanligi sezilgan holdagina termometrga murojaat qilinadi. Lekin, bilamizki, ba‘zi hollarda tananing ichidagi xavfli yuqori harorat inson peshonasida aks etmasligi mumkin. Shunday ekan, inson tanasi haroratini zamonaviy fan-texnika yutuqlaridan foydalangan holda davomli monitoring qilib borish bugungi kunning eng dolzarb muammolaridan biri hisoblanadi.

Odatdagi tibbiy termometrlarda suyuqliklar xajmining harorat ta'sirida chiziqli o'zgarishi xususiyatidan (masalan, simobli termometrlar), metallarda esa haroratga bog'liq ravishda elektr tokini o'tkazish darajasi o'zgarishi xususiyatlaridan (termorezistorlar) foydalaniladi. Lekin, bunday turdagi termometrlarning tibbiyotda qo'llanishida bir qator kamchiliklar mavjud. Bunday kamchiliklar jumlasiga:

- simob bug'ining inson uchun o'ta zararli ekanligi;
  - suyuqlikli termometrlar faqat visual informative xarakterga ega bo'lib, elektr signal ko'rinishda emasligi;
  - suyuqlik termometrlarning maksimal aniqligi 0,1 °C, termorezistorlarning aniqligi 0(1 °C) ekanligi;
- kabilarni kiritish mumkin.

Yarimo'tkazgichlar fizikasining hozirgi kundagi intensiv rivojlanib borishi natijasida yuqoridagi singari kamchiliklardan holi bo'lgan harorat sensorlaridan foydalanish imkoniyati ham ortib bormoqda, Hozirgi kundagi yarimo'tkazgichli termometrlarning ishlash prinsipi to'g'ri yo'nalishdagi p-n o'tishda kuchlanishning haroratga bog'liqligi hususiyatiga asoslangan. Yarimo'tkazgichlarning bunday xususiyatlari bugungi kunda ham ko'plab fizik tadqiqotchilar, jumladan respublikamizning yetakchi olimlari G.G'ulomov va U.Erkaboyevlar rahbarligidagi bir guruh ilmiy tadqiqotchilar tomonidan faol o'rganilmoqda [4].

**Tadqiqot metodologiyasi.** Quyida yarimo'tkazgichli termometrlarning bugungi kundagi mavjud ilg'or namoyandalaridan biri bo'lgan DS18B20 sensoridan inson tanasi harorat signallarini olish va uni qayta ishlash maqsadida foydalanish imkoniyatlarini ko'rib chiqamiz.

TO-92 korpusdagi DS 18B20 harorat sensori o'lchamlari bo'yicha kompakt (4.5x4.5x3.5mm) qurilma bo'lib, undan kichik xajmli monitoring qurilmalarini yaratishda foydalanish qulay (1-rasmga qarang).

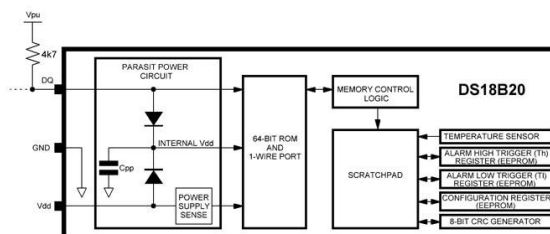


1-rasm. TO-92 korpusdagi DS18B20 sensor tasviri.

Ushbu sensor quyidagi xossalarga ega:

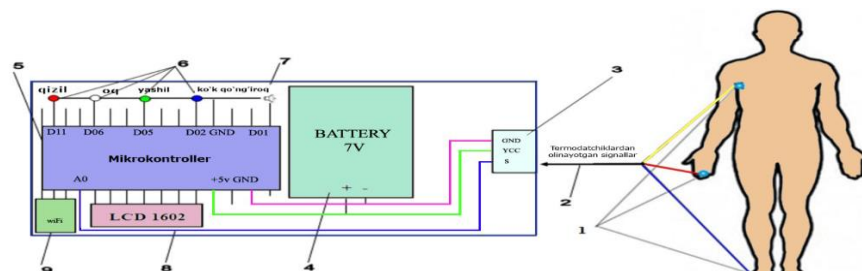
- yarimo'tkazgichli qurilma;
- 3 dan 5 voltgacha doimiy tok iste'mol qiladi;
- 9, 10, 11, 12 razryadli holatlarda ishlaydi;
- 12 razryadli holatda harorat o'lchash aniqligi – 0.0625 °C;
- 12 razryadli holatda harorat o'lchash tezligi – 750 ms gacha;
- har bir sensor unikal seriya nomeriga ega (bu 127 tagacha sensorni bitta kabelga parallel ulash imkoniyatini beradi);
- o'lchagan haroratni, havotir signalining quyi va yuqori chegara qiymatlari (Th va Tl) ni, konfiguratsiyani saqlab turuvchi RAM xotiraga ega.

Ushbu sensorni funksional imkoniyatlariga ko'ra alohida "mikrokontroller" deb atash mumkin bo'lib, uning soddalashtirilgan sxemasi 2-rasmda keltirilgan.



2-rasm. DS18B20 sensor tuzilishining soddalashtirilgan sxemasi. DQ – o'lchangan harorat signali pini, Vdd – sensorga musbat tok berish pini, GND – manfiy pin.

Ushbu sensordan inson tanasi haroratini davomli monitoring qilib borishga mo'ljallangan avtomatlashtirilgan qurilma A.Turakulov va F.Mullajonovlar tomonidan taklif qilingan bo'lib [6], uning soddalashtirilgan sxemasi 3-rasmda keltirilgan.



3-rasm. Qurilmaning soddalashtirilgan sxemasi. 1 - termosensolar, 2 - harorat o'lchash natijalarini uzatish kabeli, 3-qurilmaga kabelni ulash joyi, 4-qurilmaning o'zgarimas tok manbai, 5 - mikrokontroller, 6 - natijani monitoring qilish lampalari, 7 - xavfli holat to'g'risida ogohlantiruvchi qo'ng'iroq, 8 - LCD displey foydalanuvchi interfeysi, 9 - tashqi qurilma.

Ushbu inson tanasi haroratini monitoring qiluvchi avtomatlashtirilgan qurilma boshqa mavjud harorat o'lchovchi asboblardan shu bilan farqlanadiki, u bir vaqtning o'zida tananing bir nechta joyi haroratini o'lchaydi, barcha o'lchash natijalarini monitorida ko'rsatadi, olingan haroratlarni taqqoslash orqali avtomatik qayta ishlaydi va natijalarni ogohlantirish signallari orqali ma'lum qiladi. Shu bilan birga, u uzoq vaqt davomida tana harorati o'zgarishi dinamikasini tashqi qurilmalarga (masalan, USB kabel orqali personal kompyuterga) uzatib, davomli monitoring ma'lumotlari sifatida saqlash imkoniyatini ham beradi. Yana bir eng asosiy omillardan biri – qurilmada “miya” sifatida mitti hamda arzon Arduino Nano mikrokontrolleridan foydalanilgan. Bu esa qurilmani jamiyatning barcha tabaqadagi a'zolari uchun qurbi yetishini ta'minlaydi.

**Tahlil va natijalar.** Hozirgi vaqtda inson “yurak-qontomir” tizimi faoliyati ko'zgularidan biri sifatida elektrokardiogramma (EKG)dan keng foydalanilmoqda. Ma'lumki, EKG – bu yurakning sinus tugunida hosil bo'lgan elektr tokining inson tanasining turli nuqtalaridagi potentsiallari ayirmalarining grafik tasviri bo'lib, u asosan yurakda ro'y berib bo'lgan turli ishenik va boshqa kasalliklar simptomlarini baholash imkoniyatlarini beradi. Lekin EKG ba'zi symptomsiz kasalliklarni aniqlash uchun yetarli ma'lumot bera olmaydi.

Ma'lumki, yurakning “Sinus tuguni” hosil qilgan elektr toki yurak bo'ylab “Gis dastasi” ko'rinishda tarqaladi. Agar ushbu dasta hosil qiladigan magnit maydonidagi o'zgarishlarni qayd qilish imkoniyati bo'lganda edi, biz undan EKG ga nisbatan ko'proq ma'lumotlarni olgan bo'lar edik.

Dunyoda birinchi bo'lib ushbu go'yani 1963 yilda Amerikalik olimlar Gerhard Boul va Richard McPheeler amalga oshirishga harakat qilishgan. Ular magnit maydonini qayd qilish uchun metal o'zakli magnit g'altaklaridan foydalanganlar. Lekin inson tanasidagi bioto'klar atigi  $10^{-14}$  dan  $10^{-10}$  Teslagacha magnit maydoni hosil qilganligi sababli ular ijobiy natijaga erisha olmaganlar.

Ushbu go'ya 1964 yilda DC SQUID (Direct Current Superconducting Quantum Interference Device) – o'zgarish tokli o'ta o'kazuvchan magnit sensorlar [1], 1967 yilda RF SQUID (Radio Frequency Superconducting Quantum Interference Device) – radio chashtotali o'ta o'kazuvchan magnit sensorlar [2] ixtiro qilingandan keyin ijobiy natija bera boshladi. Lekin, bunday sensorlarning tannarxi bugungi kun texnologiyalaridan foydalangan holda ham o'ta qimmat (o'rtacha \$1-1,5mln.) bo'lganligi sababli, EKG o'rni bosa olmayapti.

2015 yilda f.-m.f.d.Vladimir Belotelov rahbarligida bir guruh Rossiya Kvant Markazi (PKЦ – Российский Квантовый Центр) olimlari tomonidan yuqori sezuvchanlik xususiyatiga ega bo'lgan magnit sensori yaratildi. Ushbu sensor SQUID sensorlarga nisbatan yuzlab marta arzon va kompakt bo'lib, u ferrit-granatning monokristall yupqa qatlamidan tayyorlanadi. Magnit maydonini aniqlash uchun mazkur qatlamdagi atomlarning magnit momentlari boshqaruvchi g'altaklar yordamida yuzlab kilogerts chastota bilan aylantiriladi [3]. Ushbu texnologiya  $10^{-13}$  dan  $10^{-11}$  Teslagacha bo'lgan magnit maydonini aniqlash imkoniyatini beradi. Lekin, ushbu sensor tashqi magnit shovqinlarga nisbatan ham o'ta sezgirliigi sababli, hozircha, isomagnit sharoitida tajribadan o'tkazilmoqda.

Hozirgi kunda yuqorida e'tirof etilgan G.G'ulomov va U.Erkaboyevlar rahbarligidagi guruh tomonidan magnit maydonining yarimo'tkazgichlar xossalriga ta'sirini o'rganish bo'yicha ham ilmiy tadqiqotlar olib borilmoqda [5].

**Xulosa.** Xulosa qilib aytish mumkinki, hozirki kunda yuqori sezuvchanlik xususiyatiga ega bo'lgan magnit sensorlaridan foydalanish uchun asosiy to'siqlardan biri – bu inson tanasidan olingan signallarni tashqi magnit maydon ta'siri, yani, shovqinlardan tozalash muammosidir. Bu muammoni signallarni vaqt momentlarida diskretlash orqali hal qilish imkoniyati mavjud. Masalan, muayyan sharoitda  $t_i$  vaqt momentida inson tanasida o'lchangan  $B_{hb}(t_i)$  miqdordan joriy vaqt momentidagi mavjud tashqi  $B_{en}(t_i)$  magnit maydon miqdori (buni shartli ravishda shovqin deb atash mumkin) ni ayirib, inson tanasining sof magnit maydoni  $B(t_i)$  ni aniqlash mumkin:

$$B(t_i) = B_{hb}(t_i) - B_{en}(t_i), \quad i = 0, 1, 2, \dots$$

#### ADABIYOTLAR

1. R. C. Jaklevic; J. Lambe; A. H. Silver & J. E. Mercereau (1964). "Quantum Interference Effects in Josephson Tunneling". Physical Review Letters. 12(7):159–60. Bibcode:1964PhRvL..12..159J. doi:10.1103/PhysRevLett.12.159
2. J. Clarke and A. I. Braginski (Eds.) (2004). The SQUID handbook. Vol. 1. Wiley-Vch.
3. <https://www.techinsider.ru/technologies/189901-na-puti-k-mielofonu/>
4. G.Gulyamov, U.I.Erkaboev, R.G.Rakhimov, J.I.Mirzaev. On temperature dependence of longitudinal electrical conductivity's oscillations in narrow-gap electronic semiconductors. Journal of Nano- and Electronic Physics Vol. No, Ulugbek Erkaev, Rustamjon Rakhimov, Jasurbek Mirzaev, Nozimjon Sayidov. The influence of external factors on quantum magnetic effects in electronic semiconductor structures. International Journal of Innovative Technology and Exploring Engineering (IJITEE) ISSN: 2278-3075, Volume-9, Issue-5, March 2020.
5. Turakulov A., Mullajonova F. An automated system for body temperature monitoring of children, people with disabilities and bedridden people using a continuous analysis. Diagnostyka, 2020, VOL. 21, NO. 3. ISSN 1641-6414. E-ISSN 2449-5220. <https://doi.org/10.29354/diag/125314>.



UDK: 331.2:681.14(045)(575.1)

*Shoh Abbos ULUG'MURODOV,*  
*O'zbekiston Milliy universitetining Jizzax filiali tayanch doktoranti*  
*E-mail: ushohabbos@gmail.com*

*PhD dots. O.Asqaraliyev taqrizi asosida*

### ADAPTIVE RESTRICTION AND A METHOD FOR DETERMINING THE ANGLE OF INCLINATION FOR BRAILLE TEXTS

Annotation

This article focuses on the principles of Optical Character Recognition (OCR) for the Latin Braille alphabet in the Uzbek language (the type of writing used by blind people). We employed multiple image processing and analysis streams to implement the text recognition process. In doing so, adaptive thresholding and tilt angle determination methods were thoroughly examined.

**Key words:** Adaptive, angle of inclination, ocr, grid.

### АДАПТИВНОЕ ОГРАНИЧЕНИЕ И МЕТОД ОПРЕДЕЛЕНИЯ УГЛА НАКЛОНА ДЛЯ ТЕКСТОВ ШРИФТОМ БРАЙЛЯ

Аннотация

Эта статья посвящена принципам оптического распознавания символов (оптическое распознавание символов) для латинского алфавита Брайля на узбекском языке (тип письма, используемый слепыми людьми). Мы использовали несколько потоков обработки и анализа изображений для реализации процесса распознавания текста. При этом были подробно рассмотрены методы адаптивного ограничения и определения угла наклона.

**Ключевые слова:** Адаптивный, угол наклона, ocr, решетка.

### BRAYL YOZUVIDAGI MATNLARNI ANIQLASHNING ADAPTIV CHEGARALASH VA EGILISH BURCHAGINI TOPISH USULI

Annotatsiya

Bu maqola O'zbek tilidagi lotincha Brayl alifbosi (ko'zi ojiz odamlar foydalanadigan yozuv turi) uchun optik belgilarni aniqlash OCR (Optical character recognition) tamoyillari bilan bog'liq. OCR jarayonini amalga oshirish uchun biz tasvirni qayta ishlash va tahlil qilishning bir nechta mavzularidan foydalandik. Bunda adaptiv chegaralash va egilish burchakni aniqlash usullari batafsil ko'rib o'tildi.

**Kalit so'zlar.** Adaptiv, egilish burchagi, ocr, panjara.

**Kirish.** Ushbu maqolaning maqsadi Brayl kodi (ko'zi ojizlar tomonidan qo'llaniladigan yozuv turi) uchun optik belgilarni tanuvchi OCRni ishlab chiqishdan iborat. Biz ushbu ishni bajarishda quyidagi 5 ta asosiy bosqich yordamida Brayl belgilarini aniqlash jarayonini ko'rib o'tdik:

✚Kiruvchi tasvirlar sifatini boshqarish;

✚Brayl alifbosida yozilgan matnning tashkil etuvchi nuqtalarning joylashuvini aniqlash uchun skanerlangan tasvirlarni qayta ishlash;

✚Matndagi satr va ustunlar o'lchov qiymatlarini olish uchun topilgan nuqtalarni qayta ishlash. Ushbu usul Brayl mesh aniqlanishi deb nomlanadi;

✚Aniqlangan nuqtalar kombinatsiyasini ASCII kodigagi ifodaga aylantirish uchun O'zbek tilidagi lotincha Brayl alifbosidan foydalanish;

✚Foydalanuvchi interfeysi.

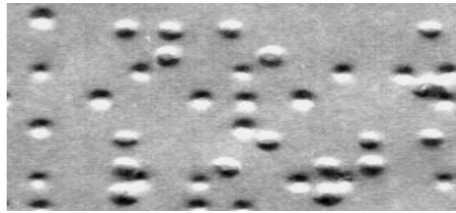
Bizda yuqoridagi besh qismga tegishli bo'lgan natijalar mavjud. Biz ushbu maqolada berilgan natijalar bilan ishlaymiz.

**Kiruvchi tasvir sifatini boshqarish.** Ushbu maqolada biz Tven standartini tanladik [1]. Ushbu standart ko'pgina sanoat firmalari (HP, Logitech, Caere va Aldus) tomonidan ilgari surilgan. Ushbu standartning maqsadi kiruvchi tasvir sifatini yaxshilash va turli shovqin qiymatlarini kamaytirishdan iborat. Ushbu standart faqat skanerlar uchun emas, balki turli xil manbalaardagi tasvirlarni olish imkonini beradi. Bu tasvirdagi belgilarni olishning ustuvor vazifadir.

#### Nuqtalarni lokallashtirish

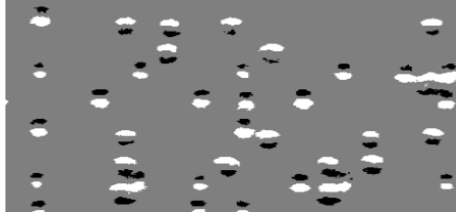
Bu mantqiy jarayonning birinchi bosqichi hisoblanib, kiruvchi tasvir kam shovqin parametrlariga ega bo'lishi kerak. Brayl alifbosida yozilgan tasvirda quyidagi ikki xil tipdagi nuqtalarni ko'rish mumkin: bo'rtgan nuqtalar va botiq nuqtalar. Ko'zi ojiz odam matnda faqat bo'rtgan nuqtalarni aniqlab, o'qish jarayonini amalga oshiradi. Botiq nuqtalar ushbu matnning orqa tomonidagi sahifasida chop etilgan, bo'rtgan nuqtalar hisoblanadi. Bu holat ikki xil turdagi nuqtalarni tasvirda farqlashda muammo tug'diradi. Ammo biz ushbu holatda tasvirni bir marotaba skanerlash orqali ikki tomondagi belgilarni ham ajratib olish taklifini beramiz.





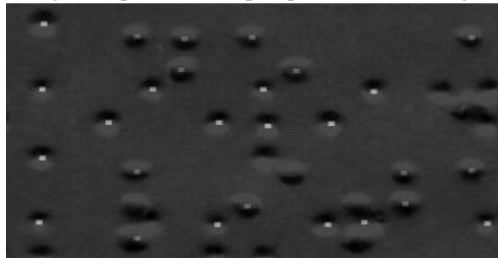
1-rasm: Brayl alifbosida yozilgan ikki tomonlama matn.

Brayl alifbosidagi boshlanish nuqta mavjud qolipning (pattern) kuzatilgan modeli hisoblanadi. Biz tajriba davomida skanerlangan tasvirlarda bo'rtgan nuqtadan yuqorida yarim oy shaklida yorqin maydon, pastki qismda esa shu shakldagi qorong'u maydon mavjud ekanligini aniqladik. Botiq nuqtalar teskari patternga ega bo'ldi (yuqoridagi qorong'u, pastdagi yorqin maydon) (2-rasmga qarang). Biz berilgan maydonlarni oq va qora dog'larga ajratishda, ikkita adaptiv chegaralash usulini qo'lladik. Chegaraviy yorqinlik darajalari yorqinlik gistogrammasidagi nuqtalar sifatida aniqlanadi [2], ular uning umumiy maydonini ikki maydonga ajratadi, shuning uchun taqsimot ma'lumotlarining berilgan ulushi tegishli chegaradan yuqori/pastda joylashgan. Foiz eksperimental ravishda 5 ga o'rnatildi%.



2-rasm. Chegaralash jarayonidan keying tasvir.

Keyinchalik, biz qora va oq maydonlarning markazlarini aniqlaymiz va ularni qora va oq nuqta koordinatalari sifatida qabul qilamiz. Keyinchalik, yuqorida joylashgan oq nuqta va quyida joylashgan qora nuqtadan iborat qo'shni juftlarni aniqlaymiz. Bu juftliklar keyinchalik "bo'rtgan nuqtalar", "botiq nuqtalar" sifatida belgilanadi.



3-rasm. Lokallashtirilgan tasvir nuqtalari

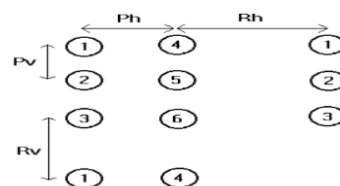
Ushbu usul foydalanish qulayligi va yuqori bajarilish tezligi bilan ajralib turadi. Shunga qaramay, ushbu usul ikkita muhim kamchilikka ega [3]. Birinchidan, ba'zi nuqtalarning yo'qolishi, ikkinchidan, soxta nuqtalarning paydo bo'lishi kuzatiladi.

Xatolar bir-biriga yaqin joylashgan dog'lar mavjudligi bilan bog'liq bo'lib, ular chegarani o'zgartirish jarayonidan so'ng birlashadi (bu, ayniqsa, bo'rtgan va botgan nuqtalar juda yaqin bo'lganda sodir bo'ladi; 2-rasmdagi oxirgi ustundagi nuqtalarga qarang). Muammoni barcha intellektual ishlov berishning keyingi bosqichga - tarmoqni aniqlashga o'tkazish orqali hal qilish mumkin [4]. Biz ishlab chiqqan panjara qurish algoritmi noto'g'ri tartibda joylashgan nuqtalarni samarali ravishda tashlab yuboradi va manbaaga tegishli yo'qolgan nuqta maydonlarini aniqlaydi.

Bu algoritm aniqlanishi zarur bo'lmagan nuqtalarni tabiiy ravishda tashlab yuboradi. Nuqtalar bilan ishlashning intuitiv yondashuvidan tashqari, biz patternni aniqlashning muqobil samaradorlikdagi usullarni aniqladik. Bu usullar bilan tanishib chiqishingiz mumkin.

#### Tarmoqni aniqlash.

Ushbu bosqichda matn satrlari, ustunlarining joylashuvi va yo'nalishini aniqlashimiz zarur. Bu pozitsiyalar biz Brayl meshi deb ataydigan usulni tashkil qiladi. Brayl alifbosida biz 6 nuqtadan iborat to'rga egamiz. Har bir nuqta faol yoki faol bo'lmasligi mumkin (matnda bo'rtgan Brayl nuqtasi sifatida belgilangan). Har bir kombinatsiya alohida xarakterni ifodalaydi. Agar bizda N ta belgi (matn) bo'lsa, ular orasidagi masofalar normallashtiriladi. Keyin, bizda  $6 \times N$  nuqtadan iborat to'r mavjud (Brayl to'ri) bo'ladi. Oldingi algoritm nuqtalarning bir qismini aniqlaydi, ammo ularning soni panjara qurish uchun yetarli hisoblanadi. To'liq panjara mavjud bo'lganda, har bir potentsial joyga yaqin nuqtalar mavjudligini tekshirish uchun uni batafsil o'rganish mumkin (har bir nuqta yuqorida va pastda joylashgan bir nechta nuqtalarga ega, ammo ba'zida ularning joylashuvi markazlashtirilmagan) bo'ladi. Ushbu algoritm yordamida biz yo'qotilgan nuqtalarni tiklaymiz. Shuningdek, soxta nuqtalarni - masofa qoidaloriga mos kelmaydigan nuqtalarni eslatib o'tish kerak. Algoritm ularni oddiy istisno tarzida tashlab yuborishni ta'minlaydi.



4-rasm. Brayl to'ri.

Standart masofalar:  $Ph = 2.5$  mm,  $Rh = 3.5$  mm,  $Pv = 2.5$  mm va  $Rv = 5$  mm. Algoritmnin birinchi bosqichi egilish burchagini aniqlash bo'lib, u quyidagi metodga asoslanadi [5]

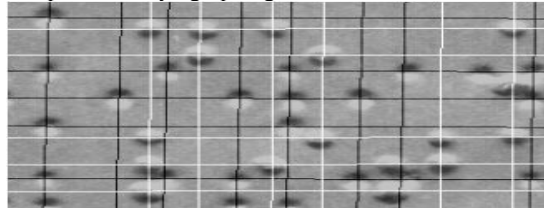


Shundan so'ng, algoritm boshlang'ich nuqtani tanlaydi va butun tarmoqni qurish uchun standart masofalarni ketma-ket siljitishni amalga oshiradi. Asosiy tanlovimiz noto'g'ri joylashgan nuqtani tanlamaslikdan iboratdir. Ushbu muammoni hal qilish uchun tizim ma'lum bir mos nuqtalar maydoniga eng yaqin 10 ta maydon nuqtasini tahlil qiladi. Ushbu nuqtalarning har biri uchun tizim dastlabki mos yozuvlar nuqtasidan belgilangan masofaga asoslangan munosabatlarni o'rnatishga harakat qiladi.

Har bir urinishda tizim standart pozitsiyalarda ma'lum usulda topilgan nuqtalar sonini hisoblab chiqadi. Ushbu 10 ta nuqtaning maksimal qiymati boshlang'ich nuqtani tanlash uchun ishlatiladi (harakat faqat vertikal ravishda amalga oshiriladi va nuqtalar gorizontal chiziqlar bo'ylab qidiriladi, bu belgi ichidagi nuqtaning nisbiy holatidan mustaqillikni ta'minlaydi).

Yana bir muhim vazifa – ko'rilayotgan Brayl belgisi ichidagi boshlang'ich nuqtaning nisbiy holatini aniqlash. 4-rasmda ko'rib turganingizdek, 6 ta pozitsiya mavjud [6]. Biz shunchaki barcha mumkin bo'lgan pozitsiyalarni taxmin qilamiz va keyin yuqorida tavsiflangan maksimal nuqtani topish usulidan foydalanamiz Birinchidan, nuqta qaysi ustunga (2 dan), so'ngra qaysi qatorga (3 dan) tegishli ekanligini aniqlaymiz.

Yakuniy bosqich sifatida boshlang'ich nuqtadan boshlab toki butun tarmoqni qurishgacha bo'lgan jarayon qaraladi. Ushbu harakat moslashuvchan tarzda amalga oshiriladi. Ushbu usulning mohiyati 6 o'lchamdagi panjarani har bir keyingi nuqtalar uchun ham siljitishdan iborat. Keyingi belgi topilgach, biz panjara tugunlari yaqinidagi nuqtalarni tekshiramiz. Keyin biz ushbu nuqtalar asosida panjara o'rnini to'g'rilaymiz. Biz bu jarayonni tasvirning o'ng chegarasiga qadar davom ettiramiz. Shundan so'ng, biz bir xil adaptiv mantiq asosida keyingi qatorga o'tamiz.



5-rasm. Tasvirning ikki sahifasi uchun hisoblangan Brayl to'ri.

Agar chegaralar to'g'ri va aniq o'rnatilgan bo'lsa noto'g'ri holatdagi nuqtalar ushbu jarayonda ko'rib chiqilmaydi.

#### ASCII kodiga tarjima

3-bosqichdan so'ng bizda olti nuqtali belgilar (1 yoki 0 ga teng bo'lishi mumkin bo'lgan oltita bit) bilan ifodalangan Brayl matni mavjud. Endi biz uni ASCII kodiga aylantirishimiz kerak. Boshqacha qilib aytganda, Brayl alifbosini qo'llaymiz.

#### Foydalanuvchi interfeysi

Foydalanuvchi interfeysi Gradio freymworki yordamida yaratilgan bo'lib, istalgan qurilmalardan foydalanish imkoniyatini beradi [7]. Dastur kodi foydalanuvchi interfeysi uchun Python hamda C++ dasturlash tillarida yozilgan va tasvirni qayta ishlash tartiblari C da yozilgan (foydalanuvchi interfeysi bilan bog'lanish uchun DLL kutubxonalar tuzilgan).



6-rasm. Dasturning umumiy ko'rinishi va ishlash prinsipi

#### Dasturdan foydalanishda zarur tavsiyalar, yutuqlar va kamchiliklar

Bugungi kunda biz hali bajarishimiz zaur bo'lgan quyidagi ishlarni ajratib ko'rsatishimiz mumkin:

- ✚ Algoritmning ishlashini tezlashtirish. Biz butun sahifani taxminan 2.8 soniyada taniymiz (Intel i5-1035G1 (8) @ 3.600GHz; GPU: Intel Iris Plus Graphics G1 Memory: 7715MiB) [8]. Bu anchayin tez ishlash hisoblanadi.

- ✚ Dasturning joriy versiyasida foydalanuvchi Brayl nuqtalari orasidagi masofani qo'lda o'rnatishi kerak. Bu nostandart Brayl alifbosi bilan ishlash qobiliyati bilan bog'liq. Tizim, albatta, sukut bo'yicha standart masofalardan foydalanadi, ammo masofalarni avtomatik aniqlash juda foydali bo'ladi. Avtomatik o'lchovlarni aniqlash uchun sun'iy intellekt texnologiyalarini qo'llash maqsadga muvofiq bo'ladi [9].

- ✚ Kompyuterlashtirilgan (8 nuqtali) Brayl alifbosi va maxsus simvolik belgilar ketma-ketliklarini (masalan, matematik belgilar) joriy etish.

- ✚ Ushbu dasturda Brayl alifbosida yozilgan matnni aniqlash xatolik qiymati 3% ni tashkil etadi.

Ushbu ilova foydalanuvchilar uchun katta qiziqish uyg'otadigan ba'zi xususiyatlarni o'z ichiga oladi. Garchi bu xususiyatlar tasvirni qayta ishlash algoritmlari bilan bog'liq bo'lmasa-da, quyida ularning qo'shimcha imkoniyati haqida aytib o'tamiz:

- ✚ Ushbu OCR dasturimiz A4 dan katta bo'lgan sahifalardagi Brayl alifbo belgilarini aniqlash uchun ishlatiladi. Bunda skaner qilinayotgan tasvir ikki qismga ajratilgan holda yuklanadi hamda ular bitta sahifa ko'rinishiga keltiriladi. Odatda ko'zi ojizlar uchun tayyorlangan o'quv adabiyotlar A4 dan katta bo'lgan sahifalarda ham bo'ladi [10].

- ✚ Foydalanuvchi loyihalarni yaratishi mumkin. Loyiha tegishli varaqlarni (masalan, kitoblarni) skanerlash uchun mo'ljallangan [11]. Dastur va skaner parametrlari loyiha bilan birga saqlanadi.

**Xulosa.** Biz Brayl alifbosida yozilgan matnlar uchun optik belgilarni aniqlash (OCR) tizimini ishlab chiqdik va amalga oshirdik. Yakuniy ilova barcha turdagi qurilmalar uchun professional dastur bo'lib, u standart matnli OCR-ga o'xshash ishlaydi va ko'zi ojizlar odamlar uchun juda foydali vositadir.

#### ADABIYOTLAR

1. "Twain, Reference Manual". HP Corporation

2. F. M. Whal. "Digital Image Signal Processing". Artech House, Inc. 1987
3. X. Fernández, F. Martín, A. Corbacho. "Algoritmos de Reconocimiento de Patrones: Aplicación a O.C.R. Braille". Proceedings of URSI-94. Gran Canaria, Spain. September, 1994
4. O.N.C.E. "Normas de Escritura Braille" (Spanish Edition of Braille Standards).
5. G. S. D. Farrow, M. A. Ireton, C.S. Xydeas. "Detecting the Skew Angle in Document Images". Signal Processing. Image Communication. Vol 6. Págs 101- 114. 1994
6. Axatov Akmal Rustamovich, and Ulug'Murodov Shoh Abbos Baxodir O'G'Li. "'Deep learning' yordamida brayl yozuvidagi matnlarni tanib olishning usullari" Илм-фан ва инновацион ривожланиш / Наука и инновационное развитие, vol. 6, no. 1, 2023, pp. 32-41. doi:10.36522/2181-9637-2023-1-5
7. Akhatov, A. R., and Sh A. B. Ulugmurodov. 'Braille Classification Algorithms Using Neural Networks'. *Artificial Intelligence, Blockchain, Computing and Security Volume 2*, CRC Press, 2023, pp. 654–659, <https://doi.org10.1201/9781032684994-106>.
8. <https://ultrashop.uz/ru/store/kompyuternaya-tehnika/noutbuki/hp-envy-x360-15m-ed0013dx>
9. Akmal Akhatov, & Shokh Abbos Ulugmurodov. (2023). TRAINING DATA SELECTION AND LABELING FOR MACHINE LEARNING BRAILLE RECOGNITION MODELS. International Journal of Contemporary Scientific and Technical Research, (Special Issue), 15 - 21. Retrieved from <https://journal.jbnuu.uz/index.php/ijcstr/article/view/326>
10. Axatov Akmal Rustamovich, & Ulug'murodov Shoh Abbos Baxodir o'g'li. (2022). INKLUZIV TA'LIMDA INNOVATSION SENSORLI O'QITISH TEXNOLOGIYASI. International Journal of Contemporary Scientific and Technical Research, 1(2), 213–216. Retrieved from <https://journal.jbnuu.uz/index.php/ijcstr/article/view/160>
11. Akhatov, A., & Ulugmurodov, A. (2022). METHODS AND ALGORITHMS FOR SEPARATION OF TEXT WRITTEN IN BRAILLE INTO CLASSES USING NEURAL NETWORK TECHNOLOGIES. Евразийский журнал математической теории и компьютерных наук, 2(11), 4 - 8. извлечено от <https://www.in-academy.uz/index.php/EJMTCS/article/view/4248>



UDK: 538.955; 621.3.082.782

**Nosirjon SHARIBAYEV**,  
Namangan muhandislik-texnologiya instituti professori, f.-m.f.d  
**Muzaffar DADAMIRZAYEV**,  
Namangan muhandislik- texnologiya instituti tayanch doktoranti  
Namangan muhandislik- qurilish instituti  
**Ulug‘bek ERKABOYEV**,  
Namangan muhandislik-texnologiya instituti professori, f.-m.f.d  
E-mail: muzaffardadamir81@gmail.com

NamMTI professori, f.-m.f.d. R.Ikramov taqrizi asosida

### ВЛИЯНИЕ ТЕМПЕРАТУРЫ И МАГНИТНОГО ПОЛЯ НА ПЛОТНОСТИ ПОВЕРХНОСТНЫХ СОСТОЯНИЙ ГЕТЕРОСТРУКТУРНОГО ПОЛУПРОВОДНИКА

Аннотация

В данной статье исследованы физические свойства поверхности гетероструктурного полупроводникового материала. Применена зависимость плотности поверхностных состояний полупроводника  $Si(p)$  р-типа от магнитного поля. Впервые разработана математическая модель, определяющая влияние сильного магнитного поля на температурную зависимость плотности поверхностных состояний в полупроводниковых гетероструктурах.

**Ключевые слова:** гетероструктура, фотоэлектрический преобразователь, глубокие уровни, вольт-фарадные характеристики, поверхностные состояния, магнитное поле.

### INFLUENCE OF TEMPERATURE AND MAGNETIC FIELD ON THE DENSITY OF SURFACE STATES OF A HETEROSTRUCTURAL SEMICONDUCTOR

Annotation

This article examines the physical properties of the surface of a heterostructure semiconductor material. The dependence of the density of surface states of the p-type  $Si(p)$  semiconductor on the magnetic field is applied. For the first time, a mathematical model has been developed that determines the influence of a strong magnetic field on the temperature dependence of the density of surface states in semiconductor heterostructures.

**Key words:** heterostructure, photoelectric converter, deep levels, capacitance-voltage characteristics, surface states, magnetic field.

### GETEROSTRUKTURALI YARIMO‘TKAZGICH SIRT HOLATLAR ZICHLIGIGA HARORAT VA MAGNIT MAYDONING TA‘SIRI

Annotasiya

Ushbu maqolada geterostrukturni yarimo‘tkazgich material sirtining fizik hossalari o‘rganildi. p-tipli  $Si(p)$  yarimo‘tkazgichning sirt holatlar zichligini magnit maydonga bog‘liqligi tadbiiq etilgan. Ilk bora, Yarimo‘tkazgichli geterostrukturnalarda sirt holatlar zichligini haroratga bog‘liqligiga kuchli magnit maydonning ta‘sirini aniqlovchi matematik model ishlab chiqildi.

**Kalit so‘zlar:** geterostrukturna, fotoelektrik o‘zgartirgich, chuqur sathlar, sig‘im-kuchlanish xususiyatlari, sirt holatlari, magnit maydon.

**Kirish.** Ma‘lumki fotoelektrik o‘zgartirgichlar sifatida keng qo‘llaniladigan  $CdS/Si(p)$  geterostrukturnali yarimo‘tkazgichning elektr, optik va magnit hossalari o‘rganish dolzarb muammolardan biri hisoblanadi. Jumladan  $CdS/Si(p)$  ni geterostrukturnasida nuqsonlarning hosil bo‘lishi, ushbu yarimo‘tkazgichli materiallarning elektr xususiyatlariga salbiy ta‘sir qilsa, chuqur energetik sathlardagi sirt holatlar zichligi esa geterostrukturnani fotoelektrik samaradorligini yomonlashishiga olib keladi.

**Mavzuga oid adabiyotlar tahlili.** Bugungi kunda, sirt holatlar zichligini o‘lchash, uni tashqi omillarga bog‘liqligini aniqlash bo‘yicha bir qator tadqiqotlar olib borilgan. Xususan, [1,2] ishlarda yarimo‘tkazgichli strukturalarda sirt holatlar zichligini Volt-Farad usuli yordamida aniqlangan.

Ishning asosiy maqsadi  $CdS/Si(p)$  geterostrukturnali yarimo‘tkazgichning sirt holatlar zichligini magnit maydonga bog‘liqligini modellashtirishdan iborat.

Keskin  $p-n$  o‘tishli diodning past chastotali sig‘im-kuchlanish xususiyatlarini  $CdS/Si(p)$  geterostrukturnali yarimo‘tkazgich uchun tavsiflash mumkin. U holda geterostrukturnani past chastotali sig‘im-kuchlanishi quyidagi ifoda orqali hisoblanadi [1]:

$$C_{pch} = \frac{dq_{pch}}{dV} = S \sqrt{\frac{\epsilon \epsilon_0 q (N_a + N_r)}{2(V_d - V - \Delta V_d)}} \quad (1)$$

(1) formulada  $V$  ni qiymati 0 dan boshlab  $V_{SS}^{max}$  gacha o‘zgaradi. U holda (1) ni  $V$  bo‘yicha 0 dan  $V_{SS}^{max}$  oraliqda integrallasak

va  $V_{SS}^{max}(B, T)$  ni hisobga olish natijasida,  $Q_{pch}$  ni aniqlash mumkin:

$$q_{pch} = q_{SS} = \int_0^{V_{SS}^{max}(B,T)} C_{pch}(V) dV \quad (2)$$

$$q_{SS} = \int_0^{V_{SS}^{max}(B,T)} S \sqrt{\frac{\epsilon\epsilon_0 q (N_a + N_t)}{2(\Phi - V)}} dV$$

Bundan tashqari, sirdagi ionlashgan zaryad miqdori akseptorni va chuqur sathdagi konsentrasiyalar bilan bog'liqligi:

$$q_{SS} = q(N_a + N_t) \delta S \quad (3)$$

$\delta$ - chuqur energetik sathlarni qayta zaryadlagan qismi (yuzi).

1-rasmga ko'ra  $\delta$  ni quyidagicha aniqlanadi:

$$W - \delta = \sqrt{\frac{\epsilon\epsilon_0 q (E_t - E_{F_p})_W}{q^2 N_a}} \quad (4)$$

Shu bilan birga,  $W$  ni  $V$  ga bog'liqligi quyidagicha [1]:

$$W(V) = \frac{\epsilon\epsilon_0 S}{C(V)} \quad (5)$$

(4) va (5) dan foydalanib  $\delta$  ni topamiz:

$$\delta = \frac{\epsilon\epsilon_0 S}{C(V)} - \sqrt{\frac{\epsilon\epsilon_0 q (E_t - E_{F_p})_W}{q^2 N_a}} \quad (6)$$

$S_i(p)$  uchun valent zona shipiga nisbatan  $E_F$  ni quyidagicha aniqlanadi [1]:

$$E_{F_p} = E_V - kT \ln\left(\frac{N_a}{N_V}\right) \quad (7)$$

(7) dan:

$$E_{F_p} = E_V - kT \ln\left(\frac{N_a}{N_V}\right) \quad (8)$$

kelib chiqadi.

(8) ni  $E_t$  ga nisbatan baholaymiz:

$$E_t - E_{F_p} = E_t - E_V - kT \ln\left(\frac{N_V}{N_a}\right) \quad (9)$$

Sirt holatlari uchun  $E_t$  ni  $E_{SS}$  ga almashtirsak va (1) formuladan foydalansak:

$$(E_{SS} - E_{F_p}) = q(\Phi - V) - kT \ln\left(\frac{N_V}{N_a}\right) \quad (10)$$

kelib chiqadi.

Sirt holatlari uchun (6) dagi  $(E_t - E_{F_p})$  ni o'rniga (10) ni qo'ysak:

$$\delta_{SS} = \frac{\epsilon\epsilon_0 S}{C_{pch}(V)} - \sqrt{\frac{\epsilon\epsilon_0}{q^2 N_a} \left( q(\Phi - V) - kT \ln\left(\frac{N_V}{N_a}\right) \right)} \quad (11)$$

ifodani olamiz.

Geterocheqaralarda sirt holatlar zichligi  $N_{SS}$  chuqur sathdagi xajmiy konsentrasiya bilan quyidagicha bog'langan:

$$N_{SS} = N_t \delta_{SS} \quad (12)$$

[1] ga ko'ra  $\delta_{SS}$  ni  $V = V_{SS}^{max}$  shart asosida (11) ni hisoblansa,  $(E_g(T) = E_g(0) - \frac{\alpha_1 T^2}{\alpha_2 + T})$  ni hisobga olamiz) u

holda  $\delta_{SS}(B, T)$  quyidagi ko'rinishga keladi:

$$\delta_{SS}(B) = \sqrt{\frac{2\epsilon\epsilon_0 \left( E_g(T) + \hbar \frac{eB}{m_c^*} \right)}{q(N_a + N_t)}} - \sqrt{\frac{\epsilon\epsilon_0}{q^2 N_a} \left( q \left( E_g(T) + \hbar \frac{eB}{m_c^*} \right) - kT \ln\left(\frac{N_V}{N_a}\right) \right)} \quad (13)$$

(2), (3), (12) va (13) lardan foydalanib, sirt holatlar zichligini kuchli magnit maydonga bog'liqligi topiladi:

$$N_{SS}^{(B)} = N_a \delta_{SS}^{(B)} - \frac{1}{qS} \int_0^{V_{SS}^{max}} C_{If} (V) dV \quad (14)$$

Shunday qilib, (13) va (14) lardan foydalanib, CV usulida aniqlangan sirt holatlar zichligini kuchli magnit maydoniga bog'lanishini topamiz:

$$N_{SS} (B) = N_a \left( \sqrt{\frac{2\epsilon\epsilon_0}{q(N_a + N_t)} \left( E_g (T) + \hbar \frac{eB}{m_c^*} \right)} - \sqrt{\frac{2\epsilon\epsilon_0}{qN_a} \left( E_g (T) + \hbar \frac{eB}{m_c^*} \right)} - kT \ln \left( \frac{N_v}{N_a} \right) \right) - \sqrt{\frac{2\epsilon\epsilon_0 (N_a + N_t)}{q}} * \left( \sqrt{\Phi - \left( E_g (T) + \hbar \frac{eB}{m_c^*} \right)} - \sqrt{\Phi} \right) \quad (15)$$

Agar ushbu ifoda  $B \rightarrow 0$  ga intilsa [1] ishda keltirilgan sirt holatlar zichligi formulasiga qaytadi. Bu esa, biz taklif qilayotgan matematik modelni nazariy tomondan to'g'ri ekanligini isbotlaydi. Taklif etilayotgan matematik modelda  $N_{SS} (B)$  sirt holatlar zichligini (15) formula bo'yicha haroratga bog'liqligini to'liq tushintira olmaydi. Chunki, past haroratlarda (15) ga ko'ra  $N_{SS} (B)$  deyarli o'zgarmaydi. Yani  $\alpha_1$  ning qiymati barcha materiallar uchun  $10^{-4}$  atrofida bo'ladi  $\alpha_2$  esa [6] ga ko'ra 100 K da yuqori haroratlarda olinadi. Bundan kelib chiqadiki,

$$\lim_{T \rightarrow 0} \left( E_g (0) - \frac{\alpha_1 T^2}{\alpha_2 + T} + \hbar \frac{eB}{m_c^*} \right) = E_g (0) + \hbar \frac{eB}{m_c^*} \quad (16)$$

Bundan tashqari, (15) formuladagi  $kT \ln \left( \frac{N_v}{N_a} \right)$  xad ham  $N_{SS} (B)$  ni haroratga bog'liqligi dinamikasiga deyarli ta'sir etmaydi. Sirt holatlar zichligini haroratga bog'liqligini aniqlash uchun chuqur energetik sathlarda (taqiqlangan zona kengligining markaziga yaqin zonalar) zaryad tashuvchilarning termik generatsiyalanish ehtimoligidan foydalaniladi.

Ma'lumki, sirt holatlarning bo'shalish ehtimoligi vaqtga, haroratga va taqiqlangan zona kengligining markazi tabiatiga bog'liq. Chuqur sathlardagi  $E_{SS}$  energiyali sathning bo'shalish ehtimoligi quyidagi formula orqali [5-8] aniqlanadi:

$$\rho (E_{SS}) = 1 - \exp \left( -\frac{t}{\tau (E_{SS})} \right) \quad (17)$$

Bunda,  $\tau (E_{SS})$  - chuqur energetik sohalarida 0 dan boshlab  $E_{SS}$  gacha elektronlarni bo'shalish vaqti. Albatta,  $E_{SS}$  ni qiymati ortishi bilan unga ko'proq vaqt ketadi. [6] ga ko'ra ( $E_{SS}$ ) funksiya  $E_{SS}$  va  $kT$  ga kuchli bog'liq bo'ladi:

$$\tau (E_{SS}, T, t) = \tau_0 \exp \left( \frac{E_{SS}}{kT} \right) \quad (18)$$

(17) va (18) lardan  $\rho (E_{SS}, T, t)$  aniqlash mumkin:

$$\rho (E_{SS}, T, t) = 1 - \exp \left( -\frac{t}{\tau_0} \exp \left( \frac{E_{SS}}{kT} \right) \right) \quad (19)$$

Bu ifoda, sirt holatidagi zaryad tashuvchilarning  $E_{SS}$  energetik sathini bo'shalish ehtimoligini haroratga bog'liqligini ifodalaydi.

Ilmiy adabiyotlardan ma'lumki, sirt holatlar sonini vaqtga bog'liqligi quyidagi ifoda orqali aniqlanadi [9]:

$$N (t) = \int_{E_v}^{E_c} N_{SS} \rho (E_{SS}, T, t) dE \quad (20)$$

(20) ifodada,  $N_{SS}$  ni qiymati energiyaga bog'liq bo'lmagan kattalik bo'lib, [1] da CV usulida hisoblangan sirt holatlar zichligiga teng. Shu bilan birga, biz taklif qilayotgan  $N_{SS}(B)$  ham  $B \rightarrow 0$  ga intilganda [1] da keltirilgan  $N_{SS}$  ga qaytadi. U holda, (15) ni (20) ga qo'yib va uni o'zgarimas vaqt oralig'ida ( $t = \text{const}$ ) sirt holatlarni energiya bo'yicha integrallanishini hisobga olsak, sirt holatlari soni quyidagicha aniqlanadi:

$$N (E, B, T) = \int_{E_v}^{E_c} N_{SS} (B) \rho (E_{SS}, T) dE_{SS} \quad (21)$$

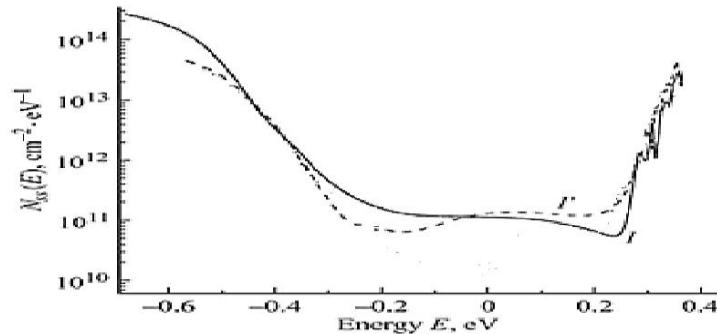
Sirt holatlar soni  $N(E, B)$  dan  $E_{SS}$  energiya bo'yicha hosilasi energetik sirt holatlar zichligi deb ataladi. Unda, (21) ni  $E_{SS}$  bo'yicha differensiallash natijasida (21) ifoda quyidagi ko'rinishga ega bo'ladi:

$$N_{SS} (E_{SS}, B, T) = \frac{dN (E_{SS}, B, T)}{dE_{SS}} \text{ yoki } N_{SS} (E_{SS}, B, T) = \sum_{N_t=0}^{N_i} N_{SSi} (B) \frac{d\rho (E_{SS}, T)}{dE_{SS}} \quad (22)$$

Ushbu keltirib chiqarilgan (22) formula energetik sirt holatlar zichligini haroratga bog'liqligiga kuchli magnit maydonning ta'sirini ifodalaydi.

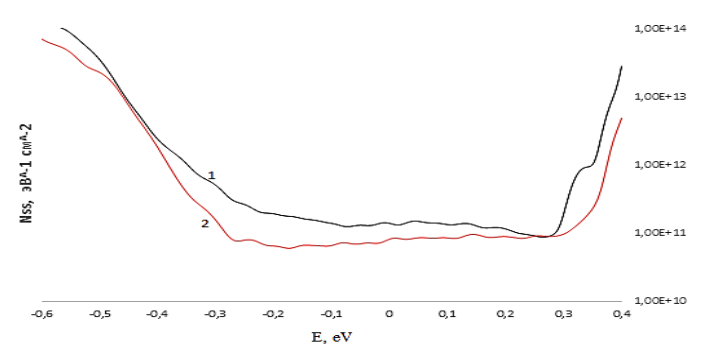
**Tahlil va natijalar.** Endi, taklif etilayotgan model asosida tashqi omillar ta'siridagi sirt holatlar zichligini aniqlashni yarimo'tkazgichli strukturalar uchun tadbiq etaylik. Jumladan, [10] ishlarda metall-oksid-yarimo'tkazgich strukturalarda sirt

holatlar zichligini radiatsiya va magnit maydonlarga bog'liqligi bo'yicha ta'iri tajriba natijalarida olingan. Ya'ni, [10] ishda *Bi-Si-Al* yarimo'tkazgichli tuzilmani sirt holatlar zichligiga magnit maydon ta'siri hona haroratida aniqlangan [1-rasm]. 1-rasmda  $N_{SS}(E)$  ni  $E$  ga bog'liqligi  $B=0$  va  $B=0.17$  Tl magnit maydonlarda grafiklari keltirilgan. Ushbu rasmdan ko'rinib turibdiki, magnit maydon ta'sir ettirilganda OY o'qi bo'yab ( $N_{SS}$  o'qi) siljishi tajribada kuzatilgan. Lekin, bu tajriba natijalari sabablari tushintiruvini mexanizmi ishlab chiqilmagan.



1-rasm. *Bi-Si-Al* tuzilmalarida (*Si* asosida) sirt holatlar zichligiga magnit maydonning ta'siri.  
1- $B=0$  Tl, 1'- $B=0.17$  Tl,  
 $T=300$  K [10].

Lekin, biz taklif qilayotgan matematik model (22-formula) tajriba natijalarini izohlashga imkon beradi. Chunonchi, [10] da keltirilgan fizik parametrlarni (22) formulaga qo'llash. Ya'ni, *Bi-Si-Al* (*Si* sirti) tuzilma uchun  $E_g(0) = 1.12$  eV,  $B=0.17$  Tl,  $T=300$  K,  $F=0.11V$ . 4-rasmda, (22) formula bo'yicha olingan  $N_{SS}(B,T)$  ni turli magnit maydonlarga bog'liqligi keltirilgan. Tajriba (1-rasm) va nazariya (2-rasm) grafiklarini solishtirilsa, albatta ba'zi qonuniyatlar bajarilganda, sifat jihatdan bir-biriga yaqin keladi. Taklif qilinayotgan modelni yana bir afzalligi shundan iboratki, (22) formula yordamida tajriba natijalari past harorat va yuqori magnit maydonlarda hisoblash mumkin.



2-rasm. Xona haroratida *Bi-Si-Al* tuzilmasida (*Si* asosida) sirt holatlar zichligiga magnit maydonning ta'siri.  
1-  $B=0$  Tl,  $T=300$  K,  
2-  $B=0.17$  Tl,  $T=300$  K

**Xulosa.** Ushbu tadqiqot ishlarini bajarish jarayonida, quyidagi xulosalarga erishildi: Ilk bora, yarimo'tkazgichli geterostrukturali materiallar uchun sirt holatlar zichligini haroratga va magnit maydonga bog'liqligini nazariy jihatdan tushuntirildi. Yarimo'tkazgich-dielektrik chegarasidagi sirt holatlar zichligiga magnit maydonning ta'sirini hisoblovchi yangi analitik ifoda taklif qilindi. Yarimo'tkazgichli geterostrukturalarda sirt holatlar zichligini haroratga bog'liqligiga kuchli magnit maydonning ta'sirini aniqlovchi matematik model ishlab chiqildi.

#### ADABIYOTLAR

1. Трегулов, В.В. Способ определения плотности поверхностных состояний в гетероструктурах CdS/Si(p) на основе анализа вольт-фарадных характеристик / В.В. Трегулов // Известия высших учебных заведений. Поволжский регион. Физико-математические науки. – 2012. – № 3 (23). – С. 124–132.
2. Трегулов, В. В. Исследование гетероструктур CdS/Si(p), изготовленных методом гидрохимического осаждения CdS / В. В. Трегулов // Вестник Рязанского государственного университета имени С. А. Есенина. – 2011. – Т. 32, № 3. – С. 169–179.
3. Шарма, Б. Л. Полупроводниковые гетеропереходы : пер. с англ. / Б. Л. Шарма, Р. К. Пурохит. – М. : Сов. радио, 1979. – 232 с.
4. Гулямов Г., Каримов И.Н., Шарибаев Н.Ю., Эркабоев У. Определение ППС на границу раздела полупроводник диэлектрик в структурах Al-SiO<sub>2</sub>-Si и Al-SiO<sub>2</sub>-n-Si<Ni> при низкой температуре // Узбекский физический журнал. - Ташкент, 2010 -12(№3), -С.143-146.



5. Erkaboev U.I., Gulyamov G., Mirzaev J.I., Rakhimov R.G., Sayidov N.A. Calculation of the Fermi–Dirac Function Distribution in Two-Dimensional Semiconductor Materials at High Temperatures and Weak Magnetic Fields // *Nano*. 2021. Vol.16, Iss.9. Article ID 2150102.
6. Erkaboev U.I., Gulyamov G., Mirzaev J.I., Rakhimov R.G., Sayidov N.A. Calculation of the Fermi–Dirac function distribution in two-dimensional semiconductor materials at high temperatures and weak magnetic fields // *NANO: Brief Reports and Reviews*. 2021. Vol. 16, No. 9. pp.2150102:1-10. (Scopus: CiteScore: 2.1. <https://www.scopus.com/sourceid/11300153732>)
7. Erkaboev U.I., Gulyamov G., Mirzaev J.I., Rakhimov R.G. Modeling on the temperature dependence of the magnetic susceptibility and electrical conductivity oscillations in narrow-gap semiconductors // *International journal of modern physics B*. 2020. Vol. 34, No. 7. pp.2050052: 1-17. (Scopus: CiteScore: 2.1. <https://www.scopus.com/sourceid/28075>).
8. Gulyamov, G., & Abdulazizov, B. T. (2016). On the thermodynamics of a two-dimensional electron gas with non-parabolic dispersion. *World Journal of Condensed Matter Physics*, 6(4), 294-299.
9. Пикус Г.Е. Основы теории полупроводниковых приборов. Москва: Наука. 1965. –448 с.
10. Б.В. Павлык, А.С. Грыпа, Д.П. Слободзян, Р.М. Лыс, И.А. Шикоряк, Р.И. Дидык, “Влияние магнитного поля на электрофизические свойства поверхностно-барьерных структур Bi-Si-Al”. *Физика и техника полупроводников*, 2011, том 45, вып. 5, С-608-611.



UDK: 538.955; 621.3.082.782

**Dilshodbek ERKABOEV**,  
*Farg‘ona politexnika instituti magistranti*  
**Nozimjon SAYIDOV**,  
*Namangan muhandislik-texnologiya instituti katta o‘qituvchisi*  
**Ulug‘bek ERKABOEV**,  
*Namangan muhandislik-texnologiya instituti professori, f.-m.f.d*  
**Ulug‘bek NEGMATOV**,  
*Namangan muhandislik-texnologiya instituti tayanch doktoranti*  
**Nodirbek NABIJONOV**,  
*Namangan davlat universiteti tayanch doktoranti*  
*E-mail: sayidovnozimjon@gmail.com*

*NamMQI professori, f.-m.f.d. M. Dadamirzayev taqrizi asosida*

### KVANT O‘LCHAMLI YARIMO‘TKAZGICHLI STRUKTURALARDA MAGNITOQARSHILIK OSSILYATSIYALARIGA KUCHLI ELEKTROMAGNIT MAYDONNING TA‘SIRI

Annatsiya

Ushbu ishda kvant o‘rali yarimo‘tkazgichli strukturalarni o‘rganishga qiziqish uni kichik o‘lchamli diapazonda ishlaydigan nanotexnologik asboblarning sifatida, shuningdek, turli xil spintronik qurilmalarda qo‘llash imkoniyati bilan belgilanmoqda. Olimlar tomonidan ushbu kvant o‘lchamli strukturalarning katta e‘tibor bilan o‘rganishiga asosiy sabab, bunday materiallarning fizik xususiyatlari bir qator qiziqarli ilmiy jarayonlarga ega bo‘lib, bu jarayonlarning turli xil tashqi omillar ta‘sirida tubdan o‘zgarishlarini to‘liqroq tushunishga imkon beradi.

**Kalit so‘zlar:** Geterostruktura, nanoo‘lcham, kvant o‘ra, holatlar zichligi, holatlar zichligi, ossillyatsiya, nanoo‘lcham, magnit maydon, ikki o‘lchamli, yarimo‘tkazgichlar.

### ВЛИЯНИЕ СИЛЬНОГО ЭЛЕКТРОМАГНИТНОГО ПОЛЯ НА ОСЦИЛЛЯЦИИ МАГНИТОСОПРОТИВЛЕНИЯ В КВАНТОВОМЕРНЫХ ПОЛУПРОВОДНИКОВЫХ СТРУКТУРАХ

Аннотация

В данной работе интерес к исследованию полупроводниковых структур с квантовой раной определяется возможностью их применения в качестве нанотехнологических устройств, работающих в малоразмерном диапазоне, а также в различных устройствах спинтроники. Основная причина, по которой эти квантовые структуры изучаются учеными с большим вниманием, заключается в том, что в физических свойствах таких материалов происходит ряд интересных научных процессов, которые приводят к более полному пониманию фундаментальных изменений этих процессов под влиянием позволяют различные внешние факторы.

**Ключевые слова:** Гетероструктура, наноразмер, квантовая катушка, плотность состояний, плотность состояний, колебание, наноразмер, магнитное поле, двумерность, полупроводники.

### INFLUENCE OF A STRONG ELECTROMAGNETIC FIELD ON MAGNETORESISTANCE OSCILLATIONS IN QUANTUM WELL OF SEMICONDUCTOR STRUCTURES

Annotation

In this work, the interest in the study of quantum-wound semiconductor structures is determined by the possibility of its application as nanotechnological devices operating in the small size range, as well as in various spintronic devices. The main reason why these quantum-scale structures are studied with great attention by scientists is that the physical properties of such materials have a number of interesting scientific processes, which lead to a more complete understanding of the fundamental changes of these processes under the influence of various external factors. allows.

**Key words:** Heterostructure, nanoscale, quantum coil, density of states, density of states, oscillation, nanoscale, magnetic field, two-dimensional, semiconductors.

**Kirish.** So‘nggi yillarda, kvant o‘rali yarimo‘tkazgichli strukturalarni o‘rganishga qiziqish uni kichik o‘lchamli diapazonda ishlaydigan nanotexnologik asboblarning sifatida, shuningdek, turli xil spintronik qurilmalarda qo‘llash imkoniyati bilan belgilanmoqda. Olimlar tomonidan ushbu kvant o‘lchamli strukturalarning katta e‘tibor bilan o‘rganishiga asosiy sabab, bunday materiallarning fizik xususiyatlari bir qator qiziqarli ilmiy jarayonlarga ega bo‘lib, bu jarayonlarning turli xil tashqi omillar ta‘sirida tubdan o‘zgarishlarini to‘liqroq tushunishga imkon beradi. Jumladan, bunday tashqi omillardan biri kvantlovchi magnit maydon va kuchli elektromagnit to‘lqin bo‘lib, u hajmiy yoki kichik o‘lchamli materiallarning kristall panjarasi bo‘ylab erkin harakatlanayotgan zaryadli zarralarning traektoriyalarini o‘zgartirib yuboradi. Bu esa, kvant Xoll effekti, Shubnikov – de Gaaz va de Gaaz – van Alfen effektlari kabi kvant – fizik hodisalarning paydo bo‘lishiga olib keladi.

**Adabiyotlar tahlili.** Kvantlovchi magnit maydon va kuchli elektromagnit maydon ta‘sirini tadbiq etish natijasida hajmiy yoki nanoo‘lchamli strukturalarning asosiy parametrlari: magnit maydon singdiruvchanligi, magnitoqarshilik, konsentratsiya, effektiv massa, harakatchanlik, g – faktor, relaksatsiya vaqti va boshqalarni aniqlash imkonini beradi [1-8]

ishlarda hajmiy yarimo'tkazgichli materiallarga kichik konsentratsiyali aralashmalar kiritish natijasida magnitoqarshilik ossilyatsiyalarining kuchli elektromagnit to'liqin ta'sirida o'zgarishlarini eksperimental natijalari keltirilgan. Bunda, past haroratlarda aralashma turi va konsentratsiyasini o'zgartirish natijasida magnitoqarshilik ossilyatsiya grafiklarini yaqqol siljishi kuzatilgan. Lekin, ushbu eksperimental tadqiqotlarning yuqori haroratlardagi ossilyatsiya jarayonlari nazariy jihatdan mukammal o'rganilmagan. Bundan tashqari, [1, 7-8] ishlarda kvant o'rali geterostrukturali yarimo'tkazgichlarning magnitoqarshilik ossilyatsiyalariga kuchli elektromagnit maydon, magnit maydon va haroratlarning ta'sirlari tadbiq etilgan. Chunonchi, ushbu ishlarda, ilk bora InAs/GaSb kvant o'ra asosida geterostruktura uchun o'ta yuqori chastotali elektromagnit maydon quvvati (P) dan magnit maydon kuchlanganligi (H) bo'yicha birinchi (dP/dH) va ikkinchi tartibli (d<sup>2</sup>P/dH<sup>2</sup>) differensial signallarning ossilyatsiyalari turli haroratlarda tajribada aniqlangan. Bunda, harorat ortishi bilan ossilyatsiya amplitudalarini keskin ravishda kamayishi kuzatilgan, lekin ushbu tajribalarda aynan shu fizik jarayonni sababi keltirib o'tilmagan.

**Tadqiqot metodologiyasi.** Kuchli elektromagnit madondagi bir jinsli tizimdagi tok zichligi quyidagi ifodaga ega [8];

$$j = \sigma(T_e)E_E \text{ yoki } j = j(E_E) \quad (1)$$

Bu yerda,  $T_e$ - kuchli elektromagnit maydondagi erkin elektron temperaturasi;  $E_E$ - kuchli elektromagnit maydonning elektr maydon kuchlanganligi.

Ushbu  $j(E_E)$  xarakteristikalarini uchun differensial elektr o'tkazuvchanlikka  $\sigma_d$  bog'liqligi haqida fikr yurutish qulaylik paydo qiladi, yani;

$$\sigma_d(E_E) = \frac{dj}{dE_E} = \sigma + E \frac{d\sigma}{dE_E} \quad (2)$$

Ushbu (2) ifodani o'zgaruvchan maydonda xisoblash uchun Furye komponentlari qo'llash orqali  $j(\omega)$  va  $E_E(\omega)$ lar tadqiq etiladi.  $\omega$ -o'zgaruvchan elektromagnit maydon chastotasi. Shuning uchun, biz hozirda na'munaga ta'sir qilayotgan kuchli elektromagnit maydoni vaqt bo'yicha o'zgarish ta'sir qilayapti deb faraz qilamiz.

U holda, muvozanat (balans) tenglamasi [7]:

$$e(v_d, E_E) = \frac{2}{3} \langle E \rangle - kT \tau_e \quad (3)$$

(3) dan foydalanib, (2) ni quyidagi ko'rinishga keltirish mumkin:

$$\sigma E_E^2 = nk \frac{T_e - T}{\tau_e} \quad (4)$$

(4) ifodada o'ng tomonda keltirilgan had kuchli elektromagnit maydonning quvvatini (P) ifodalaydi. U holda, (4) dan:

$$P = \sigma E_E^2 \quad (5)$$

ifoda kelib chiqadi.

Demak, (5) dan ko'rinish turibdiki, kuchli elektromagnit maydon quvvati materialning elektr o'tkazuvchanligi va elektromagnit to'liqinning elektr kuchlanganligini kvadratiga bog'liq ekan.

**Tahlil va natijalar.** Endi, (5) ifodadan foydalanib, kuchli elektromagnit maydondagi kvant o'rali geterostrukturalarni yarimo'tkazgichlarning elektr o'tkazuvchanlik ossilyatsiyalarini ko'rib chiqamiz.

Kuchli magnit maydondagi kvant o'rali geterostrukturali yarimo'tkazgichlarning elektr o'tkazuvchanligi  $\tau(E, B)$  quyidagicha aniqlanadi [3]:

$$\sigma(E, B) = \frac{e^2 n_s \langle \tau(E, B) \rangle}{m^*} \quad (6)$$

bunda,  $n_s$ -ikki o'lchamli materiallar uchun erkin elektronlar konsentratsiyasi;

$\langle \tau(E, B) \rangle$ -kuchli magnit maydondagi zaryad tashuvchilarning o'rtacha relaksatsiya vaqti.

Ikki o'lchovli materiallarda erkin zaryad tashuvchilarning o'rtacha relaksatsiya vaqti quyidagi ko'rinishga ega:

$$\langle \tau(E, B) \rangle = \frac{\int N_s^{2d}(E, B) \left( \frac{\partial f}{\partial E} \right) \tau(E) E dE}{n_s} \quad (7)$$

bunda,  $N_s^{2d}(E, B)$ - 2d o'lchamli yarimo'tkazgichning energetik holatlar zichligi.

[2] ishda 2d o'lchamli materiallar uchun energetik holatlar zichligini magnit maydon va haroratga bog'liqligini analitik ifodasi keltirib chiqarilgan. Bunda, mualliflar Gauss taqsimot funksiyasidan foydalangan. Yani,

$$N_s^{2d}(E, B, N_L, d, n_z) = \sum_{N_L, N_z} \frac{eB}{\pi \hbar} \cdot \frac{1}{kT} \cdot \exp \left( - \frac{\left( E - \left( \hbar \omega_c \left( N_L + \frac{1}{2} \right) + \frac{\pi^2 \hbar^2}{2m^* d^2} N_z^2 \right) \right)^2}{(kT)^2} \right) \quad (8)$$

Bu yerda,  $N_L$  – diskret Landau sathlari soni;  $d$  – kvant o'ra kengligi;  $n_z$  – o'lchamli kvantlar soni;  $\omega_c$  – siklotron chastotasi.

Kichik o'lchamli yarimo'tkazgichlar uchun sochilish mexanizmlarini elastik sochilish yaqinlashuvida  $\tau(E, T)$  relaksatsiya vaqti hamda (6), (7) va (8) ifodalardan foydalanib, kvant o'lchamli yarimo'tkazgichlar uchun kvantlovchi magnit maydondagi elektr o'tkazuvchanlik ossilyatsiyalarini haroratga bog'liqligi quyidagi ko'rinishga keladi:

$$\sigma_{\perp}^{2d}(E, B, T, d) = \frac{e^3 B}{2\pi m^* c} \sqrt{\frac{2}{\pi G}} \int_0^{\infty} \sum_{n_L} \exp \left[ -2 \left( \frac{E - \left[ \hbar \omega_c \left( n_L + \frac{1}{2} \right) + \frac{\pi^2 \hbar^2}{2m^* d^2} n_z^2 \right]}{G} \right)^2 \right] \gamma_{\perp}(k_0 T)^{\beta} E^{\alpha + \frac{3}{2}} \left( \frac{\partial f_0(E, T)}{\partial E} \right) dE \quad (9)$$

(9) dan ko'rinish turibdiki, kvant o'lchamli yarimo'tkazgichlarning ossilyatsiyalash jarayoni asosan 2d o'lchamli energetik holatlar zichligi hisobiga paydo bo'lmoqda. Ammo, (9) da kuchli elektromagnit maydon ta'siri hisobga olinmagan. (5) da esa, elektromagnit to'liqin quvvatining materialni elektr o'tkazuvchanligiga bog'liqligi keltirilgan. U holda, (5) va (9) ifodalardan foydalanib, kuchli elektromagnit maydon quvvati P ni kvantlovchi magnit maydon B, kvant o'ra kengligi d, harorat T, elektr maydon kuchlanganligi  $E_E$ larga bog'liqligi ( $P^{2d}(B, T, E_E, d)$ ) kelib chiqadi. Ya'ni:

$$P^{2d}(B, T, E_E, d) = \sigma^{2d}(E, B, T, d) \cdot E_E^2 \quad (10)$$

yoki,

$$P^{2d}(H, N_L, n_z, d, E_E, T) = \frac{e^3 B}{2\pi m^* c} \sqrt{\frac{2}{\pi}} \frac{1}{G} \int_0^\infty \sum_{n_L} \exp \left[ -2 \left( \frac{E - \left[ \frac{\hbar \cdot eH}{m^* c} \left( n_L + \frac{1}{2} \right) + \frac{\pi^2 \hbar^2}{2m^* d^2} n_z^2 \right]}{G} \right)^2 \right] \gamma_{\perp}(k_0 T)^\beta E^{\alpha + \frac{3}{2}} \left( \frac{\partial f_0(E, T)}{\partial E} \right) dE \cdot E_E^2 \quad (11)$$

Ushbu keltirib chiqarilgan formula, bir qator tajriba natijalarini tushuntirishga va ulardan fizik jarayonlar mohiyatini izohlashga hizmat qiladi.

**Xulosalar.** To'g'ri zonali kvant o'ra asosidagi geterostrukturalarda ikki o'lchamli kombinirlangan holatlar zichligini haroratga bog'liqligiga kvantlovchi magnit maydonning ta'sirini hisoblash uchun yangi model ishlab chiqilgan. Kuchli magnit maydonda kvant o'raning ikki o'lchamli kombinirlangan holatlar zichligini haroratga bog'liqligini "termik kengayishi" ni Gauss taqsimot funksiyasi yordamida tushuntirilgan. Eksperimental natijalar kvantlovchi magnit maydonidagi kvant o'raning kombinirlangan holat zichligi ossillyatsiyasi yordamida talqin qilingan. Hisoblash natijalari har xil haroratlarda kvantlovchi magnit maydonidagi InGaN/GaN kvant o'rasiga asoslangan heterostrukturalar uchun olingan eksperimental natijalar bilan taqqoslangan. Kombinirlangan holatlar zichligi ossillyatsiyalari qonuniyatidan magnitooptik yutilish mexanizmini aniqlashning yangi metodi taklif etilgan. Kvant o'rali to'g'ri zonali yarimo'tkazgichli strukturalarning magnitooptik yutilish koeffitsientining harorat, magnit maydon va kvant o'raning qalinligiga bog'liqligini hisoblovchi yangi matematik model ishlab chiqilgan.

#### ADABIYOTLAR

1. Кочман И.В., Михайлова М.П., Вейнгер А.И., Парфеньев Р.В. Магнитофонные осцилляции магнитосопротивления в квантовой яме InAs/GaSb с инвертированным зонным спектром // Физика и техника полупроводников, 2021, том 55, вып. 4, стр.313-318. <http://dx.doi.org/10.21883/FTP.2021.04.50731.9569>
2. Andrei Zbrodskii, Anatoly Veinger, and Petr Semenikhin. Anomalous Manifestation of Pauli Paramagnetism and Coulomb Blockade of Spin Exchange upon the Compensation of Doped Semiconductors // Phys. Status Solidi B 2019, pp.1900249-1-1900249-7. <http://dx.doi.org/10.1002/pssb.201900249>
3. А.И. Вейнгер, И.В. Кочман, В.И. Окулов, Т.Е. Говоркова. Особенности магнитных осцилляций в монокристалле HgSe с примесями кобальта низкой концентрации (<1 ат%) // Физика и техника полупроводников, 2022, том 56, вып. 1. Стр.69-75. <http://dx.doi.org/10.21883/FTP.2022.01.51814.9718>
4. А.И. Вейнгер, И.В. Кочман, Д.А. Фролов, В.И. Окулов, Т.Е. Говоркова, Л.Д. Паранчич. Микроволновое магнитопоглощение в HgSe с примесью Co и Ni // Физика и техника полупроводников, 2019, том 53, вып. 10. Стр.1413-1418. <http://dx.doi.org/10.21883/FTP.2019.10.48299.9149>
5. А.И. Вейнгер, И.В. Кочман, В.И. Окулов, Т.А. Говоркова, М.Д. Андрийчук, Л.Д. Паранчич. Особенности электронного парамагнитного резонанса примеси железа в кристаллах HgSe // Физика и техника полупроводников, 2019, том 53, вып. 3. Стр.317-322. <http://dx.doi.org/10.21883/FTP.2019.03.47281.8980>
6. А.И. Вейнгер, И.В. Кочман, В.И. Окулов, М.Д. Андрийчук, Л.Д. Паранчич. Осцилляции микроволнового магнитопоглощения в кристаллах HgSe с примесью Fe // Физика и техника полупроводников, 2018, том 52, вып. 8. Стр.847-852. <http://dx.doi.org/10.21883/FTP.2018.08.46208.8793>
7. Gulyamov G., Erkaboev U.I., Gulyamov A.G. Shubnikov-de Haas oscillations in semiconductors at the microwave-radiation absorption // Advances in condensed matter physics. 2019, Vol.2019. Article ID 3084631, pp.1-5. <https://doi.org/10.1155/2019/3084631>
8. Gulyamov G., Erkaboev U.I., Gulyamov A.G. Magnetic quantum effects in electronic semiconductors at microwave-radiation absorption // Journal of nano – and electronic physics. 2019, Vol.11. No.1. pp.01020-1-01020-6. [https://doi.org/10.21272/jnep.11\(1\).01020](https://doi.org/10.21272/jnep.11(1).01020)
9. Erkaboev U.I., Rakhimov R.G., Negmatov U.M., Sayidov N.A., Mirzaev J.I. Influence of a strong magnetic field on the temperature dependence of the two-dimensional combined density of states in InGaN/GaN quantum well heterostructures // Romanian Journal of Physics. 2023. Vol.68, Iss.5-6, pp.614-1-614-14. <https://www.scopus.com/sourceid/11500153309>
10. Erkaboev U.I., Rakhimov R.G., Mirzaev J.I., Negmatov U.M., Sayidov N.A. Influence of a magnetic field and temperature on the oscillations of the combined density of states in two-dimensional semiconductor materials // Indian Journal of Physics. 2024. Vol.98, pp.189-197. <https://www.scopus.com/sourceid/145208>
11. Gulyamov G., Erkaboev U.I., Rakhimov R.G., Mirzaev J.I., Sayidov N.A. Determination of the dependence of the two-dimensional combined density of states on external factors in quantum-dimensional heterostructures // Modern Physics Letters B. 2023. Vol.37, No.10, pp.2350015-1-2350015-14. <https://www.scopus.com/sourceid/29055>



UDK: 538.955; 621.3.082.782

*Ulug‘bek ERKABOYEV,*  
*Namangan muhandislik-texnologiya instituti professori, f.-m.f.d*  
*Jasurbek MIRZAYEV,*  
*Namangan muhandislik-texnologiya instituti, PhD*  
*Muzaffar DADAMIRZAYEV,*  
*Namangan muhandislik- texnologiya instituti tayanch doktoranti*  
*E-mail: muzaffardadamir81@gmail.com*

*NamMTI professori, f.-m.f.d. N.Shariboyev taqrizi asosida*

### ОСЦИЛЛЯЦИИ ПЛОТНОСТИ ЭНЕРГЕТИЧЕСКИХ СОСТОЯНИЙ В НАНОРАЗМЕРНЫХ ПОЛУПРОВОДНИКАХ ПРИ ПРОДОЛЬНЫХ И ПОПЕРЕЧНЫХ КВАНТУЮЩИХ МАГНИТНЫХ ПОЛЯХ

Аннотация

С учетом гауссовой функции распределения удастся рассчитать влияние квантованного магнитного поля на температурную зависимость колебаний плотности энергии состояний в квантоворазмерных полупроводниках на основе метода растекания дельта-функции. С помощью численных методов расчета разработана новая математическая модель температурной зависимости колебаний плотности энергии состояний разрешенного поля в наноразмерных полупроводниках под действием поперечного квантующего магнитного поля.

**Ключевые слова:** магнитное поле, квантующее магнитное поле, гетероструктура, квантовая яма, плотность состояний, осцилляция, наноразмер, двумерные полупроводники.

### OSCILLATIONS OF THE ENERGY DENSITY OF STATES IN NANO-SIZED SEMICONDUCTORS IN LONGITUDINAL AND TRANSVERSE QUANTIZING MAGNETIC FIELDS

Annotation

Taking into account the Gaussian distribution function, it is possible to calculate the effect of a quantized magnetic field on the temperature dependence of fluctuations in the energy density of states in quantum-sized semiconductors based on the delta-function spreading method. Using numerical calculation methods, a new mathematical model of the temperature dependence of fluctuations in the energy density of states of the allowed field in nanosized semiconductors under the action of a transverse quantizing magnetic field has been developed.

**Key words:** magnetic field, quantum magnetic field, heterostructure, quantum well, density of states, oscillation, nanosize, two-dimensional semiconductors.

### BO‘YLAMA VA KO‘NDALANG KVANTLOVCHI MAGNIT MAYDONDAI NANOO‘LCHAMLI YARIMO‘TKAZGICHLARDA ENERGETIK HOLATLAR ZICHLIGI OSSILLYATSIIYASILARI

Аннотация

Gauss taqsimot funksiyasini hisobga olgan holda kvant o‘lchamli yarimo‘tkazgichlarda energetik holatlar zichligi ossillyatsiyalarini haroratga bog‘liqligiga kvantlovchi magnit maydonning ta‘sirini hisoblash mumkinligi delta – funktsiyalarni qatorga yoyish usuli yordamida asoslangan. Sonli hisoblash usullaridan foydalanib, ko‘ndalang kvantlovchi magnit maydon ta‘siridagi nano o‘lchamli yarimo‘tkazgichlarda ruhsat etilgan sohasining energetik holatlar zichligi ossillyatsiyalarini haroratga bog‘liqligi aniqlangan.

**Kalit so‘zlar:** magnit maydon, kvantlovchi magnit maydon, geterostruktura, kvant o‘ra, holatlar zichligi, ossillyatsiya, nanoo‘lcham, ikki o‘lchamli yarimo‘tkazgichlar

**Kirish.** Hozirgi vaqtda yarimo‘tkazgichlar fizikasi sohasidagi amaliy va fundamental tadqiqotlarga bo‘lgan qiziqish hajmi materiallardan nanoo‘lchamli materiallarga o‘tdi. Ayniqsa, kvantlovchi magnit maydon ta‘sirida bo‘lgan nanoo‘lchamli yarimo‘tkazgichlarda zaryad tashuvchilarning energetik spektrining xususiyatlarini tubdan o‘zgarishi, olimlarning spintronika va nanoelektronika sohalari bilan ilmiy tadqiqot ishlarini olib borishga qiziqish uyg‘otdi. Natijada kvantlovchi magnit maydonidagi erkin elektronlar va teshiklarning energetik sathlarini kvantlantirish kvant o‘rali yarimo‘tkazgichlardagi energetik holatlar zichligi ossillyatsiyalarini sezilarli o‘zgarishlarga olib kelishi tajribalarda kuzatilmoqda.

**Adabiyotlar tahlili.** Kvant o‘rali yarimo‘tkazgichlarda energetik holatlar zichligini kvantlovchi magnit maydonning kattaligiga bog‘liqligini o‘rganish zaryad tashuvchilarning energetik spektrlari to‘g‘risida muhim ma‘lumotlarni olish imkonini beradi. Kinetik, dinamik va termodinamik kattaliklar, jumladan magnit qarshilik, magnit singdiruvchanlik, elektronlarning issiqlik sig‘imi, Fermi sathi va boshqa kattaliklarning ossillyatsiya jarayoni asosan energetik holatlar zichligining ossillyatsiyalanishi hisobiga hosil bo‘ladi.

Bundan kelib chiqadiki, ko‘ndalang va bo‘ylama magnit maydon ta‘siridagi to‘g‘ri burchakli kvant o‘rali yarimo‘tkazgichning o‘tkazuvchanlik sohasida energetik holatlar zichligi ossillyatsiyalarini o‘rganish zamonaviy qattiq jismlar fizikasining dolzarb muammolaridan biri hisoblanadi.

Jumladan, ushbu ishlarda, [1, 2, 3], bir jinsli perpendikulyar magnit maydonidagi va tasodifiy ixtiyoriy korrelyatsiya maydonidagi ikki o‘lchamli elektron gazlarda Landau sathlari holatlar zichligi hisob-kitoblari ko‘rib chiqilgan. Keskin



o'zgaraydigan trayektoriya bo'yicha integrallar yarim klassik usuli yaratilgan korrelyasiyaning tasodifiy maydoni uchun yo'li integrallarning noan'anaviy yondashuvi ishlab chiqilgan va bu Landau sathlari holatlar zichligi uchun analitik yechim beradi. Magnit maydonning zaiflashishi va korrelyasiya uzunligining kamayishi bilan holatlar zichligining og'ishi Gauss shaklidan ortadi [1, 2]

Bu ishlarda erishilgan yutuqlarga qaramay, ularda ba'zi savollar ochiq qolmoqda. Masalan: ko'ndalang va bo'yilma magnit maydondagi kvant o'rali yarimo'tkazgichlarning energetik holatlar zichligini haroratga bog'liqligini termik o'zgarishni hisobga olgan holda qanday aniqlash mumkin? Umuman, uning harorat bo'yicha o'zgarish dinamikasi qanday bo'ladi kabi muammolar hozirgacha ochiq qolmoqda.

**Tadqiqot metodologiyasi.** Keling, ko'ndalang kvantlovchi magnit maydon ta'sirida kichik o'lchamli qattiq jismlardagi holatlar zichligi ossillyatsiyalarining haroratga bog'liqligini ko'rib chiqaylik. Ma'lumki, Landau sathlariga haroratning ta'sirini aniqlashda, energetik holatlar zichligi ossillyatsiyalarini delta o'xshash funksiyalar bo'yicha qatorga yoyish usulidan foydalaniladi [4, 5, 6, 7]. Delta shaklidagi funksiyalarning ketma-ket qatorga yoyish yo'li bilan energetik holatlar zichligi ossillyatsiyalarini o'rganish orqali kvant o'rali yarimo'tkazgichlarda o'tkazuvchanlik sohasini diskret Landau sathining haroratga bog'liqligini tushuntirish mumkin bo'ladi. Kvantlovchi magnit maydonda holatlar zichligi ossillyatsiyalarining haroratga bog'liqligi diskret Landau sathlarining termik kengayishi bilan aniqlanadi. Mutloq nol haroratda Gauss taqsimot funksiyasi delta shaklida bo'lib, quyidagi ifoda bilan hisoblanadi [8]:

$$Gauss(E, T) = \frac{1}{kT} \cdot \exp\left(-\frac{(E - E_i)^2}{(kT)^2}\right) \quad (1)$$

U holda, termik kengayishni Gauss taqsimot funksiyasini haroratga bog'liqligi bilan tavsiflash mumkin. Cheksiz chuqur to'g'ri burchakli kvant o'ra uchun, zaryad tashuvchilarning  $E_i$  chuqur sathidan o'tkazuvchanlik sohasiga va  $E$  energiyali valentlik sohasiga termik chiqarish vaqti eksponent faktor  $\exp\left(-\frac{(E - E_i)^2}{(kT)^2}\right)$  bilan belgilanadi. Demak, chuqur to'ldirilgan diskret

Landau sathlari eksponent sifatida energetik holatlar zichligi ossillyatsiyalariga va haroratga bog'liq. Energetik holatlarning zichligi ossillyatsiyalarining haroratga bog'liqligini aniqlash uchun  $T = 0$  holatidagi energiya zichligi ma'lum energiya  $E_i$  ( $N_L, N_Z$ ) funksiyasiga teng deb faraz qilamiz. Ikki o'lchamli elektron gazlar uchun, ko'ndalang kvantlovchi magnit maydonda, holatlar zichligining ossillyatsiyalari (2) formula bo'yicha hisoblanadi.

$$N_{S,Z}^{2d}(E, B) = \frac{eB}{\pi\hbar} \sum_{N_L, N_Z}^{\infty} \delta(E - E(N_L, N_Z)) \quad (2)$$

Haroratning oshishi bilan har bir holat energiya  $E_i(N_L, N_Z)$  bilan o'zgaradi. Diskret Landau sathlarini  $E_i(N_L, N_Z)$  energiya bilan termik kengayishi Shokli-Rid-Xoll statistikasiga bo'ysinadi [9]. Shunday qilib, o'tkazuvchanlik va valent sohalarida, barcha holatlarning termik kengayishini hisobga olgan holda, hosil bo'ladigan holatlar zichligi ossillyatsiyalari barcha termik kengayishlarni yig'indisi bilan aniqlanadi. Demak kvant o'rali yarimo'tkazgichlar uchun  $T$  cheklangan haroratda energetik holatlar zichligi ossillyatsiyalari  $N_{S,Z}^{2d}(E, B, T, d)$  Gauss funksiyani qatorga yoyish orqali termik kengayishini (haroratga bog'liqligini) tushuntirishga imkon beradi.

Agar  $N_{S,Z}^{2d}(E, B, T, d)$  ni Gauss funksiyalari bo'yicha qatorga yoyib kengaytirsak, u holda ikki o'lchamli elektron gazlardagi energetik holatlar zichligi ossillyatsiyalarining haroratga bog'liqligini hisoblash mumkin. Bundan, ko'ndalang kvantlovchi magnit maydonidagi energetik holatlar zichligi ossillyatsiyalarining haroratga bog'liqligini olish mumkin.

**Tahlil va natijalar.** Ko'ndalang kvantlovchi magnit maydonda Landau sathining termik kengayishi diskret sathlarning silliqlashiga olib keladi va termik kengayish Gauss funksiyasi yordamida aniqlanadi. Past haroratlarda Gauss taqsimot funksiyalari delta shaklidagi funksiyaga aylanadi:

$$Gauss(E, E_i, T) \xrightarrow{T \rightarrow 0} \delta(E - E_i) \quad (3.21)$$

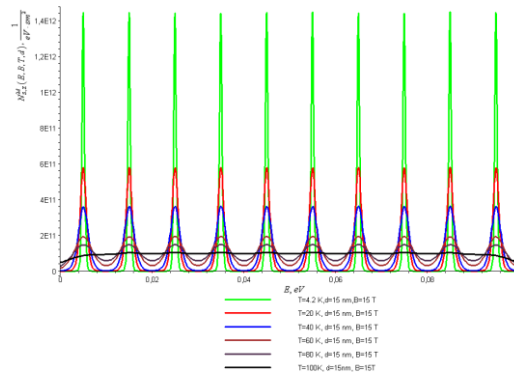
Shunday qilib, to'g'ri burchakli kvant o'ra uchun energetik holatlar zichligi ossillyatsiyalarini quyidagi analitik ifoda orqali olamiz:

$$N_{S,Z}^{2d}(E, B, T, d) = \sum_{N_L, N_Z}^{\infty} \frac{eB}{\pi\hbar} \cdot \frac{1}{kT} \cdot \exp\left(-\frac{\left(E - \left(\hbar\omega_c \left(N_L + \frac{1}{2}\right) + \frac{\pi^2\hbar^2}{2m^*d^2} N_Z^2\right)\right)^2}{(kT)^2}\right) \quad (3)$$

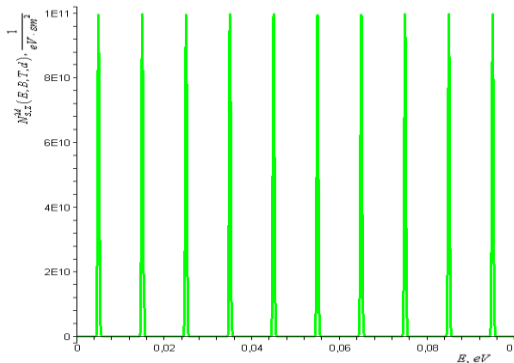
Bu yerda,  $d$  - kvant o'raning qalinligi;  $N_L$  - to'g'ri burchakli kvant o'ra uchun Landau sathlari soni;  $N_Z$  -  $Z$  o'qi bo'yilma o'lchamli kvantlar soni;  $B$  - ko'ndalang kvantlovchi magnit maydonning induksiyasi. Bu formula ko'ndalang kvantlovchi magnit maydon ta'siridagi kvant o'rali yarimo'tkazgichlarda, energetik holatlar zichligi ossillyatsiyasining haroratga bog'liqligini anglatadi. Olingan ifoda turli harorat va ko'ndalang magnit maydonda, ikki o'lchamli elektron gazlarda energetik holatlar zichligi ossillyatsiyalari bo'yicha eksperimental ma'lumotlarni qayta ishlash uchun qulaydir. Shunday qilib, nanoo'lchamli yarimo'tkazgichlardagi energetik holatlar zichligi ossillyatsiyalarining haroratga bog'liqligini ifodalaydigan yangi matematik model ishlab chiqildi. Taklif etilayotgan model yordamida kvantlovchi magnit maydondagi nanoo'lchamli yarimo'tkazgichlarning energetik holatlar zichligini haroratga bog'liqligini tahlil qilaylik. Ushbu ishda [10], HgCdTe/CdHgTe kvant o'rali assimetrik yarimo'tkazgichlarda klassik va kvantlovchi magnit maydonlar ta'siridagi erkin elektronlarning siklotron rezonans spektrlarining o'zgarishi o'rganilgan. Bu yerda Cd<sub>x</sub>Hg<sub>1-x</sub>Te kvant o'raning qalinligi  $d=15$  nm, magnit maydoni  $B=15$  T va harorati  $T=4,2$  K ni tashkil etadi. Bu ishda materiallar uchun energetik holatlar zichligining haroratga bog'liqligi muhokama qilinmagan. 1-rasmda ko'ndalang kvantlovchi magnit maydon  $B=15$  Tl. va harorat  $4.2$  K bo'lganda kvant o'raning qalinligi  $d=15$



nm uchun  $\text{Cd}_x\text{Hg}_{1-x}\text{Te}$  ni energetik holatlar zichligi ossillyatsiyalari keltirilgan. Rasmda keltirilgan kvant o'raning o'tkazuvchanlik sohasidagi diskret energetik sathlari (3) formula bo'yicha hisoblangan. Bunda diskret energetik sathlari soni 10 ga teng. Har bir diskret energiya cho'qqilari Landau sathlari deyiladi. Grafikda diskret Landau sathlarini kuzatilishiga sabab,  $B=15 \text{ Tl}$  da,  $\hbar\omega_c = 0,02 \text{ eV}$ ,  $T=4.2 \text{ K}$  da  $kT=4.10^{-4} \text{ eV}$  hamda  $\frac{\hbar\omega_c}{kT} = 50$  yoki  $kT \ll \hbar\omega_c$  sharti bajariladi. Bunday holda Landau sathining termik kengayishi juda kuchsiz va energetik holatlar zichligining ossillyatsiyasi, ideal shakldan chetga chiqishni sezmaydi. Birinchi diskret Landau sathi ( $N_L=0$ ) kvant o'raning o'tkazuvchanlik sohasining pastki qismida paydo bo'ldi. Ikkinchi ( $N_L=1$ ), uchinchi ( $N_L=2$ ) va boshqa diskret Landau sathlari kvant o'raning o'tkazuvchanlik sohasi tubidan yuqorida joylashgan. Shu tarzda, past haroratlarda kvant o'raning valentlik sohasida ham Landau sathining cho'qqilarini hisoblash mumkin. Ushbu hisob-kitoblarga dissertatsiyaning keyingi bobida ko'rib o'tamiz. 2-rasmda energetik xolatlar zichligi  $N_{S,Z}^{2d}(E, B, T, d)$  4.2 K, 20 K, 40 K, 60 K, 80 K va 100 K haroratlar uchun ossillyatsiya keltirilgan. Bu rasmdan ko'rinib turibdiki, harorat ko'tarilishi bilan Landau sathining cho'qqilari keskin silliqlasha boshlaydi va etarlicha yuqori haroratlarda holatlarning diskret holatlar zichligi uzluksiz energetik spektrlariga aylanadi.



**1 -rasm.** HgCdTe/CdHgTe kvant o'radagi energetik holatlar zichligi ossillyatsiyalari. Kvant o'ra  $\text{Cd}_x\text{Hg}_{1-x}\text{Te}$  ning qalinligi  $d=15 \text{ nm}$ ,  $B=15 \text{ T}$  va  $T=4.2 \text{ K}$ , [10]. Ushbu grafik (3) formula bo'yicha olingan



**2-rasm.** Ko'ndalang kvantlovchi magnit maydon ( $B=15 \text{ Tl}$ ) gacha HgCdTe/CdHgTe kvant o'raning ( $d=15 \text{ nm}$ ) o'tkazuvchanlik sohasidagi energetik holatlar zichligi ossillyatsiyalarining haroratga bog'liqligi. Rasmda keltirilgan energetik spektrlar (3) formula bo'yicha hisoblangan

**Xulosa.** Parabolik dispersiya qonuni asosida bo'ylama va ko'ndalang magnit maydon ta'siridagi ikki o'lchamli materiallarning energetik holatlar zichligi ossillyatsiyalarini hisoblash uchun yangi analitik ifodalar olindi. Ko'ndalang kvantlovchi magnit maydon ta'sirida ikki o'lchamli yarimo'tkazgichli materiallarda energetik holatlar zichligi ossillyatsiyalarining haroratga bog'liqligini aniqlash uchun yangi matematik model ishlab chiqildi. Kvant o'rali yarimo'tkazgichlarda harorat ortishi bilan termik kengayish hisobiga diskret Landau sathlari yuvilishi ko'rsatildi va energetik holatlar zichligi ossillyatsiyalari kuzatilmadi.

#### ADABIYOTLAR

1. Дубровский И.М. Новая теория электронного газа в магнитном поле и задачи для теории и эксперимента // Успехи физ. мет. 2016. Т.17, С.53–81.
2. Kytin V.G., Bisquert J., Abayev I., Zaban A. Determination of density of electronic states using the potential dependence of electron density measured at nonzero temp // Physical review B. 2004. Vol.70, pp.193304-1- 193304-4.
3. Sablikova V. A., Tkacha Yu.Ya. Singularity of the density of states and transport anisotropy in a two-dimensional electron gas with spin-orbit interaction in an in-plane magnetic field // Semiconductors, 2018. Vol. 52, No.12, pp.1581–1585.
4. Gulyamov G., Erkaboev U.I., Sharibaev N.Yu. Effect of temperature on the thermodynamic density of states in a quantizing magnetic field // Semiconductors. 2014, Vol. 48, No.10, pp. 1323-1328.
5. Gulyamov G., Erkaboev U.I., Sharibaev N.Yu. The de Haas-van Alphen effect at high temperatures and in low magnetic fields in semiconductors // Modern physics letters B. 2016. Vol. 30, No.7. pp.1650077-1-1650077-7.
6. Gulyamov G., Erkaboev U.I., Baymatov P.J. Determination of the density of energy states in a quantizing magnetic field for model Kane // Advances in condensed matter physics. 2016. Vol.2016. pp.5434717-1-5434717-1.
7. Gulyamov G., Erkaboev U.I., Gulyamov A.G. Influence of pressure on the temperature dependence of quantum oscillation phenomena in semiconductors // Advances in condensed matter physics. 2017. Vol.2017. pp.6747853-1-6747853-6.
8. Schoenberg D. Magnetic oscillations in metals. New York, Wiley. 1986. pp.350-400.

9. Сильбанс Л.С. Физика полупроводников. Москва, «Советское радио». 1967. С.416-421.
10. Бовкун Л.С., Маремьянин К.В., Иконников А.В., Спирин К.Е., Алешкин В.Я., Potemski M., Piot B., Orlita M., Михайлов Н.Н., Дворецкий С.А., Гавриленко В.И. Магнитооптика квантовых ям на основе *HgTe/CdTe* с гигантским расщеплением Рашбы в магнитных полях до 34 Тл // ФТП. 2018. Т.52, вып.11, С.1274-1279.